海洋開発及地球科学技術調査研究促進費

地球科学技術特定調査研究

アジアモンスーン機構に関する研究

JAPANESE EXPERIMENT ON ASIAN MONSOON (JEXAM)

（平成元年度～平成10年度）

（ＦＹ1989～ＦＹ1998）

平成８年度　成果報告書

ANNUAL REPORT

(APRIL 1996～MARCH 1997)

平成９年８月

August 1997

科学技術庁研究開発局

Research and Development Bureau

Science and Technology Agency

Japan

はじめに

大規模な季節変動として知られているアジアモンスーンは、インド洋・東南アジア周辺の海洋とチベット・ヒマラヤを始めとしたアジア大陸の地表面が、大気を媒体として熱・水蒸気等の交換により、相互に影響を及ぼし合っている現象です。その活動の年々変動は、東南アジア地域や、日本を始めとした周辺地域の気候のみならず、大気大循環を介して世界の気候に大きな影響を与えています。また、アジアモンスーンの活動が西部熱帯太平洋域の大気・海洋変動を引き起こし、太平洋規模で発生するエル・ニーニョ／南方振動の引き金になっている可能性があるという指摘もあり、この点からも注目されています。しかし、これらの地域・海域は広大であり、また観測環境が厳しいこと等から観測体制の整備が遅れており、気象・海象・陸象に関するデータの収集は必ずしも十分に行われていませんでした。

このため科学技術庁では、海洋開発及地球科学技術調査研究促進費により「アジアモンスーン機構に関する研究」を平成元年度より開始し、さらに、平成5年に「『アジアモンスーン機構に関する研究』プロジェクトに関する日本国科学技術庁と中華人民共和国国家気象局との間の実施取極」を結び、日中の協力体制を整えて、観測・解析を進めてきました。

本研究の成果が、アジアモンスーン機構の解明に寄与し、さらには気候変動に対する理解を深めることを期待しています。

最後になりましたが、本研究に携わられた関係各位に対し感謝するとともに、今後とも御協力をお願いする次第です。

平成9年8月

科学技術庁研究開発局長
青江　茂

目　次

Contents

研究計画の概要

Outline of the Study

Ⅰ. General Introduction

Asian Monsoon is caused by the thermal contrast between the Indian Ocean and surrounding oceans, and the land surface of Asian Continent. These two land and ocean areas interact with each other through the exchange of the heat and moisture. Its consequence is observed as a seasonal phenomenon in the regions of Southeast Asia and East Asia, including Japan.

The year-to-year variation of the Asian Monsoon has a significant influence not only on the climate of Southeast Asia and the surrounding area including Japan, but also on the worldwide climate through the global atmospheric circulations. Furthermore, it is recently reported that the anomalous activities of the Asian Monsoon causes the atmospheric/oceanic variations over the tropical western Pacific which, in turn, trigger the El Nino/Southern Oscillation events over the whole Pacific Ocean.

Though it is recognized that Asian Monsoon plays an important role in the global climate system, its mechanism has not yet been made clear. This is mainly attributable to the fact that the atmospheric and oceanographic data are sparse over those regions due to the technical difficulties in the observations and the insufficiencies of conventional observation network.

Japan, as a member of the Asian countries, is situated under the direct influence of the Asian monsoon and has a capability to conduct the atmospheric and oceanographic observations. Therefore, it is an important role of Japan to carry out the research projects for the study on Asian Monsoon in cooperation with the countries such as China and India.

This project is expected to make a contribution for the improvement of the long-range forecast of the global climate change as well as the forecasting technique of the unusual weather, such as drought and long spell of rain.

Based on the understandings as mentioned above, Science and Technology Agency (STA) of Japan has launched this ten-year research project since April 1989.

Ⅰ．研究の趣旨

アジアモンスーンは、インド洋・東南アジア周辺の海洋とチベット・ヒマラヤを始めとしたアジア大陸の地表面が、その熱的特性の相違により大気を媒体とした熱・水蒸気等の交換を通じて、それぞれ相互に影響を及ぼし合う結果、東南アジア・東アジア地域における季節的な現象として発現している。その活動の年次の変動は、東南アジア地域や、日本を始めとした周辺地域の気候の変動に大きな影響を及ぼすばかりでなく、大気大循環変動を介して世界の気候にも大きな影響を与えている。また最近、アジアモンスーンの活動の異常は西部熱帯太平洋域の大気・海洋変動を引き起こし、これが太平洋規模で発生するエル・ニーニョ／南方振動の引き金となっている可能性があるという研究報告もあり、この点からも注目する必要がある。しかしながら、これらの地域・海域は、対象域の広大さや観測環境の厳しさ等から観測体制が整備されておらず、気象・海象・陸象の基本的な要素に係るデータの収集が必ずしも十分に行なわれているとは言えない。

従って、アジアの一員であり、アジアモンスーンの直接的影響を受け、大気・海洋観測の十分なポテンシャルを有する我が国が、世界の気候を形成する複雑なシステムの一つであるアジアモンスーンの機構を解明するため長期的・総合的な研究を実施することが緊要となっている。本研究を実施することにより、我が国を含むアジア地域における旱ばつや長雨といった異常気象発現の予測技術のみならず、世界的規模の気候変動を予測する技術の発展に寄与することが期待される。

以上のような状況を踏まえて、本研究は１９８９年度から１０年間の計画で行っている。

Ⅱ. Outline of the Study

1. Observation and Analysis on the Process of the Atmosphere-Ocean-Land Interactions

(1) Observation and Analysis on the Process in the Atmosphere

-To construct a database of the Japanese and Indian satellites and make an analysis of the large scale cloudiness changes.

-To observe and three dimensional structures of the tropical convective clouds related to the heat budget of the atmosphere-ocean interaction by wind Doppler radar.

(2) Observation and Analysis on the Process over the Ocean

-To observe sub-surface temperature throughout the year by voluntary, official, commercial and fishing ships over the Southeast Asia and the Indian Ocean.

-To observe larg-scale oceanic current throughout the year by drifting buoys over the Indian Ocean.

-To standardize and construct a database of the oceanic data and promote a data exchange. To construct an information exchange systemconcerning to the observation in the Indian Ocean.

(3) Observation and Analysis on the Process over the Land

-To observe weather and land surface conditions over the Tibetan area and estimate an energy budget of the atmosphere-land interaction.

-To observe three dimensional structures of low level air flow related to the heat budget of the atmosphere-land interaction by wind profiler.

-To promote a maritime meteorological observation by voluntary commercial ships and estimate an energy budget of the atmosphere-ocean interaction.

-To construct a database of the polar orbiting earth observation satellites and make an analysis of the atmosphere-ocean-land situations related to the large scale hydrological variations.

-To collect daily hydro-meteorological data over the Yangtze River basin and make an analysis of the long-term variations.

2. Experiment of the Atmosphere-Ocean-Land Interactions by the Use of Numerical Models

(1) Development of the Four Dimensional Data Assimilation System by the Use of Numerical Model

-To develop the four dimensional data assimilation system by the use of numerical models for the analysis on the process of the atmosphere-ocean-land interactions.

(2) Development of the Water Balance Model over the Wide Area

-To develop numerical models for the investigation of the large scale hydrological budget over the Tibet,India and Southeast Asia related to the heat transport.

3 . Synthetic Study on the Atmosphere-Ocean-Land Interactions

(1) Experiment of the Atmosphere-Ocean-Land Interactions by the Use of General Circulation Models

-To perform numerical experiments of the effect of intraseasonal 30-60 day variation on Asian monsoon.

-To perform numerical experiments by the atmosphere-ocean coupled model for the investigation of the effects of oceanic conditions on the long-term variation of the atmosphere-land condition.

(2) Analysis of the Energy Balance of Monsoon

-To construct a database of Earth radiation budget through the polar orbiting meteorological satellites and make an analysis of an effect of the monsoon variation.

(3) Synthetic Study of the Monsoon Circulations

-To make a comprehensive analysis of the monsoon circulation by the use of the standardized data.

Ⅱ. 研究の概要

1. 大気・海洋・陸域間相互作用の諸過程に関する観測・解析研究

(1) 大気における諸過程に関する観測・解析研究

- 静止気象衛星資料をデータベース化し、モンスーン活動の年々変動、降水システム、エルニーニョとの関連についての解析を行う。
- 前期に観測した対流雲のデータを解析し、対流雲の構造、対流雲による熱、水、運動量の輸送過程を明らかにする。

(2) 海洋における諸過程に関する観測・解析研究

- 東南アジア周辺海域及びインド洋を航行する公庁船、商船及び漁船により海洋表層水温の通年観測を行う。
- インド洋に漂流ブイを放流し、大規模海流循環の通年観測を行う。
- 上記で取得した海洋データの標準化、データベース化を促進する。また、インド洋及び東南アジア周辺海域の海洋観測情報交換システムを構築し、取得データを交換する。

(3) 陸域における諸過程に関する観測・解析研究

- チベット地域における気象及び陸面の観測を行い、大気陸面間のエネルギー収支を見積もる。
- 商船委託により、インド洋から東南アジア周辺に至る海域での海上気象・高層気象観測、及びウィンドプロファイラーにより下層大気の観測を行い、大気海洋間、大気陸面間のエネルギー収支を見積もる。
- 極軌道地球観測衛星資料から、積雪、雲分布、土壌水分量を算出し、解析する。
- 中国の代表流域の水文資料、水文・気象データを収集し、水収支解析及び蒸発発散解析を行う。

2. 数値モデルによる大気・海洋・陸域間相互作用の実験研究

(1) 数値モデルによる4次元資料同化システムの開発に関する研究

- 現在の4次元資料同化システムに、現在使用されていない衛星データ等を組み込めるように高度化を図り、得られた物理量からモンスーン機構を考察する。

(2) 広域水収支モデルの開発に関する研究

- 前期に開発した流出量モデル、蒸発散量モデルへの検証・改良を行うと共に、積雪・流出量サブモデルを開発し、積雪地域への広域水収支モデルの適用を図る。

3. 大気・海洋・陸面間の相互作用に関する総合研究

(1) 大規模モデルによる大気・海洋・陸面間の相互作用に関する実験研究

- 前期に用いたモデルの改良を行う。また、大気海洋結合モデルを導入し、アジアモンスーンの機構に対する海洋や陸面の役割を評価する。さらに高分解能の大気大循環モデルを開発し、地表面状態や対流活動の影響を評価する。

(2) モンスーンのエネルギー収支に関する解析研究

- モデルのシミュレーション結果を衛星観測データの解析結果によって検証し、モンスーン機構のエネルギー収支解析を行う。

(3) モンスーン循環系の総合解析

- 海洋や雪氷分布の変動と、モンスーン循環を含む大気大循環や日本の天候の関連を調査する。また、高層・地上・海洋・陸面観測データを用いて総合的に解析することによって、モンスーン循環系を解明する。

Ⅲ. 研究実施体制
Research Items and Institutes

研 究 項 目 Research Items	担 当 機 関 Research Institutes
Ⅰ. 大気・海洋・陸域間相互作用の諸過程に関する観測・解析研究 Observation and Analysis on the Process of the Atmosphere-Ocean-Land Interactions	
1. 大気における諸過程に関する観測・解析研究 Observation and Analysis on the Process in the Atmosphere	
(1) 大規模積雲対流活動と降水系に関する解析研究 Analysis on the Large scale Convective Activity and Precipitation Systems	気象庁 気象研究所 Meteorological Research Institute (MRI), Japan Meteorological Agency (JMA)
(2) 大規模雲域内における対流雲構造に関する研究 Observation of Structure of Convective Clouds in Large-scale Cloud Systems	気象庁 気象研究所 MRI/JMA
(3) モンスーン域対流雲の維持過程と水収支に関する研究 Analysis on the evolution of Convective cloud systems	科学技術庁 防災科学技術研究所 National Research Institute for Earth Science and Disaster Prevention (NIED), Science and Technology Agency (STA)
2. 海洋における諸過程に関する観測・解析研究 Observation and Analysis on the Process over the Ocean	
(1) 表層水温に関する観測研究 Observation on Subsurface Temperature by Voluntary Ships	水産庁 遠洋水産研究所 Far seas Fisheries Research Laboratory, Fisheries Agency 気象庁 海洋気象部 Marine Department, JMA
(2) 海流循環に関する観測研究 Observation on Oceanic Currents with Drifting Buoys	海上保安庁 水路部 Hydrographic Department (HD), Maritime Safety Agency (MSA)
(3) 海洋データの標準化及び海洋データ交換の推進 Standardization of Oceanic Data and Promotion of Exchange of Oceanic Data and Information	海上保安庁 水路部 HD/MSA
3. 陸域における諸過程に関する観測・解析研究 Observation and Analysis on the Process over the Land	
(1) チベット・ヒマラヤにおける水文変動に関する観測研究 Observation on Hydrology over the Tibetan Plateau and Himalayas	科学技術庁 防災科学技術研究所 NIED/STA

研 究 項 目 Research Items	担 当 機 関 Research Institutes
(2) 地表面熱収支に関する観測研究 Observation on Regional Surface Heat Budget Observational Study of the Ground Surface Heat Budgets	気象庁 気象研究所 MRI/JMA 郵政省 通信総合研究所 Communications Research Laboratory, Ministry of Posts and Telecommunications
(3) モンスーン循環広域条件及び雪氷変動状況に関する解析研究 Analysis on Environmental Condition and Snow-Ice Cover Changes Affecting Monsoon Cycle in Asia	科学技術庁 防災科学技術研究所 NIED/STA
(4) 地域水収支に関する解析研究 Analytical study of water balance on representative river basins	科学技術庁 防災科学技術研究所 NIED/STA
Ⅱ. 数値モデルによる大気・海洋・陸域間相互作用の実験研究 Experiment of the Atmosphere-Ocean-Land Interactions by the Use of Numerical Models	
1. 数値モデルによる4次元資料同化システムの開発に関する研究 Development of the Four Dimensional Data Assimilation System by the Use of Numerical Model	気象庁 予報部 Forecasting Department (FD), JMA
2. 広域水収支モデルの開発に関する研究 Development of the Water Balance Model over the Wide Area	科学技術庁 防災科学技術研究所 NIED/STA
Ⅲ. 大気・海洋・陸面間の相互作用に関する総合研究 Synthetic Study on the Atmosphere-Ocean-Land Interactions	
1. 大規模モデルによる大気・海洋・陸面間の相互作用に関する実験研究 Experiment of the Atmosphere-Ocean-Land Interactions by the Use of General Circulation Models	気象庁 気象研究所 MRI/JMA
2. モンスーンのエネルギー収支に関する解析研究 Analysis of the Energy Balance of Monsoon	気象庁 気象研究所 MRI/JMA
3. モンスーン循環系の総合解析 Synthetic Study of the Monsoon Circulations	気象庁 予報部 FD/JMA
Ⅳ. 検討委員会の開催等 Research Steering Committee	気象庁 気象研究所 MRI/JMA 科学技術庁 研究開発局 Research and Development Bureau, STA

Ⅳ. 研究検討委員会

Research Steering Committee

委　員　名 Membership		所　　属 Affiliation
委員長 Chairman:	浅井　冨雄 Prof. Tomio Asai	千葉大学環境リモートセンシング研究センター教授 Center for Environmental Remote Sensing, University of Chiba
委員 Member:	大畑　哲夫 Dr. Tetsuo Oh'hata	滋賀県立大学環境科学部助教授 School of Environmental Science, University of Shiga Prefecture
	加藤　内蔵進 Dr. Kuranoshin Kato	名古屋大学大気水圏科学研究所助手 Institute for Hydrospheric-Atmospheric Sciences, Nagoya University
	久保田　雅久 Prof. Masahisa Kubota	東海大学海洋学部教授 School of Marine Science and Technology, Tokai University
	住　　明正 Prof. Akimasa Sumi	東京大学気候システム研究センター長 Center for Climate System Research, University of Tokyo
	辰野　忠夫 Mr. Tadao Tatsuno	海上保安庁水路部海洋情報課長 HD/MSA
	露木　　義 Mr. Tadashi Tsuyuki	気象庁予報部数値予報課予報官 FD/JMA
	西田　英男 Mr. Hideo Nishida	海上保安庁水路部企画課沿岸調査課長 HD/MSA
	新田　　勍 Prof. Tsuyoshi Nitta	東京大学気候システム研究センター教授 Center for Climate System Research, University of Tokyo

委　員　名 Membership	所　　属 Affiliation
萩野谷　成徳 Dr. Shigenori Haginoya	気象庁気象研究所物理気象研究部主任研究官 MRI/JMA
増田　悦久 Dr. Yoshihisa Masuda	郵政省通信総合研究所 沖縄電波観測所長 Communications Research Laboratory, Ministry of Posts and Telecommunications
三河　哲也 Mr. Tetsuya Mikawa	気象庁海洋気象部海洋課エルニーニョ監視センター調査官 MD/JMA
水野　恵介 Dr. Keisuke Mizuno	水産庁遠洋水産研究所海洋・南大洋部低緯度域海洋研究室長 Far Seas Fisheries Research Laboratory, Fisheries Agency
安成　哲三 Prof. Tetsuzoh Yasunari	筑波大学地球科学系教授 Institute of Geosciences, University of Tsukuba
山形　俊男 Prof. Toshio Yamagata	東京大学大学院理学系研究科教授 Graduate School of Science, University of Tokyo
吉住　禎夫 Dr. Sadao Yoshizumi	気象庁気象研究所台風研究部長 MRI/JMA
丸山　剛司 Mr. Takeshi Maruyama	科学技術庁研究開発局海洋地球課長 Ocean and Earth Division, Research and Development Bureau, STA

研究成果報告

Result of the Study

I. Observation and analysis on the process of the atmosphere-ocean-land interactions
大気・海洋・陸域間相互作用の諸過程に関する解析・観測研究

1. Observation and analysis on the process in the atmosphere
大気における諸過程に関する解析・観測研究

(1) Analysis on the Large scale Convective Activity and Precipitation Systems
大規模積雲対流活動と降水系に関する解析研究

Meteorological Research Institute,
Japan Meteorological Agency
Nobuo Yamazaki, Toshiro Inoue, Minoru Tanaka
Tetsuo Nakazawa, Kiyotoshi Takahashi,
Meteorological Satellite Center
Kiyoshi Sasamoto
気象庁
気象研究所
山崎信雄、井上豊志郎
田中実、高橋清利
中澤哲夫
気象衛星センター
笹本清

(Abstract)

Using 3 hourly mean GMS infrared data, diurnal and semi-diurnal variations over the Asian monsoon region are investigated. The tendency can be seen that diurnal amplitude becomes smaller and the ratio of semi-diurnal amplitude becomes larger in proportion to the distance from the land. This tendency can be seen over both the equatorial Pacific and Indian ocean.

The water budget analysis over the Tibetan Plateau in the northern summer of 1994 was performed. The vertically integrated moisture sink <Q2> shows that over the East Tibet it is smaller than that of the West Tibet. This result is different from the previous study, such as Yanai et al. (1992).

The split window (11 and 12um in combination) on board NOAA-9 was used to see the contrast of convective activity, sea surface temperature (SST) and water vapor amount associated with the 1987 and 1988 Indian summer monsoons. Convective activity estimated by the split window over the southern India was depressed in 1987, especially during July, and was enhanced in 1988. SST over the Arabian Sea was a little colder in 1988 than in 1987. On the other hand, water vapor amount over the Arabian Sea was higher in 1988 than in 1987. The enhancement (suppression) of convection over India corresponded to larger (smaller) water

vapor amount and to cooler (warmer) SST over the Arabian Sea.

The analysis of the precipitation systems using 5-day mean Sea-level pressure and the rainfall data in East Asia for a 30-year period from 1963 to 1992 are conducted. Significant positive correlations between the July rainfall in Kyushu and NINO3 SST (4°N-4°S, 150°W-90°W) are observed during this period. Since most of the rainfall in July are observed during the Baiu season, the Baiu rainfall are heavy in the El Nino years.

1. Objectives

This study aims to reveal the large scale features of the Asian Monsoon by using satellite data and the objective analysis data. The diurnal and intraseasonal variations (ISVs) are known as principle variations in the tropical convective activity and the monsoon activities.

It is well known that the Tibetan Plateau plays an important role in the global general circulation. During the northern summer, the Tibetan Plateau provides a huge heat source in the upper troposphere through the latent heat as well as sensible heat flux from the Tibetan Plateau. It is also reported that the regional difference or east-west contrast of the heating is evident. The purpose of this study is to analyze the water budget over the Tibetan Plateau using the objective analysis dataset of Japan Meteorological Agency (JMA) and the rainfall dataset from China.

Split window data is effective to classify convective clouds and non-precipitating cold cirrus clouds. Convective activity can be assessed more reliably by split window than single infrared data. Split window is also effective in retrieving SST and water vapor amount over the cloud free ocean area. We can study ISV of convective activity in relation to these oceanic parameters.

For the analysis of decadal variations of the precipitation system the objects in this study are to analyze the precipitation systems in the Asian and adjacent monsoon region and to investigate the possible relationship to the ENSO and the interdecadal changes in the climate system.

2. Data and Method

For the analysis of diurnal variations one degree square mesh mean equivalent Black Body Temperature (TBB) data observed 3 hourly by GMS were utilized. Using these TBB data Index of convection (IC) were defined as follows.

$$IC = 255 - TBB(K) \quad \text{for } TBB < 255K,$$
$$IC = 0 \quad \text{otherwise.}$$

Analysis was done for the average IC of summer season (May-Sep) for 1980-94 except for 1984. Amplitude and phase of diurnal variation were obtained by Fourier analysis. First and second components corresponds to diurnal and semi-diurnal ones respectively.

The data used for the analysis of water budget over the Tibetan Plateau are

1) Objective analysis water budget dataset from JMA with every 6 hours and 2.5 degree latitude-longitude grid.
2) Outgoing longwave radiation dataset from NOAA polar orbiting satellite with twice daily and 2.5 degree latitude-longitude grid.
3) Geostationary Meteorological Satellite (GMS) Infrared brightness temperature data with 3 hourly and 1 degree latitude-longitude grid.
4) Global precipitation data from the National Climate Data Center (NCDC) of National Oceanography and Atmosphere Agency (NOAA).
5) Rainfall data from Chinese Meteorological Satellite Center(CMSA).

The period in this study is May to September in 1994. The Tibetan Plateau is divided into two regions, one is located west of 90°E, another is east of it between 30°N and 37.5°N.

The split window (11 and 12um in combination) on board NOAA-9 was used to see the contrast of convective activity, sea surface temperature (SST) and water vapor amount associated with the 1987 and 1988 Indian summer monsoons.

Using the 5-day mean rainfall and sea-level pressure data, the analysis of the precipitation systems was carried out with emphasis on the interannual and interdecadal variations, and its relationship to the ENSO.

3. Results

Fig. 1 shows the distribution of number of peaks in one day time series. Fig. 2 shows the distribution of ratio of diurnal amplitude to semi-diurnal one. In both figures contours show the distribution of a diurnal amplitude.

Apparently from both figures over the land and the ocean adjacent to the land diurnal component is predominant.

On the other hand, over the ocean far from the land like the central pacific and Indian ocean existence of semi-diurnal component becomes clear.

Especially over the bay of Bengal and the South China Sea diurnal component prevails. This suggests strong influences over these areas from the surrounding land areas.

The seasonal change of the daily averaged GMS infrared (IR) data in 1994 is shown in Fig. 3. During July and August the temperature of GMS IR is the same in both the East (open circle) and West (black dot) Tibet. In June and early September it is lower in the East Tibet. Comparing the GMS IR data in 1994 with the climatological data (1980-1994), it is suggested that the year of 1994 is a weak monsoon year.

The vertically integrated apparent moisture sink <Q2> is the sum of the temporal change of the precipitable water and the divergent component of the vertically integrated moisture flux. We calculated the apparent moisture sink Q2 (Yanai et al. (1992)), using the objective analysis water budget dataset which consists of the precipitable water, vertically

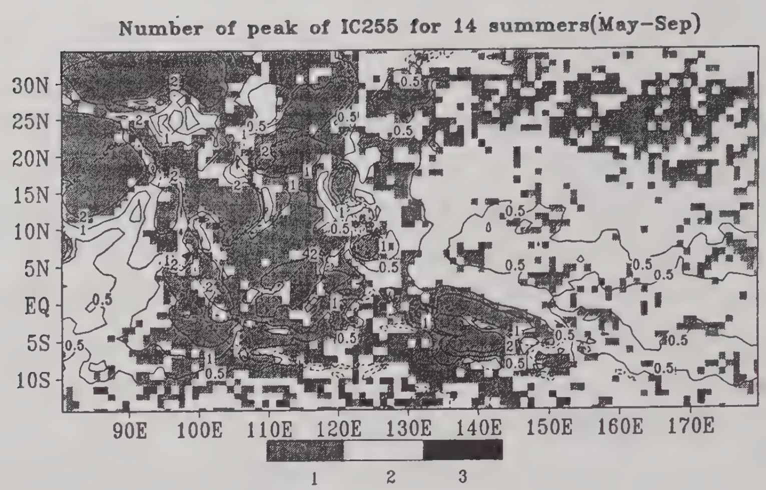


Fig. 1 The distribution of number of peaks within one day time series.
Contours shows the amplitude distribution of diurnal component.

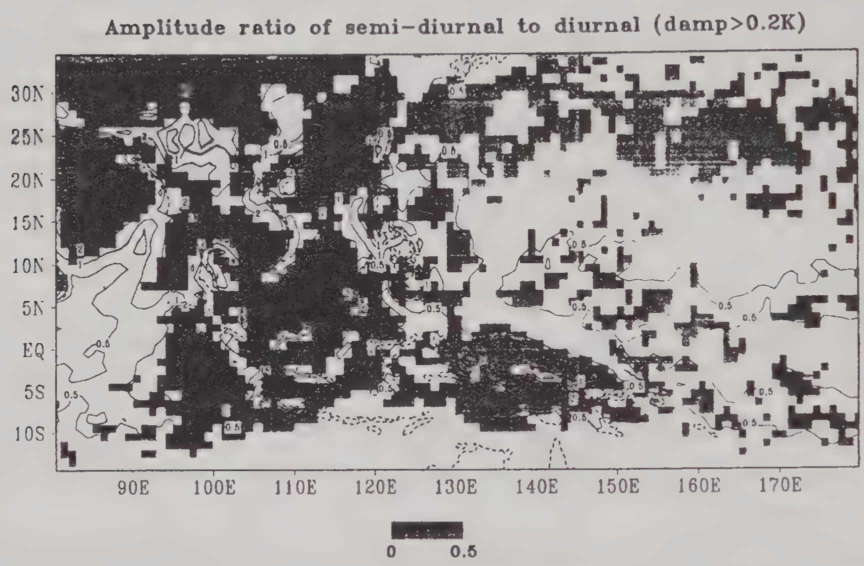


Fig. 2 The distribution of ratio of diurnal amplitude to semi-diurnal one.
Contours shows the amplitude distribution of diurnal component.

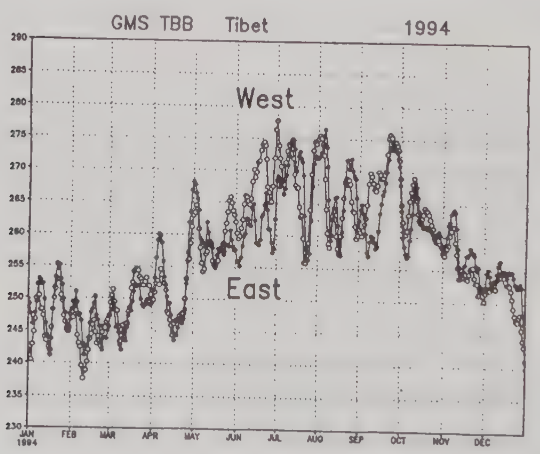


Fig. 3 The seasonal change of the daily averaged GMS IR data in 1994.

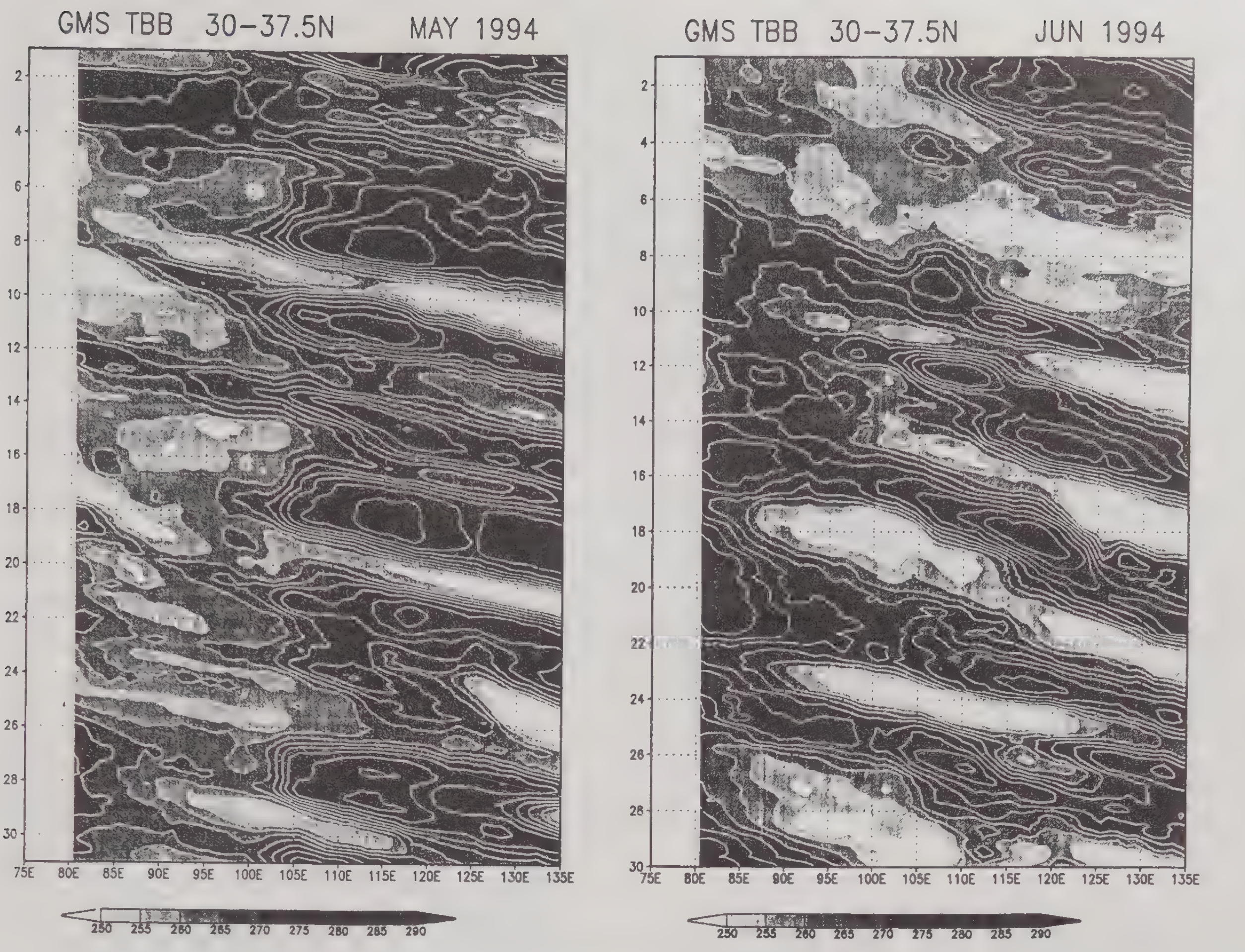


Fig. 4 The time-longitude section of the GMS IR averaged between 30° -37.5° N in June 1994.

integrated zonal / meridional moisture flux, 6 hourly accumulated rainfall (both convective and stratus) and evaporation.

The monthly mean of <Q2> in 1994 over the Tibetan Plateau is summarized in Table 1. The bracket is from the Yanai et al.(1992) 's paper.

<Q2> (Wm-2)	June	July	August
East Tibet	65 (16)	30 (48)	36 (35)
West Tibet	34 (-1)	84 (10)	76 (22)

Table 1 Monthly mean of the vertically integrated apparent moisture sink Q2

The apparent moisture sink is large in June over the East Tibet and in July and August over the West Tibet. The same tendency is found in the precipitable water, but the GMS IR dataset shows the temperature is the same in July and August in both Tibet regions. The geographical dependency or the diurnal component of the GMS IR may affect this.

We also examined the moving characteristics of the active convection over the Tibetan Plateau. It is found that there is a time lag of several days in the GMS IR time series over the both East and West Tibet. The change in the West Tibet is leading, telling that the disturbance moves eastward. Fig. 4 shows the time-longitude section of the GMS IR averaged

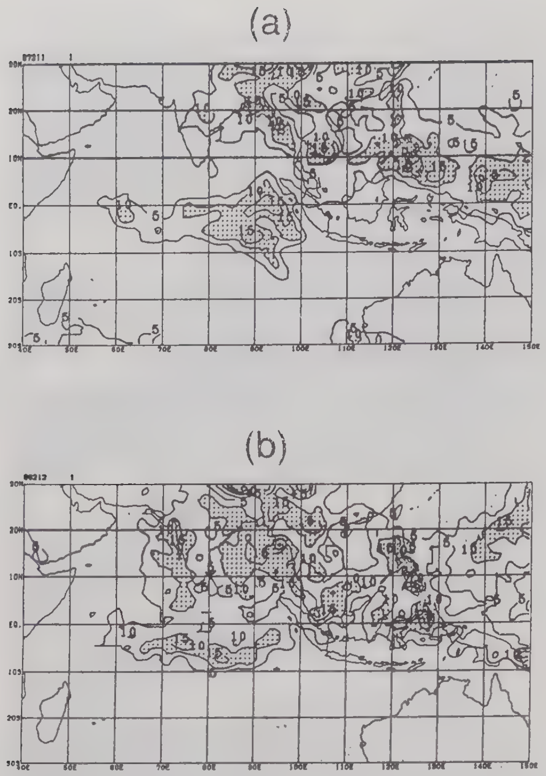


Fig. 5 The monthly mean distribution of cumulonimbus cloud in July of 1987 (a) and 1988(b).

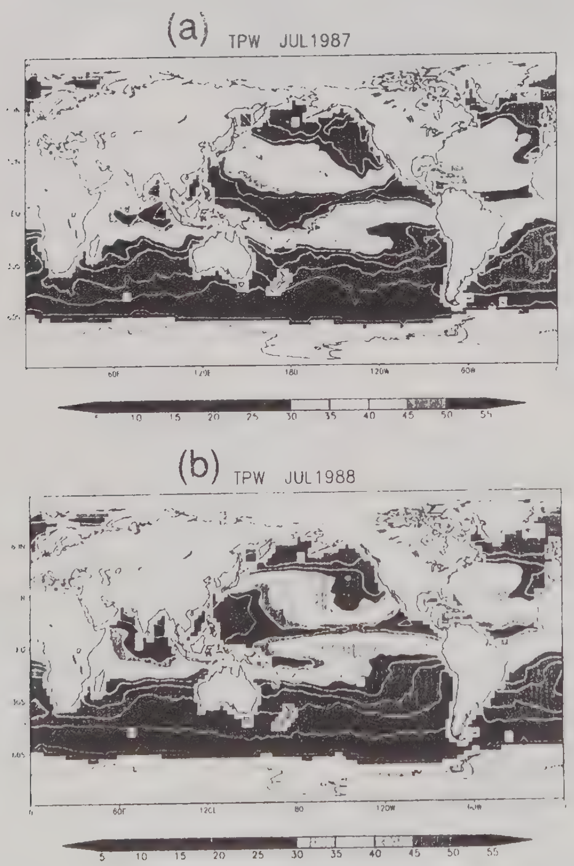


Fig. 6 The monthly mean total precipitable water vapor (TPW) estimated from SSM/I in July of 1987 (a) and 1988(b).

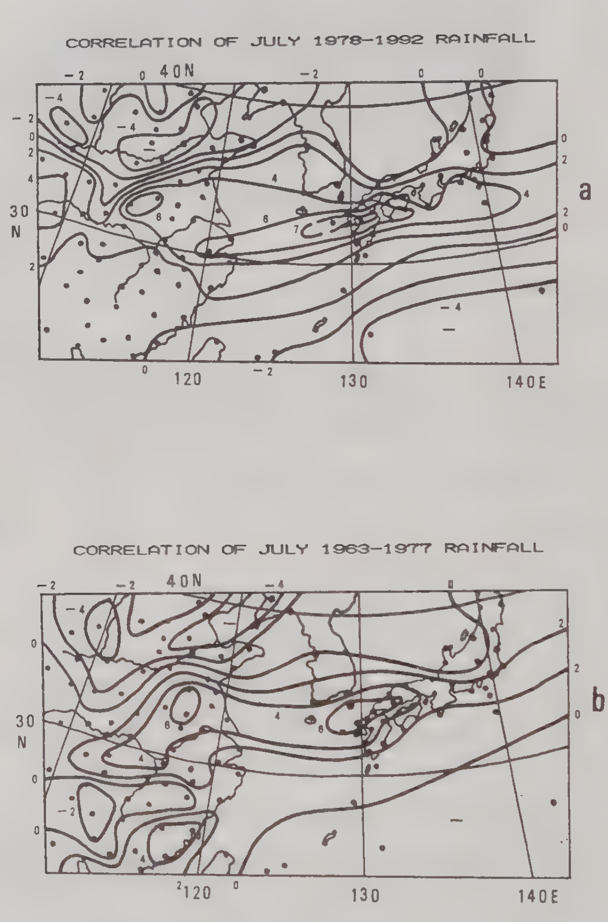


Fig. 7 Lag-correlations between the July rainfall in East Asia and NINO3 SST (4°N-4°S,150°W-90°W)

a) Rainfall for 1978-1992 and September NINO3 SST

b) Rainfall for 1963-1977 and May NINO3 SST

between 30° -37.5° N in June 1994. This figure clearly demonstrates the progression of the eastward-moving disturbance, which originates over the western Tibet and further develops over the East China, and forms the Mei-yu or Baiu front.

Figs. 5-a,b show the monthly mean distribution of cumulonimbus cloud in July of 1987 and 1988. Larger cloud amounts are seen along the west coast of Indian in 1988, while less cloud amounts are seen over south India in 1987. The difference of cloud cover distribution in 1987 and 1988 shows general agreement with the seasonal GPI rainfall difference between 1987 and 1988 (Janowiak and Arkin,1991). The winds of the operational global analysis (GANAL) by JMA show big difference of low level monsoon westerly. The wind at 850 hPa over east of Somalia was about 18 m/s in 1987 and was about 27 m/s in 1988. In the last annual reports of JEXAM, we reported the big difference of water vapor amount over the Arabian Sea between 1987 and 1988, although SST was a little colder in 1988. The larger amount of water vapor over the Arabian Sea corresponds to enhanced convective activity over the south India. Figs. 6-a,b show the monthly mean total precipitable water vapor (TPW) estimated from SSM/I. The TPW over the Arabian Sea is about 45 mm in 1987 and is about 55 mm. This results are consistent with the split window measurements. Further, we can see about 20% increase of water vapor amount in comparison between east of Somalia and Arabian Sea. This suggests the importance of Arabian Sea in terms of moisture supply for the Indian summer monsoon.

The analysis of the precipitation systems using the 5-day mean Rainfall data from 1963 to 1992 showed that the Baiu rainfall in July shows significant positive correlations to the NINO3 SST (4° N-4° S,150° W-90° W)during this period as shown in Fig. 7.

4. Discussions

As it is seen around the New Guinea island in Fig.1, the tendency can be seen that diurnal amplitude becomes smaller and the ratio of semi-diurnal amplitude becomes larger in proportion to the distance from the land. This tendency can be seen over both the equatorial Pacific and Indian ocean. It can be said that this is one of general features concerning the geographical distribution of diurnal and semi-diurnal variation.

But more investigation is necessary to reveal the cause of diurnal and semi-diurnal variation of convective activity including statistical point of view.

The water budget analysis over the Tibetan Plateau in the northern summer of 1994 was performed. The year of 1994 is the weak monsoon year over the Tibet.

The vertically integrated moisture sink <Q2> shows that over the East Tibet it is smaller than that of the West Tibet. This result is different from the previous study, such as Yanai et al. (1992).It is necessary to extend the analysis period to confirm this result.

The eastward-moving active convection was demonstrated. It is noticed that this disturbance corresponds with the activity of the Mei-yu or Baiu front.

6. Publications

(Reports)

T. Inoue: Contrast of 87/88 Indian summer monsoon observed by split window measurements. Advances in Space Research , Accepted for publication

(Oral presentation)

M. Tanaka: Interannual variations of the summer monsoon over Asia and western Pacific. --Its relationship to Baiu and the El Ninos. 1996 Spring meeting of MSJ, May 1996

K.Takahashi and M. Murakami: Analysis of the influence of the intraseasonal variation on the diurnal variation using the geosynchronous satellite data --Part 4. 1996 Spring meeting of MSJ, May 1996

T. Inoue: Contrast of 87/88 Indian summer monsoon observed by split window measurements. 31st COSPAR Scientific Assembly, July 1996.

T. Nakazawa: Water vapor analysis over the Tibetan Plateau during the northern summer in 1994. 1996 Autumn meeting of MSJ, October 1996.

T. Nakazawa, Chen Longxun and T. Iwasaki: Water vapor analysis over the Tibetan Plateau during the northern summer in 1994. International Workshop on Climate System of Monsoon Asia, December 1996.

K. Takahashi: Analysis of diurnal convective activities over Asian monsoon region using infrared data observed by geostationary satellites. International Workshop on Climate System of Monsoon Asia, December 1996.

7. International Cooperation

The cooperation with China has been carried out based on the agreement signed in 1993 between Japan Science and Technology Agency and China Meteorological Administration. During FY 1995, three Chinese experts were invited to M.R.I. and performed the joint study on the interannual aspects and air-sea interaction of Asian monsoon by using the GMS satellite data. From Japanese side, one research official visited China during FY 1996 and performed the joint study on the analysis of monsoon related rainfall activity.

要旨

ＧＭＳ衛星資料による１度格子平均赤外データを用いてアジアモンスーン域における日変化と半日周期変動の解析を行い、日変化の振幅は陸域から離れるにつれて小さくなり、日変化の振幅に対する半日周期変動の振幅は逆に大きくなる傾向があることを見出した。この傾向は赤道太平洋でもインド洋でも共に見られた。

１９９４年夏季のチベット付近の水収支解析を行い、鉛直に積分された水蒸気のシンクQ2は以前の解析とは異なり、西チベット域より東チベット域で小さいことが分かった。

スプリットウィンドウのデータを用いて、１９８７年と１９８８年のアラビア海における海面水温と水蒸気量、インド付近の対流活動を調べ、南インドにおける１９８８（１９８７）年の活発な（不活発）対流活動はアラビア海における海面水温の負（正）偏差と、より大きな（小さな）水蒸気量に対応している事が分かった。

１９６３年から１９９２年の３０年間の東アジアの５日平均の海面気圧と降水量データを用いて東アジアにおける降水系の変動を調べ､九州の７月の降水量と赤道東太平洋のＮＩＮＯ３（北緯４度ー南緯４度、西経１５０度ー西経９０度）の海面水温の間に統計的に有意な正の相関が見出された。７月の九州の降水は多くは梅雨時にある事から、梅雨の降水量はエルニーニョ時に多くなることが分かった。

I. Observation and analysis on the process of the atmosphere-ocean-land interactions
大気・海洋・陸域間相互作用の諸過程に関する観測・解析研究

1. Observation and analysis on the process in the atmosphere
大気における諸過程に関する観測・解析研究

(2) Observation of structure of convective clouds in large-scale cloud systems
大規模雲域内における対流雲構造に関する観測研究

Meteorological Research Institute,
Japan Meteorological Agency
気象庁気象研究所
H.Sakakibara, H.Okamura, K.Mori,
Y.Shimazu, Y.Tanaka, K.Bessho
榊原均、岡村博文、森一正、
島津好男、田中恵信、別所康太郎

(Abstract)

In order to reveal the structure of convective clouds in cloud clusters, convective clouds in typhoons and cloud clusters associated with the Baiu front which is a stationary front extending from China to Japan in early summer months were observed by using X-band Doppler radars and omega-sondes in the island of Miyako (24.8N,125.4E) from 1990 to 1992.

In this report, large-scale environment of cloud clusters in the Baiu front in 1992 is outlined. Period mean eqivalent black-body temperature (TBB) distribution and large-scale circulation during the Baiu season are examined. A cloud zone from southern China to Japan lay along the Okinawa area from west-southwest to east-northeast. Corresponding to this cloud zone, southwesterly flow from Southeast Asia and southerly or southeasterly flow from the subtropical anticyclonic circulation over the northwestern Pacific were confluent around the Okinawa area. The Baiu cloud zone roughly corresponded to low-level (850hPa) positive vorticity area and sharp latitudinal gradient zone of equivalent potential temperature. Depending on the latitude of the Baiu cloud zone, the Baiu period is divide into five periods. Period 3 (6-13 June) and Period 4 (14-20 June) were active rainy periods in the Okinawa area. Low-level warm and moist southwesterly confluent flow was remarkable around the cloud zone over the Okinawa area in Period 3 and Period 4. Over the Okinawa area, deep southwesterly flow prevailed almost through the troposphere to the east of upper level trough in Period 3, especially in the first half, while southwesterly flow only appeared in the middle and lower troposphere and northerly prevailed in the upper troposphere in Period 4. Twelve cases of mesoscale precipitation systems (MPSs) were observed by Doppler radars. In case 9, three MPSs containing an active convective band or bands in their central part successively passed over the island of Miyako. Dual Doppler analysis of

the first MPS indicates that intense low-level convergence by southwesterly flow in front and northwesterly flow in rear maintained the active convective band.

In order to compare the large-scale environment of the cloud clusters in the Baiu front with that in 1992, the data obtained in the Torrential Rain Experiment (TREX) in Kyushu in 1996 was analyzed. Latitude-time cross sections of TBB, low-level θe and middle-level θes indicate that cloud areas moved north and south reflecting the motion of the Baiu front. The subtropical ridge south of Kyushu was not strong from 15 June to 23 June (Period A), and the location of the front largely changed with the passage of lows. From 24 June to 29 June (Period B) the front shifted northward because of intensification of the subtropical ridge. From 30 June to 7 July (Period C) the subtropical ridge weakened and the front shifted southward. After 8 July (Period D) the subtropical ridge diminished and the front disappeared.

1. Objectives

Cloud clusters which form and develop over the warm sea transport upward heat and water vapor added through the sea surface. Water vapor condenses during the upward transportation. Some fraction of condensed water falls and reaches the sea surface as rain. Latent heat released by condensation of water vapor to form raindrops remains in the atmosphere and heats the air in the cloud cluster. This heating is not only the energy source of the cloud cluster but one of the energy sources of monsoon.

In this study we aimed to reveal the structure of convective clouds in cloud clusters and the interaction between convective clouds and cloud clusters and to discuss the processes of precipitation and vertical transport of heat and water substances.

In this report, outline of the Baiu season in the Okinawa area in 1992 is described and some observed MPSs are examined. Characteristics of the evolution of the Baiu front in the Okinawa area and the MPSs are briefly discussed. Furthermore, the Baiu front in the Kyushu area in 1996 is also outlined to compare with the above one.

2. Methods

Convective clouds in cloud clusters associated with the Baiu front which is a stationary front extending from China to Japan in early summer months were observed by using X-band Doppler radars of Meteorological Research Institute and National Research Institute for Earth Science and Disaster Prevention and omega-sondes in the island of Miyako (24.8N, 125.4E) in 1992.

Large-scale environment of cloud clusters in the Baiu-frontal zone were analyzed by using routinely obtained data of Geostationary Meteorological Satellite (GMS) and conventional radar and global objective analysis data (GANAL) made every twelve hours by the Numerical Prediction Division, Japan Meteorological Agency.

In order to compare the large-scale environment of cloud clusters in the Baiu front in 1992, we also made preliminary analysis of the large-scale situations in the Baiu season in 1996 when Torrential Rain Experiment (TREX) was performed in the Kyushu area by several universities and research institutes.

3. Results

(1) Large-scale environment of the cloud clusters in the Baiu front in 1992

The Baiu season, which is a rainy season in early summer, in the Okinawa area in 1992 started on 8 May and ended on 25 June, so its duration was 49 days. Doppler radar observation in the island of Miyako was conducted during 23 May to 18 June. During the Baiu season, precipitation over several tens mm/day were frequently observed in the islands of Okinawa, Miyako and Ishigaki. These heavy rains were centered on 22 May, 10 June and 18 June. Especially on 10 June, heavy rains of about 200mm/day were observed in the islands of Miyako and Ishigaki. Total rainfall amount in the island of Miyako during the Baiu season was 519mm which was slightly larger than the climate mean of 410mm.

Period mean equivalent black body temperature (TBB) distribution and large-scale circulation during the Baiu season (not shown) are examined. A cloud zone originating from southern China lay along the Okinawa area from west-southwest to east-northeast. Corresponding to this cloud zone, southwesterly flow from Southeast Asia and southerly or southeasterly flow from the subtropical anticyclonic circulation over the northwestern Pacific were confluent around the Okinawa area.

Variation of the Baiu cloud zone is investigated using latitude-time cross sections of TBB and GANAL data (Fig.1). The Baiu cloud zone roughly corresponded to low-level (850hPa) positive vorticity area and sharp latitudinal gradient zone of equivalent potential temperature (θe). Depending on the latitude of the Baiu cloud zone, the Baiu period is divide into following five periods. Period 1(P1); 8-17 May; the Baiu season in the Okinawa area started corresponding to a passage of cold front on 8 May. After that, the Baiu cloud zone or front stayed mainly 30-35N and precipitation in the Okinawa area was caused at the southern tip of the middle-latitude disturbances. Period 2(P2); 18 May-5 June; During this period, cold air mass intruded over the Okinawa area in the middle and upper troposphere. The Baiu cloud zone moved southward after a passage of cold front on 18 May and stayed along 20N. Active convective regions were organized in the southern part of the cloud zone around 24, 28 and 31 May. The Baiu cloud zone abruptly returned to 30-33N on 5 June after a passage of an eastward moving anticyclone. Period 3(P3); 6-13 June; The Baiu cloud zone shifted to the south as an cold front passed on 7 June. After that, the cloud zone developed around 25N, though the Baiu frontal zone was sustained mainly to the north of 30N. The heaviest precipitation during the Baiu season at the island of Miyako occurred on 10 June. Period 4(P4); 14-20 June; The Baiu front moved southward gradually accompanying the cloud zone. The cloud zone was formed along the Baiu front. Period 5(P5); 21 -25 June; The Baiu cloud zone moved to the north up to 30N corresponding to an intensification of subtropical anticyclone over the northwestern Pacific. The Baiu season in the Okinawa area ended on 25 June. In summary, P3 and P4 were active rainy periods in the Okinawa area.

The mean TBB distribution in each period is shown in Fig.2. Main part of the west-southwest to east-northeast oriented Baiu cloud zone stayed to the north of 30N in P1, sifted to the south of 20N in P2, and lay along the Okinawa area in P3, while the Baiu front remained north of 30N. The cloud zone shifted to the south with the Baiu front and lay over the Okinawa area in P4, and migrated northward to 30-35N in P5. Low-level warm and moist southwesterly confluent flow was remarkable around the cloud zone over the Okinawa area in P3 and P4 (not shown). Over the Okinawa area, deep southwesterly flow prevailed almost through the troposphere to the east of upper level trough in P3, especially in the first half, while southwesterly flow only appeared in the middle and lower troposphere

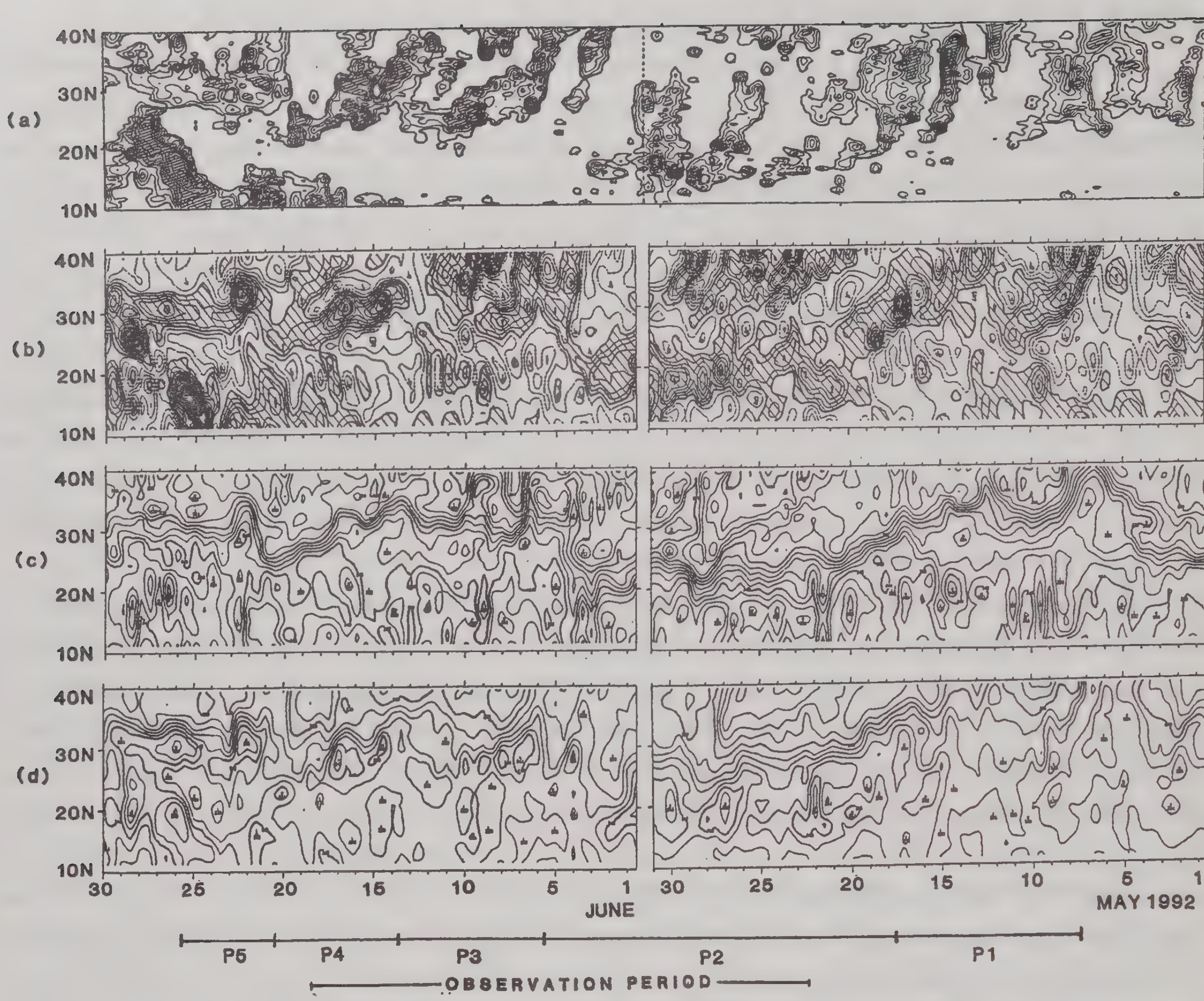


Fig.1 Latitude–time cross section along 125E of (a)TBB, (b)vorticity at 850hPa, (c) θe at 850 hPa and θe at 500hPa. TBB lower than 0℃ is contoured every 10℃. TBB lower than −30℃ is shaded in (a). Positive vorticity is shaded in(b). Five periods of the Baiu season, P1 to P5, are determined depending on the latitude of the Baiu cloud zone.

and northerly prevailed in the upper troposphere in P4.

Twelve cases of MPSs were observed by Doppler radars in P2, P3 and P4. Structures of these MPSs were variable depending on the environmental conditions such as large scale circulation or stability. Here, an example of the case 9 which caused the heaviest precipitation at the island of Miyako on 10 June (P3) is shown in Fig.3. In this case, three MPSs containing an active convective band or bands in their central part successively passed over the island of Miyako. The first MPS is presented in Fig.3. Dual Doppler analysis indicates that intense low level convergence by southwesterly flow in front and northwesterly flow in rear maintained the active convective band.

(2) Large–scale environment of cloud clusters during TREX

Observations of TREX were carried out from 15 June to 10 July 1996 in southern Kyushu (Fig.4). Three Doppler radars were placed in the islands of Tane and Yaku south of Kyushu. Special upper–air

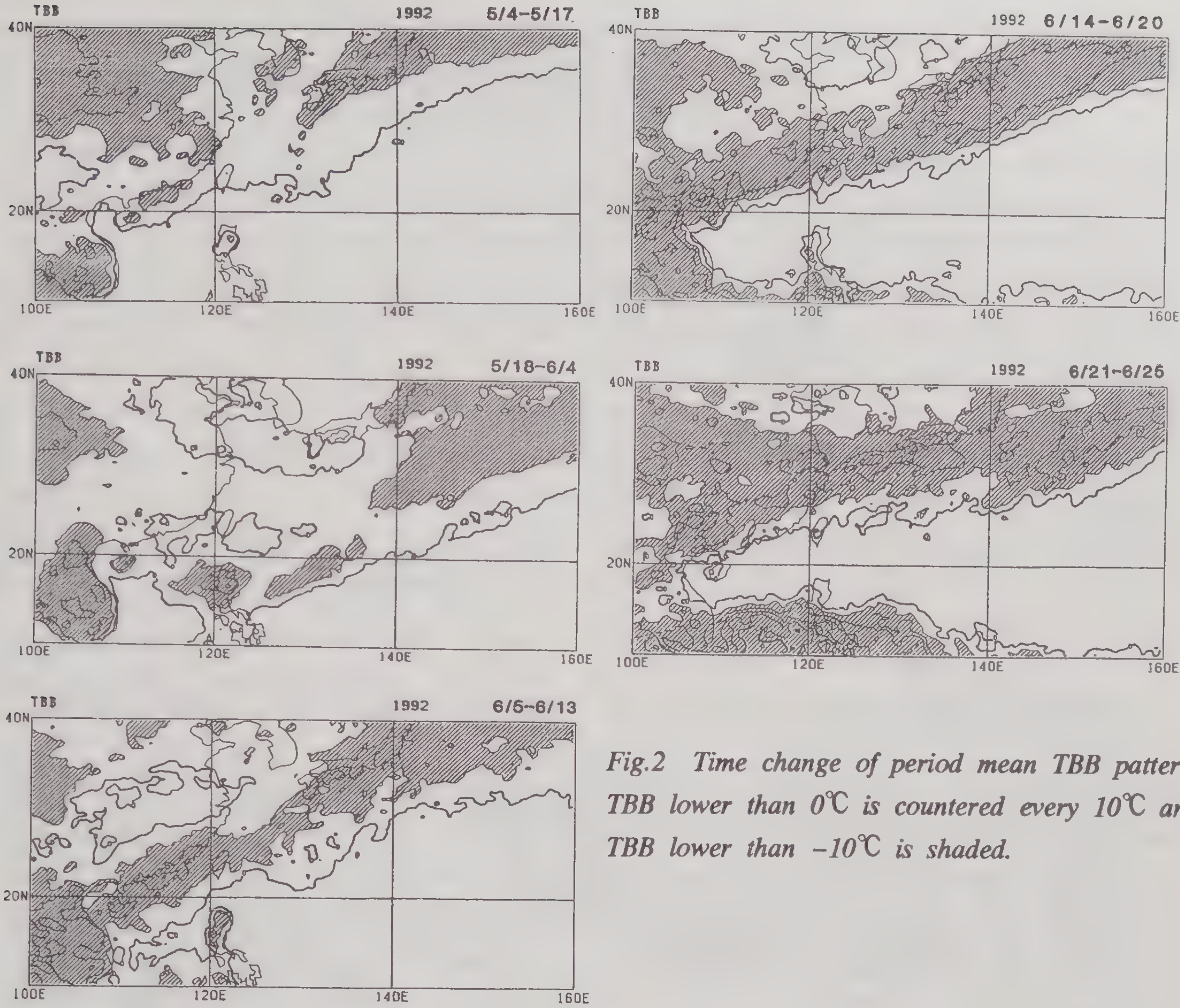
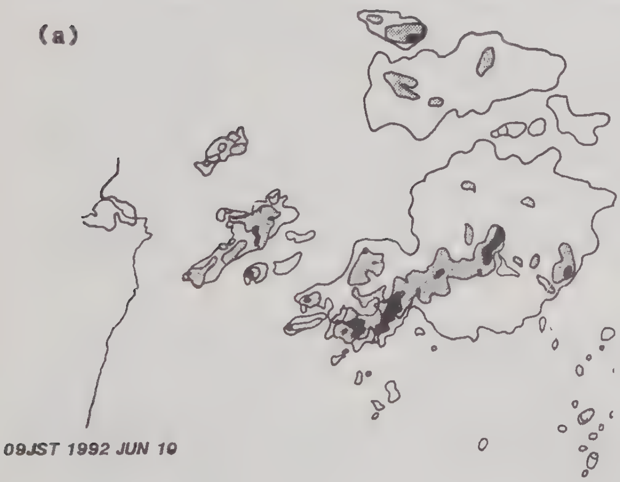


Fig.2 Time change of period mean TBB pattern. TBB lower than 0℃ is countered every 10℃ and TBB lower than −10℃ is shaded.



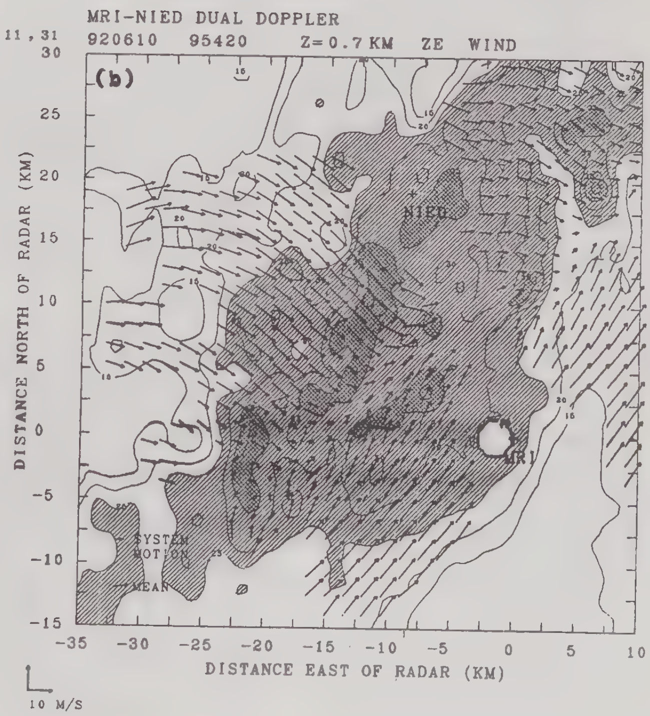


Fig.3 PPI echo pattern of MPS in case 9 at 09 JST (a) and low level(0.7km) echo and flow pattern of the convective band in the MPS at 0954JST on 10 June 1992(b).

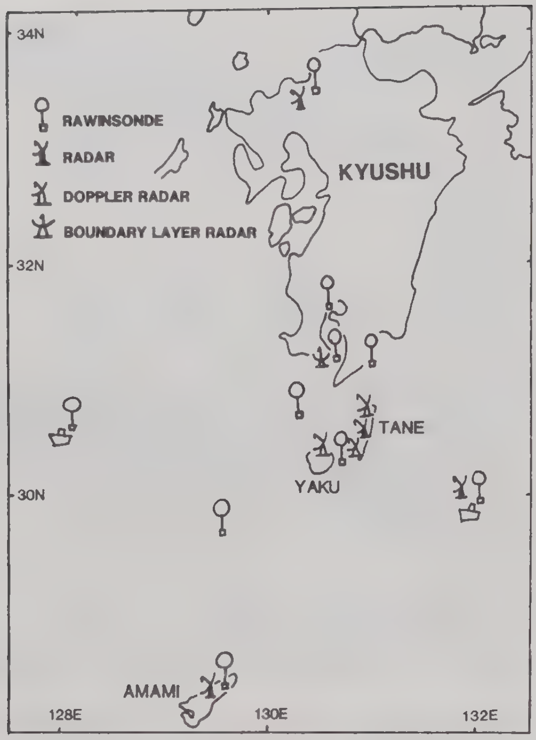
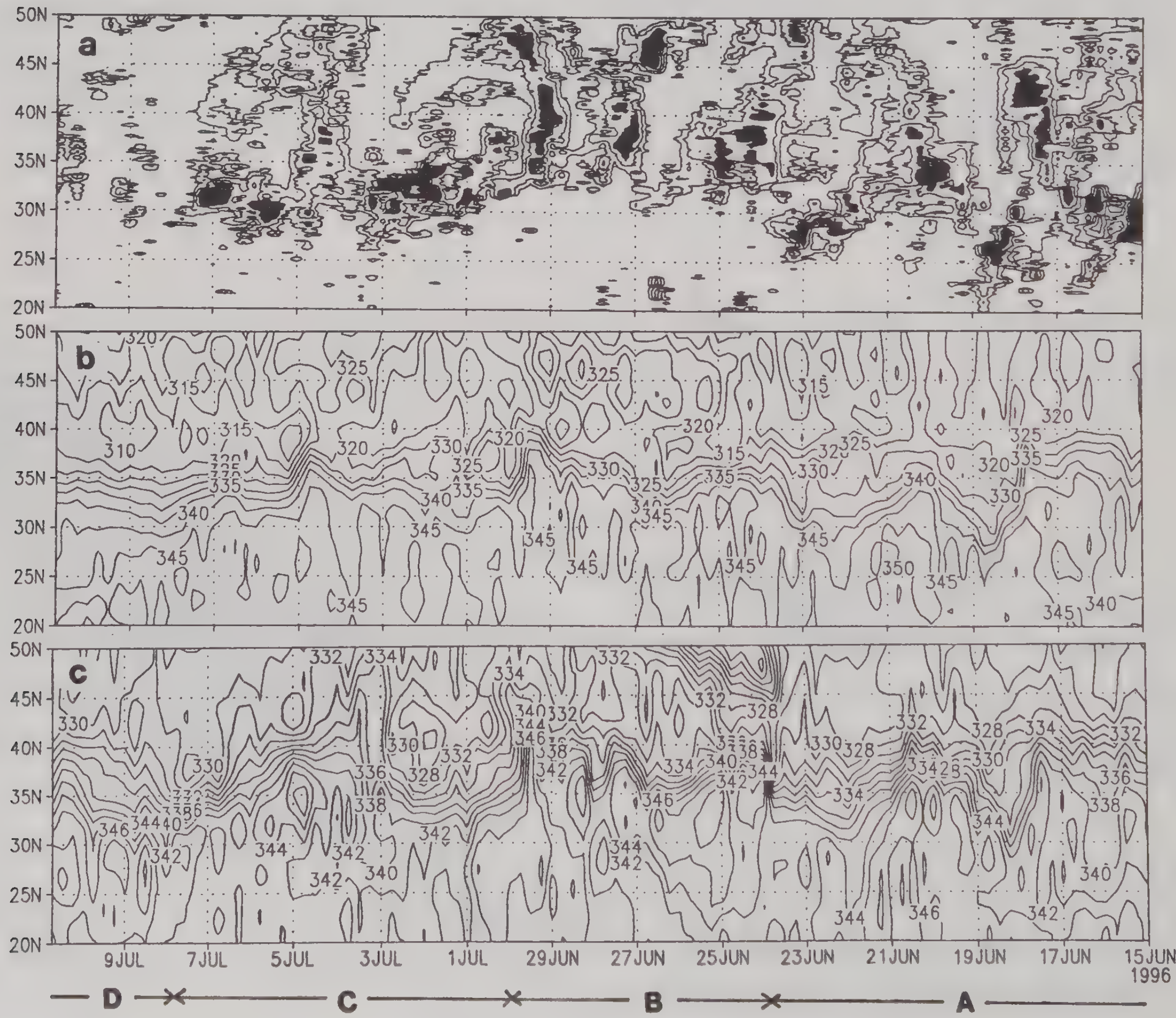


Fig.4 Observation network of TREX.

Fig.5 Latitude–time cross section along 130E of (a)TBB, (b)θe at 925hPa and (c) θes at 500hPa. TBB lower than 0℃ was contoured every 20℃. TBB lower than −60℃ was shaded in (a).



soundings were made at five stations by universities and research institutes. Upper-air soundings were also made at two research vessels of JMA to the southwest and southeast of Kyushu. Enhanced upper-air soundings were made at three routine stations around Kyushu.

Large-scale environment of cloud clusters during TREX is examined using latitude-time cross sections along 130E of TBB, θe at 925 hPa and θes at 500 hPa (Fig.5). Low TBB areas below -60C are found near extratropical cyclones to the north of Kyushu and along the Baiu front. The location of the Baiu front is seen as sharp latitudinal gradient in the cross section of θe at 925 hPa. Depending on the latitude of the Baiu cloud zone, the observation period is divided into four periods. Period A; 15-23 June; The subtropical ridge south of Kyushu was not strong and the location of the front largely changed with the passage of lows. Active convection occurred in both two cold-frontal cases and two warm-frontal cases. Period B; 24-29 June; The Baiu front shifted northward because of intensification of the subtropical ridge and convection along the Baiu front was not active. Period C; 30 June-7 July; The subtropical ridge weakened and the front shifted southward. Period D; 8-10 July; The subtropical ridge weakened and the front disappeared.

4. Discussions

Recently, seasonal cycle of summer monsoon in east Asia was investigated using GMS data (Tanaka,1992). He pointed out rapidly southward movement of a cloud band from 30N to 20-25N during the middle of May, which coincides with the onset of the Baiu season in Okinawa. He also showed subsequent sudden northward advance of this cloud band from 20-25N to Japan main land during 5-9 June. In 1992, sudden southward shift of the cloud zone on 18 May and subsequent northward shift of the cloud band on 5 June were well corresponded with these climatic seasonal cycle. Hirasawa(1995) also investigated on the abrupt southward shift of cloud zone in the middle of May and showed that after the abrupt change, convective activity north of South China Sea is intensified in association with intensification of low-level southwesterly flow. MPSs in P2 may be examples of MPSs in the activated cloud zone.

The internal structure of MPS in case 9 , in which an intense convective band was embedded in its central part (Fig.3), was maintained at least for two hours. In this case another two MPSs with similar structure containing intense convective band or bands in their central parts formed successively around the island of Miyako. The case 9 was in P3 when southwesterly monsoon flow was intensified through the troposphere and occurred on 10 June just before upper level trough passed over the Okinawa area.

Characteristics of the MPSs in the observed twelve cases including the case 9 will be summarized and related with environmental conditions such as stability or large-scale circulation.

Large-scale environment of the cloud clusters during the TREX period is somewhat different from that of the cloud clusters in Okinawa in 1992. The cloud clusters during TREX occurred near the Baiu front, while some of those in Okinawa in 1992 occurred far south of the Baiu front. In addition, abrupt shift of the Baiu front like that on 5 June 1992 was not observed during the TREX period, although the front shifted north and south with the passage of lows.

Analysis of structure of cloud clusters during the TREX period is necessary to compare the structure with that found in the cloud clusters in the Okinawa area.

5. References

Hirasawa, N., 1995: Abrupt change in the characteristics of the cloud zone in subtropical East Asia around the middle of May. J.Meteor. Soc. Japan, 73, 221–239.

Tanaka, M., 1992: Intraseasonal oscillation and the onset and retreat dates of the summer monsoon over East, Southeast Asia and the western Pacific region using GMS high cloud amount data. J. Meteor. Soc. Japan, 70, 613–629.

6. Publications

(oral)

Sakakibara,H., M.Yoshizaki and MRI TREX group, Activity of the Baiu front around Kyushu during TREX. Meteorological Society of Japan. Preprints of the presentation, 70, pp117, 1995.

Mori,K., Y.Shimazu, Y.Tanaka, K.Bessho, H.Sakakibara, K.Akaeda and MRI TREX group, Doppler radar observation of the Baiu front in the island of Yaku in 1996. Meteorological Society of Japan. Preprints of the presentation, 70, pp118, 1995.

（要旨）

熱、水の輸送過程に関連する対流雲の構造と対流雲と大規模雲域の相互作用を調べる目的で、１９９０年から９２年まで宮古島（北緯２５度、東経１２５度）でドップラーレーダーとオメガゾンデによる大規模雲域（台風と梅雨期クラウドクラスター）内の対流雲の３次元構造の観測を行った。

今年度は１９９２年の梅雨前線に伴い発生するクラウドクラスターについてその発生環境を調べた。期間平均のTBBと大規模循環から、中国南部から沖縄地方、さらに本州にかけて雲の帯が存在し、これに対応して東南アジアからの南西流と亜熱帯高気圧循環の一部である南または南東の流れが沖縄付近で合流している。梅雨前線の雲帯はおおよそ下層の正渦度域と相当温位の南北方向の傾度が大きいところに対応する。梅雨前線帯の緯度をもとに梅雨期間を５つに分けた。第３期（６月６－１３日）と第４期（６月１４－２０日）は沖縄地方でよく雨が降った。この両期間、沖縄地方の雲帯付近では下層の暖かく湿った合流する南西流が顕著である。沖縄地方では第３期（特に前半）には上層のトラフの東で深い南西流が卓越していた。一方第４期では南西流は中、下層だけに見られ、上層では北風が卓越していた。１２ケースの中規模降水システムがドップラーレーダーで観測された。９番目のケースでは活発な帯状対流を含む３個の中規模降水システムが宮古島上空を次々と通過した。２台のドップラーレーダーデータの解析によると最初の降水システムでは前方の南西流と後方の北西流による下層の強い収束が活発な帯状対流を維持していた。

また、１９９２年の沖縄の梅雨と比較するために、九州の梅雨についての豪雨特別観測（ＴＲＥＸ）データを用いて梅雨期の雲域の発生環境を調べた。時間緯度断面では雲域は前線の南北変動に対応して変位していた。その中に積乱雲域が中層への北からの寒気の流入に伴って発生していた。６月１５－２３日（期間Ａ）には九州の南の亜熱帯高圧帯は強くなく、前線の位置は低気圧の通過に伴い大きく変化した。６月２４－２９日（期間Ｂ）には亜熱帯高圧帯の強化に伴い前線は北上した。６月３０－７月７日（期間Ｃ）には亜熱帯高圧帯が弱くなり前線は南下した。７月８日以降（期間Ｄ）は亜熱帯高圧帯は縮小し、前線も消えた。

I. Observation and analysis on the process of the atmosphere-ocean-land interactions
1. Observation and analysis on the process in the atmosphere
(3) Analysis on the evolution of convective cloud systems

Advanced Measurement and Analysis Technology Division
National Research Institute for Earth Science and Disaster Prevention (NIED)
Science and Technology Agency
S. Nakai

Abstract

Baiu frontal zone over the East China sea and the northwestern Pacific is one of the regions that generate many convective cloud systems. They play an important role on the water cycle of Baiu front. The activity of Baiu front is closely related to the global Monsoon circulation. So, it is important to clarify the water cycle of the Baiu frontal zone focusing on the evolution of convective cloud systems. In FY1996, the attenuation correction method, developed in the previous financial year (attenuation rate K_2 of Nakai(1996)), was improved introducing convective/stratiform area definition. The echo area was divided into 'convective' and 'stratiform' area defined respectively by $|\nabla_{PPI} I|>2$ dB km^{-1} and $|\nabla_{PPI} I|\leqq 2$ dB km^{-1}, where $|\nabla_{PPI} I|$ was the magnitude of gradient of Ze(equivalent radar reflectivity factor) in decibel unit on PPI planes. The attenuation rate was decided for each of them as $K=a_c\ Ze^b$ (dB km^{-1}) and $K=a_s\ Ze^b$ (dB km^{-1}). b was fixed to K-MP value, 0.755. $a_c=2.3\times10^{-4}$ and $a_s=1.3\times10^{-4}$ were considered as the best values, which gave the minimum RMS of the Ze difference on a horizontal section. The effect of the attenuation correction was examined by three-dimensional display of Ze field and comparison with SSM/I rain rate. The attenuation correction improved the appearance of Ze field in three-dimensional display, and decreased the difference between radar- and SSM/I- derived rain rate.

1. Objectives

The characteristics of the convective clouds vary from place to place in the world. Baiu frontal zone over the East China sea and the northwestern Pacific is one of the regions that generate many convective clouds. Especially, mesoscale convective systems (MCSs) play an important role on the water cycle of Baiu front. The activity of Baiu front closely related to the global Monsoon circulation (*e.g.*, Kato, 1993). It is important to clarify the evolution and the water cycle in MCSs observed in the Baiu frontal zone.

Cooperative observations on the structure of convective clouds were made in June 1992 by Meteorological Research Institute (MRI) and National Research Institute for Earth Science and Disaster Prevention (NIED). The investigation of the observed precipitating clouds has been carried out mainly using the observation data and the satellite data. The primary interest is on 1) the process that MCSs vertically transport water, 2) redistribution of water as precipitation, upper level cloud and water vapor, and 3) the mesoscale circulation and its role in the maintenance of MCSs.

Combined analysis of the radar data and satellite microwave radiometer data (ex. SSM/I) requires correct conversion from received intensity to rain rate (or rain mass). The attenuation correction is important for the quantitative analysis of X-band equivalent radar reflectivity factor (Ze) data. Methods using 'specific differential phase' is hopeful for the attenuation correction (*e.g.*, Ryzhkov and Zrnić, 1995). However, there are a lot of cases that such polarization information is not available, and it is important to develop alternative attenuation correction method using observed Ze data only. In FY1996, the attenuation correction method, developed in the previous financial year (attenuation rate K_2 of Nakai(1996)), was improved and examined by three-dimensional display of the Ze field.

Spatial resolution of SSM/I is a few tens of kilometers, that is two order coarser than that of a X-band radar. A suitable averaging is necessary for the radar data. The SSM/I rain rate was calculated under some assumptions at present, and the values are not necessary reliable. In FY1996, averaged Ze was qualitatively compared with SSM/I rain rate. Preliminary result of the comparison is shown.

2. Methods

The attenuation rate K is defined for one-way attenuation and expressed as $K=a\ Ze^b$ (dB km^{-1}). There are a lot of attenuation rate derived from microphysical observations. Kozu(1991) deduced the attenuation rate as $K=1.78\times10^{-4}Ze^{0.755}$ for the famous Marshall-Palmer raindrop-size distribution. This formula, hereafter referred to as K-MP, gave better result when applied to JEXAM-Miyako radar observation data than the other Ks, especially than Ks with larger b. However, the corrected Ze field still had some attenuated features (Nakai, 1996).

Figure 1 shows the root mean square (RMS) of the Ze difference of two radars in decibel unit on horizontal sections at a height of 3.0km. RMS was large when the number of grid data was less than 5000 (among 121x121). In these cases, the data of at least one radar was practically unavailable because of the strong attenuation by strong rainfall in the vicinity of the radar. Attenuation correction by K-MP generally improved the reflectivity field (decreased the RMS). The exceptions were seen from 19JST to 21JST when strong stratiform echoes were embedded around the two radars.

Nakai (1996) showed that attenuation rate that minimize the Ze difference on the horizontal sections was about $K=2.3\times10^{-4}Ze^{0.755}$. It gave better result than K-MP formula, however, the RMS increase by the correction from 19JST to 21JST remained unsolved. Corrected Ze field of these cases suggested underestimation of attenuation, while overestimation occurred at strong convective bands of other cases. He gave as attenuation rate with common a and b for both convective and stratiform rain. Kozu(1991) derived quite similar b for three types of rain. Considering that attenuation rate is sensitive to a small change of b, it may be better to fix b at K-MP value and to change a by the type of rain.

The rain type was defined in a conventional manner as 'convective' rain and 'stratiform' rain with attenuation parameters a_c and a_s , respectively. The rain area was divided into these types by the magnitude of gradient of Ze in decibel unit on PPI planes, $|\nabla_{PPI} I|$. $|\nabla_{PPI} I|$ was calculated on the polar coordinate centered at the radar after smoothing as

$$|\nabla_{PPI} I| = \left[\left(\frac{I_{i+2,j} - I_{i-2,j}}{4\Delta r}\right)^2 + \left(\frac{I_{i,j+2} - I_{i,j-2}}{4r\Delta\theta}\right)^2\right]^{\frac{1}{2}}, \quad (1)$$

where I=dBZe. Δr and $\Delta\theta$ are grid intervals of the polar coordinate. $|\nabla_{PPI} I|$ was less than 2 dB km^{-1} in most of the rain area (Fig. 2). 'Convective' rain area can be characterized by small areas that have large $|\nabla_{PPI} I|$. So, the 'convective' and 'stratiform' areas were defined respectively as $|\nabla_{PPI} I|>2$ dB km^{-1} and $|\nabla_{PPI} I|\leqq 2$ dB km^{-1}.

The rest of the method is the same as that described for K_2 by Nakai (1996). Ze of the two radars were derived with given a_c, a_s and b on a common horizontal section by usual coordinate conversion for the volume data processing. Then, the root mean square (RMS) of the Ze difference in decibel unit was calculated using all of the derived pairs of Ze. The calculation was done varying a_c and a_s. b was fixed to K-MP value, 0.755. a_c and a_s those give the minimum RMS were considered as the best values.

3. Results

Figure 3 is an example of data whose Ze difference was significant before attenuation correction by rain. A strong convective echo was between the two radars and caused significant attenuation behind it. Convective cells were coexisted with nearly uniform stratiform precipitation. The $|\nabla_{PPI} I|$ was large around convective cells and small in the stratiform echo area (Fig. 3b,d). Hatched area in Fig. 3b and d was defined as 'convective' area.

RMS of the Ze difference in decibel unit was calculated on a 3.0km high horizontal section varying both a_c and a_s from 0.8×10^{-4} to 2.8×10^{-4} (Fig. 4). RMS minimum was found around $a_c=2.3\times10^{-4}$ and $a_s=1.3\times10^{-4}$ at 1742JST. The other two examples in Fig. 4 does not indicate clear RMS minimum. It seems that RMS minimum existed around $a_c=2.8$ at 1256JST, while the RMS contour lines are nearly vertical and RMS was strongly dependant on a_c. There was no RMS minimum at 1934JST and RMS increased as either of a_c or a_s increased. In this case, RMS is more dependent on a_s than on a_c. Convective cells were in the vicinity of the radars at 1256JST and 1742JST, and uniform stratiform rain area extended around the radars at 1934JST. The dependence of RMS on a_c and a_s can be related to the type of echoes in the vicinity of the radars. The pair of a_c and a_s at RMS minimum at 1742JST gave fairly

small RMS (<3.70dB) also at 1256JST and 1934JST, which was better than a_c=a_s=2.3x10^{-4} (Nakai, 1996). So, it was inferred that

$$K \sim \begin{cases} 2.3\times10^{-4}Ze^{0.755} & (\nabla_{PPI} I>2) \\ 1.3\times10^{-4}Ze^{0.755} & (\nabla_{PPI} I\leq2) \end{cases} \quad (2)$$

was the best value approximately applicable to various Ze fields.

Applying this K to the observed data increased the similarity of two Ze fields, though the Ze difference still remained (Fig. 5). Comparing with the previous values, a_c=a_s=2.3x10^{-4}, overcorrection of the case such as 1934JST was avoided by adopting smaller a_s. It can be said that the method described here gives good approximate attenuation correction. This method can be used as a preprocessing of X-band Ze data with reasonably selected a_c and a_s.

4. Discussions

The selection of a_c and a_s is important to derive good attenuation correction using the method described in this report. These parameters affect the corrected Ze field and the following analyses in two ways.

One is the influence to the appearance of the structure of precipitating cloud systems. The attenuation by rain can be subjectively considered in conventional analysis procedures. However, recent three-dimensional visualization technique is sensitive to the numerical correction. Figure 6 shows the three-dimensional display of Ze=26dBZ isosurface at 1742JST. Three panels were drawn using the same observation data and different a_cs and a_ss. Comparison of these panels indicated that the shape of isosurface varied significantly with the change of a_c and a_s. Figure. 6(c) used a_c=a_s=2.3x10^{-4}, the result of previous financial year. The exaggeration at the edge of the isosurface was apparent in Fig. 6(c). It was improved in Fig. 6(b), which used a_c=2.3x10^{-4} and a_s=1.3x10^{-4}, the result of this report. The change of Ze seen on a horizontal section was not significant as in Fig. 6. The attenuation correction is necessary for correct interpretation of cloud structure using three-dimensional display, and may contribute to increase the efficiency of the other analysis procedures.

The other is the influence on the quantitative analysis of rain rate, such as the comparison with SSM/I. GMS and SSM/I observed the same mesoscale cloud system as the radars observed at 1742JST. Miyako island, where radar observation was held, was near the center of a MCS (Fig. 7a). Rain rate derived from SSM/I data was about 5mm hour^{-1} in average around Miyako island (Fig. 7b). The size of SSM/I footprint is of the order of the radar observation area, and rain rate derived from SSM/I has some ambiguity at present, especially, inhomogeneous precipitation within a footprint causes bias of rain rate estimation (Browning, 1990). Rain rate derived from Ze field varied significantly within the observation area. Average rain rate, with the assumption of Z=200R$^{1.6}$, was 1.02mm h^{-1} without attenuation correction and 1.38mm h^{-1} with a_c=2.3x10^{-4} and a_s=1.3x10^{-4}. They were much smaller than the SSM/I rain rate. The peak value of radar-derived rain rate exceeded 6.0mm h^{-1}, which was comparable with the peak value of SSM/I rain rate. The difference between these rain rate decreased by applying the attenuation correction to the radar data. The mean values still differed by a factor of three or more, however, part of it was attributed to the data processing and was expected to decrease to some extent. For quantitative evaluation of rain rate, more examination of characteristics of both radar and SSM/I data is necessary. It will contribute to the investigation of the structure and maintenance mechanism of convective systems.

Considering the wide variety of the convective systems, it is important to analyze as many cases as possible. The result described here is limited to the data in June 1992 around 25^{o}N. In FY1997, it is planned to analyze satellite microwave data of June-July 1996 around 30^{o}N as well as the data in 1992. Continuing analysis of the radar observation data is also necessary as the basis of satellite data analyses.

5. References

Browning, K. A., 1990: Rain, rainclouds and climate. Quart. J. Roy. Meteor. Soc., 116, 1025-1051.

Kato, K, 1993: The processes of the seasonal transition of Baiu front in East Asia: The effect of Indian Monsoon and the semiarid region around China (Japanese). Kaiyo Monthly, extra issue No.5, 96-101.

Kozu, T., 1991: Estimation of raindrop size distribution from space-borne radar measurements. Ph. D.

dissertation, Kyoto University, 196pp.
Nakai, S., 1996: Analysis on the evolution of convective cloud systems. Japanese experiment on Asian Monsoon (JEXAM): Annual report (April 1995 - March 1996), Research and Development Bureau, STA, Japan, I-1-(3).
Ryzhkov, A. and D. S. Zrnić, 1995: Precipitation and attenuation measurements at a 10-cm wavelength. J. Appl. Meteor., 34, 2121-2134.

6. Publications

①oral presentations

Nakai, S., K. Akaeda and H. Sakakibara, 1996: Correction of rain attenuation using dual radar observation data (Japanese). Preprints of the 1996 Spring Semi-annual Meeting of the Meteorological Society of Japan, 21-23 May 1996, Omiya, B155.

Nakai, S., 1997: Orographic cumulus at Yakushima (Japanese). Preprints of the 1997 Spring Semi-annual Meeting of the Meteorological Society of Japan, 21-23 May 1997, Tsukuba, G220.

Nakai, S., R. Kawamura, 1997: Characteristics of cloud clusters appeared around the Baiu front: 5-18 June 1992 case (Japanese). Preprints of the 1997 Spring Semi-annual Meeting of the Meteorological Society of Japan, 21-23 May 1997, Tsukuba, G307.

和文アブストラクト

本研究では、4年度に取得したデュアルドップラー観測データの解析によって対流雲内の雨水量、気流の分布を明らかにすること、およびその結果を基にした衛星データ（主にマイクロ波センサ）の解析によって、対流雲による水蒸気消費量および鉛直輸送量を調査し、対流雲の維持過程、モンスーン雲域の水収支、およびこれらの関係を解明することを目的としている。

平成８年度は、前年度に開発した降雨減衰補正法の改良として、対流域／層状域の区分を導入した。'対流域'と'層状域'はPPI面上におけるZe(等価レーダー反射強度因子)傾度の大きさ$|\nabla_{PPI} I|$によって区分し、$|\nabla_{PPI} I|>2$ dB km^{-1}を対流域、$|\nabla_{PPI} I|\leqq 2$ dB km^{-1}を層状域とした。減衰係数は$K=a\ Ze^{b}$ (dB km^{-1})の形とし、bは共通で0.755、aは対流域(a_c)と層状域(a_s)で独立とした。高度3kmの水平面上で２台のレーダーの反射強度差が最小となる値を最適値として求めたところ、a_c=2.3x10^{-4}、a_s=1.3x10^{-4}となった。これらの値による降雨減衰補正の効果をZe分布の３次元表示とSSM/Iとの比較で見たところ、いずれにおいても改良が見られた。ZeとSSM/Iからの降雨強度の比較では、両者の値は一致しなかったがその差は減衰補正によって小さくなった。

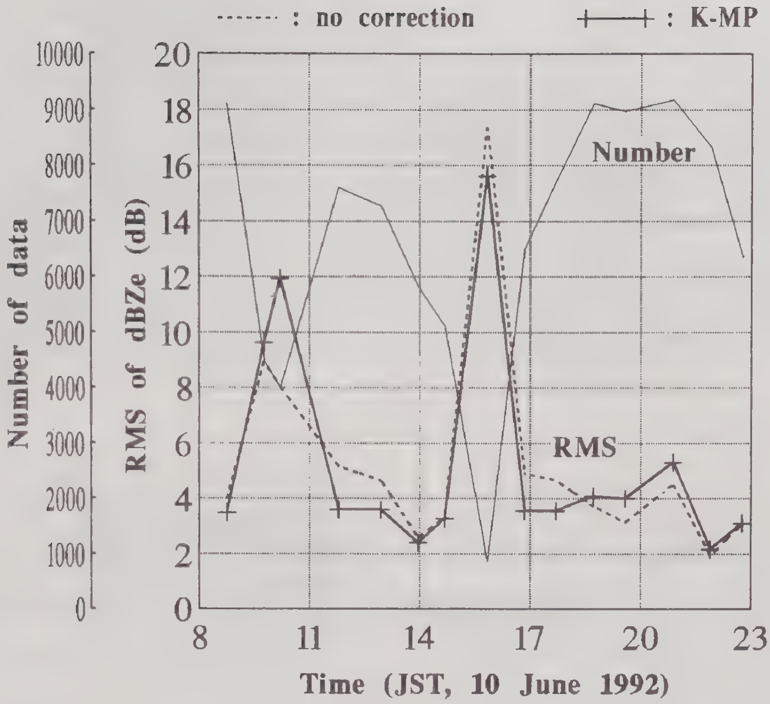


Fig. 1. RMS of Ze difference in decibel unit on 15 horizontal sections at a height of 3km about 1-hour intervals. Thick solid and dashed lines indicate RMS calculated without attenuation correction and with correction by K-MP formula, respectively. Thin line indicates the number of available grid points among 121x121 points.

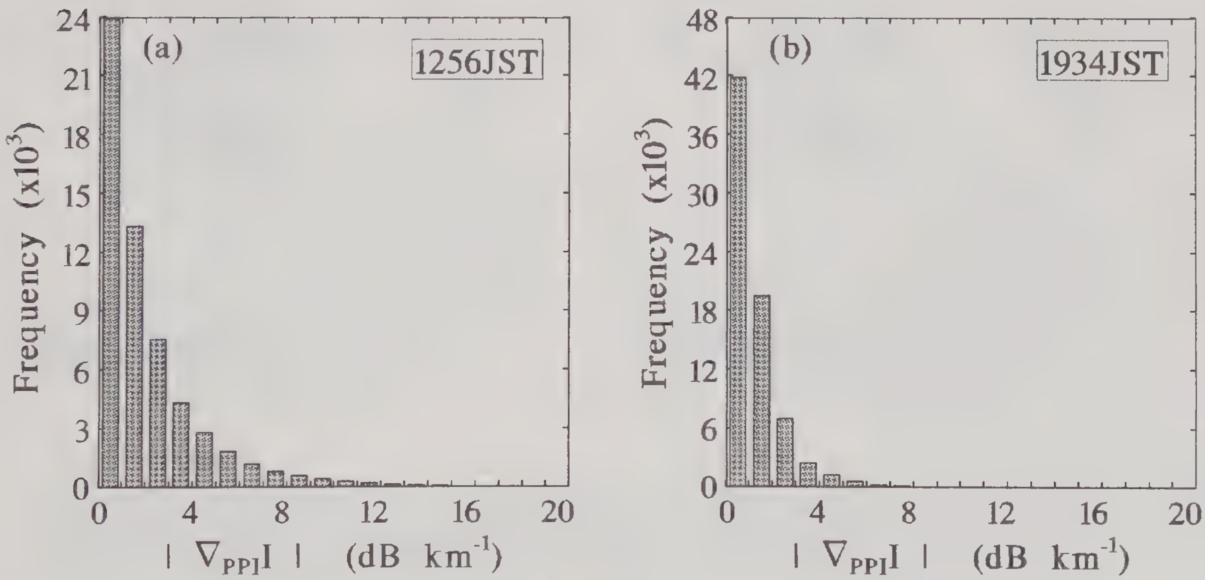


Fig. 2. Histogram of $|\nabla_{PPI}I|$ on a PPI plane at an elevation of 2.8°. (a) for 1256JST and (b) for 1934JST.

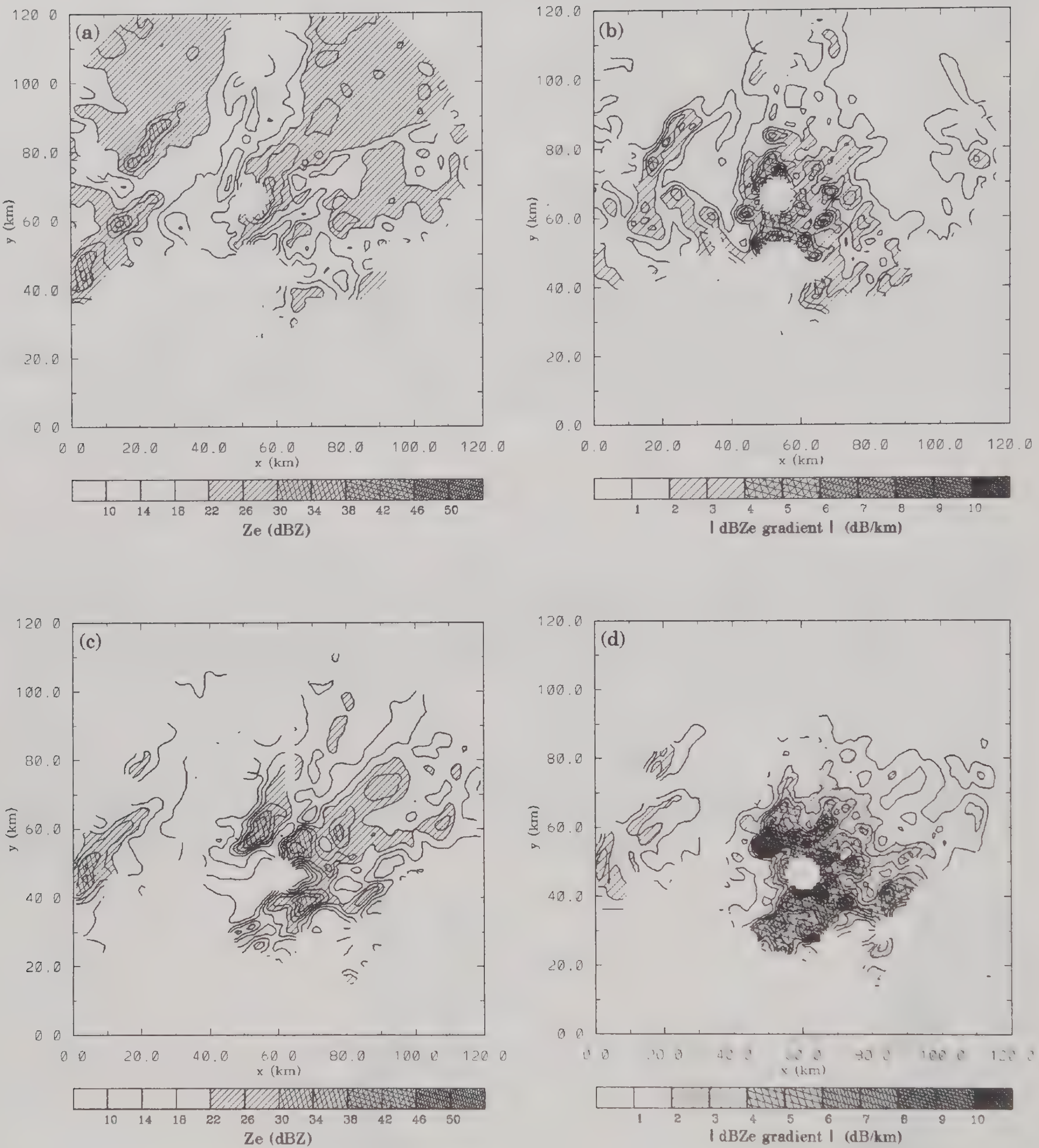
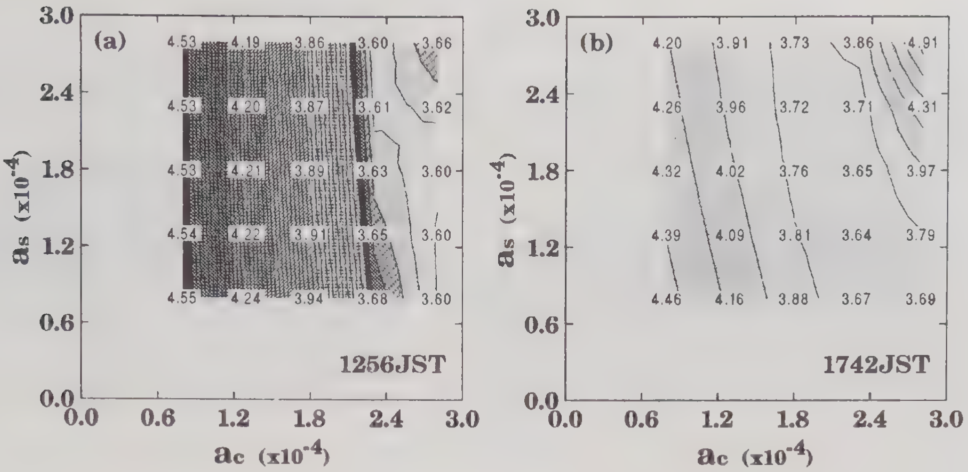


Fig. 3. Horizontal sections of radar-observed data at a height of 3.0km at 1256JST without attenuation correction. (a) Ze of NIED-BD radar, (b) $|\nabla_{PPI}|$ of NIED-BD radar, (c) Ze of MRI-3cm Doppler radar, and (d) $|\nabla_{PPI}|$ of MRI-3cm Doppler radar. NIED-BD radar located at (x,y)=(55.80,69.43) (km), and MRI-3cm Doppler radar located at (x,y)=(64.20,50.57) (km).



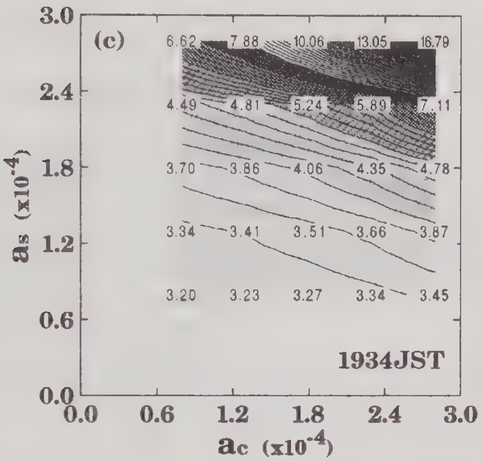


Fig. 4. RMS of Ze difference in decibel unit on horizontal sections at a height of 3km. RMSs calculated varying a_c and a_s are shown by contourplot. (a) 1256JST, (b) 1742JST, and (c) 1934JST.

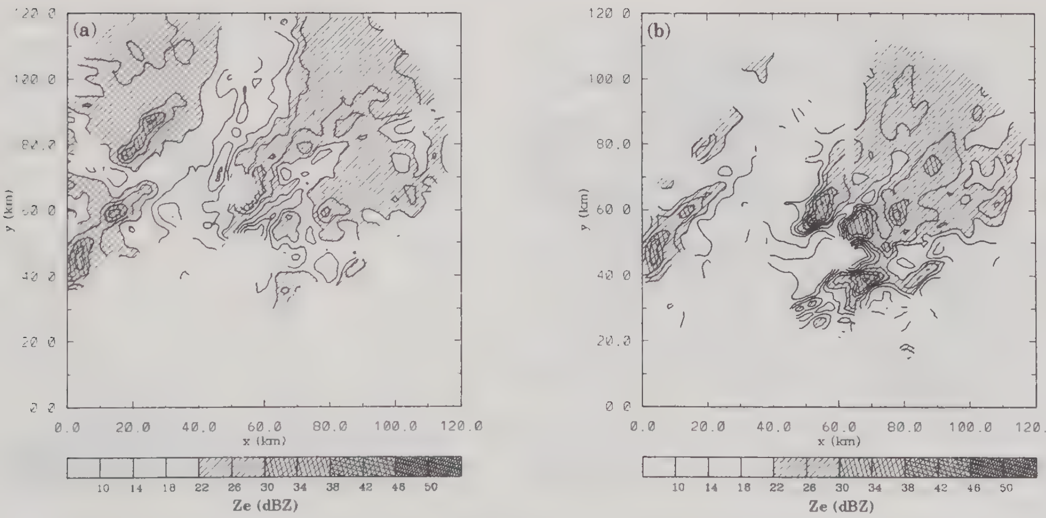


Fig. 5. As in Fig. 3, except that the attenuation correction was done using a_c=2.3x10^{-4} and a_s=1.3x10^{-4}. (a) Ze of NIED-BD radar, (b) Ze of MRI-3cm Doppler radar.

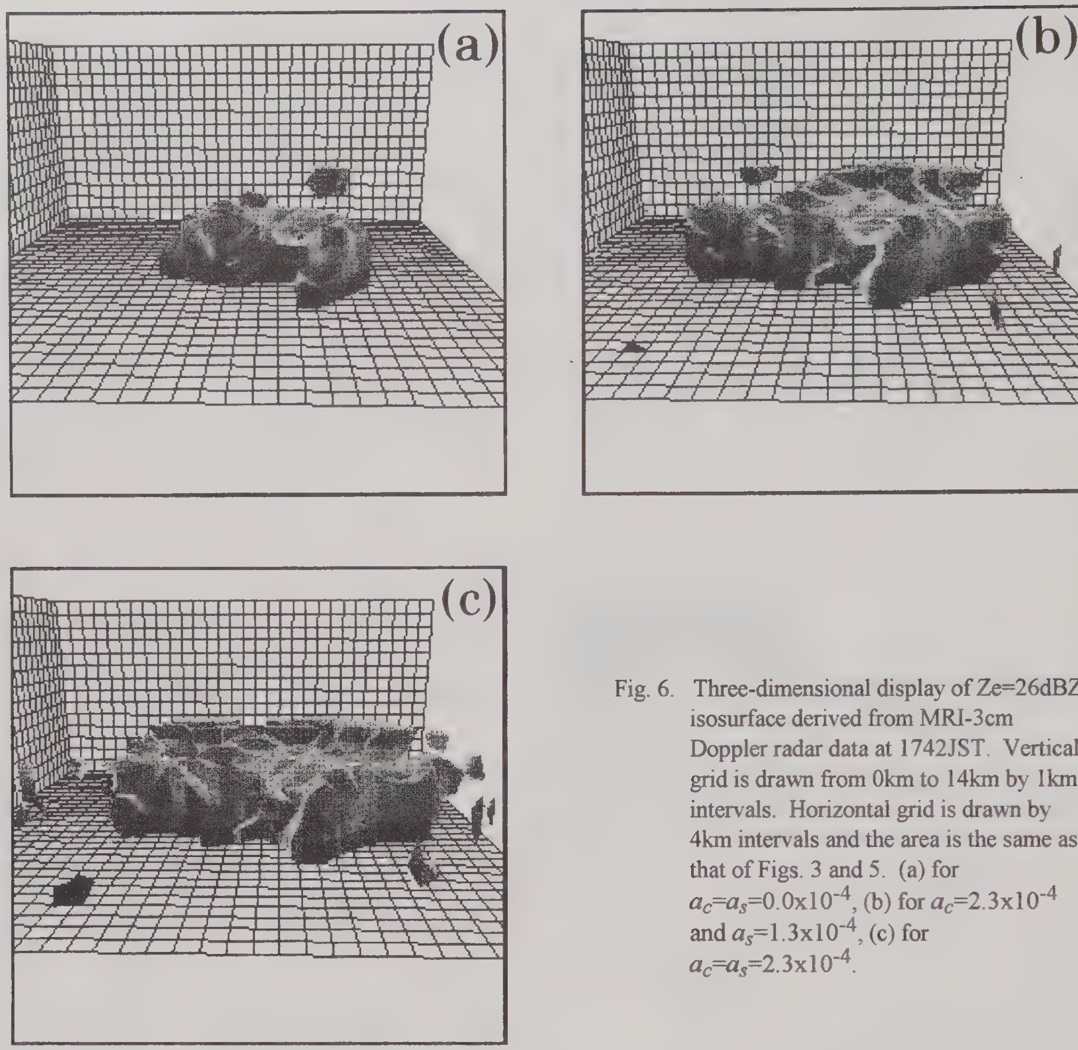


Fig. 6. Three-dimensional display of Ze=26dBZe isosurface derived from MRI-3cm Doppler radar data at 1742JST. Vertical grid is drawn from 0km to 14km by 1km intervals. Horizontal grid is drawn by 4km intervals and the area is the same as that of Figs. 3 and 5. (a) for a_c=a_s=0.0x10^{-4}, (b) for a_c=2.3x10^{-4} and a_s=1.3x10^{-4}, (c) for a_c=a_s=2.3x10^{-4}.

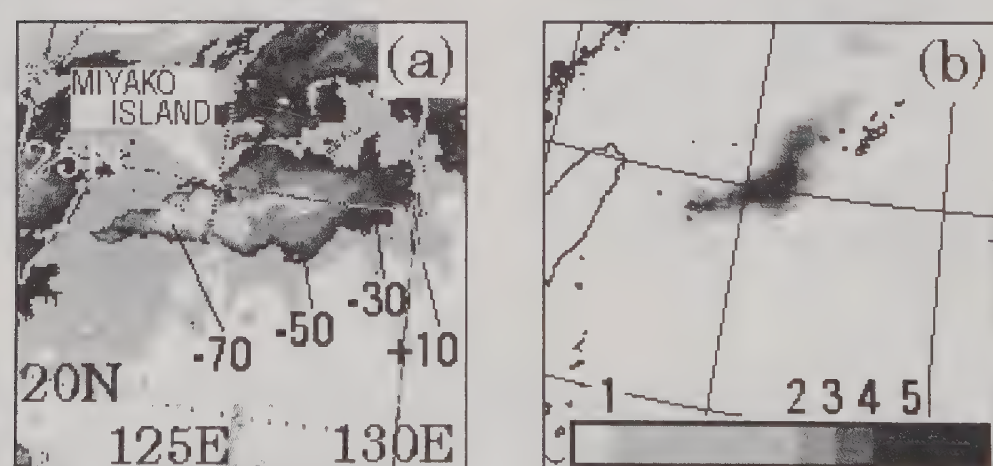


Fig. 7. (a) Cloud-top T_{BB}(^oC) distribution from GMS-IR data (WEFAX H-image) at 1739JST. Radar observations were held at Miyako island. (b) Rain rate (mm h^{-1}) retrieved from SSM/I data at 1744JST.

I. Observation and analysis on the process of the atmosphere-ocean-land interactions

I. 大気・海洋・陸域間相互の諸過程に関する観測・解析研究

2. Observation and analysis on the process over the ocean

2. 海洋における諸過程に関する観測・解析研究

(1) Observation on Sub-Surface Temperature by Voluntary Ships

(1) 表層水温に関する観測研究

Keisuke Mizuno* , Tomowo Watanabe*, and Makoto Okazaki

水野　恵介*, 渡辺　朝生*, 岡崎　誠 *

National Research Institute of Far Seas Fisheries

遠洋水産研究所

ABSTRACT

Shipboard hydrographic observation in the eastern Indian Ocean were conducted in January 1997 (winter monsoon season) in order to obtain detailed upper layer hydrographic structure for better understanding of heat flux in the area. Near Sunda strait, coast side of the South Java Current, a westward current with subsurface velocity maximum interleaves southward below the South Java Current. The current has significant westward volume transport. Water in the South Equatorial Current is characterized by mixed water, and its characteristics are formed by confluence of different currents. The westward transport along a section south of Sunda strait(105 E) is large (23Sv), but the that of Lombok strait(115 E) is estimated to be small. It is suggested that the deficit causes the shallow upper layer thickness which changes the heat storage of the area.

1. Objectives

Large scale upper layer thermal field of the ocean is important for the mechanism of Asia Monsoon as a major boundary condition which plays as a sink/source of heat of the atmosphere. Since the upper layer of the ocean is not quiet and stable, heat storage of oceanic upper layer and its transport by oceanic current, which make net oceanic heat gain, play an important role for the heat exchange between atmosphere and ocean. In fact, Arabian Sea is a annual mean heat-gain area entirely by upwelled cool water, although upwelling area is limited to narrow coastal area but the water spreads broadly.

Previously, we described that upper layer thermal field in the eastern tropical Indian Ocean tended to correlate with ENSO signal in the Pacific Ocean by using historical temperature/depth data(Mizuno and Watanabe 1994). When warm episode occurs in the Pacific, depth of the upper layer decreases and the temperature becomes colder than normal with a few months time lag. Also, the area is important for the outlet of the water from the Pacific Ocean (i.e. Indonesian Throughflow; ITF) which annual cycle of mass transport were previously estimated quantitatively (Mizuno and Watanabe 1995).

However, the atmosphere-ocean heat flux in the eastern Indian Ocean has not attained to a consensus among several previous studies. In terms of annual mean atmosphere-ocean heat flux in this area, a model (Macreary et al. 1993) calculated to be heat-loss area, a climatology (Hastenrath and Lamb 1979) described to be heat-gain area. The difference is remarkable especially in the area under the effect of ITF.

In order to investigate the difference, detailed description of the current and temperature/salinity structure and their variability in that area is necessary, which has not yet conducted adequately. So, we conducted hydrographic observation by using a research ship in winter 1997.

2. Method

Hydrographic observation was conducted in the eastern tropical Indian Ocean by using Shoyo Maru (Fisheries Agency Research Ship ; 1362 gloss ton) during January

1997(Figure 1). The area of interest is between the north western coast of Australia and the lesser Sunda archipelago where the ITF enters the Indian Ocean and the area is subjected to the impact of ENSO signal in the Pacific.

Observation lines are shown in Figure 1. Meridional lines were taken along 105 E and 115 E in order to obtain zonal structure of current system. At each CTD station (solid triangle in the figure), a CTD sensor(Sea Bird Instrument Co. model 911 plus) with Rosset sampler (12 Niskin bottle array) was lowered down to 3000m. Measured salinity and dissolved oxygen by CTD were corrected by comparing with the laboratory measurements of sampled sea water. Additionally, XCTD was dropped midway of the CTD stations(solid circles).

Currents were directly measured by Acoustic Doppler Current Profiler (ADCP; RD instrument Co.) during all steaming time. Although five minutes ensemble mean of 1 second pinging interval surface to 500m for every 16m bin were taken, the data is under processing.

3. Result

Since the upper layer is important for short term climate study, we focus on the upper ocean structure, although we observed deeper than 3000m.

3-1. Upper layer thermal/salinity structure along 105° E

Sea surface temperature is higher in the northern end, and the water warmer than 28° C extends southward from the Sunda strait to nearly 16° S (Figure 2 upper panel). The thermocline (15-20° C) generally becomes shallower and thinner from south to north, while isotherms warmer than 25° C become deeper. Eventually a very sharp thermocline appears at the north end around 120m depth. A thermocline ridge appears at 10° S which indicates a boundary of different currents.

Salinity section(Figure 2 middle panel) shows quite different structure from that of temperature which means different water types are there. High salinity core appears at 200m of south end (22 S) and extends to the north with a sharp front at 15 S. This water type is South Indian Central Water (SICW) which is salty.

Low salinity water of upper layer extends from the north end having a surface

salinity front around 8° S which is possibly from Java Sea or southern coast of Java or Sumatra. Below this low salinity water at 7° S, comparatively higher salinity water (>34.7psu) appears, which is estimated to be North Indian Water(NIW). Between 8-12° S and below 100m, vertically uniform low salinity water is appears. According to Wijffels et al. (1996), this water is thought to be Banda Sea Water. Three different water type are found in this section.

In terms of upper layer structure, weak ridge of halocline in the upper layer can be seen at 8-9° S which location is different from that of thermocline ridge.

3-2. Transport along 105° E

Geostrophic transport were computed based on 1000db reference level. South Java Current can be seen around 8-10° S, which flows eastward and has shallow structure extending only upper 100m depth. The flow transports warm and very low salinity water to the east. At its coast side (i.e. north of 8° S), westward current appears with maximum at 150m, and interleaved southward below the SJC. The SJC transports comparatively low salinity water to the east.

Off the SJC, a strong westward current appears with maximum at 11° S. The flow correspond to the upstream side of westward South Equatorial Current, and significant part of the flow originates from the ITF. The SEC transports near surface warm and low salinity water to the west. The boundary of SEC and SJC corresponds to the thermocline ridge at 10 S. South of the SEC, there is a broad and comparatively weak eastward flow, and their boundary location is consistent with subsurface salinity front around 15° S. The eastward flow transports high salinity SICW, but is rather modified.

Zonal geostrophic mass transport of upper 400m at each latitude bin is calculated (Figure 3). Westward transport is generally dominant, and the total transport along the section is -23Sv(1Sv is $10^6 m^3/sec$; negative value indicates westward direction). The SJC at 9-10 S is apparently small. It is not only because seasonal weakness, but because it is a shallow current and reversed current flows below it. The SEC at 10-14 S has large transport nearly -13Sv westward, although some part of the transport might be a contribution of recirculation of eastward flow

south of it.

3-3. Upper layer thermal/salinity structure along 115° E

Warm water higher than 28 C extends surface layer of entire section (Figure 4, upper panel). The thermocline (15-20 C) becomes shallower to the north similarly to that in 105° E section. In terms of the salinity structure (Figure 4, middle panel), comparatively low salinity water (<34.5psu) near the surface at northern edge (14-15 S) and high salinity core at southern area (18° S and 20° S) between 200-250m are remarkable. This basic structure is common in both sections.

3-4. Transport along 115° E

Geostrophic transports were computed in the same way as the previous section (Figure 4 lower panel). Four zonal current bands appears, eastward bands at 13° S and 17 S , and westward one at 15° S and 19° S. Northernmost eastward band is probably an edge of SJC, and westward band at 15° S might be the main body of the ITF. This water shows scattered T-S relation (not shown) suggesting mixing process. Eastward flow at 17° S carries high salinity core of SICW(200-250m). Another high salinity core at 20 S also flows to the east, but upper layer westward flow at 19° S is probably the Leeuwin Current along the Australian coast.

Net zonal transport along this section is small(1.2Sv), although the section does not extend to the Indonesian coast.

4. Discussion

North of the SJC, counter current was found with subsurface velocity maximum, and the current interleaved below the SJC at 105 E section. So far, it is not known whether the current is robust structure. Calculated transport of the current is significant for zonal transport in the area, which may not be negligible for heat flux.

Upper layer water in the SEC area has scattered T-S characteristics which suggest mixing process occurs in the layer. Surface mixing layer tends to be thin and the isotherm interval of the upper layer(20-25° C) increases to the south. The upper layer water in SEC at 105° E has lower salinity than that at 115° E. Source of SEC has not a single water type, but is thought to be formed by confluence of more than two

different currents as Wijffels et al.(1996). So, the heat in the upper layer is capable to be transported downward to deeper layer by vertical mixing. If so, the mixing helps to gain heat from the atmosphere to the ocean.

Observed SJC has not significant transport because of its seasonal change. According to Wijffel et al. (1996), SJC is strongest in May and November due to Indian Ocean Equatorial Jet (it intrudes into the area along the west coast of Sumatra by coastal Kelvin wave), but weak in monsoon time.

Obtained westward zonal transport across 105 E section is exceptionally large(23Sv) due to strong SEC compared to the previous works, but no significant zonal transport can be found at 115 E. Although the volume may be supplied by ITF near Java to the north of this section, this possibility is small because ITF is seasonally weak in January. The deficit of the volume probably makes the change of the upper layer thickness of this area. The change of upper layer thickness causes the upper layer heat storage and its advection which are important for heat flux.

Although this is one time observation, it brings several important aspects of hydrographic structure in the eastern tropical Indian Ocean, where the mechanism of heat flux is still open to question. Fortunately several hydrographic observations have been conducted in the international frame work (i.e. WOCE) in 1995-1996. Synthesis of the results would bring us clearer aspects in heat flux mechanism in the near future.

5. References

Hastenrath,S.and P.J.Lamb (1979): Clmatic Atlas of the Indian Ocean. PartII: The oceanic heat budget. The University of Wisconsin Press.

McCreary,J.P.,P.K.Kundu, and R.L.Molinari(1993): A numerical investigation of dynamics, thermodynamics and mixed-layer processes in the Indian Ocean. Prog. Oceanogr. 31, 181-244.

Meyers,G., R.J.Bailey, and A.P.Worby (1994): Volume Transport of Indonesian throufhflow. Deep-Sea Res.,Part I,42,1163-1174.

Mizuno,K. and T.Watanabe (1994): Observation on sub-surface temperature by

voluntary ships. JEXAM annual report (FY1993), 15-24.
Mizuno,K. and T.Watanabe (1995): Observation on sub-surface temperature by voluntary ships. JEXAM annual report (FY1994), 12-22.
Wijffel,S.E., N.Bray, G.Meyers, and W.M.L.Morawitz (1996): The WOCE Indonesian Throughflow repeat hydrography sections: I10 and IR6. International WOCE Newsletter, 24,24-28.

6. Publications

Mizuno,K.(1996): Observation of the Indian Ocean –Equatorial Jet-. Proceedings of international workshop on ocean climate variations from seasons to decades with special emphasis on Pacific Ocean buoy network. 149-156.

Watanabe,T.(1996): Interannual variation of upper ocean in the western North Pacific and its relationship to East Asian wintertime monsoon. Proceedings of the international workshop on the climate system of monsoon Asia. 288-290.

7. International Cooperation

None

和文要旨

インドネシア通過流はインド洋内部の熱輸送に大きな影響があると考えられている。海洋内部の熱輸送機構の理解に必要な海流と表層の水温構造を調べるため、１９９７年１月に、ジャワ・オーストラリア間の海域において水産庁調査船照洋丸を用いて海洋観測を実施した。スンダ海峡付近では東流する南ジャワ海流の岸よりに、かなり大きな流量をもつ反流が見出され、これは南ジャワ海流の下側にも及んでいた。南赤道海流の運ぶ水の水塊特性は混合水の特徴を示し、ジャワ島南方海域では海水の混合が強いことが示唆された。また、この海域全体では南赤道海流による東側への流出量がインドネシア通過流の流入量を上回り、表層の厚みの変化が起きていることが示された。

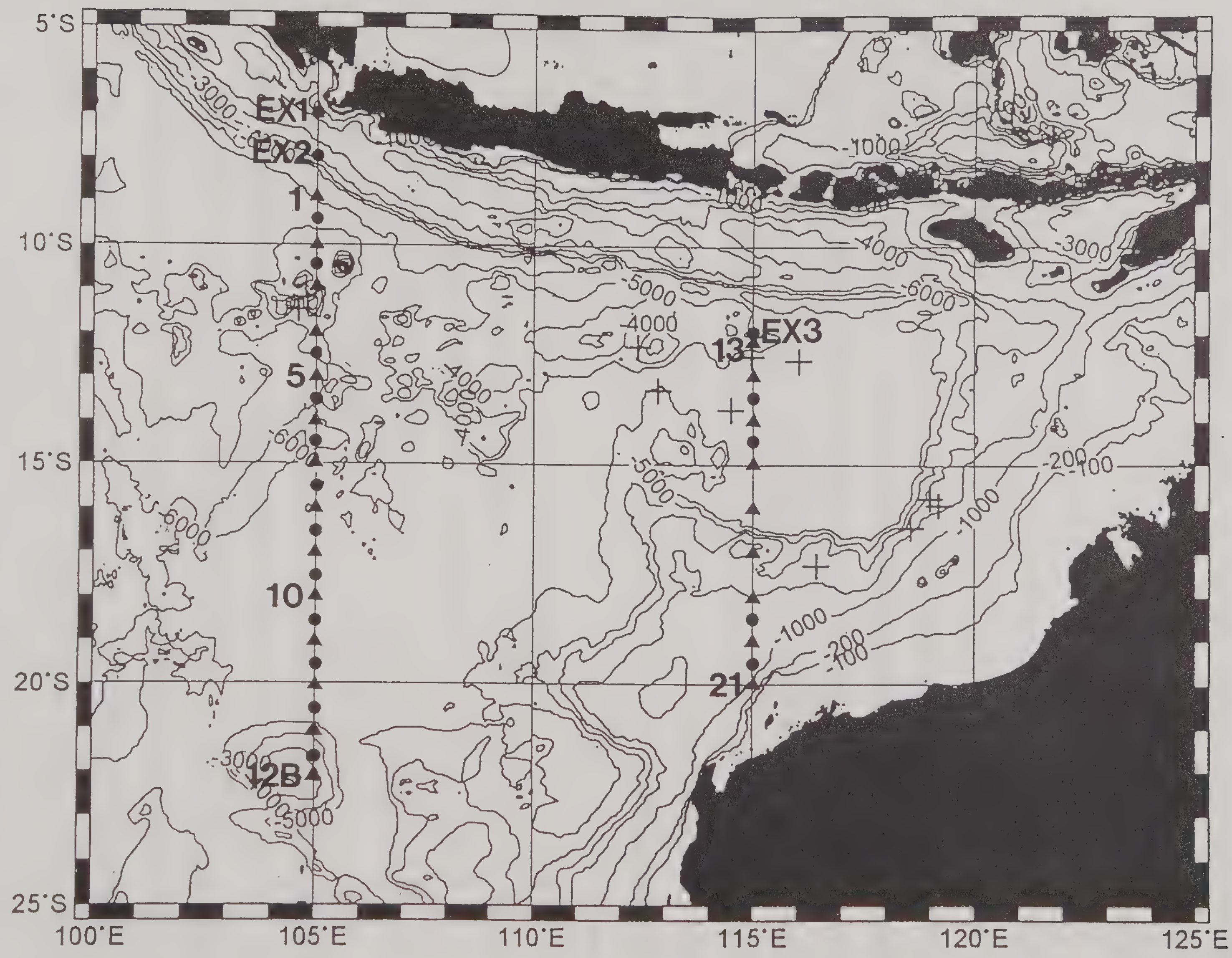


Figure 1. Observed hydrographic stations (▲ CTD, ● XCTD).

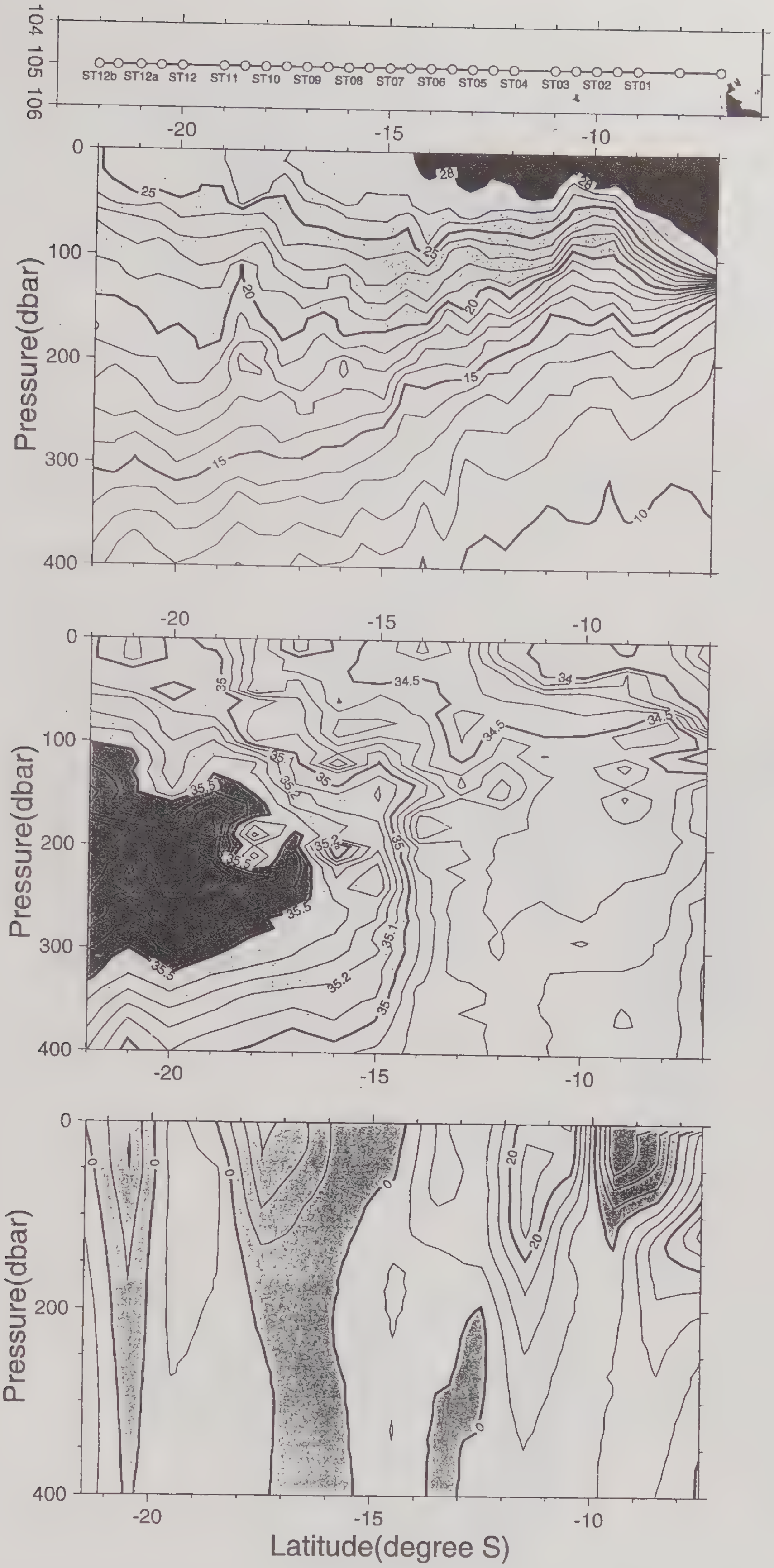


Figure 2. Vertical sections along 105°E. upper panel; temperature(°C) section, contour interval is 1°C. middle panel: Salinity (psu) section, contour interval is 0.1psu. lower panel; Zonal geostrophic velocity section(cm/sec), contour interval is 5cm/sec, Eastward velocity is shaded.

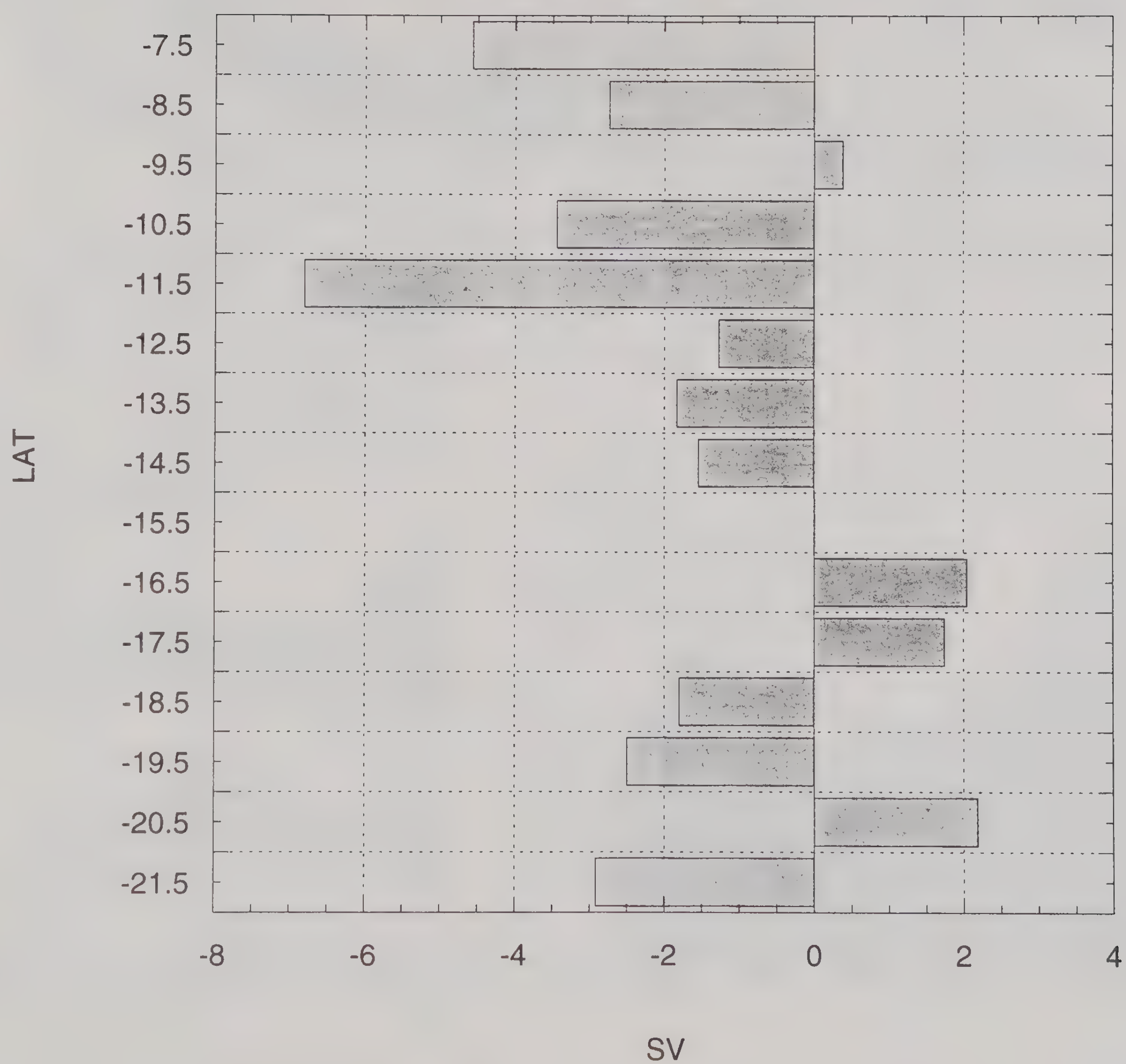


Figure 3. Zonal geostrophic mass transport of upper 400m at each latitude (1000db reference level) across 105°E

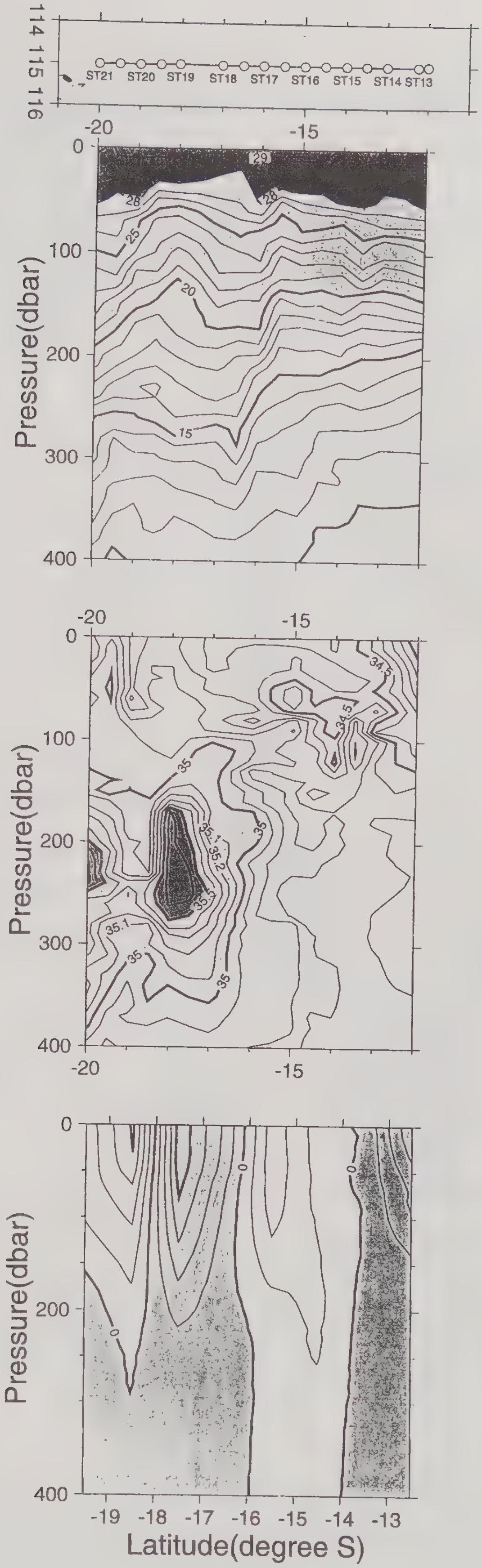


Figure 4. Same as figure 2, but 115°E.

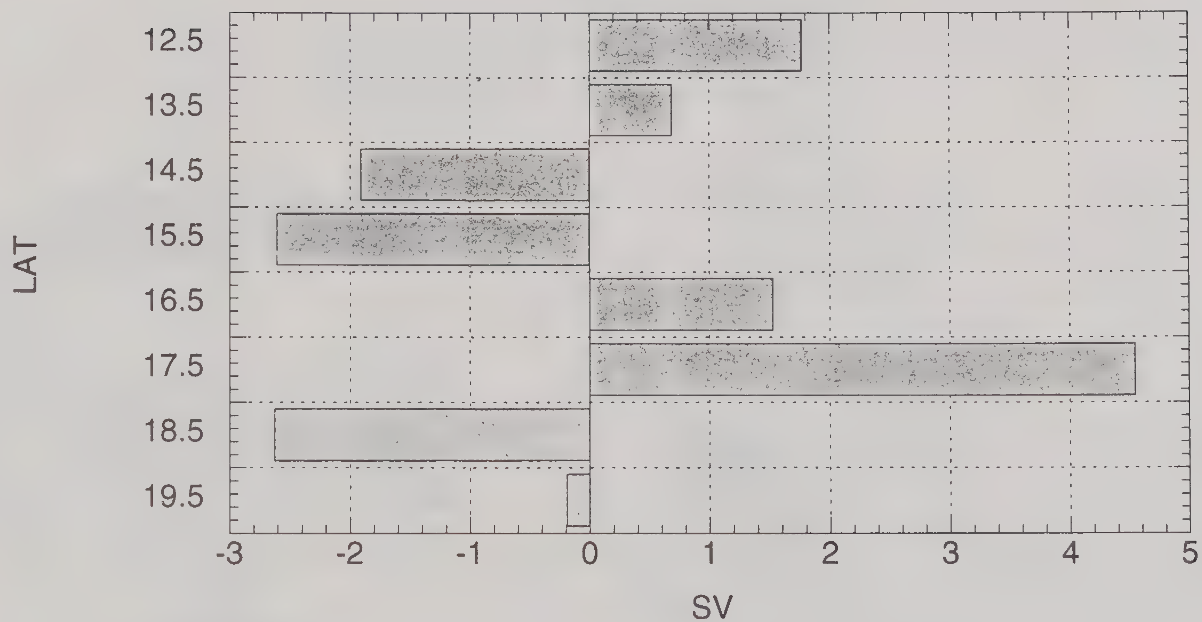


Figure 5. Same as figure 3, but 115°E.

I．大気・海洋・陸域間相互作用の諸過程に関する観測・解析研究
Observation and analysis on the process of the atmosphere-ocean-land interactions
2．海洋における諸過程に関する観測・解析研究
Observation and analysis on the process over the ocean
（1）表層水温に関する観測研究
Observation on Subsurface Temperature by Voluntary Ships

気象庁　気候・海洋気象部
三河哲也、吉田隆、吉川郁夫、水野孝則、石川一郎
Climate and Marine Department,
Japan Meteorological Agency
Tetsuya Mikawa , Takashi Yoshida, Ikuo Yoshikawa,
Takanori Mizuno and Ichiro Ishikawa

(Abstract)

Subsurface temperature observations in the Indian Ocean and the South China Sea have been made by a voluntary observing ship, "Kashimasan-Maru" with expendable bathythermograph (XBT) since 1990. Subsurface temperature data collected via the Global Telecommunication System of the World Meteorological Organization, including XBT data observed by the above mentioned ship have been assimilated in the Ocean Data Assimilation System (ODAS) of Japan Meteorological Agency. The depth of 20°C isotherm derived from the ODAS are compared with subsurface temperature observations along regular shipping routes. The result is that the ODAS shows well the variation of the observed subsurface thermal structure in the tropical Indian Ocean. Using the results of the ODAS, the time-space evolution of the ocean heat content anomalies in the tropical Indian Ocean is investigated via empirical orthogonal function (EOF) analysis. The first EOF mode displays positive loadings around 5°S to 10°S in the western equatorial Indian Ocean and negative loadings off Sumatra Island in the eastern equatorial Indian Ocean. The correspondence of the time evolution of the mode with the variation of monthly mean of u-component of wind stress anomalies over the central equatorial Indian Ocean and SST anomalies for Region B (between 4°N and 4°S from 150°W to 90°W; nearly equal to so-called NINO.3) suggests that the subsurface thermal structure in the Indian Ocean is in close connection with El Niño-Southern Oscillation.

1. Objectives

The Asian Monsoon over the Indian Ocean and the seas around Southeast Asia is considered to be related to El Niño-Southern Oscillation (ENSO) events which affect the global climate, through the interaction between the ocean and the atmosphere in the Indonesian region (Barnett 1983, Nicholls 1984). Recently, a further understanding of the physical structure of the ocean in these regions, and a clearer elucidations of the relation between the Asian Monsoon and ENSO have been required. However, the oceanographic data in these regions are too sparse to fully understand the physical structure of the ocean.

In this study, Japan Meteorological Agency (JMA) have conducted the subsurface temperature observation with expendable bathythermograph (XBT) in the Indian Ocean where the oceanographic data are too poor,

by a voluntary observing ship (VOS), a crude oil tanker "Kashimasan-Maru" cruising between Japan and the Persian Gulf since October 1990. The subsurface temperature data observed and reported by the ship have been distributed to national meteorological/oceanographical services throughout the world via the Global Telecommunication System (GTS) of the World Meteorological Organization (WMO). XBT data collected via GTS including those from the crude oil tanker are used to investigate annual variation of subsurface waters in this region.

2. Methods

Subsurface temperature in the Indian Ocean and the South China Sea is observed by a crude oil tanker, "Kashimasan-Maru" which makes fifty-day round trips between Japan and the Persian Gulf via the Strait of Malacca.

In this study, first, we compare the subsurface thermal structure appeared in the output derived from the Ocean Data Assimilation System (ODAS) of JMA (Kimoto et al. 1997) with that appeared in actually observed subsurface temperature. Next, in order to understand annual variation of the thermal structure in the Indian Ocean, we investigate the ocean heat content (OHC) derived from ODAS via empirical orthogonal function (EOF) analysis.

Although the spatial density of the subsurface temperature observation is with a rather high along the regular shipping routes, observations other than the routes are very sparsely distributed both in time and space. Thus, it is very difficult to understand the time-serial three-dimensional structure of the ocean only from the observed data. However, this difficulty can be removed by the ODAS that reproduces the oceanic structure reasonably. Subsurface temperature data collected via GTS including XBT data observed by "Kashimasan-Maru" have been assimilated into the ODAS of JMA. The five-day averaged output of the ODAS operated by JMA have obtained every 5 days. Climatology was computed by the ODAS from the data observed during the 1987-1995 base period.

3. Results

(1) Observation of subsurface temperature by "Kashimasan-Maru"

As many as 2,428 subsurface temperature data were obtained by "Kashimasan-Maru" in the South China Sea, south of the Bay of Bengal and the Arabian Sea for the period from October 1990 to April 1997. Those subsurface temperatures were usually observed four times a day. The interval of observation points is about one hundred and seventy kilometers. Fig. 1 shows the distribution of XBT's observation along the cruise tracks of "Kashimasan-Maru" on 1996.

(2) The depth of 20°C isotherm (D20) derived from ODAS and the observed data

To make sure the ODAS represents the actual subsurface thermal structure in the Indian Ocean, we verify the subsurface thermal structure displayed by the ODAS prior to investigation of annual variation of that derived from the ODAS. D20 in comparison with ODAS and the observed data is adopted as a parameter to indicate the variation of the thermocline depth in the tropical Indian Ocean.

Fig. 2 shows a time-longitude section and the analysis line of D20 estimated from data observed by "Kashimasan-Maru" and other ships. The time-longitude section of D20 along 6°N derived from the ODAS

are shown in Fig. 3. In general, seasonal and annual variation of D20 derived from the ODAS well corresponds that in the observation data, only the correspondence of annual variation is not sufficiently clear, because two lines do not agree and there are some lack of observations.

(3) Annual variation in the Indian Ocean

On the time-space evolution of heat storage of the upper 400 m, Tourre and White (1995) performed EOF analysis using the time series of anomalies derived from observed subsurface temperature data for the 13-year period 1979-1991, and showed that the signal over the subsurface of the Indian Ocean was approximately in phase with the ENSO signals. But the number of data used by them is not large enough at all.

In the present study, EOF analysis for OHC anomalies from ODAS are performed to investigate annual variation of the subsurface thermal structure. The region for EOF analysis is between 20°N and 20°S, from 40°E to 120°E with 2.5 degrees interval in longitude and latitude in the Indian Ocean. The analysis period is 10 years (1987-1996).

The spatial pattern of the first EOF mode for OHC anomalies is shown in Fig. 4. The spatial pattern displays positive loadings around 5°S to 10°S in the western equatorial Indian Ocean and negative loadings off Sumatra Island in the eastern equatorial Indian Ocean, explaining 17.6% of the total variance. To investigate the relationship between this first mode EOF pattern and Monsoon wind strength, we shows the time sequence of the first mode for OHC anomalies (solid line) and wind index (chain line) in Fig. 5. Wind index is the regional monthly mean of u-component of wind stress anomalies over the central equatorial Indian Ocean (between 5°N and 5°S from 70°E to 90°E). The time series of EOF correspond very well with that of wind in reverse sign. The latter goes about two months ahead of the former and the correlation is rather high (lagged correlation coefficient is -0.77), which implies that OHC is considerably affected by the Asian Monsoon wind.

The relationships between the Asian Monsoon wind and ENSO have studied by many researchers. We have already showed that the Asian Monsoon wind and OHC in the Indian Ocean have close connection, and thus the variation of OHC in the Indian Ocean would correspond to ENSO signals. In Fig. 6, a solid line is the time sequence of the first EOF mode for OHC anomalies in the Indian Ocean and a broken line is a regional monthly mean of Sea Surface Temperature (SST) anomalies averaged over Region B (between 4°N and 4°S from 150°W to 90°W; nearly equal to so-called NINO.3) which is often used as a index of ENSO signals. Both signals are in phase of each other without time lag. In fact, the correlation coefficient of the two parameter (0.56) is higher than that between SST anomalies for Region B and the Asian Monsoon wind (lagged correlation coefficient is -0.42). These results suggests that the subsurface thermal structure in the Indian Ocean is in close connection with ENSO.

In the spatial pattern of the second EOF mode for OHC anomalies (Fig. 7), there are negative loadings around 10°S, 60°E and positive loadings around 10°N in the western tropical Indian Ocean, explaining 12.9% of the total variance. Annual mean of D20 in the Indian Ocean derived from the ODAS (Fig. 8) shows that the depth of thermocline is shallowest around 10°S, 60°E and deepest between 15-20°S. The horizontal gradient of D20 is very steep in the area between the shallowest region and the deepest region to the south, and hence Southern Equatorial Current (SEC) flows westward there. The pattern of the second EOF mode is similar to the map of annual mean D20 in the western Indian Ocean. It suggests this pattern is possibly

correlated with the intensity of SEC. Fig. 9 shows the time sequence of the second EOF mode and SST anomalies for Region B. There also exists some relationships between the variations of the two existing in the first mode.

4. Discussions

We investigated time-space evolution of the ocean heat content (OHC) anomalies in the tropical Indian Ocean applying EOF analysis technique to the output derived from the ODAS. The time evolution of the first mode corresponds with the variations of monthly mean of u-component of wind stress anomalies over the central equatorial Indian Ocean and SST anomalies for Region B (nearly equal to NINO.3). This results suggests that the subsurface thermal structure in the Indian Ocean is in close connection with ENSO.

It is more difficult to investigate the physical structure in the Indian Ocean than the Pacific and the Atlantic, because of lack of observed data there. More *in situ* data such as the XBT data by "Kashimasan-Maru" are useful to understand the thermal structure of the Indian Ocean. We intend to further study the subsurface thermal structure in Indian Ocean further in order to understand the relation between the Asian Monsoon and ENSO which affect the global climate.

5. References

Ando, T., T. Yoshida and M. Kumamoto, 1994: JEXAM Annual report (April 1989 - March 1990), 33-44 (in Japanese).

Barnett, T. P., 1983: Interaction of the Monsoon and Pacific Trade Wind System at Interannual Time Scales. Part Ⅰ: The equatorial Zone. Mon. Wea. Rev., 111, 756-773.

Kimoto M., I. Yoshikawa and M. Ishii, 1997: An Ocean Data Assimilation System for Climate Monitoring, Journal of the Meteorological Society of Japan, 75, 1B, 471-487

Mikawa, T., and T. Mizuno, 1996: JEXAM Annual report (April 1995 - March 1996), 55-66.

Nicholls, N., 1984: The Southern Oscillation and Indonesian Sea Surface Temperature. Mon. Weather Rev., 112, 424-432.

Ropelewski, C. F., and M. S. Halpert 1989: Precipitation Patterns Associated with the High Index Phase of the Southern Oscillation. J. Climate, 2, 268-284.

Tourre Y., and W. White, 1995: ENSO Signals in Global Upper-Ocean Temperature. J. Phys. Oceanogr., 25, 1317-1332.

6. Publications

(Oral Presentation)

Mikawa T., and T. Mizuno, 1996: Seasonal Variation of the Subsurface Thermal Structure in the Indian Ocean in the Ocean Data Assimilation System of JMA. The International Workshop on the Climate System of Monsoon Asia. 3-7 December, 1996, Kyoto.

7. International Cooperation

None

（要旨）

日本とペルシャ湾を往復するタンカー「鹿島山丸」に、航路に沿った表層水温の観測・通報を依頼し、インド洋及び南シナ海の表層水温データを取得した。鹿島山丸及びその他の船舶により観測された表層水温データは気象庁の海洋データ同化システムで同化されている。本年度は同システムの結果を用いてインド洋における表層貯熱量の年々変動について調べた。まず、同システムの結果を表層水温観測データと比較した結果、同システムの結果は、表層水温の変動のパターンをかなり良く表現していることが判った。次に、同システムのインド洋熱帯域における表層貯熱量について、経験的直交関数(EOF)による解析を行った。その結果、EOFの第１モードには、南緯５～10度を中心としてインド洋西部赤道域に広がる変動パターンとスマトラ島沖のインド洋東部赤道域に逆符号で広がる変動パターンが見られた。その時系列は、アジアモンスーンの指標となるインド洋中部赤道域の海面応力の東西成分とともに、ENSOの変動シグナルであるＢ海域（NINO.3）の平均海面水温偏差の変動とかなり良く一致していた。これらの結果は、インド洋における表層貯熱量とENSOの関連が深いことを示唆している。

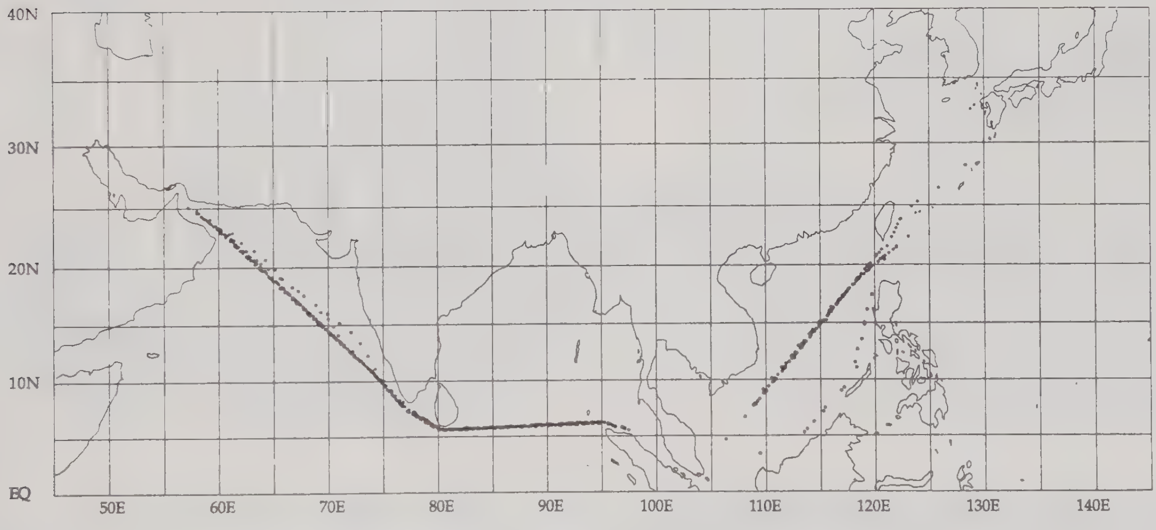
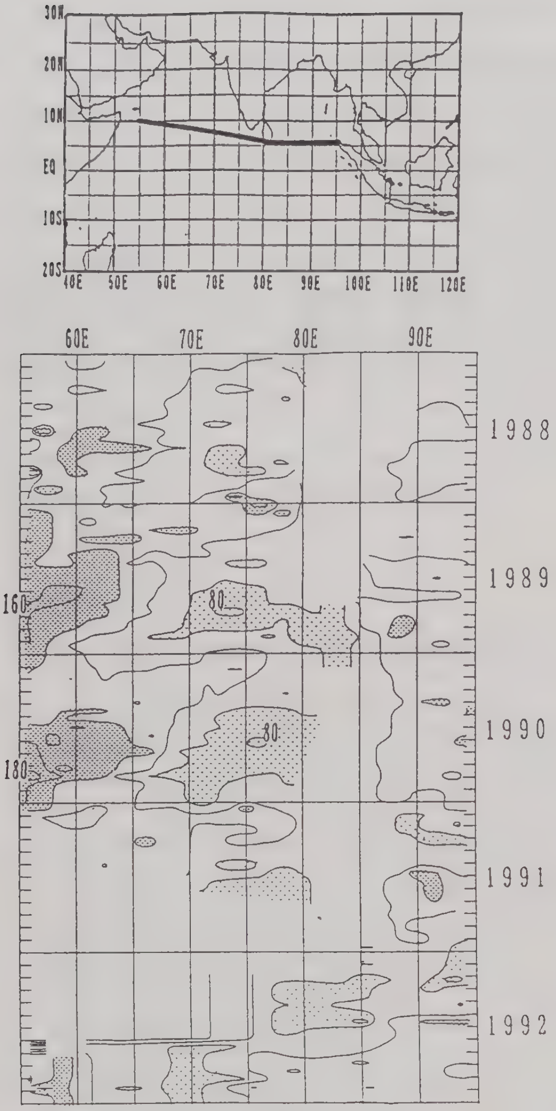


図１　委託商船「鹿島山丸」が航路上で1996年に観測した測点分布。

Fig. 1 Distribution of XBT's observation along the cruise tracks of "Kashimasan-Maru" for 1996.



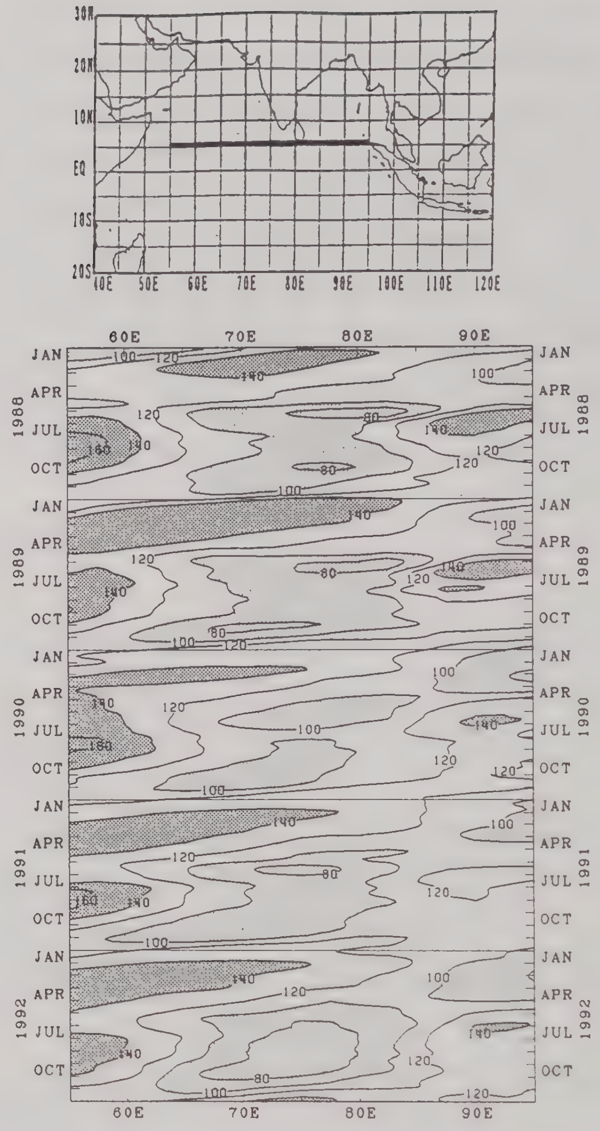


図2　安藤ら（1994）が表層水温観測データを基に解析した20℃等温線深度の時間－経度断面図。上図は解析したラインを示しており、船舶の定期航路に沿っている。

Fig. 2 Time-longitude section of D20 analyzed by Ando et al. (1994) using observed subsurface temperature data. Upper panel shows the analysis line along a regular ship route.

図3　気象庁の海洋データ同化システム（ODAS）による北緯6度線に沿った20℃等温線深度の時間－経度断面図。上図は解析したラインを示している。

Fig. 3 Time-longitude section of D20 along 6°N derived from the Ocean Data Assimilation System of JMA . Upper panel shows the analysis line along 6°N.

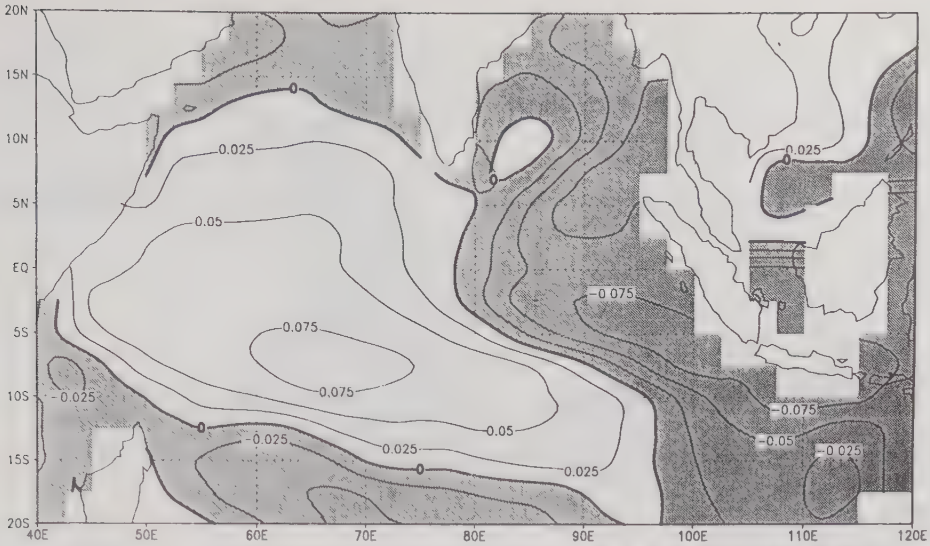


図４　気象庁の海洋データ同化システム（ODAS）による海洋表層貯熱量の平年偏差のEOF解析第１モードのパターン。EOF解析には緯度・経度ともに2.5度間隔の10年間（1987-1996年）のデータを用いた。

Fig. 4 The spatial pattern of the first EOF mode for OHC anomalies derived from ODAS of JMA. Data spacing is 2.5 degrees in longitude and latitude. The analysis period is 10 years (1987-1996).

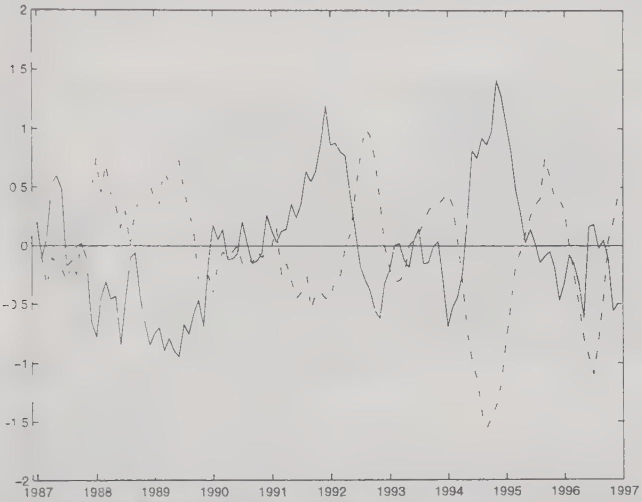


図５　気象庁のODASによる海洋表層貯熱量の平年偏差のEOF解析第１モードの時系列（実線）及びインド洋中部赤道域において領域平均した海面応力の東西成分（x50N/m^2）の平年偏差（一点鎖線）。

Fig. 5 The time sequence of the first EOF mode for OHC anomalies derived from ODAS of JMA (solid line) and the regional monthly mean of u-component of wind stress anomalies (x50N/m^2) over the central equatorial Indian Ocean (chain line).

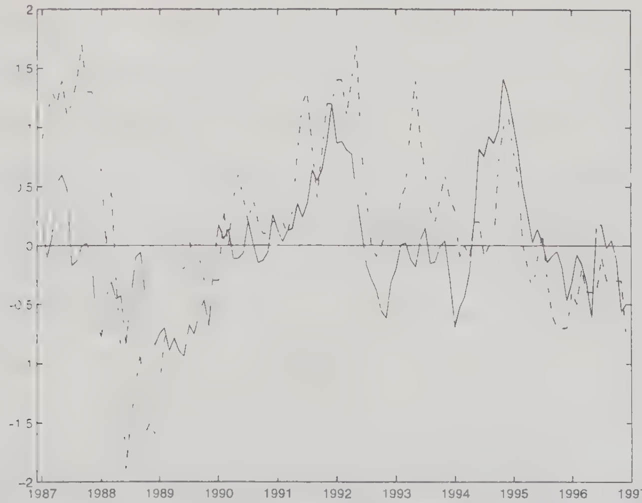


図６　実線は図５と同じ。破線は、太平洋東部赤道域のＢ海域（NINO.3とほぼ同じ）における海面水温の平年偏差（℃）。

Fig. 6 A solid line is the save in Fig. 5 and a broken line is the regional monthly mean of sea surface temperature anomalies (℃) for Region B (nearly equal to so-called NINO.3) in the eastern equatorial Pacific Ocean.

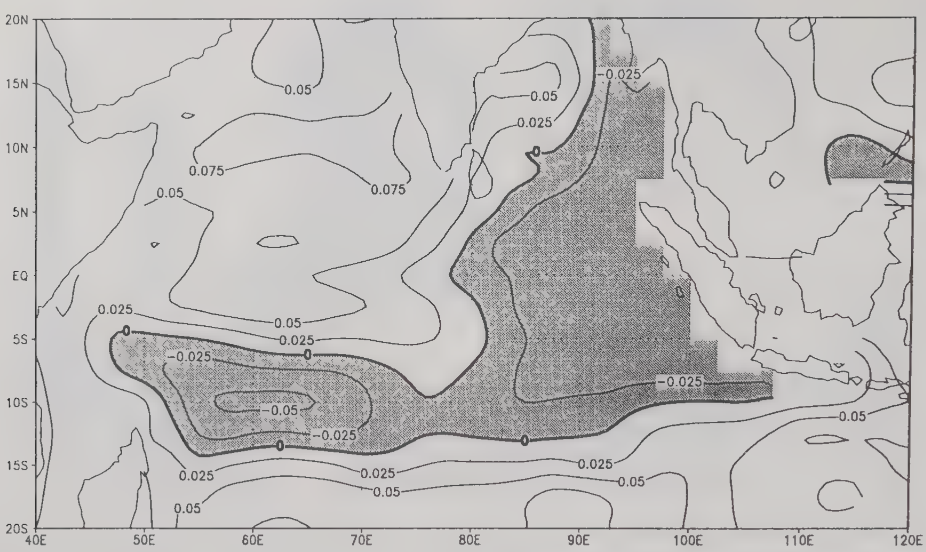


図７ 気象庁の海洋データ同化システム（ODAS）による海洋表層貯熱量の平年偏差のEOF解析第２モードのパターン。EOF解析には緯度・経度ともに2.5度間隔の10年間（1987-1996年）のデータを用いた。

Fig. 7 The spatial pattern of the second EOF mode for OHC anomalies derived from ODAS of JMA. Data spacing is 2.5 degrees in longitude and latitude. The analysis period is 10 years (1987-1996).

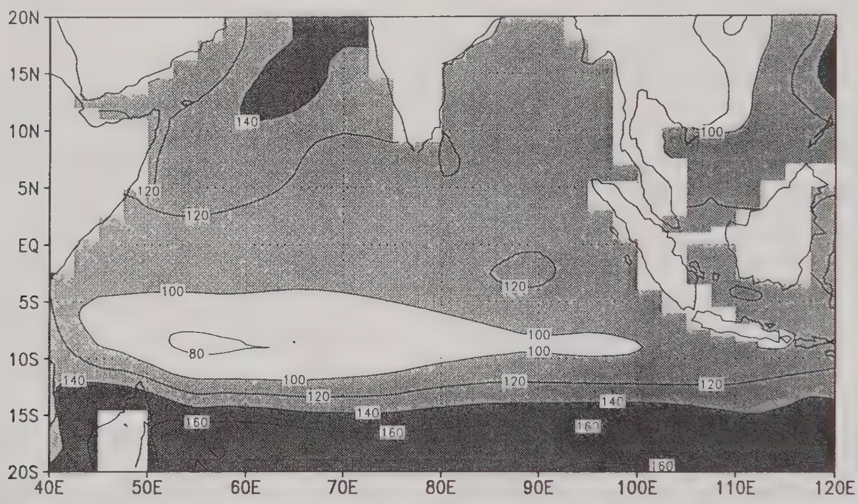


図８ 気象庁のODASによるインド洋における年平均20度等温線深度（m）。

Fig. 8 Annual mean of the depth of 20℃ isotherm (m) in the Indian Ocean derived from the ODAS of JMA.

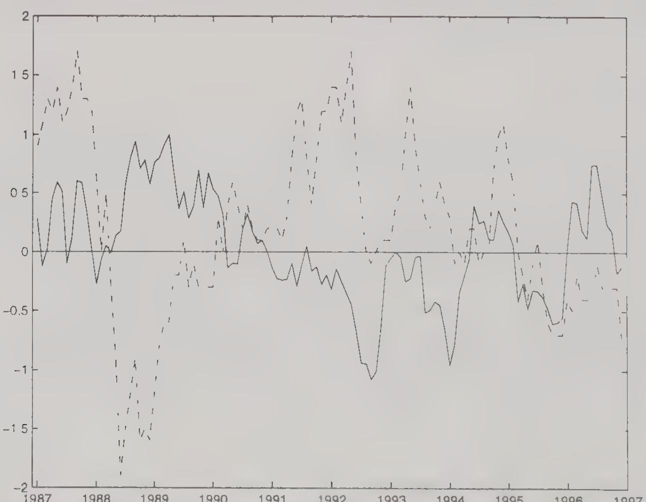


図９ 気象庁のODASによる海洋表層貯熱量の平年偏差のEOF解析第２モードの時系列（実線）及び太平洋東部赤道域のＢ海域（NINO.3とほぼ同じ）における海面水温の平年偏差（℃）（破線）。

Fig. 9 The time sequence of the second EOF mode for OHC anomalies derived from ODAS of JMA (solid line) and regional monthly mean of sea surface temperature anomalies (℃) for Region B (nearly equal to so-called NINO.3) in the eastern equatorial Pacific Ocean (broken line).

I. Observation and analysis on the process of the atmosphere-ocean-land interactions
2. Observation and analysis on the process over the ocean
(2) Observation on Oceanic Currents with Drifting Buoys

Hydrographic Department, Maritime Safety Agency
Hiroyuki Yoritaka, Yutaka Michida and Hideki Kinoshita

(Abstract)

Five drifters were deployed in the Arabian Sea on October 1996, to cover the area where very few buoys have been tracked in JEXAM programme. They were all released by National Institute for Far Seas Fisheries, Fisheries Agency, from a research vessel '*Wakatori-maru*' of Sakai Fisheries High School. Their tracks are described together with those of the previous drifters in this paper as the results of investigation for fiscal 1995. One drifter described reversal of the coastal current along Sumatra twice in two months. The drifters released in the Arabian Sea showed westward current in boreal winter due to north-east monsoon with the drifting velocity about 20 cm/s.

1. Objectives

Interannual variation of the Asian Monsoon, which has big influence upon the climatical variabilities in the region of south east Asia, may play an important role in the global climate change through the atmospheric general circulation. Some of previous studies have suggested that the Aisan Monsoon would cause changes in the oceanographic condition in the western tropical Pacific and should have close relationship with ENSO events. As a successful example of oceanographic research related to climate change, TOGA (Tropical Ocean and Global Atmosphere), whose major field was the tropical Pacific, provided so much knowledge on ENSO mechanism. In the Indian Ocean, on the other hand, there have been very few oceanographic data available in comparison with other oceans.

Forty-eight surface drifters were deployed by the end of 1996 in the Indian Ocean and tracked with ARGOS system within this research programme, Japanese EXperiment on Asian Monsoon (JEXAM) to illustrate the surface current system of the tropical Indian Ocean and the Seas adjacent to Indonesia, which is very interesting issue for oceanographers from the view points of, for examples, mass/heat/salt exchange between the Pacific Ocean and the Indian Ocean, or air-sea interactions there.

A schematic representation of the Indian Ocean currents and their seasonal changes has been proposed by *Molinari et al.* (1990), who have presented a monthly

climatology of surface currents by analysing historical drifter data. To investigate their results and to complement their study, trajectories of the drifters which are uniformly designed according to the recommendation of WOCE/TOGA SVP (Surface Velocity Programme) have been analysed in this study. The results of analysis for the drifters deployed in 1995 and 1996 are mainly described in this paper.

2. Methods

Six to ten drifters have been deployed in the Indian Ocean every year since 1990, the commencement of JEXAM programme. The drifters are designed according to the WOCE/TOGA SVP standard. A holey sock drogue of 8.6m in length whose drag center is at 15m below the sea surface is attached to the surface float that contains a processing unit for sensor data (sea surface temperature, on/off of the drogue and battery voltage) and a transmitter for ARGOS system. There is also a small subsurface float, which would reduce the tension of the tether between the surface float and the drogue (cf. *Michida and Ishii*, 1993; *Michida and Yoritaka,* 1995).

Five drifters were deployed in the Arabian Sea in October 1996, to cover the area where very few buoys have been tracked not only in JEXAM programme, but also in SVP. All the above drifters were released by National Institute for Far Seas Fisheries, Fisheries Agency, from a research vessel '*Wakatori-maru*' of Sakai Fisheries High School.

3. Results

The tracks of six drifters deployed in the western equatorial Indian Ocean and Arabian Sea in 1995 are shown in Figure 1. They were released along a meridional line across the Arabian Sea and on the equator east of Somalian coast during an expedition in the Indian Ocean on board the research vessel '*Shoyo-maru*' of Fisheries Agency.

These tracks in fiscal 1995 were analysed in *Michida and Kinoshita* (1996). Only one drifter(23914) trapped in the equatorial jet kept drifting in fiscal 1996, by the end of November. This drifter described reversal of the coastal current along Sumatra twice. Figure 2 shows daily drifting velocity and direction off Sumatra. It drifted south-eastward from April 30 to May 6 (Jurian day 121-127) with the drifting velocity 56-106 cm/s. It made cyclonic loop and drifted north-westward by June 1 (Jurian day 153) with drifting velocity 18-68 cm/s. It turned again south-eastward and drifted with drifting velocity 20-61 cm/s by June 18 (Jurian day 170). Then it drifted westward with South Equatorial Current.

The tracks of five drifters deployed in the Arabian Sea in 1996 are shown in Figure 3. They were released along a meridional line (64E) across the Arabian

Sea. They drifted westward and reached to the Arabian or Somarian coast except for the drifters with short life. Figure 4 shows westward velocity of these drifters including ones released in 1995. They generally drifted at 20 cm/s from November to February according to north-east monsoon.

4. Discussions

The drifters released in the Arabian Sea showed westward current in boreal winter due to north-east monsoon. In GFDL model (*Wacongne and Pacanowski*, 1996), there are no prominent circulation in the Arabian Sea in boreal winter. So they were drifted with north-east monsoon drift current. One drifter(27318) traced small eddy, but no drifter described large eddy simulated in the regional model (*Pal and Ali*, 1996).

The equatorial jet was described with the drifters (Michida and Kinoshita, 1996) and ADCP (*Mizuno and Watanabe*, 1996) in JEXAM programme. Figure 5 shows the positions of the drifters in JEXAM (1990-1997) around the equator (1S-1N). These show the westward monsoon drift current in boreal winter (from January to March) and the eastward equatorial jet in intermonsoon season (from April to June and from November to December). We can not discuss the longitudinal and year-to-year variations of the equatorial circulation due to few samples. For further analysis, preliminary examination of the satellite altimeter data was carried out. Figure 6 shows sea surface height anomaly in TOPEX/POSEIDON altimeter data on the equator. The higher surface in boreal summer and the lower surface in boreal winter are shown according to wind direction. On June and July, the lower surface appears in the westernmost part of the equator due to coastal upwelling. Only for 1994, the lower surface appears in the easternmost part according to weak westerly wind (*Mikawa and Mizuno*, 1996). For clarifying the mechanism of the variation in the tropical Indian Ocean, it is needed to continue investigating surface current with another source including altimeter.

5. References

Michida, Y. and H. Ishii, Observation of ocean circulation with surface drifters, *Kaiyo monthly,* extra 4 ,115-122,1993 (in Japanese).

Michida, Y. and H. Yoritaka, Survivability of the surface drifters deployed by Hydrographic Department of Japan for the period from 1988 to 1993, *J. Japan Soc. Mar. Surv. Tech.* 7(2), 21-28, 1995.

Michida, Y. and H. Kinoshita, Annual Report of JEXAM for FY1995, 67-74, 1996.

Mikawa, T. and T. Mizuno, Annual Report of JEXAM for FY1995, 55-66, 1996.

Mizuno, K. and T. Watanabe, Annual Report of JEXAM for FY1995, 45-54, 1996.

Molinari, R. L., D. Olson and G. Reverdin, Surface current distributions in the

tropical Indian Ocean derived from compilations of surface buoy trajectories, *J. Geophys. Res.* 95, 7217-7238, 1990.

Pal, P. K. and M. M. Ali, Arabian Sea eddies simulated by an ocean model with thermodynamics, *International WOCE Newsletter*, 24, 34-36, 1996.

Reverdin, G., The upper equatorial Indian Ocean: The climatological seasonal cycle, *J. Phys. Oceanogr.*, 17, 903-927, 1987.

Wacongne, S. and R. Pacanowski, Seasonal heat transport in a primitive equations model of the tropical Indian Ocean, *J. Phys. Oceanogr.*, 26, 2666-2699, 1996.

6. Publications

(1) Scientific Journals

Y. Michida and H. Yoritaka, Surface currents in the areas of Indo-Pacific throughflow and tropical Indian Ocean observed with surface drifters, *J. Geophys. Res..*, 101, 12475-12482, 1996.

Y. Michida and M. Yoritaka, A Comparison between the Tracks of Surface Drifters and Sea Levels Derived from Satellite Altimetry in the Seas Adjacent to Indonesia, Proceedings of International Workshop on the Throughflow Studies in and around Indonesian Waters, 177-183, 1996.

(2) Oral Presentations

Y. Michida and M. Yoritaka, A Comparison between the Tracks of Surface Drifters and Sea Levels Derived from Satellite Altimetry in the Seas Adjacent to Indonesia, Jakarta, Oct. 9-11, 1995.

7. International Cooperation

The deployments of drifters in JEXAM Programme have been contributing to WOCE/TOGA Surface Velocity Programme for re-description of ocean surface circulation.

（要旨）

「アジアモンスーン機構に関する研究（JEXAM）」の一環として、1989年以来実施してきた表面漂流ブイによる海流観測の空白域を埋めるため、1996年10月に水産庁遠洋水産研究所の協力を得て、境水産高校の「若鳥丸」から、アラビア海に計５個の漂流ブイを投入した。ここでは、平成８年度の研究成果としてそれらの軌跡及び過去のブイの軌跡を記述する。平成７年度に投入したブイのうち１個によってスマトラ沿岸の海流データが得られ、２カ月の間に２回反転する様子が得られた。アラビア海に投入されたブイからは、北半球の冬季に北東モンスーンによって駆動される西向きのモンスーン・ドリフトが観測され、その平均流速は約20cm/sであった。

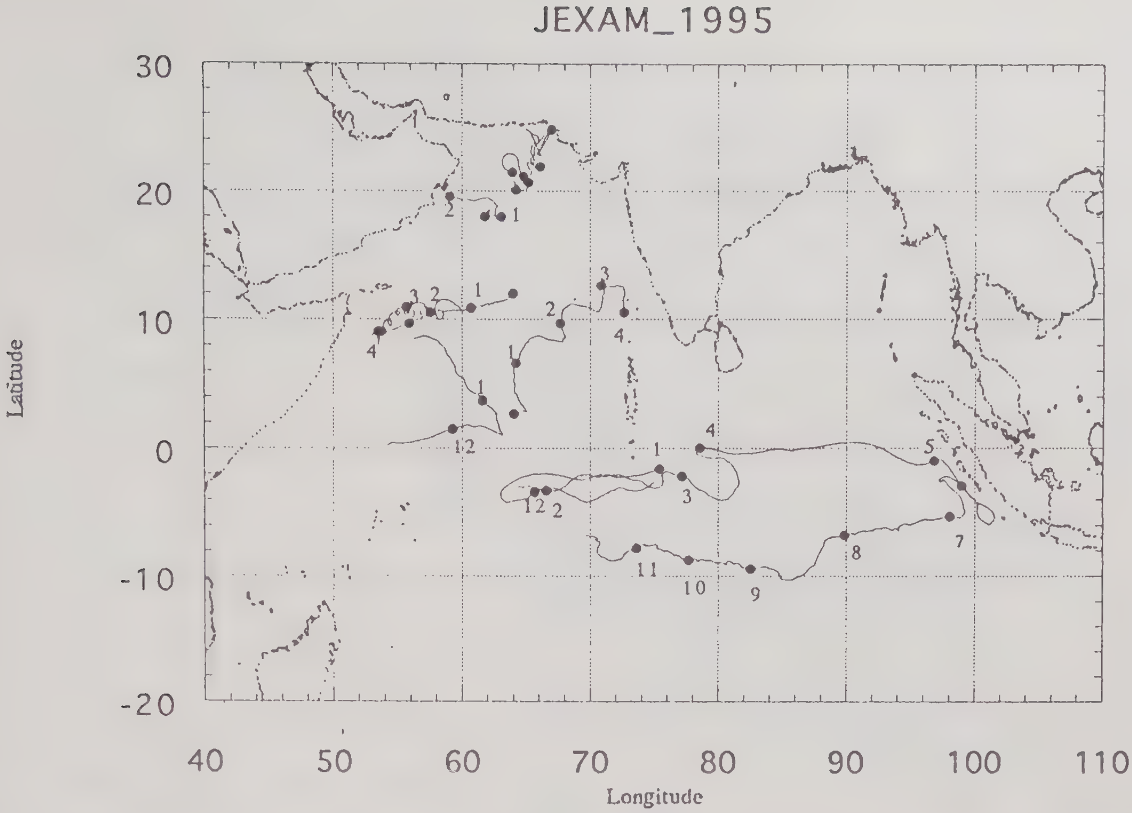


Figure 1. Trajectories of the drifters deployed in the western tropical Indian Ocean and Arabian Sea in November-December 1995. Solid circles mark the locations on the first day of every month, with the month number (January is 1, February is 2,..).

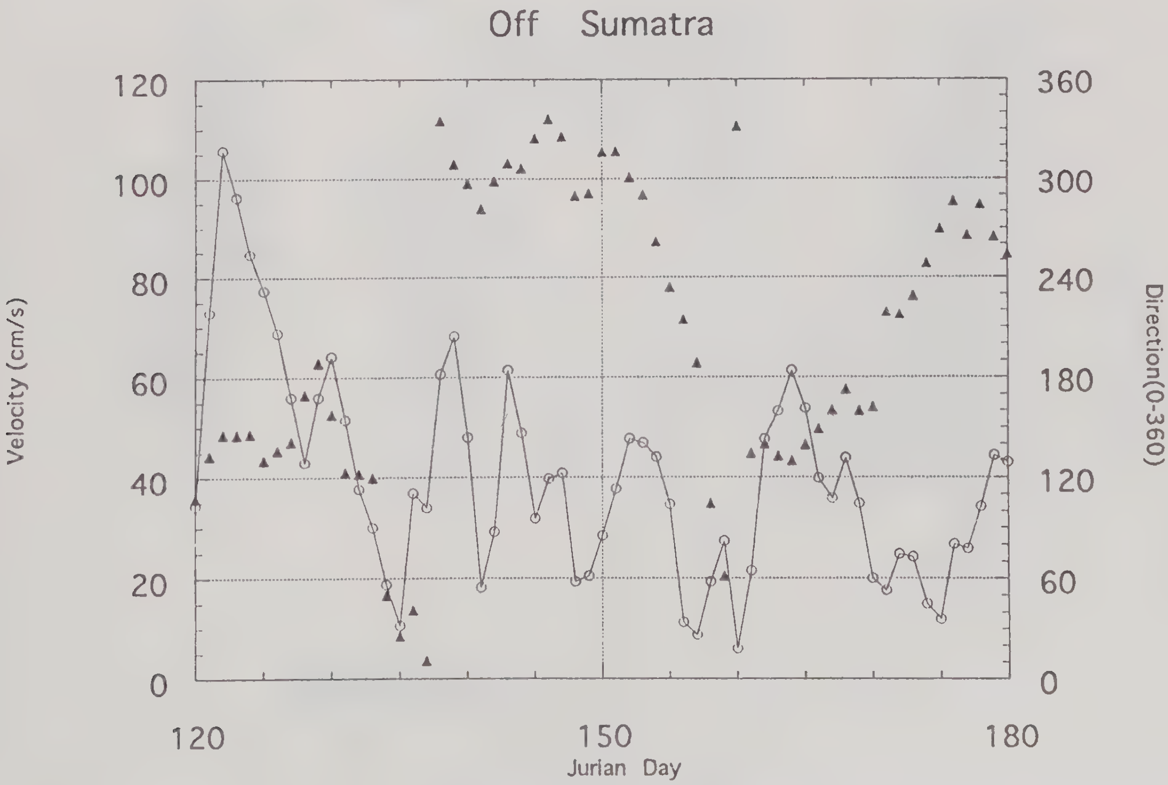


Figure 2. Time series of daily drifting velocity and direction off Sumatra. Solid line with open circles show velocity and solid triangles show direction.

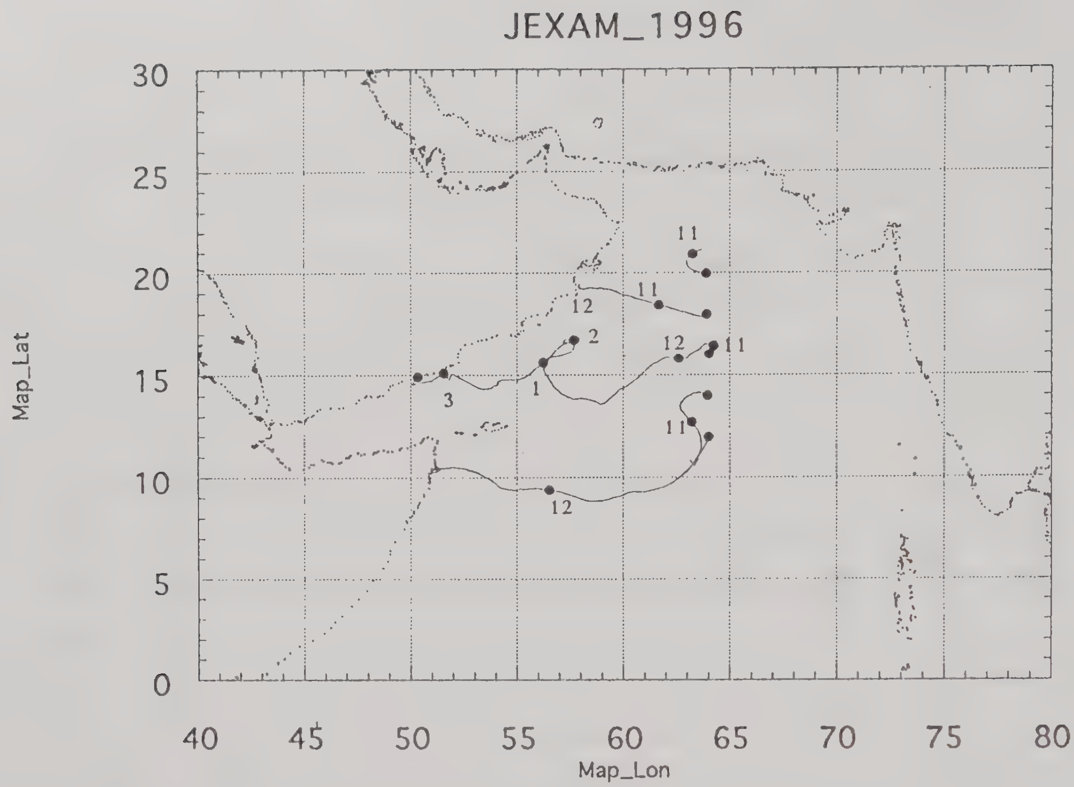


Figure 3. Same as Figure 1, except for the drifters deployed in the Arabian Sea on October 1996.

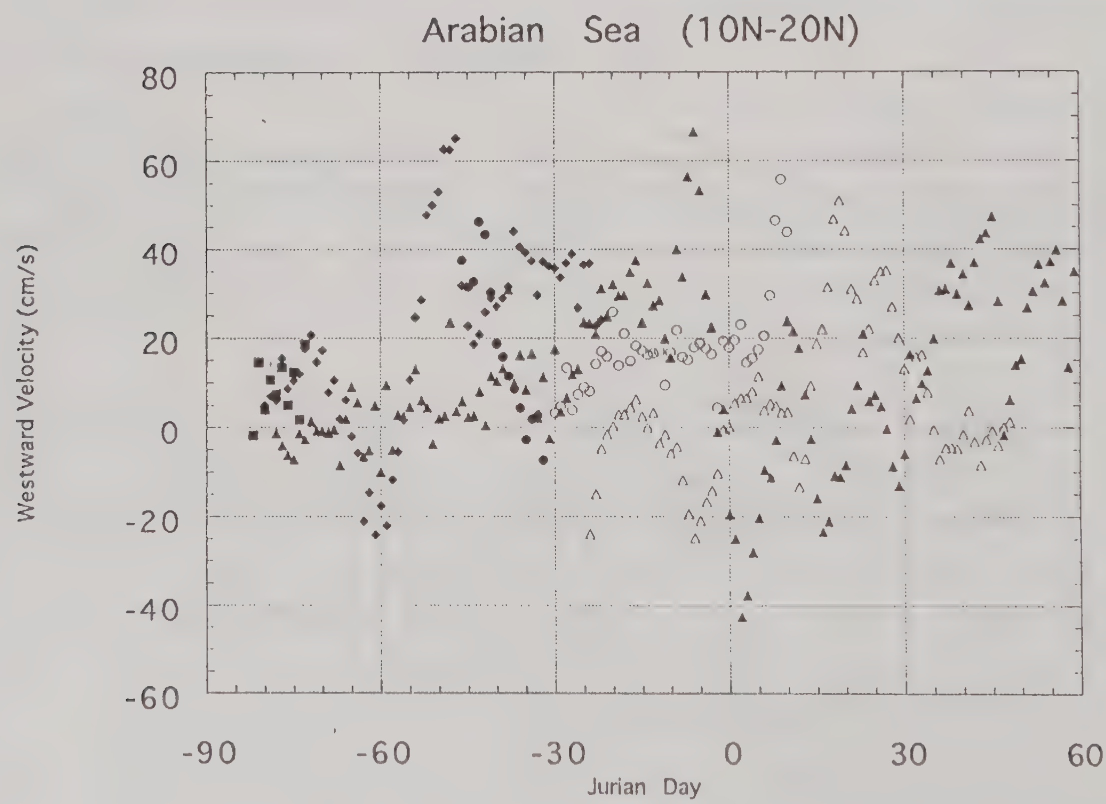


Figure 4. Time series of daily drifting westward velocity in the Arabian Sea (10N-20N). Open marks show velocity for the drifters released in 1995 and solid mark for ones released in 1996.

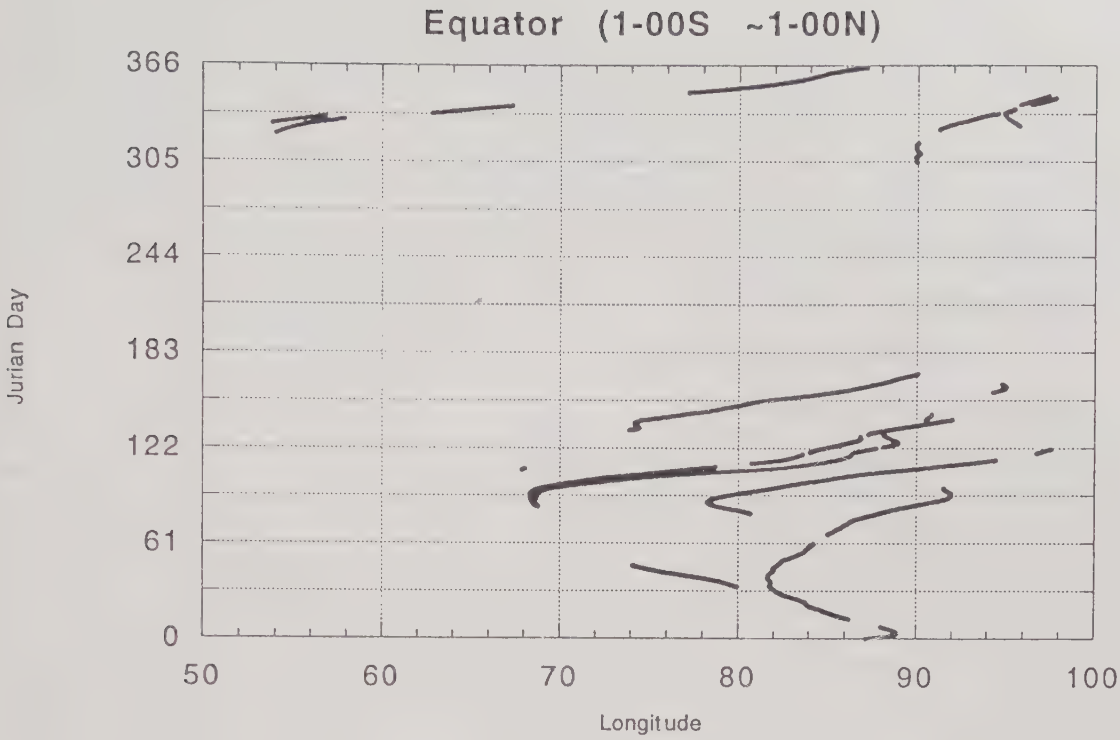


Figure 5. East-west trajectories of the drifters deployed in JEXAM since 1990 around the equator.

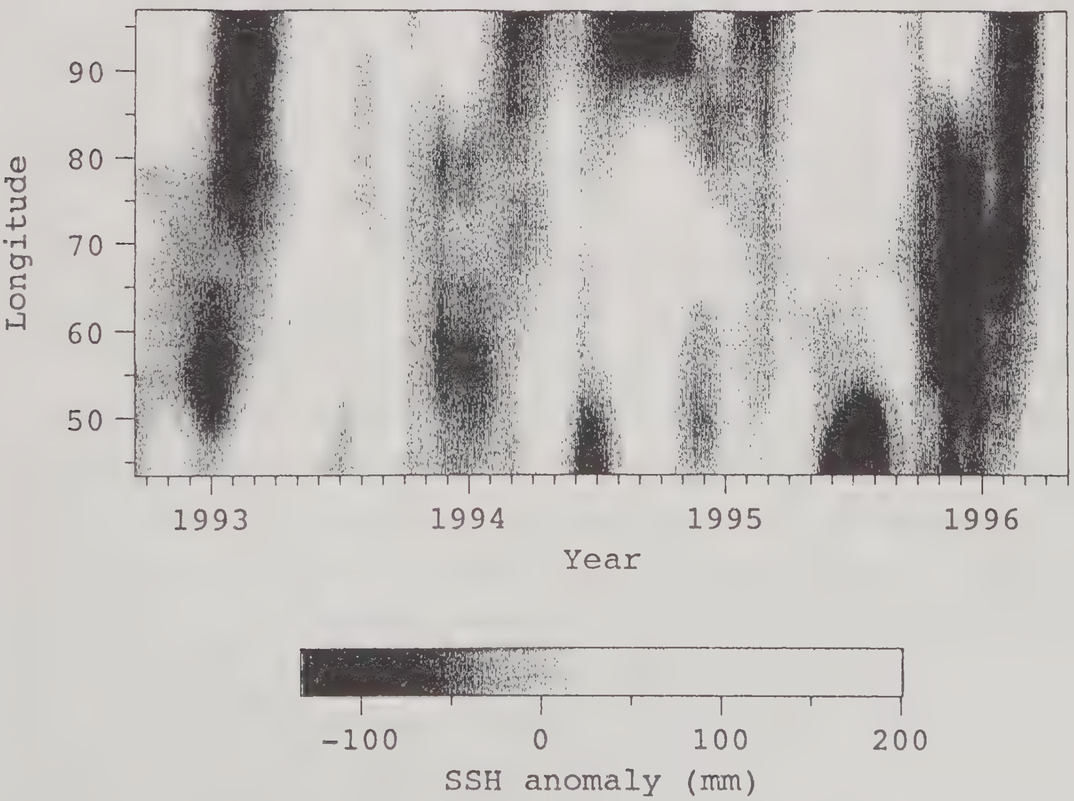


Figure 6. Sea surface height anomaly on the equator from TOPEX/POSEIDON altimetry.

I. Study on Air-Sea-Land Interactions and their Long Term Variations

2. Observation in the Indian Ocean

(3) Standardization of Oceanic Data and Promotion of Exchange of Oceanic Data and Information

Japan Oceanographic Data Center
Hydrographic Department
Maritime Safety Agency
Taiji Imoto, Yoshio Shimizu

(Abstract)

The purpose of study is to provide a sufficient data set and timely information for promoting the JEXAM programme. In order to suffice this goal, sub-themes have been established; data standardization and quality control of JEXAM data ; collection of existing data from other nations; establishment of international online network system for data and information exchange.

The JODC Online Information and Data Exchange Service (JOIDES) was added with information exchange system for NODCs, and JODC collected the information of oceanographic data resources for JEXAM in 1996.

1. Objectives

The purpose of this study is to provide researchers engaged in the "Japanese Experiment on Asian Monsoon" (hereinafter referred to as JEXAM) and research study on the Indian Ocean with the best available data set as well as information on research so that those studies can be carried out smoothly and effectively.

To achieve this purpose, oceanic data such as water temperature obtained through the "Observation in the Indian Ocean", one of the research subjects of JEXAM, will be standardized so that researchers can share their data with each other smoothly. In addition, existing oceanic data and information will be collected in order to provide full basic data for each study of JEXAM. Efforts will be also made to improve the accuracy of quality control of data by enhancing the reliability of statistics based on the obtained data.

In addition to such data management activity, a data base will be built, which permits on-line input/output or retrieval of information to check the state of data management or marine research programs with the view of speeding up distribution of information. Furthermore, a data information network system will

be established between national oceanographic centers of various countries and JODC to allow it to easily obtain cooperation from various countries for acquisition of data and information while another system will be established to allow Japan and other countries to share consistent oceanic data and information. Those systems will contribute to easy, fast and smooth use of oceanic data for JEXAM and to effective use of such data for various projects related to global environment.

2. Methods

(1) Support the system for fast and smooth distribution of data in this project through on-line computer network system, JOIDES.

(2) Standardize obtained data (water temperatures, ocean currents, drifting buoys), and building a data base of such data.

(3) Collect information and data on the marine research in the Indian Ocean.

3. Results

(1) On-line computer network system JOIDES

The system for fast and smooth distribution of information for this project is supported by the on-line computer network system JOIDES.

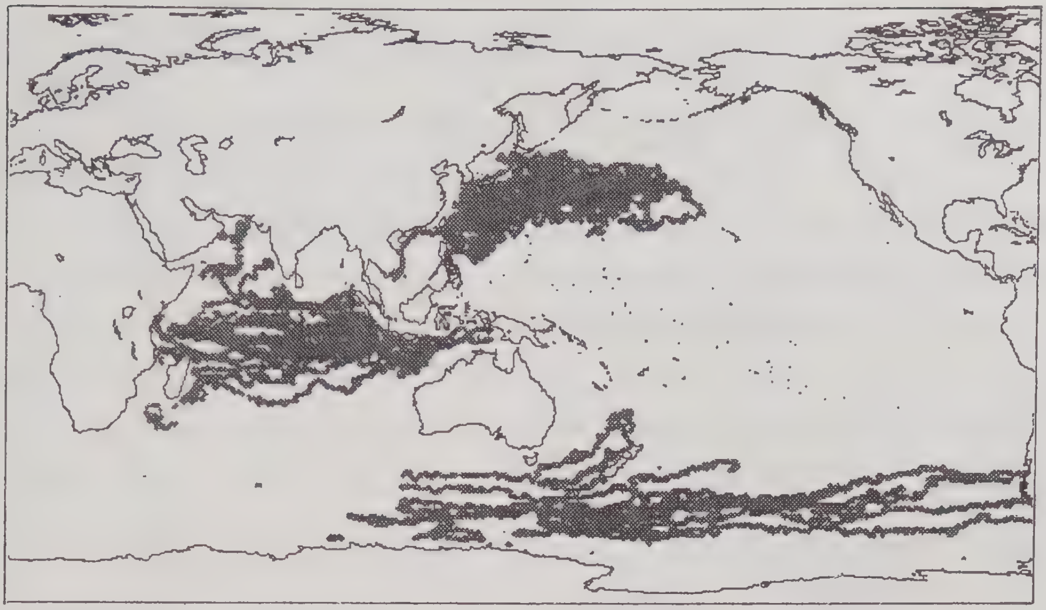
(2) Building a data base of observation data on the Japanese Experiment on Asian Monsoon

We received the drifting buoy data collected through ARGOS system from 1990 to 1996 from Hydrographic Department of Maritime Safety Agency and merge them into the database system developed in 1996 after standardization.

By providing the buoy number, observation date, latitude, longitude and project code, the necessary data can be extracted from the data base.
It is possible not only to see a catalogue of the observation areas of drifters but also to draw trajectories of selected drifters.

All trajectories of the drifters are shown in Fig. 1.

Fig. 1 All trajectories of the drifters deployed



(3)Collecting oceanographic information and data in the Indian Ocean

In order to support this research, a staff of JODC visited the organizations in charge of management of oceanographic data in India and Malaysia from March 11 to March 21, 1997 promoting the exchange of oceanographic data from the two countries.

The IODC (India Oceanographic Data Center) which belongs to the Indian Ocean Research Laboratory, collects and manages all data from its 11 coastal laboratories in India as well as the data from related domestic organizations (including those from nearby countries). A network system is being prepared in those laboratories and it has been confirmed that in the near future, there will be extensive online information exchange between the two countries.

In Malaysia, a staff of JODC visited the Coastal and Offshore Engineering Institute of University Technology Malaysia (the organization planning to establish an oceanographic data center) and the Hydrographic Department of the Navy (Designated National Agency : DNA).

At present, there is no organization in charge of management of all oceanographic data in Malaysia. However, the chief of the Hydrographic Department acts as chairperson of the committee which manages national oceanographic data. And procedures to establish an organization in charge of management of oceanographic data in the future is well underway. Not only the necessity for oceanographic data management is recognized; one can see that the technology in both countries has improved and it was confirmed that systematization of oceanographic data management is rapidly taking place.

4. Discussions

In the past, JODC has supported the information flow system of this project through the JOIDES computer network. However, recently the number of researchers using the internet has increased and in the future, in order to quickly exchange information and data within the project , a transfer is quickly being made to a data exchange system through the internet.

In addition, for international mutual exchanges of data, the IODC (India Oceanographic Data Center) began activities as the Responsible National Oceanographic Data Center (RNODC) for Indian Ocean in 1996. This center is compiling an online database and because it is scheduled to undergo major improvements in the first half of 1997, mutual exchange of oceanographic data is expected to go smoothly in the future.

（和文アブストラクト）

本研究は、「アジアモンスーン機構に関する研究」（以降JEXAM）及びインド洋に関する調査研究の円滑かつ効果的な実施を図るため、当該研究に携わる研究者に対し、利用可能な最良のデータセット及び調査に係る情報を提供するためのものである。この目的を達成するために、JEXAM関連データとして海上保安庁水路部から、漂流ブイデータを受領し、これを標準化した後データベースシステムに登録するとともに、パソコン通信システムJOIDESにより、本プロジェクトにおける情報の円滑かつ迅速な流通体制の支援を行なった。

また、インド洋での海洋調査情報及びデータの収集を図ることを目的として、JODC職員がインド及びマレーシア両国の海洋データ管理担当機関を訪問し、両国の現状を調査した結果、今後日本とのオンラインによる情報交換が緊密になること等が確認できた。

Ⅰ. Observation and analysis on the process of the atmosphere-ocean-land interactions

大気・海洋・陸域間相互作用の諸過程に関する観測・解析研究

3. Observation and analysis on the process over the land

陸域における諸過程に関する観測研究

(1) Observation on Hydrology over the Tibetan Plateau and Himalayas

チベット・ヒマラヤにおける水文変動に関する観測研究

Shinjo Branch of Snow and Ice Studies,
National Research Institute for Earth Science
and Disaster Prevention,
Science and Technology Agency
Takeshi Sato
防災科学技術研究所
新庄雪氷防災研究支所
科学技術庁
佐藤　威

1. Objective

Snow cover and frozen ground in the Tibetan Plateau have great influence not only on the Asian Monsoon activity but also on the global climate system (e.g. Yasunari et al., 1991). In order to understand the mechanism of the Asian Monsoon, seasonal and inter-annual variations of snow cover and frozen ground should be clarified and the quantitative relationship between them and the Asian Monsoon activity should be studied. In this study, automatic observations of snow cover and frozen ground have been carried out since 1993 summer at three sites (Lhasa, Rikeze and Nagqu) in the Tibetan Plateau, as the cooperative study with China Meteorological Administration.

2. Methods

The snow weight meter to measure the weight (water equivalent) of accumulated snow is almost the same as that commonly used in Japan (Kimura, 1983). Four metal wafer units are used to support the accumulated snow, in which unti-frozen liquid is filled. The snow on the metal wafer units leads to the change of inner pressure within the units, which is detected by the pressure sensor and converted to the snow weight. The ground temperature just below the metal wafer unit is measured by Pt resistance thermometer to correct the temperature dependence of the snow weight meter.

The sensor unit of the frozen ground depth meter (FDM2) is a FRP cylinder, 225cm long and 1.6cm in diameter, in a Silicon rubber tube. Deaired water is filled between the sensor unit and the tube (Kimura, 1992). The sensor has 104 electric terminals, separated 2cm from each other, to detect the freezing of deaired water around the terminals by measuring the resistance between the detection

terminals and the one common terminal. In July, 1995, the frozen ground depth meter was changed from FDM2 to FDM3, whose scanning method is improved and the structure of sensor unit is changed (Sato, 1996). However, the principle of the measurement is the same.

At every site, the instruments were installed in the precinct of the meteorological observatory. Meteorological Research Institute started micrometeorological observations at the same sites. Summary of the observations are shown in Table 1. No significant snow weight was recorded at Lhasa and Rikeze in 93/94 and 94/95 winters.

3. Results

3.1. Frozen ground depth

An observed frozen ground at Nagqu in 93/94 winter is shown in Fig.1 together with the routinely measured frozen ground. Until the end of December, frozen ground layer grew and the observed data coincided with the routine data. After that, the observation indicates that the frozen ground layer was getting deep until the beginning of March and it attained maximum (158cm). However, the routine data shows that the development continued until the beginning of April and the maximum depth was 200cm. The decay of the frozen ground layer was faster in the observed data than in the routine data. The data in 94/95 winter has a similar tendency as in 93/94 winter.

The discrepancy between the observed and routine data in the decay stage may be ascribed to the fact that the soil temperature between the depths of 40cm and 160cm at this stage was close to 0°C and its vertical gradient was very small. In this situation, small disturbance of the soil and/or sensor temperature would affect the measurement of frozen ground layer.

The maximum frozen ground depths at the three sites are summarized in Table 2. The frozen ground layer at Lhasa and Rikeze was thin and confined to near the ground surface.

The maximum frozen ground depth D (cm) can roughly be expressed by the following equation (Kinoshita, 1982):

$$D=\alpha\sqrt{I}, \qquad (1)$$

where I (°C·day) is an accumulated freezing index defined by

$$I=\Sigma T. \qquad (2)$$

Here, T (°C) is a daily mean ground surface temperature, and the summation is made for only negative values of T. The values of α for the three sites are listed in Table 2. At Nagqu, α is larger than 2.0-2.5, which were obtained in Hokkaido, Japan, where the soil would be wetter than Nagqu.

The heat budget of the ground at Nagqu during the freezing stage will be discussed below. Here, the freezing stage is the 90 days period from the date when the ground surface temperature attained 0°C. The routine soil temperature profile was integrated to estimate the heat storage. The heat capacity for each winter was assumed based on the observed soil moisture in the autumn of 1995, amount of precipitation in the preceding summer (July to September) and the measured soil density. The latent heat associated with the soil freezing was also estimated with the assumed soil moisture. The observed net radiation was averaged over the period and the sum of turbulent sensible and latent heat fluxes was obtained as the residual. The results are shown in Fig.2. Due to strong solar radiation and low albedo, the net radiation is positive and the ground is cooled by the turbulent fluxes.

The latent heat of freezing cannot be neglected in the heat budget.

3.2. Snow Weight

The snow cover at Nagqu did not last for a long period in both 93/94 and 94/95 winters. An example of the snow weight at Nagqu is shown in Fig.3(a), where the routinely measured snow depth is also shown in the lower part. The daily averaged albedo and air temperature are shown in Fig.3(b) and Fig.3(c), respectively. The snow weight in 94/95 winter was corrected by using the ground temperature, and the error in the snow weight values is considered to be within $\pm 3kg/m^2$.

The snow density at Nagqu was calculated from the observed snow weight and the routine data of snow depth (Fig.4). During the snow covered periods from January to February, 1995, the snow density did not change largely and was about $0.1g/cm^3$. This value corresponds to the that for the new snow observed in Japan. Small snow density indicates that the densification of snow was not remarkable due to the thin snow cover and low temperature.

4. Concluding Remarks

Since the development of frozen ground is governed by the heat conduction with the phase change of water in the soil, frozen ground depth depends on the thermodynamic property of the soil including the soil moisture. After July, 1995, the soil moisture has been observed continuously at the three sites, which will be useful in the quantitative discussion on the variation of frozen ground depth and in the heat budget analysis.

5. References

Kimura, T., 1983 : Observation of water equivalent of snow cover by metal wafer., *Report of the National Research Center for Disaster Prevention*, 31, 203-217. (in Japanese with English abstract)

Kimura, T., 1992 : Observation on hydrologic variations in Tibet-Himalaya area., *Annual Report of Japanese Experiment on Asian Monsoon,* Research and Development Bureau, STA, 80-83. (in Japanese)

Kinosita, S. (ed.), 1982 : *Physics of frozen ground.*, Morikita Shuppan, 227pp. (in Japanese)

Sato, T., 1996 : Observation on hydrology over the Tibetan Plateau and Himalayas., *Annual Report of Japanese Experiment on Asian Monsoon*, Research and Development Bureau, STA. (in English with Japanese abstract, in press)

Yasunari, T., A. Kitoh, and T. Tokioka, 1991 : Local and remote responses to excessive snow mass over Eurasia appearing in the northern spring and summer climate., *Journal of Met. Society of Japan*, 69, 1033-1049.

6. Publications

Author	Title	Name of Publications	Notes
(report)			
T. Sato and S. Haginoya	Continuous measurements of frozen ground and snow in Tibet	Proceedings of the International Workshop on the Climate System of Monsoon, Dec., 1996.	
(oral)			
T. Sato *et al.*	Continuous measurements of snow weight and frozen ground depth in the Tibetan Plateau (3)	Japanese Society of Snow and Ice. Preprints of the presentation, Sept., 1996.	

7. International cooperation

The observations of the snow weight and frozen ground have been carried out as the cooperative study with China Meteorological Administration. National Research Institute for Earth Science and Disaster Prevention invited Prof. Liu Guangxuan (Tibetan Meteorological Bureau of China) for 17 days in 1996. At the same time, Meteorological Research Institute invited Mr. Li Guoping (Chengdu Institute of Meteorology). During their stay in Japan, we discussed the cooperative study, research themes and so on.

（要旨）

本研究ではチベット高原に３ヶ所（ラサ、シガセ、ナチュ）の積雪重量（相当水量），地温，凍結深度の自動観測点を設置し、長期間のデータを蓄積するとともに、積雪、凍土の変動ならびにそれらとアジアモンスーンの関係を解析する。1993年７月に中国側研究者の協力を得て、積雪重量計及び凍結深度計を設置し連続観測を開始している。

1993年７月から1995年７月のデータを解析し、以下の結果を得た。ナチュにおける93/94冬期及び94/95冬期の最大凍結深度は、いずれもルーチン観測より小さい値であった。また、凍結深度の季節変化をみると、厳冬期以前は観測値とルーチンデータは一致するが、厳冬期以降は一致しなかった。これらの食い違いの原因として、地中の温度勾配が小さいために、わずかの温度の誤差や場所による違いが凍結深度の値を大きく変える可能性が示唆された。

ナチュにおける凍土の発達期（90日間）の平均的な熱収支を、土壌の熱物理定数と含水率を推定して求めた。この結果、正味入力放射は正であり、地表面は乱流熱輸送により冷却していることが明らかになった。また、土壌の凍結の潜熱が無視できないことがわかった。

積雪重量の補正方法を改良することにより、測定精度は±３kg/m²まで向上することができた。ナチュにおいて積雪が長期間継続することはなかったが、1995年１月～２月の間の積雪があるときの積雪密度は、変化が小さく0.1g/cm³程度であった。これは積雪が少なく、また低温であるために圧密があまり起こらなかったことを意味する。

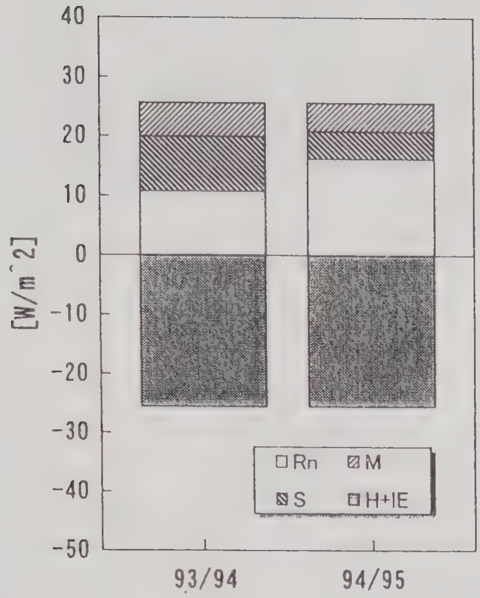


Figure 2 Heat budget of the ground during the freezing stage (Nagqu).
ナチュの凍土発達期の熱収支。

Rn: net radiation, S:heat storage, M:latent heat of freezing, H+lE: sum of turbulent sensible and latent heat fluxes.
Rn: 正味入力放射, S:貯熱量,
M:凍結の潜熱,
H+lE:乱流による顕熱と潜熱の和

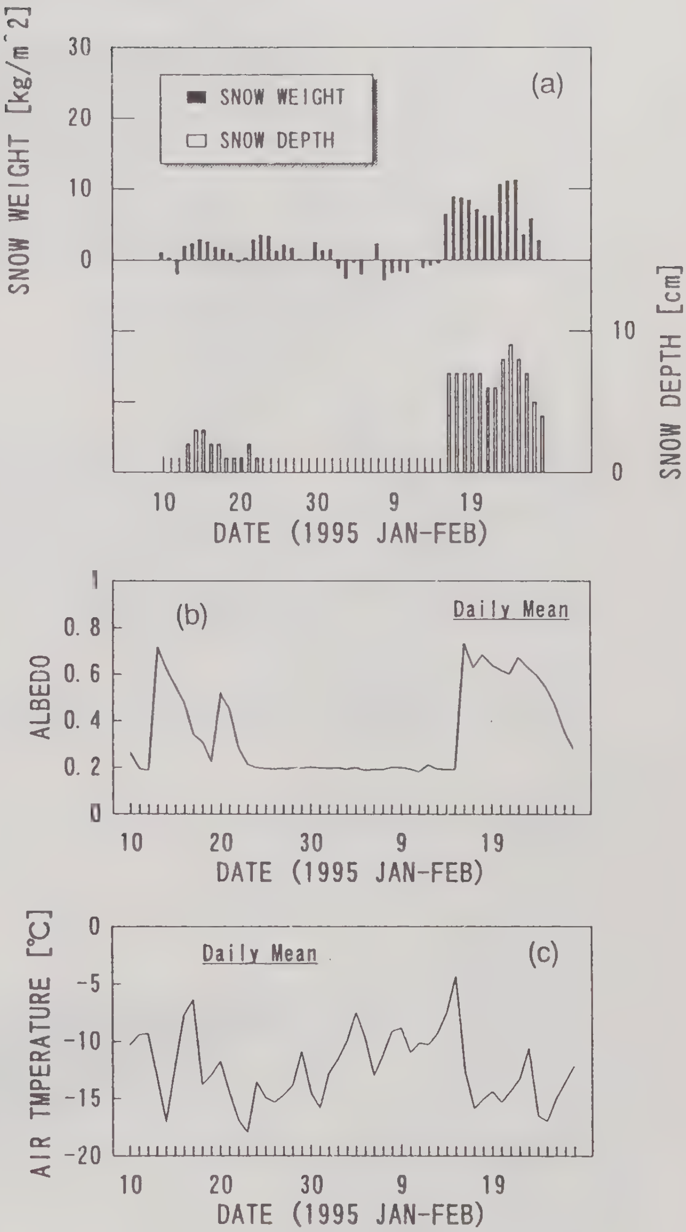


Figure 3 Time series of observed snow weight (upper) and routinely measured snow depth (lower) at Nagqu in 94/95 winter (a), and those of albedo (b) and air temperature (c).
ナチュにおける94/95冬期の積雪重量(上)とルーチン観測による積雪密度(下)(a)、アルベド(b)、気温(c)

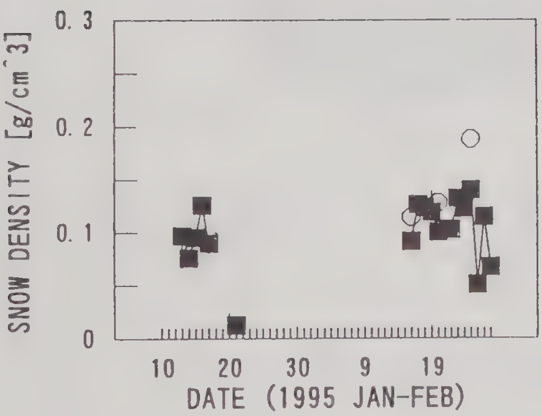


Figure 4 Snow density at Nagqu in 94/95 winter.
ナチュにおける94/95冬期の積雪密度。
■:observation,
○:routine measurement.
■:観測値, ○:ルーチン観測値

Table 1 Summary of observations in 93/94 winter and in 94/95 winter.
93/94冬期と94/95冬期の観測のまとめ。

Site	Frozen Ground Depth		Snow Weight		Ground Temperature	
	93/94	94/95	93/94	94/95	93/94	94/95
Lhasa	×	△*1	○	○	○	○
Rikeze	△*1	○	△*2	△*4	○	○
Nagqu	○*1	△*3	○	○	×	△*4

○: no trouble, △:see captions , ×: sensor broke.
*1 : Total number of data disagrees with snow weight data
*2 : Large drift
*3 : Some ambiguity in data
*4 : Partly bad

Table 2 Summary of the maximum frozen ground depth D and the coefficient α obtained from the routine data.
最大凍結深度Dとルーチンデータから求めた係数 α

Site	93/94			94/95		
	D (cm)		α	D (cm)		α
	Obs.	Routine		Obs.	Routine	
Lhasa	-	13	1.5	0	15	1.6
Rikeze	12	35	3.0	12	42	3.0
Nagqu	158	200	6.0	134	177	5.0

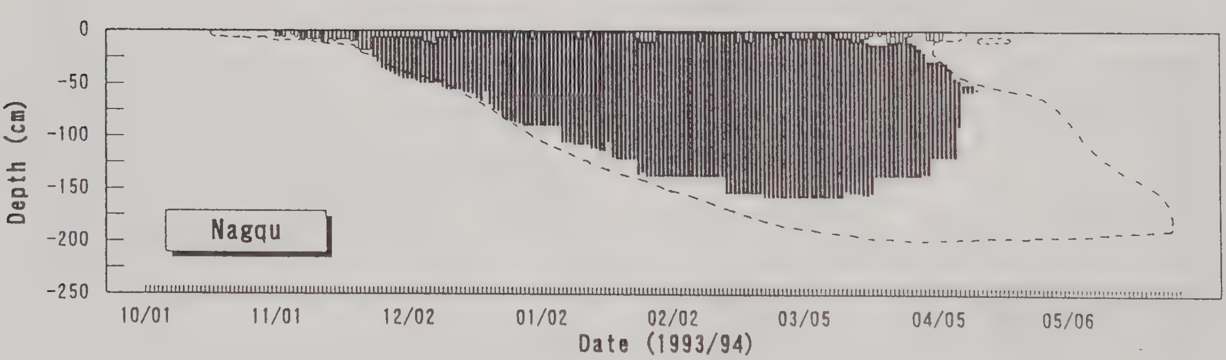


Figure 1 Seasonal variation of the frozen ground at Nagqu (93/94 winter).
ナチュにおける93/94冬期の凍結深度の季節変化。

White bar indicates a daily active layer near the ground surface and the black bar indicates a frozen ground layer. Dashed line is the routine measurement.
白棒は地表面付近の日活動層、黒棒は凍結層を表す。
破線はルーチン観測による凍結深度。

I. Observation and analysis on the process of the atmosphere-ocean-land interactions
大気・海洋・陸域間相互作用の諸過程に関する観測・解析研究

3. Observation and analysis on the process over the land
陸域における諸過程に関する観測・解析研究

(2) Observation on Regional Surface Heat Budget
地表面熱収支に関する観測研究

Meteorological Research Institute,
Japan Meteorological Agency
S. Haginoya and H. Naoe
気象庁 気象研究所
萩野谷 成徳・直江 寛明

(Abstract)

In order to clarify the mechanism of the Asian Monsoon caused through Air-Sea-Land interactions, the large-scale heat budgets over two different areas should be estimated: Tibetan-Himalaya Mountains Area and the Indian Ocean-South China Sea Area. This study aims to collect the basic meteorological data and to estimate large-scale heat budgets over the two areas.

Field observation has been carrying out in the Tibetan Plateau in 1996 FY. This paper describes the following results through the observations and data analysis.

(1) Tibetan Plateau

The four sets of Automatic Weather Station (AWS) were installed and continued observation in the Tibetan area since summer 1993. Japanese scientist visited four AWS sites (Lhasa, Rikeze, Nagqu and Lingzi) and one western station (Gaize) in June to July 1996. Gaize station is representative place in western Tibet which is located in the rural area on the opened plateau. Its elevation is about 4,400m. There is an undulating plain. Ground surface is bare soil, few grass and no tree. To estimate the regional averaged sensible heat flux, barometer was installed at the middle of the mountain area near Lhasa site. The wind field at Lhasa site was investigated. Surface wind direction is along the valley which shows typical mountain and valley wind. This accompanies the daily variation of surface layer pressure and temperature. The regional averaged sensible heat flux at Lhasa site was estimated from surface pressure variation and upper air data. The averaged sensible heat flux is much larger than the local surface heat flux at Lhasa site. This is caused by the effect of horizontal convection. Downward and upward long wave radiation were estimated. Void ratio and saturated hydraulic conductivity of sampled soil were measured. Void ratio is scattered from 40% to 50%. Saturated hydraulic conductivity is about $1 \times 10^{-4} ms^{-1}$. The water content is good correlation to the rainfall amount in monsoon period. Just after rainfall, water content of the shallower layer increased up to 30%. After non rainfall condition continues for a few days, water content decreased by 10%. Its variation of the deeper layer delayed several days and its amplitude was smaller than the shallower layer.

(2) Indian Ocean

AWS observations were made on Osaka-Maru from October 1991 to October 1995. She made six times round trips between Japan and Republic of South Africa through the South China Sea, the Strait of Malacca and the Indian Ocean. Heat balance are estimated from observation data. In the Indian Ocean (from 25S to the

equator), yearly net heat flux is about $+20Wm^{-2}$. This means that net heat flow is from the atmosphere to the Ocean.

1. Objectives

In order to clarify the mechanism of the Asian Monsoon caused through Atmosphere-Ocean-Land interactions, the large-scale heat budgets over two different areas should be estimated: Tibetan-Himalaya Mountains Area and the Indian Ocean-South China Sea Area. Because of the vastness of the areas and of their unsuitable conditions for observations, observatories or ships in these areas are very sparsely distributed. Therefore the basic meteorological data to clarify the mechanism of the Asian Monsoon has been lacking. This study aims to collect these basic data and estimate large-scale heat budgets over the two areas.

2. Methods

Since the heat budgets in two areas are studied by different methods, they are described separately.

(1) Tibetan Plateau

The four sets of Automatic Weather Station (AWS) were installed in the Tibetan area in summer 1993. Observation sites are Lhasa, Rikeze, Nagqu and Lingzi[1)]. The observation were carried out continued from last fiscal year. Japanese scientist visited 4 AWS sites mentioned above and one western station (Gaize) in June to July 1996. The last station, together with another western station (Shiquanhe), is planned to be installed new AWS in 1997F.Y. He investigated the road conditions on the way to Gaize, its filed of observatory and around the topography. Japanese and Chinese side installed the barometer at the middle of the mountain area near Lhasa site. It's elevation is about 4700m above mean sea level. The aim of this observation is to estimate regional sensible heat flux from the time and height variation of pressure. He also supported data collection and AWS maintenance. Soil samples were collected in each site and soil water content and soil parameter were measured. Chinese side checked AWS every month and collected data twice a year. Chinese side finished the first data collection in July 1996, the second data collection in January 1997. Collected data were sent to Japan by mail. Routine surface meteorological data of 9 stations in Tibetan area from January to December 1995 were collected. Routine aerological data of 2 stations (Lhasa and Nagqu) in Tibetan area from January to December 1995 were collected. Routine radiation data of 2 stations (Shiquanhe and Changdu) in Tibetan area from May 1993 to December 1995 were collected.

(2) Indian Ocean

AWS observations were made on the Osaka-Maru (31,382GT) of Mitsui O.S.K. Lines, which made 24 times round trips between Japan and Republic of South Africa through the South China Sea, the Strait of Malacca and the Indian Ocean from October 1991 to October 1995[1)]. Surface heat balance are estimated from observation data.

3. Results

(1) Tibetan Plateau

Japanese scientist visited 4 AWS sites and one western station in summer 1996. The four AWS sites had been already summarized[1)]. Gaize site is summarized here. This site is located at the middle of western Plateau, about 730km west-north-west of Lhasa. Its elevation is about 4,400m mean sea level. This site is representative place in western Tibet which is located in the rural area on the opened plateau. There is an undulating plain. Ground surface is bare soil, few grass and no tree. Gaize climate

conditions are characterized by large sunshine duration, strong wind, large amplitude of air temperature and dry air.

The wind field at Lhasa site was investigated. This site is located at the bottom of valley and its direction is west to east. The valley inclines toward the west. The wind characteristics on daily cycle are as follows. Surface wind direction is along the valley which is eastward in the daytime and westward in the night time. This shows typical mountain and valley wind. This accompanies the daily pressure and surface layer temperature variation. Upper air wind direction is also analyzed. In the morning, wind direction at 300m level above the ground is independent of above 600m level. In the afternoon, 300m level wind correspond to 600m and 900m level wind.

Surface pressure variation is the measure of the heating or cooling amount of air column. So that the pressure variation is used to estimate the regional averaged sensible heat flux surrounded by mountains. The data at Lhasa site is suitable for this purpose. The average sensible heat flux at Lhasa site was estimated. This site also carries out routine upper air soundings twice a day. We can assume the detail vertical temperature profile from the pressure variation and the temperature profiles. Then we can calculate heating rate averaged for 12 hours. We can also estimate the time variation of sensible heat flux using the pressure data. Figure 1 shows the calculated pressure difference and observed one. If estimated temperature profile is proper, these two values agree with each other. Figure 2 shows heating rate of vertical air column above Lhasa site. Pressure difference is good correlation to heating rate. Next average sensible heat flux over the valley can be estimated taking into account the surrounding topography. The regional averaged sensible heat flux is much larger than the local surface heat flux at Lhasa site. This shows the surface heat flux from the slope around the site is much larger than that from the basin bottom. The effect of horizontal advection is very important in horizontally inhomogeneous region.

Long wave radiation was estimated from AWS data and the results compared with empirical formula. The present AWS measured Sd: downward short wave radiation (global solar radiation), Su: upward short wave radiation, Rtd: downward total radiation and Rtu: upward total radiation. These values have the following relations;

$$Rn = Rtd - Rtu = Sd - Su + Ld - Lu,$$

where Rn: net radiation, Ld: downward long wave radiation and Lu: upward one.

$$Lu = \varepsilon \sigma Ts^4 + (1 - \varepsilon) Ld,$$

where ε : emissibity (=0.95 in this case), Ts: ground surface temperature in Kelvin temperature, σ : Stefan-Boltzman constant. The following relationship is obtained from the above equations.

$$Ld = \{Rtd - Rtu - Sd + Su\} / \varepsilon + \sigma Ts^4 \quad (1).$$

Figure 3 shows the relation between Ld calculated from equation (1) and the theoretical values calculated from air temperature, relative humidity and pressure[2)]. Observation data is scattered between clear condition and cloudy one. This shows that the data is not inconsistent.

Void ratio and saturated hydraulic conductivity of sampled soil were measured. Void ratio is scattered from 40% to 50%. Saturated hydraulic conductivity is about 1×10^{-4} ms^{-1}, this is near sand condition.

The data of soil water content (w) measured by AWS were examined. Measured data are average of the shallower layer (from the surface up to 15cm in depth) water content and the deeper one (from 15cm up to 30cm) at Lhasa and Rikeze. The water content is good correlation to the rainfall amount in monsoon period. Just after rainfall, water content of the shallower layer increased up to 30%. After non rainfall condition continues 5 days, water content decreased by 10% to 16%. The change of the deeper layer was delayed a few days and the difference was smaller than the shallower

layer (Figure 4).

(2) Indian Ocean

AWS observation were made on the Osaka-Maru for four years. Figure 5 shows the latitudinal variation of daily heat budget. Sensible and latent heat fluxes are estimated by Kondo's bulk method[2]. In the Indian Ocean (from 25S to the equator), yearly net heat flux is about $+20Wm^{-2}$. This means that net heat flow is from the atmosphere to the Ocean.

4. Discussions

AWS observation sites are located in the eastern part of Tibetan Plateau. These area are relatively wet region over the Plateau. On the other hand, the western part of Plateau is dry region. To estimate an energy balance over the Plateau, it is necessary to install AWS in the western part of Tibetan Plateau. We plan to install two additional AWSs in this area.

Osaka-Maru observation accumulated the basic data for estimating heat balance over the Indian Ocean for four years. The results showed that net heat flow towards from the atmosphere to the Ocean.

5. References

1) Haginoya, S. et al.: Observation on Regional Surface Heat Budget. Annual Report of Japanese Experiment on Asian Monsoon, Research and Development Bureau, STA, 91-103. (1996)

2) Kondo J.(ed.): Meteorology on water environment. -ground surface water balance/heat balance-, pp.350. (1994)

6. Publications

(report)

S. Haginoya et al., Observation on Regional Surface Heat Budget. Research and Development Bureau, Science and Technology Agency, Japan. Annual Report of Japanese Experiment on Asian Monsoon, 1995JFY, pp91-103, 1996.

(oral)

S. Haginoya, Automatic Meteorological Observation over Tibetan Plateau (5). Meteorological Society of Japan. Preprints of the presentation, 69, pp47, 1996.

H. Naoe and S. Haginoya, Wind characteristic over Tibetan Plateau. Meteorological Society of Japan. Preprints of the presentation, 69, pp323, 1996.

S. Haginoya, Observation on surface heat budget over the Tibetan Plateau. Preprints of "Interbational Workshop on the Climate System of Monsoon Asia" Dec. 3-7, 1996, pp233-236, 1996.

7. International cooperation

Meteorological observation over the Tibetan Plateau is carried out the cooperative study with China Meteorological Administration. Meteorological Research Institute invited one Chinese scientist named Prof. Li Guoping (Chengdu Institute of Meteorology) for 17 days. In the same time, National Research Institute for Earth Science and Disaster Prevention, Science and Technology Agency invited another scientist named Mr. Liu Guangxuan (Tibetan Mteorological Bureau). Japanese and Chinese sides discussed the results of the Tibet observation. They attended the international Workshop which were held in Kyoto from 3 to 6 December, 1996. Prof. Li Guoping presented his study at the workshop. Japanese and Chinese sides examined the results of 1995 J.F.Y. and the plan of 1996 J.F.Y. They summarized the results of

discussion as "Working Plan". Both sides agreed the "Working Plan" in the 5th Working Group Meeting held from 5 to 6 December, 1996 in Kyoto, Japan. Details concerning the "Working Plan" are summarized in the Appendix 1 of "SUMMARY REPORT ON THE 5TH WGM OF JAPAN-PRC COOPERATIVE PROGRAM ON ASIAN MONSOON".

要旨

本研究は，大気を媒体として海洋と陸面間の相互作用として発現しているアジアモンスーンの機構を解明するため、２つの異なる地域における広域のエネルギー収支を評価するものである。そのうちの１つはチベット・ヒマラヤの山岳地帯の地表面フラックス，もう１つはインド洋・東南アジア地域の海面フラックスである。これらの地域において、熱収支解析に必要な気象要素を現地観測により収集し，それに基づいて広域熱収支解析を行うことを目的としている。

チベット関連：

現在、拉薩（ラサ）、日喀則（シガセ）、那曲（ナチュ）および林芝（ニンチ）の4ヶ所の観測地点には山岳用自動気象観測装置(AWS)が設置してあり、1993年夏から熱収支の観測を継続実施している。なお、1997年に西チベット2ヶ所に新たにAWSの設置を計画している。場所は改則（ガイゼ）と獅泉河（シーチョワンホー）である。

今年度は、既存AWSがある4ヶ所の訪問と西側の改則の現地調査を行った。まず、拉薩では付近の山岳地帯に気圧計を取り付けて、気圧の自動観測を開始した。これは、拉薩地域の平均的な顕熱輸送量を求めるためである。引き続きAWSデータの回収を行った。なお、各AWSで使用している気象関連の全てのセンサを回収し、日本において再較正をし、データの品質をチェックした。また、改則においては現地気象データや周辺の状況を調査し、AWS設置のための基礎データを得た。このほか、チベット地域のルーチン観測所のデータ（地上、高層および放射量）の入手、1996年12月までのAWS観測データの解析を行い、さらに中国人研究者を日本に招聘し、共同研究の打ち合わせ等を行った。

データ解析の結果、以下の成果が得られた。

拉薩の風速日変化とそれに及ぼす地形との関連を調べた。その結果、拉薩は東西の走行を持つ谷間に位置し、日中は東風、夜間は西風が卓越しており、典型的な山谷風循環が生じていることがわかった。また、気圧の日変化の様子も同様の様相を呈していることがわかった。

拉薩の気圧の日変化から拉薩周辺の谷間の平均顕熱輸送量を求めた。平均顕熱輸送量は拉薩の谷間の顕熱輸送量に比べて数倍も大きく、起伏地上では水平移流の効果が重要であることがわかった。

長波放射量の観測データから、チベット高原上の下向き長波放射量は冬季快晴時に200Wm^{-2}、夏期の曇天時に400Wm^{-2}近くになることがわかった。

チベットで採取した土壌の間隙率と飽和透水係数を測定し、間隙率は40%から50%の間、飽和透水係数は1×10^{-4}ms^{-1}前後の値をそれぞれ示し、砂土の値に近いことがわかった。

拉薩および日喀則において自動観測している土壌の含水率のデータを解析した。降水直後、第1層の含水率は30%近くまで上昇するが、無降水の日が続くと徐々に減り、5日間で16%まで減少した。第2層は数日遅れて含水率の変化が認められ、その大きさは第1層よりも小さい。以上のことから、モンスーン季は0cmから15cm（第1層）および15cmから30cm（第2層）の平均含水率が降水量によく対応していることが分かった。

インド洋関連：

大阪商船三井船舶株式会社の定期コンテナ船「大阪丸(31,382GT)」に搭載した船舶用AWSで得られたインド洋航路のデータを解析した。本船の観測は1991年10月から1995年10月まで行われた。この期間の航路に沿った海面熱収支解析の結果、インド洋海域の南緯25度以北の海域は海面に入る正味の熱フラックスが正になっており、大気から海洋への熱輸送が認められた。その大きさは20Wm^{-2}程度であることがわかった。

Table 1 Summary of additional AWS sites and the pressure observation site.

site name	Gaize	Shiquanhe	Lhasa-P
latitude	32° 18'N	32° 30'N	29° 44'N
longitude	84° 03'E	80° 05'E	91° 07'E
altitude(m)	4,420	4,279	4,690
around the topography	flat	flat	slope
conditions around the site	rural	rural	middle of mountain
ground surface conditions	bare soil (sand)	bare soil (sand ?)	rock
observation period	from Sept. 1997	from Sept. 1997	from June 1996

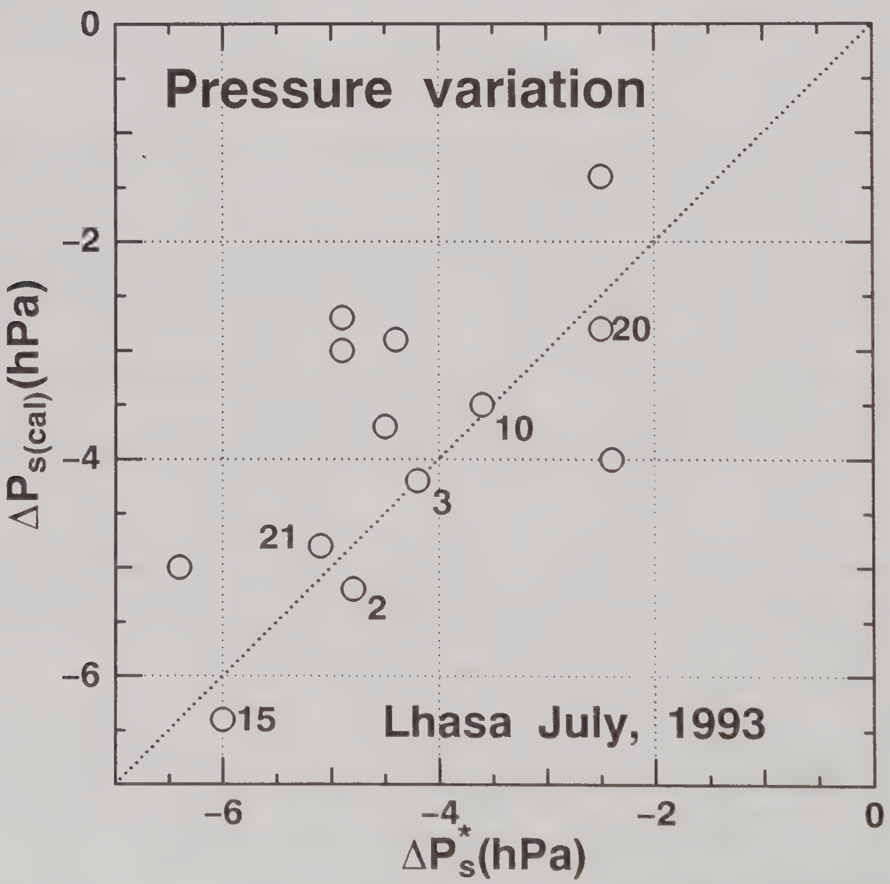


Figure 1 The relation between the observed pressure differences at Lhasa site (△Ps*) and the calculated pressure differences from temperature profile (△Ps(cal)). The number shows day.

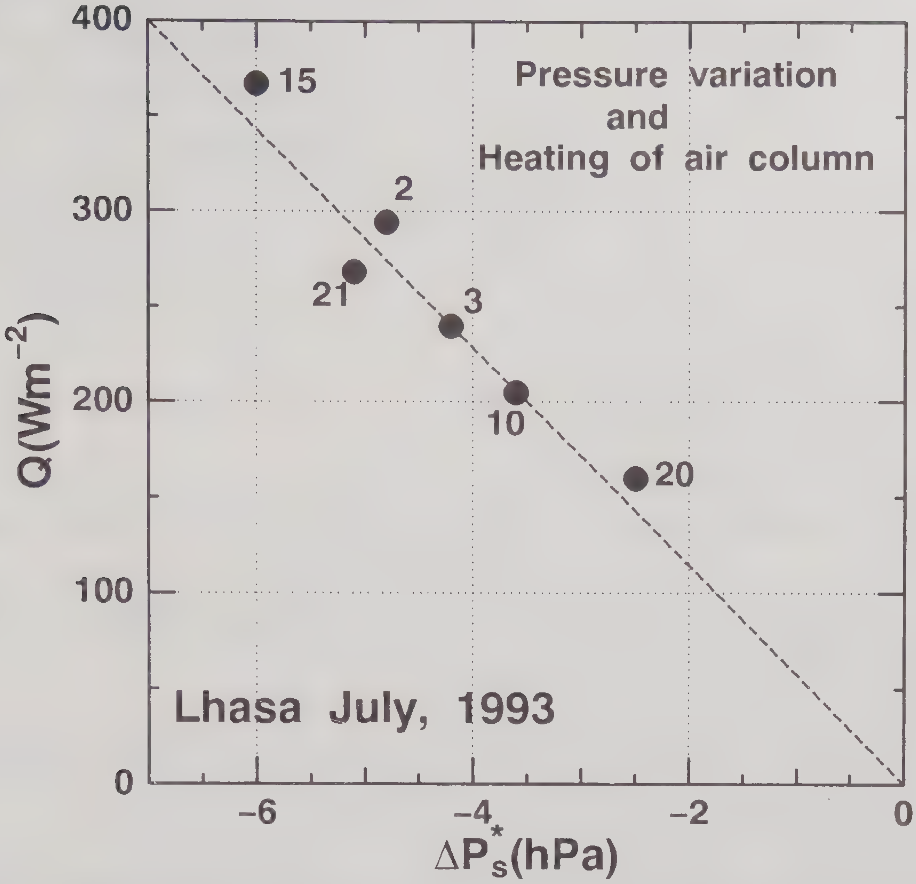


Figure 2 The relation between $\triangle Ps^*$ and heating rate of vertical air column above Lhasa site (Q).

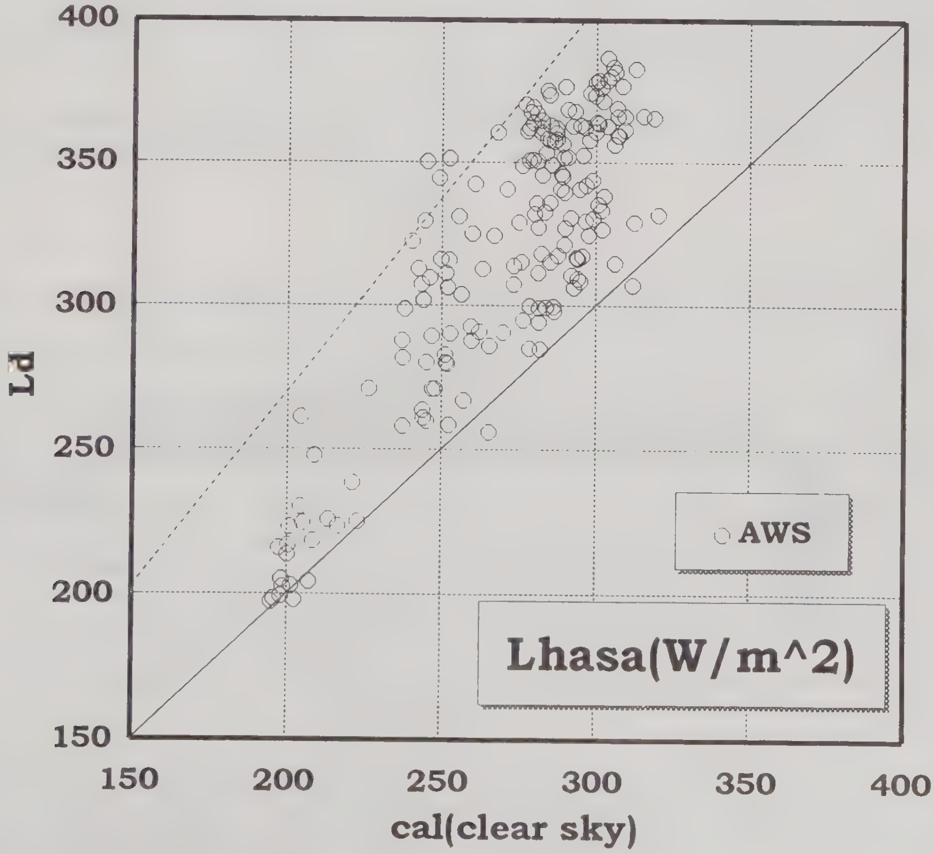


Figure 3 Comparison of long wave radiation. Open circle shows AWS data. Solid and dashed line indicate empirical formula in the case of clear and cloudy condition, respectively.

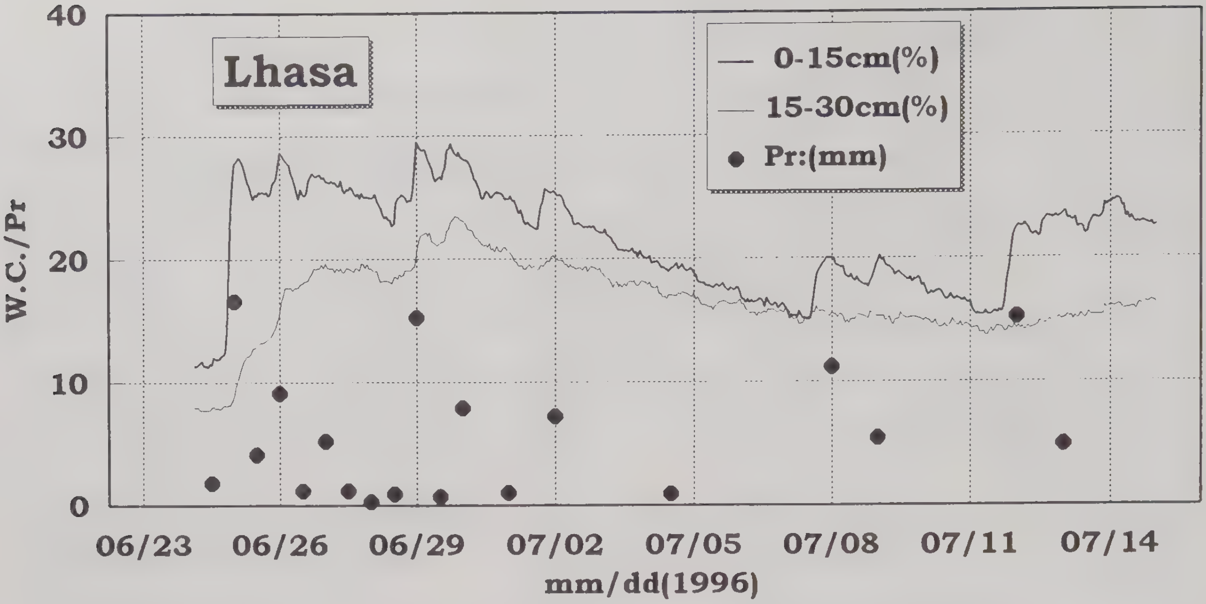


Figure 4 The time variation of soil water content at Lhasa site. Filled circle shows 12 hourly rainfall amount.

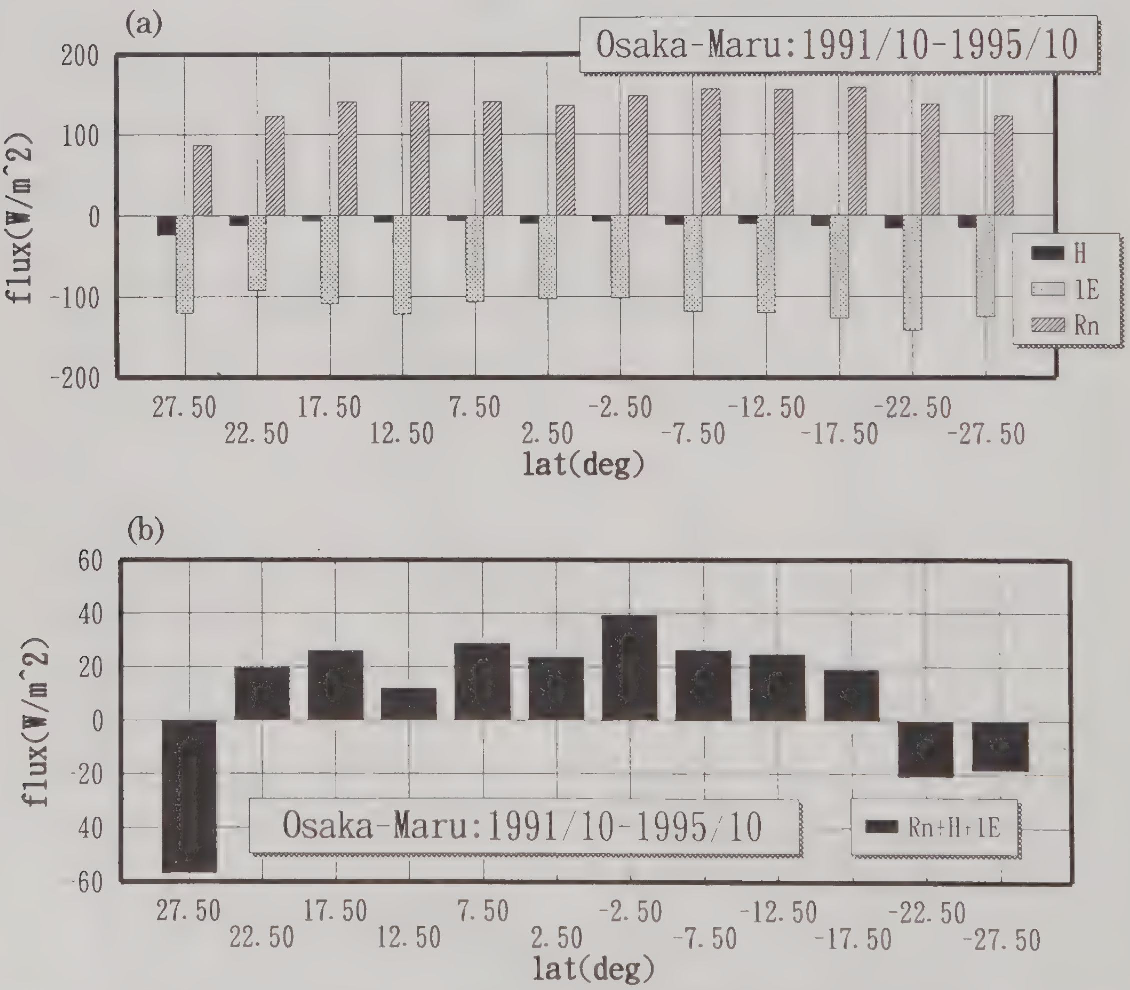


Figure 5 (a) Latitudinal variation of averaged energy fluxes. H: sensible heat flux, lE: latent heat flux and Rn: net radiation flux. Positive fluxes show the direction from the atmosphere to the Ocean. (b) Same as (a) but net flux.

Ⅰ. Observation and analysis on the process of atmosphere-ocean-land interactions

大気・海洋・陸域間相互作用の諸過程に関する観測・解析研究

3. Observation and analysis of over the land

陸域における諸過程に関する観測研究

(2) Observational study of ground surface heat budgets

地表面熱収支に関する観測研究

Communications Research Laboratory
Ministry of Posts and Telecommunications
Yoshihisa Masuda and Yuichi Ohno
郵政省通信総合研究所
増田悦久、大野裕一

(Abstract)

Radar wind profilers are very useful tool to measure directly the vertical motion above the radar site. The Communications Research Laboratory (CRL) developed the first L-band wind profiler in 1991. We are calling the radar Boundary Layer radar (BLR) , since the radar can measures the vertival motion from 300 m up to about 3 km in height. This is now operating at the Okinawa Radio Observatory. Three other BLRs have since been developed, two has been operating at the CRL in Tokyo since 1992 and 1995, respectively, other one has been operating in a joint research/experiment project on environmental monitoring technology between the CRL and the King Monkut's Institute of Technology Ladkrabang (KMITL) since 1993, which is located in Bangkok, Thailand. These radars are used to measure the altitude profiles of the wind and temperature, and the fluctuation intensity of the atmospheric refractive index. They are thus powerful tools for meteorological research.

This paper describes the seasonal wind variations of wind profiles measured for two years since 1994 at Bangkok in Thailand.

1.Objectives

Our developed wind profiler [1] is a Doppler radar that measures atmospheric wind speed and direction directly above its location and will provide timely information on wind conditions from about 300m to 3 km above ground level . The information obtained will help meteorogists to predict more precisely and accurately the development and movement of atmospheric phenomena. Therefore, weather forecasting is dependent on computer models of the atmosphere. To produce accurate forecasts, these models require large quantities of timely wind and temperature observations.

Our BLR can measures vertical wind velocity immediately above its antenna, where a conventional radiosonde is unable to measure, in addition with horizontal wind.A windprofiler/RASS, combined with a windprofiler and an acoustic source, is also the most effective system for measuring temperature profiles under all weather conditions. We previously determined the effect of wind and temperature profiles on the measurable height coverage for RASS[2], and showed how to design a useful acoustic waveform for accurately measuring temperature[3]. The validity of the windprofiler/RASS was

confirmed by the MU (Middle and Upper atmosphere) Radar/RASS experiment [4]. Wind profiler/RASS is useful tool to obtain timely data for computer models on the atmosphere.

Our purpose is to develop radar wind profiler and to show that the wind profiler is useful tool for continuously monitoring the atmospheric dynamic structures such as Asia monsoon, and land and sea breeze circulation [5]. We shows the seasonal change of wind profiles at Thailand in tropical region.

2. Methods

We now know that Doppler radar of high sensitivity could detect backscattered signals from irregularities produced by variations in air temperature and humidity. For this reason, wind profilers are often referred to as clear-air Doppler radar.

Our BLR systems have an antenna radiation pattern that is essentially straight up, with greatly reduced side lobes, and that determine the velocity of the air within the main beam. The BLR transmits and receives signals sequentially in one vertical and two near-vertical beams from steerable parabolic antenna. The BLR specifications are shown in Table 1.

Table 1: Specifications of our developed BLRs

Frequency	1357.5 MHz
Transmit peak power	1 kW
Pulse width	1.0 μ s (variable)
Data sampling rate	0.5 μ s (variable)
Time resolution	5 min.
Antenna type	parabolic
Antenna bean width	3.9 degrees
Beam directions (azimuth, zenith)	Vertical(0,0), East (90,15), North(0,15)

Therefore, the main beam of the antenna is aimed straight up or steered 15 degree from vertical. In the atmospheric refractive index, irregularities, whose wavelength along the radar line-of-sight is half the radio wavelength, causes Bragg scattering in the BLR. The irregularities are transported by the atmospheric wind, so they always move at the local velocity. The BLR transmits radio waves in three radial directions immediately above its antenna and receives the echoes scattered by the moving irregularities from three directions of antenna beam .

The power of the received echoes is proportional to the square of both the number density and the fluctuation-amplitude of the refractive index. The frequency of the received echoes is Doppler shifted to be proportional to the wind velocity. The velocity of the targets measured by the BLR is a line-of-sight velocity, which is the projection of a velocity vector in the radial direction. That is, the BLR uses the Doppler-beam-swing method to determine the three components of the velocity vector.

3. Results

We are now conducting the Asia Monsoon research using data gathered by the BLRs since 1993. Figures 1 and 2 , for 1994 and 1995, respectively, show an example of the measured wind profiles,

averaged the data obtained every five minutes over a day. The upward and rightward arrows indicate northward and eastward winds, respectively. In Figs.1 and 2, we can see the seasonal variation of wind over Bangkok from the data of daily mean horizontal wind change. Even though data for same days is missing due to radar trouble, but an outline of the wind change can be seen in Figs. 1 and 2. As shown in Fig. 1, the dominant wind directions are easterly in April and westerly in May, indicating the seasonal change from northeast monsoon to southwest monsoon. The reverse change is seen at the end and first of September in Fig. 1 and 2, respectively. We can see the difference of reverse changes between 1994 and 1995. Therefore, the time of the reverse change in 1995 is about half month fast to that in 1994. The reason is not understanding.

In tropical Asia monsoon areas, fundamentally, the wind direction changes abruptly. from May to September, the wind is mainly southwest; this period corresponds to the rainy season in Bangkok.

The maximum coverage height of the BLR depends on the intensity of the fluctuations and the system specifications, such as the average transmitting power and the effective antenna area. It is also different by the condition of humid weather. For example, the coverage height can be observed up to 2-3 km at Tokyo and 3-4 km at Bangkok [5].

4. Discussions

Our BLRs provide accurate data on the atmospheric dynamic structures with high time and height resolutions. The BLR located in Thailand has been shown to be a useful tool for continuously observing dynamic structures, such as Asia monsoons and land and sea breeze circulation. However, we have not yet clarified the constituent of fluctuation contrbuting to BLR scatterer and the causes of short- and long-term changes in wind direction. We are thus planing to conduct a comparative study using BLR and convensional radiosonde and will continue measurement of wind profiles for using BLR in Bangkok and Japan, to answer these question. Especially, the reason that the reverse change in 1995 is half month fast is not understanding, it is necessary to observe wind profiles by using the BLR for a long term.

5. References

1) Y. Masuda, K. Okamoto, K. Nakamura, T. Ihara, and T. Onishi; J. Remote Sensing Soc. Japan, 12, 1, pp.43-56, 1992.
2) Y. Masuda; Radio Sci., 23, 4, pp.647-654, 1988.
3) Y. Masuda, J. Awaka, K. Nakanura, T. Adachi, and T. Tsuda; Radio Sci., 27, 5, pp.681-691, 1992.
4) T. Tsuda, T. Adachi, Y. Masuda, S. Fukao, and S. Kato; J. Atmos., Ocean Tech., 1, 1, pp.50-62, 1994.
5) Y. Ohno, A. Manyano, N. Leelaruji, and N. Hemmakon; Proc. COST-76 Profiler Workshop 1997 in Switzerland., pp. 78-81, 1997.

6. Publications

1) Y. Ohno, A. Manyano, N. Leelaruji, and N. Hemmakon; Proc. COST-76 Profiler Workshop 1997 in Switzerland., pp. 78-81, 1997.

7. International Cooperation

The BLR with RASS operating in Thailand to study the dynamic structure of the tropical atmosphere is a joint project between the CRL and the KMITL and is sponsored by the Japanese Ministry of Posts and Telecommunications.

(要約)

郵政省通信総合研究所は、１９９１年にＬバンド境界層観測用レーダ１号機の観測を開始している。同種の境界層観測用レ-ダは、既に 4 台が開発され地球環境観測を目的として 1993 年末にタイ国キングモンクット工科大学内に一台、１９９４年に沖縄電波観測所に一台、更に２台が開発され、１９９２年と１９９５年に東京国分寺の通信総合研究所構内に設置されている.

これらのレ--ダは、境界層の風向風速及び気温高度分布の観測が可能であり、大気擾乱に伴う電波屈折率の乱れをターゲットとしており、乱れ強度の観測も可能である。 即ち、同レーダは、大気運動及び大気の熱的構造の観測に有用な装置である。

この報告では、境界層観測用レ--ダをモンス--ン域のタイ国に設置し 1994 年と 1995 年の 2 年間観測した大気運動の結果を紹介する。 タイの観測は、偏東風（乾期）から偏西風（雨期）のモンスーン変化を連続観測する事に成功している。1994 年と
1995 年の 9 月に起きる偏西風から偏東風への変化時期が、1995 年では前年より半月程度、進んでいる点に特徴がある。その原因の解明は、タイ国との共同による長期観測を必要としている。

Seasonal Change of Wind (JAN - JUN, 1994)

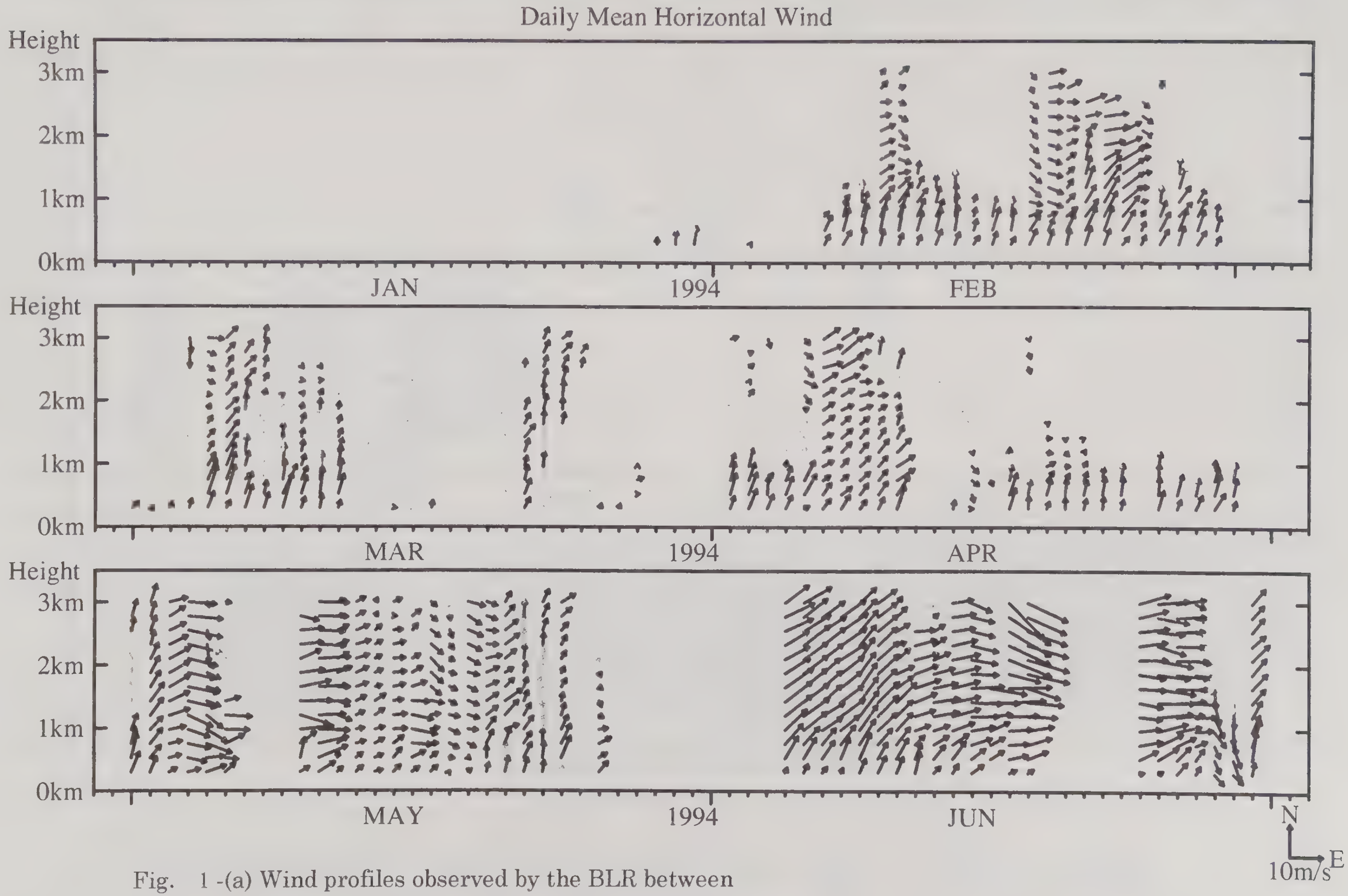


Fig. 1 -(a) Wind profiles observed by the BLR between January and June in 1994 at Bangkok, Thailand.

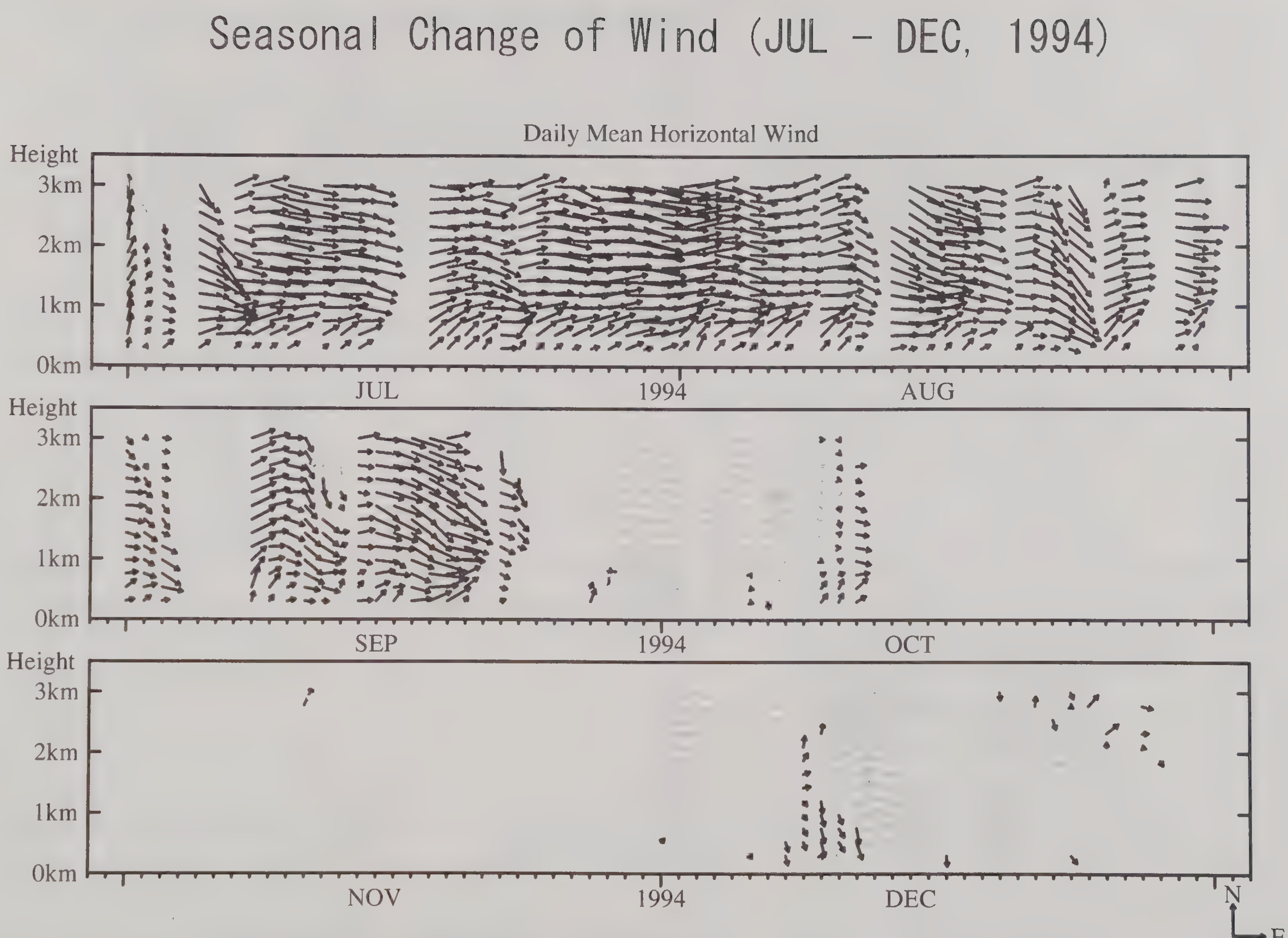


Fig. 1-(b) Wind profiles observed by the BLR between July and December in 1994 at Bangkok, Thailand.

Seasonal Change of Wind (JAN - JUN, 1995)

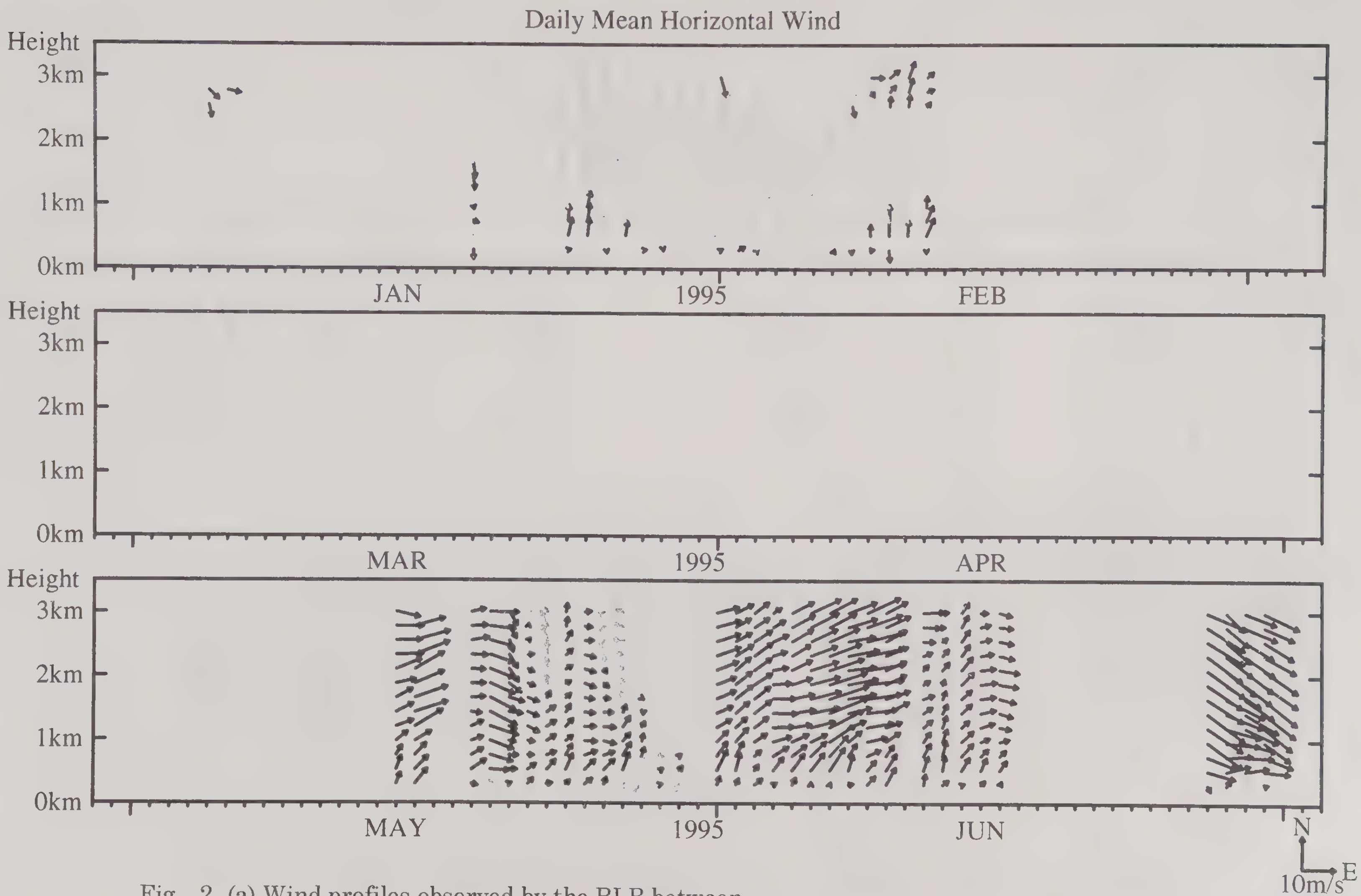


Fig. 2 -(a) Wind profiles observed by the BLR between January and June in 1995 at Bangkok, Thailand.

Seasonal Change of Wind (JUL - DEC, 1995)

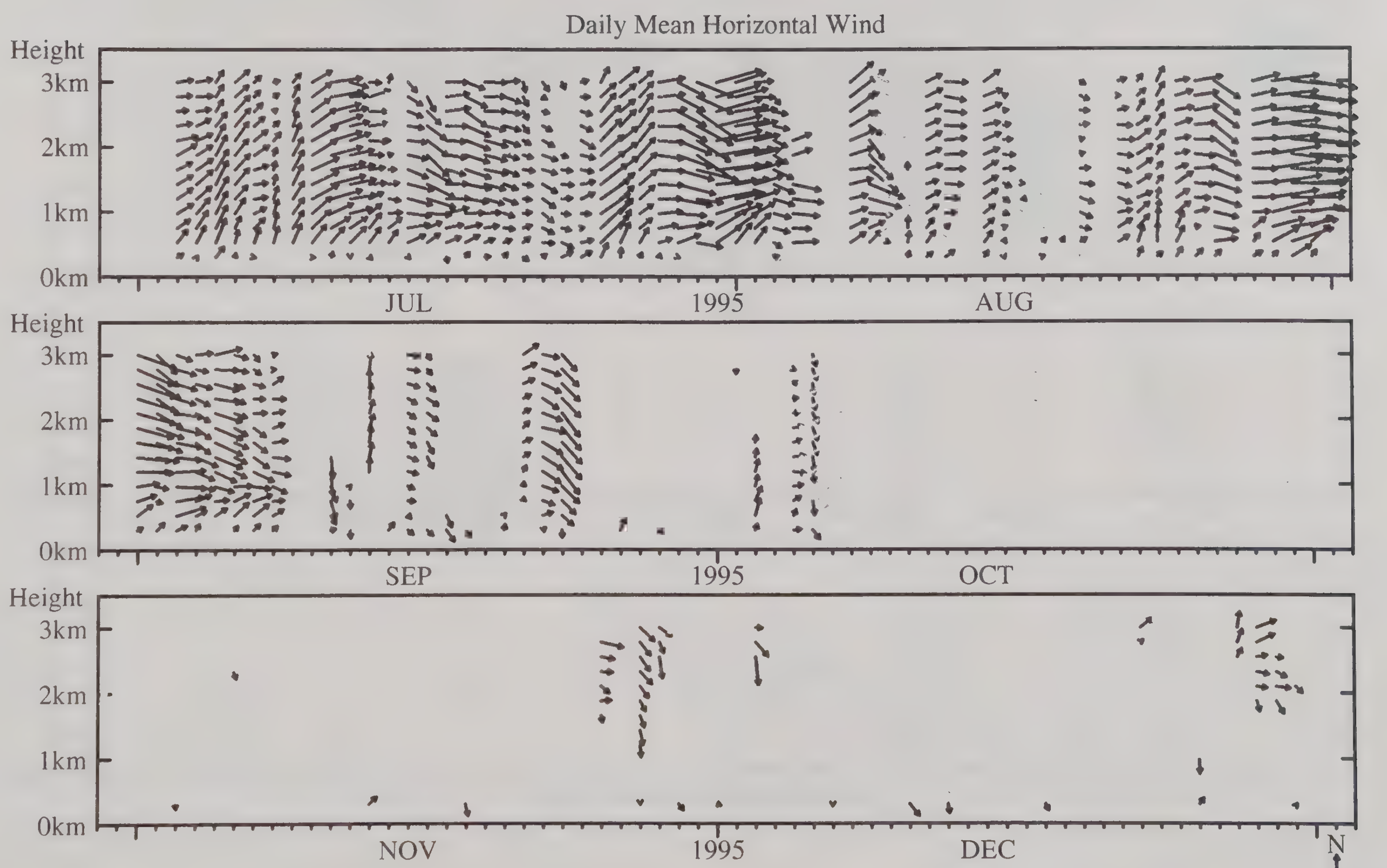


Fig. 2-(b) Wind profiles observed by the BLR between July and December in 1995 at Bangkok, Thailand.

Ｉ．大気・海洋・陸域間の諸過程に関する観測・解析研究
I. Observation and Analysis on the Process of the Atmosphere-Ocean-Land Interactions
３．陸域の諸過程に関する観測・解析研究
3. Observation and Analysis on the Process over the Land
（３）モンスーン循環広域条件及び雪氷変動状況に関する解析研究
(3) Analysis on Environmental Conditions and Snow-Ice Cover Changes Affecting Monsoon Cycle in Asia

科学技術庁防災科学技術研究所
矢崎　忍、宋　献方、中根 和郎、諸星 敏一
National Research Institute for Earth Science and Disaster Prevention, Science and Technology Agency
S. Yazaki, X. Song, K. Nakane, T. Morohosi

(Abstract) The aspect of Asian monsoon activities is considered storongly affected by environ- mental conditions of the area especially SST of Indian ocian and snow-ice cover over the continent. The purpose of this study is to make clear the relation between them mainlyby analyzing satellite data.

Our method is

(1) To make regional satellite image date base covering whole Asian area with NOAA/AVHRR data in a regular period(one in 7 days).

(2) To establish algorithms to detect various air, sea and land conditions with the satellite image data.

(3) For snow-ice cover in Tibetan-Himalayan area, sea ice in the Sea of Okhotsk or air water content over ocians, another adequate satellite data will be adopted for precise analysis.

This year's results are as following.

(1) The algolithm to detect snow covered area with the regional satellite image data is improved and applied to whole area of the image. To distinguish snow from cloud both spectral information and temporal change are used. As a result almost cloud free image of snow cover is obtained.

(2) Detectability of soil moisture with NOAA/AVHRR data and JERS-1/SAR data is verified for Shangdong area. The result was examined with ground observation data.

(3) The method of estimation of ground temperature with the regional satellite data is improved continuously.

1. Objectives

Activity of Asia monsoon is deeply afected by sea surface temperatur in Indian See and west Pacific Sea and snow cover in Eurasian Continent. On the other hand precipitation as a result of Asian monsoon activity has much relation with disastar, water resourse amount and vegetation. In this study methods to detect various environmental conditions: such as see surface temperature, land surface temperature, snow cover, vegetation with the earth observation data by satellite are developed. And relation between the environmental conditions and monsoon activity are clearified.

アジアモンスーンの変動はインド洋、西太平洋の海水温、ユーラシア大陸の積雪面積と深く関わっていることが指摘されており、またモンスーン活動によってもたらされる降水は災害、水資源、植生活性度に大きく関係する．本研究ではアジアモンスーン地域を対象として、モンスーン循環活動に関わる各種環境条件（海面水温、地表面温度、積雪、海氷、植生指標、雲頂温度、大気水分量等）の分布状況を各種の地球観測衛星データを用いて検出し、時系列的なデータベースとして整備するとともに、それらを用いて環境条件とモンスーン循環変動との関係を明らかにする．

2. Methods

(1) NOAA/AVHRR data are geometrically corected on a map then composed over a range :30°E-160°E, 20°S-60°N to make environmental condition data over Asia. The data are made periodically in every seven days and the whole data are called the regional satellite image data set.

アジアモンスーンの変動に大きく影響すると考えられるインド洋、西太平洋、ユーラシア大陸を含む東経３０°～１６０°、南緯２０°～北緯６０°の範囲を解析対象領域として、この領域をカバーするＮＯＡＡ／ＡＶＨＲＲ画像を幾何補正、モザイク合成して広域衛星画像データベースを一定期間（７日）毎に作成する．

(2) Methods to detect various environmental conditions with the regional satellite image data set are developed. And using the method images of every conditions are made in time series.

（１）で作成する広域衛星画像データベースを用いて、前記の各種環境条件を検出する手法を開発し、その手法を用いて環境条件画像を時系列に作成する．

(3) Snow-ice condition over Himalayan area are analized precisely using high resolution satellite image data such as LANDSAT/TM and MOS-1/MESSR.

アジアモンスーンの変動に影響が大きいヒマラヤ地域の雪氷分布を分解能の高いＬＡＮＤＳＡＴ／ＴＭ，ＭＯＳ－１／ＭＥＳＳＲ等を用いて詳細に解析する．

(4) Relationship between above mensioned various environmental conditions and variation of Asian monsoon activity especially variation of precipitation is made clear .

以上のような各種環境条件画像を長期間にわたって整備し、その季節変動、経年変動を解析する．さらにこれらの環境条件とモンスーン循環の変動、特に降水量との関係を明らかにする．

3. Results

(1) Detection of snow cover area and its time change over Tibetan-Hymarayan area.

To detect snow cover area with cloud comtanined satellite images both spectral and temporal information are used. Most of cloud are distinguishable from snow with the difference of spectral charactristics. But some cloud still remains undistinguished.

With using multi-temporal images more cloud are removed and snow cover area is detected more accurately. With about four images are used to make one month snow cover distribution map.

上記の広域衛星画像を用いて、主としてチベット・ヒマラヤ地域を対象に広域の積雪分布を検出する手法の開発を引き続き行った．スペクトル特性だけからは積雪と雲は完全には識別できないことが分かった．そこで時期のわずかに異なる複数のデータを用い、スペクトル情報と時間変動情報を併用することにより検出精度の向上をはかった．この手法を用い、約４日分の画像から月毎の積雪分布図を作成した。

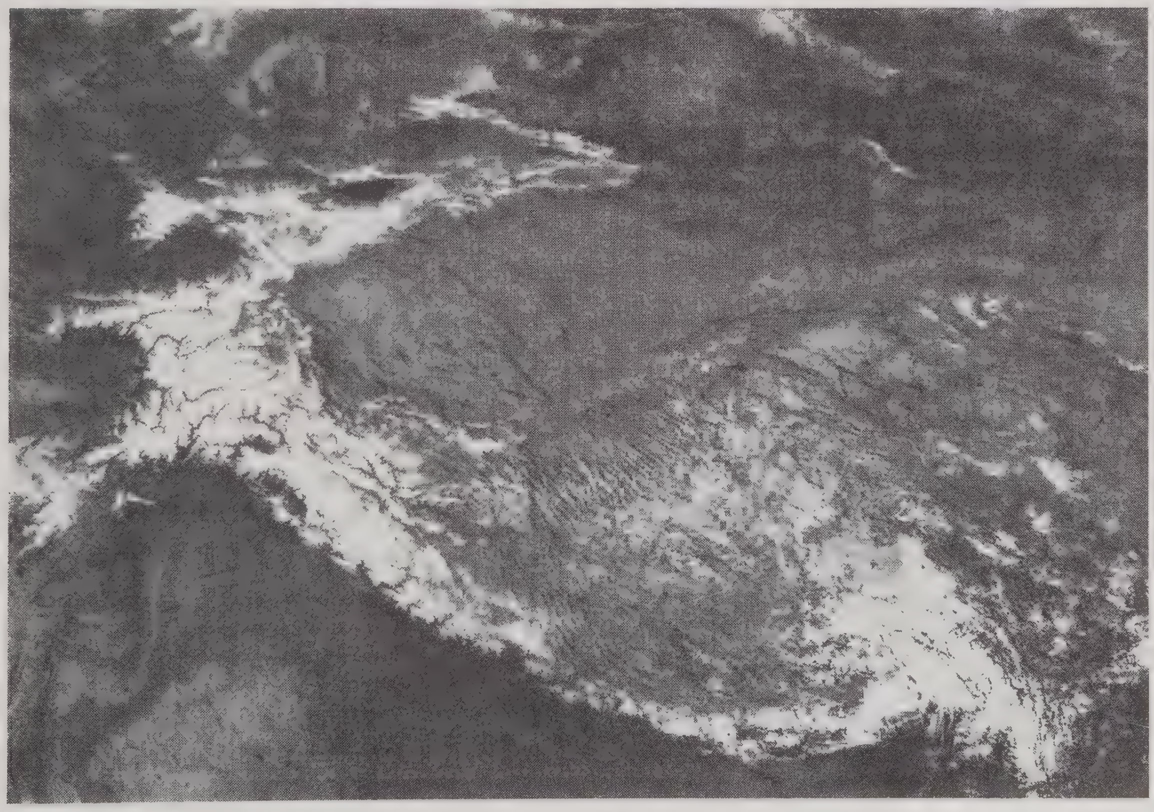


Fig.1 Detected snow cover distribution in March, 1994

図１　積雪分布図（１９９４年３月）

(2) Detection of soil moisuture

Detection of soil moisuture with NOAA data and JERS-1/SAR data are continued to be studied. To verify the method continuous observation with soil moisuture guage at Shangdong province is being carried out.

ＪＥＲＳ－１／ＳＡＲとＮＯＡＡデータを用いた土壌水分の検出手法の開発を引き続き行った．また、中国山東省で土壌水分計による土壌水分の連続観測を行い、本手法の検証を行った．

4. Discussions

It has been clearified that snow cover area is well detected by using both spectral and temporal information. But for more accurate and frequent analysis present data period: one image in seven days is not enough. Simular method must be adopted to one image in one day data frequency.

積雪分布について、現在は４日間のデータから１月の分布図を作成している．しかし、この方法では雲が完全には取り除けない．今後毎日のデータを用い、時間間隔を１０日程度とした積雪分布図の作成を予定している．

7. International Cooperation

This study has been carried out under cooperation between NIED and Satellite Meteolorogical Center of China. One researcher of NIED visited SMC and two researchers of SMC are invited to NIED for cooperative study. Joint observation of soil moisture at a station in Shandong China are maintained.

中国国家気象局衛星気象センターとの協力を行っている．本年度は防災科研の１名の研究者が同センターを訪問し、また同センターより２名の研究者を防災科研に招請し、共同研究を行った．また、本研究項目の研究分担者が１名同センターを訪問し、中国山東省で共同で行っている土壌水分の自動観測施設の視察を行った．

I．大気・海洋・陸域間相互作用の諸過程に関する観測・研究

Observation and analysis on the process of the atmosphere-ocean-land interactions

3. 陸域における諸過程に関する観測・解析研究

Observation and analysis on the process over the land

(4)地域水収支に関する解析研究

Analytical study of water balance on representative river basin

科学技術庁防災科学技術研究所
岸井徳雄、葛葉泰久、矢崎　忍、
杉田　文
National Research Institute for Earth
Science and Disaster Prevention,
Science and Technology Agency
T.Kishii, Y. Kuzuha, S.Yazaki and
F.Sugita

(Abstract)

The activity of Asia monsoon is influenced by water cycle and change of water cycle affects Asian monsoon. This study aims to clarify water balance of the regional scale in China. For these purposes hydrological data base, the elements are precipitation, runoff, evaporation, temperature, humidity and wind velocity are made. Using this data base, the characteristics of rainfall, runoff and evaporation is analysed in the Huai he river basin.

This report shows the result of the hydrological characteristics at Hoai pin in the Huai he river basin by the runoff model (Tank model). As the result, hydrological characteristics of rainfall, runoff and evaporation was determined and runoff characteristics in the upstream of the Huai he river.

1. Objective

This study aims to clarify the characteristics of the runoff in the upstream of the Huai he river in China. This river is located on the area between the Yellow river and the Chang Jiang river. So the river basin is strongly affected by the Asian monsoon. Tank model is used for analyzing daily runoff in this river.

2. Method

The analyzed area is the upstream of the Huai he river basin. The target station is "Hoai pin" , area of basin 16,005 km(Fig.1). Hydrological data used are, rainfall, runoff and evaporation from 1983 to 1991 by "Remote Sensing Technology Application Center, Department of

Water Resources of China". Areal rainfall amounts are calculated by arithmetic mean of two stations, Hoai pin and Shi shen. Evapotranspiration is calculated from evaporation data of Shensh en multiplied by some coefficients.

3. Results

a. Characteristics of monthly change of rainfall, runoff and evaporation.

Monthly and seasonal change of hydro-meteorological as follow. Rainfall occur's mainly in June to October. Especially much rainfall in June, July and October. Runoff amounts is also large from June to October similar to rainfall. Evaporation is larger than 4 mm/day from April to September. A example of the change of this elements are shown as Fig. 2 and Fig.3.

b. Runoff model (Tank model) analysis (Fig. 4)

Four series Tank model is used for analyzing runoff of the Huai he river. Hydrorological data from 1983 to 1991 are used. Runoff data are used at Hoai pin, rainfall data as arithmetic mean of Hoai pin and Shi shen and evaporation data at Shi shen as Fig.1. Evapotranspiration for this analysis is used for half amounts of observed pan evaporation at Shi shen. This is due to results by annual rainfall loss analysis.

Results are following. In summer season, of large amounts of discharge, the simulated result is coincided with observed one. But not so good in low flow period. The part of the cause may be artificial drainage, irrigation for paddy field, cultivated land etc. Runoff coefficients of the first & the second tank of tank model larger than that of the down stream basin analyzed last year reported on the annual report 1995. It means that rapid runoff component is larger than that of downstream basin as the last year analysis.

4. Discussion

Runoff ratio and total discharge are shown as Table 1.

Annual rainfall ranges from 700 mm to 1400 mm, runoff 160 mm to 700 mm and runoff ratio from 0.22 to 0.48. Mean annual loss is about 600 mm.

From these results, runoff ratio is smaller than that of the river in Japan.That shows evapotranspiration have major role in water balance. Mean annual than that of the downstream l arge basin, Bengbu. One of this reason is due to the height of basin area. This basin include large part of mountainous area.

5. Reference

Y. Kuzuha, S. Ikebuchi and T. Kishii (1996) : The estimation of fluxes on the complex land-use surface -Basic Study on Local Circulation Model-. Journal of Japan Society of Hydrology & Water Resources, Vol. 9, No. 2, pp.153-161.

6. Publications

Publication beside Society

2) Publication in foreign country

T. Kishii, Y. Kuzuha and C.X. Yan (1996) : Evapotranspiration in the Huai He River Basin. Proceedings of the International workshop on Macro-scale Hydrological Modeling

7. International Cooperation

One researcher was invited to our institute from "Remote Sensing Technology Application Center, Department of Water Resources of China" and exchanged information of water balance and land use mapping in the Huai he basin.

（要旨）

アジアモンスーンの変動は、アジア地域の水循環に大きな影響を及ぼし、その変動は、地表面の水文過程、特に水収支の特性を変えることが推定される。

本研究は、中国を対象とし、この地域の水収支の特性を明らかにすることを主目的とする。この目的のため、水文要素、すなわち、降雨、流出、蒸発、気温、湿度、風速および日射等のデータベースが作成される。 このデータベースを利用して、代表流域としての淮河流域の水収支の主要な要素である降雨、流出および蒸発散の解析を行う。

本年度は、淮河流域を対象に水文要素の特性を解析し、昨年のBengbuでの流出ﾓﾃﾞﾙ（ﾀﾝｸﾓﾃﾞﾙ）での解析に引き続き上流のHoai pinでの流出解析を行った。

その結果、降雨、流出および蒸発等の水文要素の特性が解析され、水文ﾓﾃﾞﾙにより淮河上流域の水収支特性が明らかとなった。

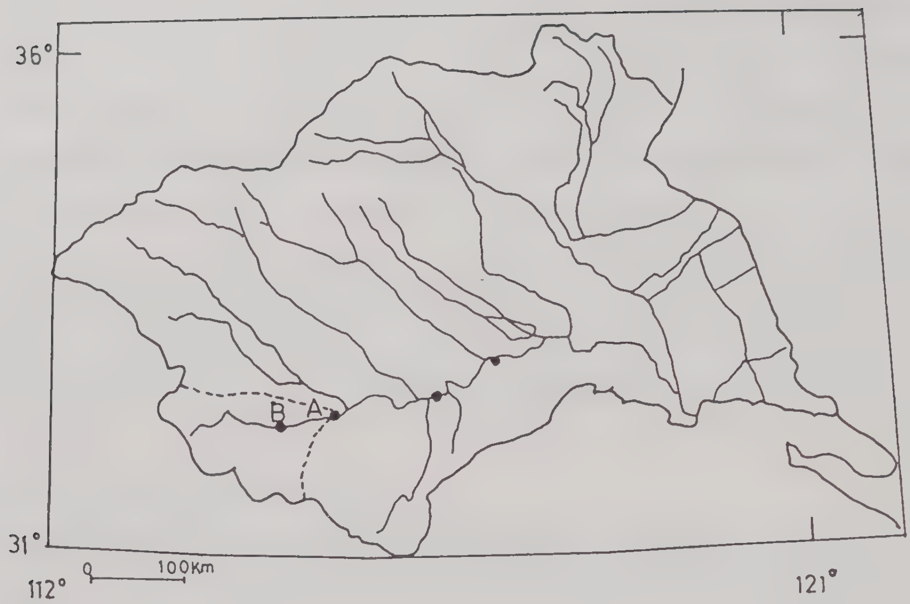


Fig.1 Location of the hydrological stations in the Huai he river basin
(A: Hoai pin, B: Shi shen)

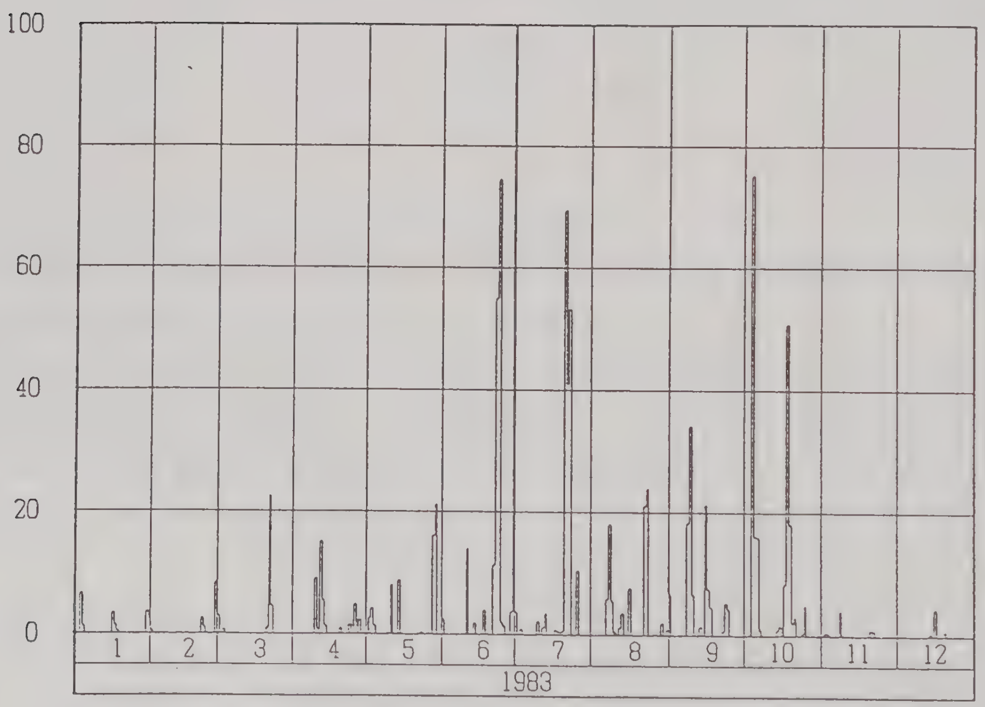


Fig.2 Monthly mean rainfall to the upstream basin of Hoai pin in 1983

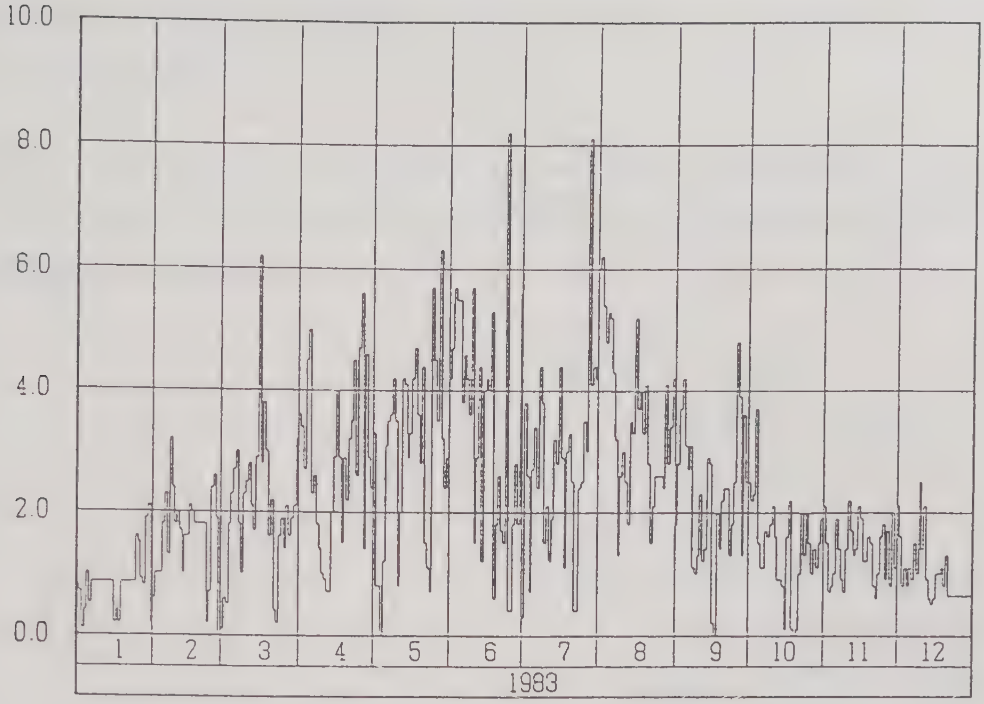


Fig.3 Monthly evaporation at Shi shen in 1983

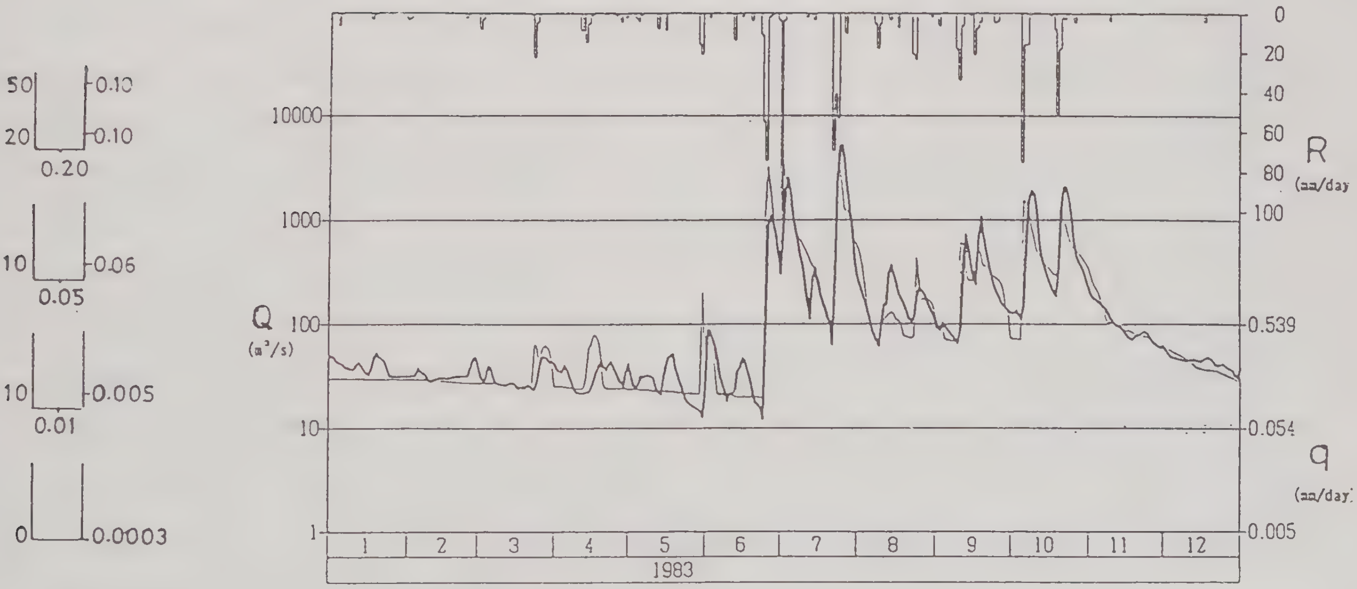


Fig.4 Tank model to the upstream basin of Hoai pin

II. 数値モデルによる大気・海洋・陸域間相互作用の実験研究
Experiment of the Atmosphere-Ocean-Land Interactions by the Use of Numerical Model

1. 数値モデルによる４次元資料同化システムの開発に関する研究
Development of the Four Dimensional Data Assimilation System by the Use of Numerical Model

気象庁　予報部
岩崎俊樹、隈　健一、北川裕人、
露木　義
Forecast Department,
Japan Meteorological Agency
Toshiki Iwasaki, Ken-ichi Kuma,
Hiroto Kitagawa, Tadashi Tsuyuki

(Abstract)

Extended-range forecast experiments for the Asian summer monsoon are carried out by using a global model with modified parameterization schemes for cloud fraction and cumulus convection in order to obtain insights into possible improvements to the numerical model that is used in the four-dimensional data assimilation system.

The cloud parameterization scheme is modified to enhance (reduce) the cloud fraction over the land (ocean). The effective radii of cloud droplets are set to 9 μm over the land and 12 μm over the ocean. It is found that the modified scheme leads to significant reduction of the systematic error in the absorbed solar radiation. Over the Eurasian continent, the reduction of absorbed solar radiation decreases low-level temperature through the land-atmosphere interaction and increases mean-sea-level pressure. It also has a significant impact on the water cycle between the land and ocean, particularly around the monsoon Asia.

The cumulus convection scheme is modified to enhance the coupling between dynamics and cumulus convection by allowing the time scale for the adjustment toward the equilibrium to vary according to the vertical motion near the top of the mixed layer. When a constant value is used for this time scale, the Madden-Julian oscillation (MJO) is not well simulated and the tropical cyclone activity is weak. With the above modification, MJO is successfully simulated and the tropical cyclone activity is increased.

1. Objectives

The performance of the four-dimensional data assimilation system strongly depends on the performance of a numerical model used in the system. In order to improve the global numerical weather prediction model of the Japan Meteorological Agency (JMA), extended-range forecast

experiments for the Asian summer monsoon are carried out by using modified parameterization schemes for cloud fraction and cumulus convection.

The Asian summer monsoon is the large-scale circulation system between the land and ocean excited by diabatic heatings of surface heat fluxes and deep cumulus convections. Yanai et al. (1992) showed that the sensible heat flux plays a primary role in the formation of the monsoon circulation by triggering the deep cumulus convection. In this respect, the absorbed solar radiation at the ground are of great concern, because total heat flux at the surface is heavily dependent on the ground absorption of solar radiation.

The cloud fraction, cloud water and droplet size are important control parameters of the solar radiation at the ground. Recent studies have clarified that the effective radii of cloud droplet over the land are smaller than that over the ocean. The small effective radius suggests that cloud droplets are easier to form due to plenty of condensation nuclei (Martin et al., 1994). When relative humidity is the same, the cloud fraction may be larger over the land than over the ocean. We investigate the impact of using different cloud droplet sizes over the land and ocean in the model, focusing on the land-atmosphere interaction.

The Madden and Julian oscillation (MJO) is one of the key targets for extended-range prediction of Asian monsoon because of its long time scales (30-60 days). There have been many studies on the performance of general circulation models (GCMs) in simulating MJO, and it has been shown that the performance of simulation is sensitive to the formulation of cumulus parameterization schemes. We found from a preliminary study that MJO was not well simulated by the current JMA global model. We examine the sensitivity of MJO simulation to the coupling between dynamics and cumulus convection.

2. Methods

The numerical model used in this study is a low-resolution version of the operational global model of JMA. It has a truncation wave number of T63 in the horizontal and 30 levels in the vertical up to 10 hPa.

(1) Experiment 1

The cloud fraction in the model is diagnostically determined from relative humidity r as follows:

$$Cloud\ fraction = \begin{cases} \left(\frac{r-r_c}{1-r_c}\right)^2 & (r \geq r_c) \\ 0 & (r < 0) \end{cases},$$

where the parameter r_c is the critical relative humidity of cloud formation given by a function of pressure. In the experimental run, the critical relative humidity r_c is reduced over the land and enhanced over the ocean by 10 % at most. The effective radii are set to 12 μm over the ocean and 9 μm over the land, following the observation by Han et al. (1994). We carry out a one-month

forecast run from the initial condition of 30 May 1993 with the above modification, and compare the result with the result of the control run in which a constant effective radius is used.

(2) Experiment 2

Deep cumulus convection in the model is parameterized by an economical prognostic Arakawa-Schubert scheme (Randall and Pan, 1993). In the original version of the scheme (AS1), the time scale for the adjustment toward the equilibrium value for the cloud work function is set to a constant. In the modified version of the scheme (AS2), the time scale is allowed to vary according to the vertical motion near the top of the mixed layer. If downward motion is found there, the time scale is increased so as to suppress cumulus convection. It should be noted that we have a stronger coupling between dynamics and cumulus convection in the AS2 scheme than in the AS1 scheme. Comparing the closure assumption between the Kuo scheme (Kuo, 1974) and the Arakawa-Schubert scheme, the Kuo scheme gives more direct response to the dynamical fields, since its closure is the moisture convergence. We carry out seven-month time integrations from 30 May 1990 with the Kuo, AS1 and AS2 schemes, and compare the results focusing the simulation of MJO.

3. Results

(1) Experiment 1

Figure 1 shows the monthly averaged forecast error of the earth's absorbed solar radiation compared with observational data provided by NOAA satellites. The control run overestimates the absorbed solar radiation over the continent but underestimates it over the ocean. Both errors are reduced in the experimental run as is easily expected from the modification of the cloud scheme.

The reduction of downward solar radiation decreases the ground temperature and sensible heat fluxes. Figure 2 shows the impact of the modified scheme on temperature at 850 hPa and mean-sea-level pressure. We find temperature decrease and pressure increase over the Eurasian continent. This is regarded as a direct effect of reduced solar radiation at the ground. Over North America, however, transient effects are dominant and the primary effect is not clear.

The modified scheme changes the atmospheric water cycle. Figure 3 shows the change in the horizontal moisture flux around the monsoon Asia. It is found that the use of different cloud droplet sizes leads to stronger eastward moisture flux in low latitudes.

(2) Experiment 2

Figure 4 shows the time-longitude cross section for 200 hPa velocity potential along the equator as well as the location in longitude of tropical cyclones in the northern hemisphere. A time filter which only passes period of 30-60 days is applied for the velocity potential field. This figure indicates that the model using the AS1 scheme gives weaker intensity of MJO and weaker

activity of tropical cyclones compared to the analysis and the model using the Kuo scheme. The simulation of MJO and tropical cyclone activity is improved by allowing the time scale to vary according to the vertical motion near the top of the mixed layer.

4. Discussions

The result of Experiment 1 suggests that the cloud scheme may have considerable impacts on forecast performance of the Asian summer monsoon. It is very important to simulate the ground absorption of the short wave radiation as accurately as possible. Wide et al. (1995) indicated that most of the GCMs overestimated the clear sky downward radiation. Intensive validation of the surface radiation against field observations is planned to investigate the radiation scheme, cloud formation scheme and cloud optical parameters.

Besides the cloud radiation, we must consider other physical processes that influence forecast performance for the Asian summer monsoon. Among them, the cumulus parameterization scheme, which is the major driving force of the general circulation in low latitudes, may have great influences on monsoon forecasts. The result of Experiment 2 suggests that we need to include the effect of coupling between the vertical motion at the top of the mixed layer and cumulus convection for successful simulation of MJO and the tropical cyclone activity. It should be further explored why the vertical motion near the top of the mixed layer is important for the cumulus convection. One possibility is that downward motion above the mixed layer increases the static stability, which may result in the negative buoyancy of a parcel lifted from the mixed layer.

5. References

1) Han, Q., W. B. Rossow and A. A. Lacis, 1994: Near-global survey of effective droplet radii in liquid water clouds using ISCCP data. *J. Climate*, **7**, 465-497.

2) Kuo, H. L., 1974: Further studies of the influence of cumulus convection on large scale flow. *J. Atmos. Sci.*, **31**, 1232-1240.

3) Martin, G. M., D. W. Johnson and A. Spice, 1994: The measurement and parameterization of effective radius of droplets in warm stratocumulus clouds. *J. Atmos. Sci.*, **51**, 1823-1842.

4) Randall, D., and D.-M. Pan, 1993: Implementation of the Arakawa-Schubert cumulus parameterization with a prognostic closure. *The Representation of Cumulus Convection in Numerical Models*, American Meteorological Society, Boston, 137-144.

5) Wide, M., A. Ohmura, H. Gilgen and E. Roeckner, 1995: Validation of general circulation model radiative fluxes using observations. *J. Climate*, **8**, 1309-1324.

6) Yanai, M., C. Li and Z. Song, 1992: Seasonal heating of the Tibetan Plateau and its effects on the evolution of the Asian summer monsoon. *J. Meteor. Soc. Japan*, **70**, 319-351.

6. Publications

K. Kuma, The convection schemes and the Madden-Julian oscillation. The WGNE Workshop on Numerical Weather Prediction and Data Assimilation for Climate, 23-25 October 1996, Tokyo, Japan (1996).

T. Iwasaki, Impacts of parametrization scheme of cloud formations on one-month dynamical forecast of the Asian summer monsoon. Proceedings of the International Workshop on the Climate System on Monsoon Asia, 3-7 December 1996, Kyoto, Japan, 164-167 (1996).

K. Kuma, The Madden-Julian oscillation and the onset of Asian summer monsoon — Prelude to numerical prediction of monsoon onset —. Proceedings of the International Workshop on the Climate System on Monsoon Asia, 3-7 December 1996, Kyoto, Japan, 202-205 (1996).

T. Iwasaki and H. Kitagawa, Extended forecast experiment of the Asian monsoon using a global model with a cloud scheme different over between the land and ocean. The First WMO International workshop on Monsoon Studies, 24-28 February 1997, Bali, Indonesia (1997).

H. Kitagawa and T. Iwasaki, A cloud scheme different over between the land and ocean and its impact on prediction of the Asian summer monsoon. Proceedings of the Semiannual Meeting of the Meteorological Society of Japan, 21-23 May 1997, Tsukuba, Japan, 35 (in Japanese) (1997).

K. Kuma, Improvements in cloud-radiation and cumulus convection schemes and their impacts. Proceedings of the Semiannual Meeting of the Meteorological Society of Japan, 21-23 May 1997, Tsukuba, Japan, 38 (in Japanese) (1997).

7. International Cooperation

None

（和文アブストラクト）

4次元資料同化システムに用いられている全球モデルを改善するために、雲と積雲対流のパラメタリゼーションを変更して夏季アジアモンスーンに対する予報実験を行い、その効果を調べた。

雲粒の有効半径を陸上で9μm、海上で12μmに設定して、雲量が陸上で大きく海上で小さくなるようにした。これによって、大気と地表面による太陽放射の全吸収量にみられたモデルの系統的誤差がかなり減少した。ユーラシア大陸上では、太陽放射の吸収が減少することにより、下層の気温が下降し、海面気圧が上昇した。また、海陸間、特にアジアモンスーン域周辺の水収支に大きな影響が現れた。

積雲対流スキームにおいて、平衡状態への緩和時間を混合層上端における上昇流に応じて変化させることにより、力学と積雲対流のカップリングを強くなるようにした。緩和時間を一定にした場合には、マデン・ジュリアン振動はよくシミュレートされず、熱帯低気圧の活動も弱かったが、この変更によってこれらの問題点が改善した。

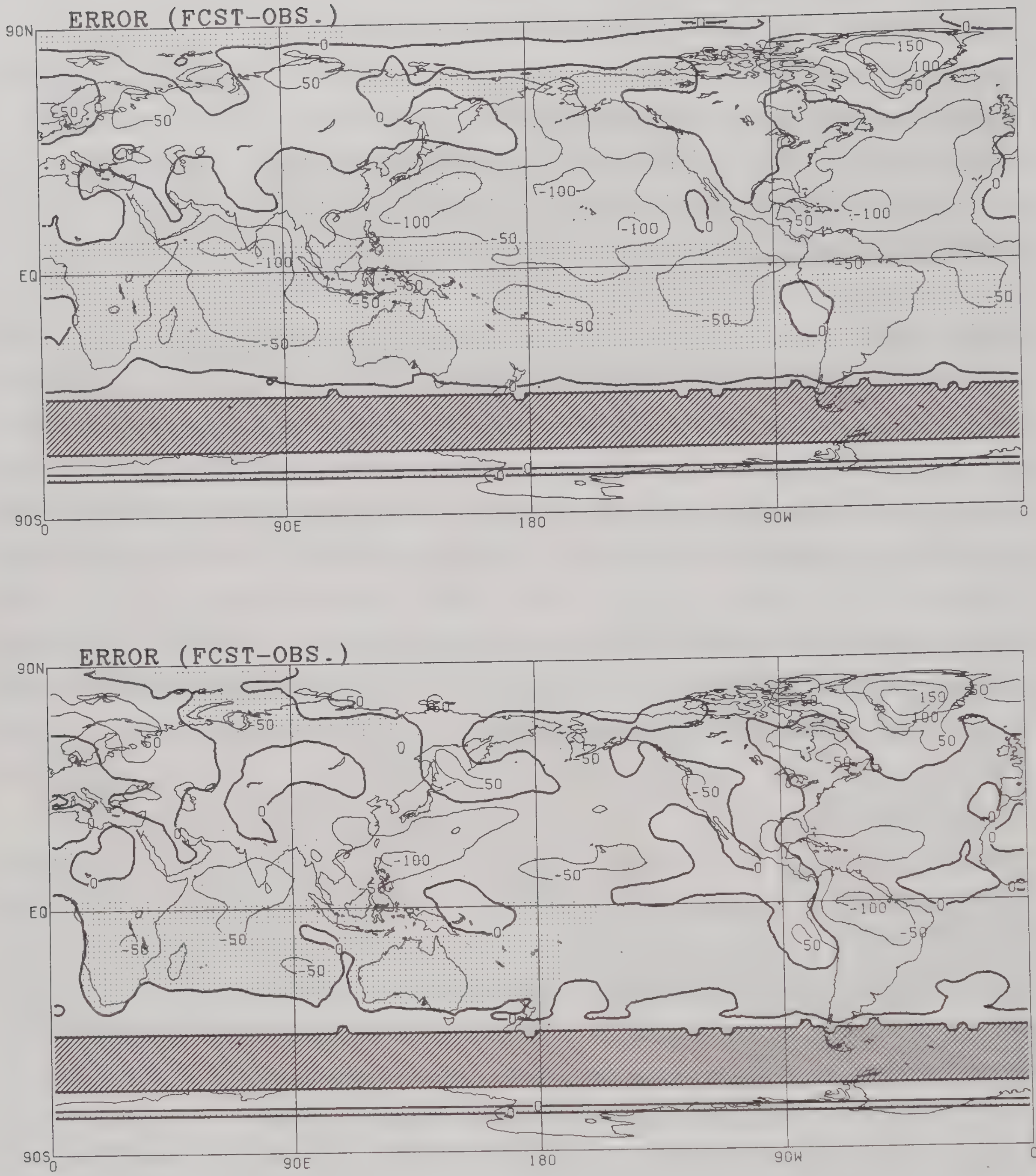


Fig. 1 Monthly averaged forecast error of the total earth's absorbed solar radiation. Upper and lower panels show the control run and the experimental run, respectively. Contour interval is 50 W/m^2 and negative area is shaded. Observational data are missing south of 45°S.

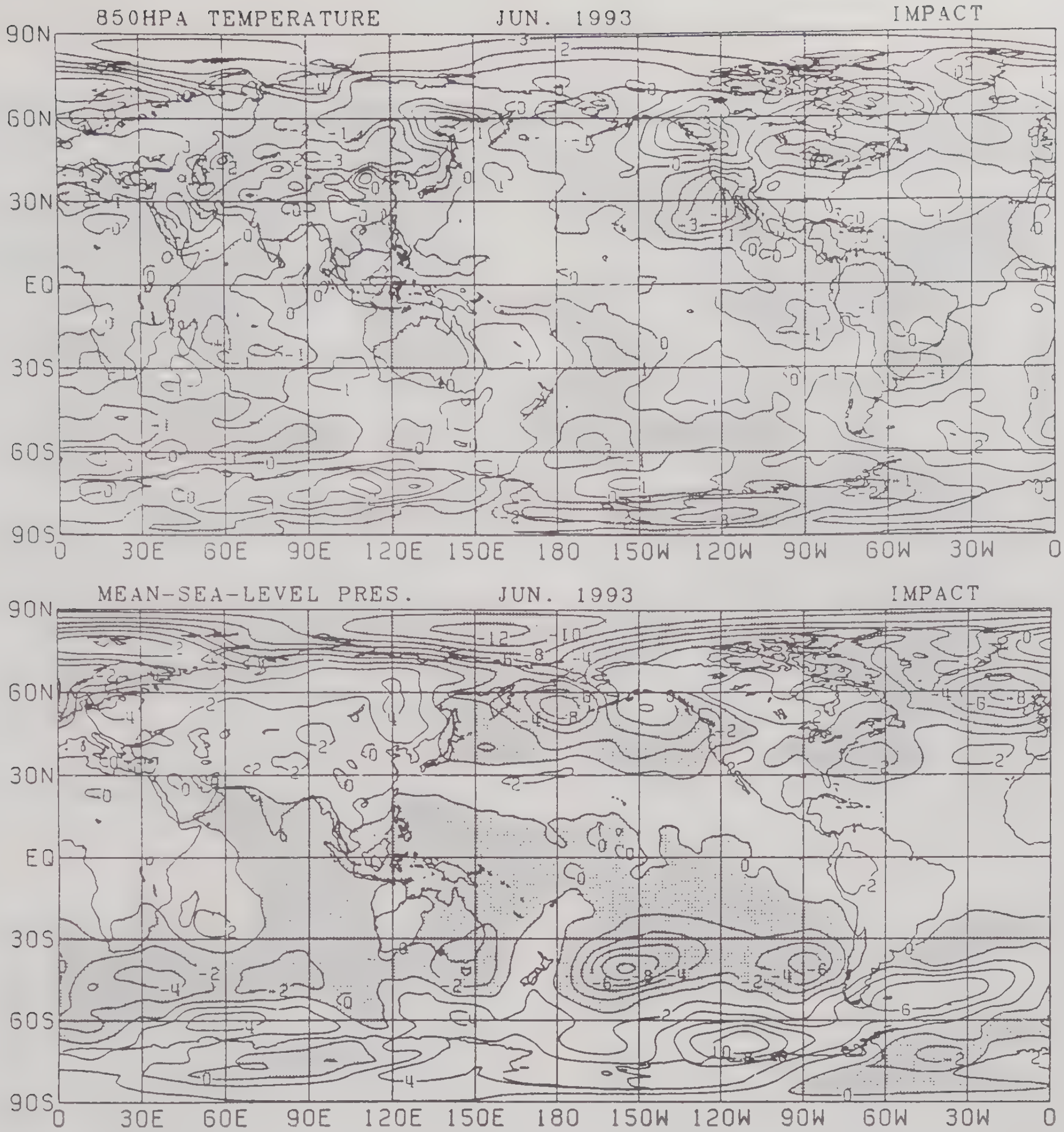


Fig. 2 Global distribution of monthly mean 850 hPa temperature (top) and mean-sea-level pressure (bottom) differences between the experimental run and the control run. Contour intervals are 1 K and 2 hPa, respectively. Areas of negative values are shaded.

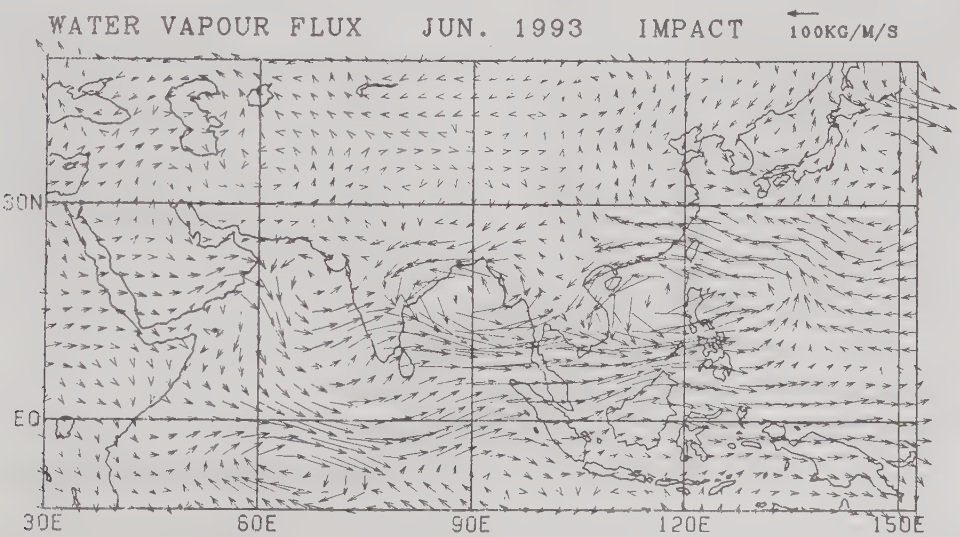


Fig. 3 Monthly mean difference in horizontal moisture flux around monsoon Asia between the experimental run and the control run.

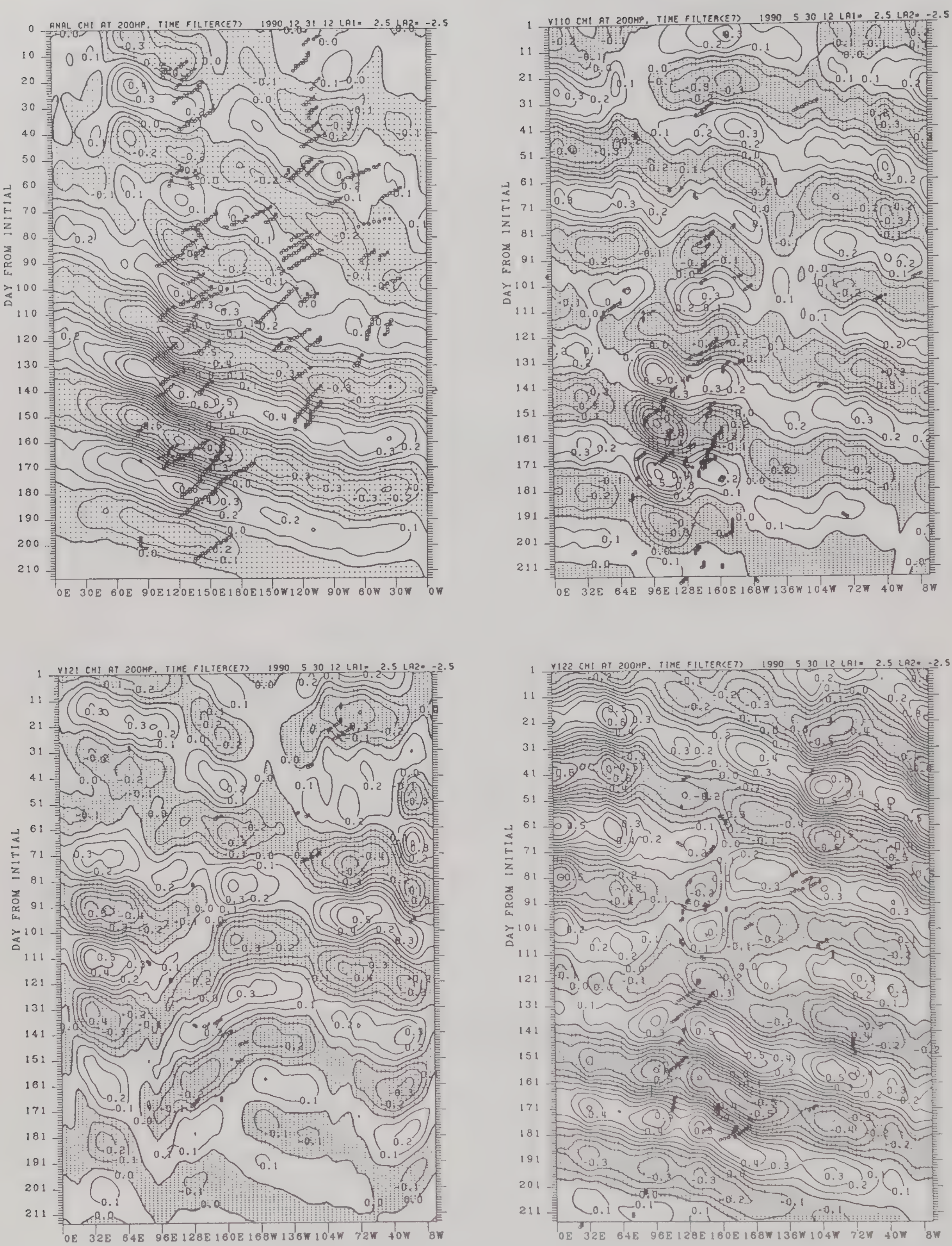


Fig. 4 Time-longitude cross section of 200 hPa velocity potential ($\times 10^7 m^2/s$) along the equator as well as the location (○) in longitude of the tropical cyclones in the northern hemisphere. Contour interval is $0.1 \times 10^7 m^2/s$. Negative area is shaded. See text for details. Upper left: JMA analysis and Navy best track. Upper right: Kuo scheme. Lower left: AS1 scheme. Lower right: AS2 scheme.

II. 数値モデルによる大気・海洋・陸域間相互作用の実験研究
Experiment of the atmosphere-ocean-land interactions by the use of numerical models

2. 広域水収支モデルの開発に関する研究
Development of water balance model over the wide area

科学技術庁防災科学技術研究所
中根 和郎、幾志 新吉
National Research Institute for Earth Science and Disaster Prevention,Science and Technology Agency.
K. Nakane and S. Kishi

(Abstract) The purpose of this study is to develop the Regional Water Balance model for assessing the variation of water resources and soil moisture over the wide area due to the fluctuation of Asian Monsoon activity. The model could predict hydrological surface condition, namely river discharge, water contents in the soil, storage amount of water in the ground, snow deposit, snow melt and actual evapotranspiration, on each area with 0.5° x 0.5° in latitude and longitude by using observed precipitation, evaporation and air-temperature. The model is made on the basis of the concepts of Tank Model. The prototype of the Regional Water Balance model had been developed and had been applied to Chaophraya River basin(110 thousand km^2) in Thailand. The results were satisfied, though the weather in this region changes from the dry season to the wet season alternately. Now, the model is going to be applied to Huaihe River basin(121 thousand km^2) in China and Ohyodo River basin(2 thousand km^2) in Japan. The model requires huge conventional observed data for input data. However it is difficult to acquire these data over the wide area densely, especially evaporation. Therefore, it is necessary to estimate evaporation in wide area by using satellite data. Satellites could observe Brightness Temperature and Albedo, which are related with evaporation, on the land from the space globally and frequently. Evaporation relates with air-temperature strongly. The air-temperature could be derived from split window data of infrared channel on NOAA AVHRR GAC data potentially. Up to this time, the new regression equation estimating the monthly mean air-temperature had been obtained. Now, generalization of the regression equation is curried out for applying to the Asian Continent.

These results in this fiscal year are summarized as follows;

(1) The Regional Water Balance model were applied to Huaihe River basin from 1983 to 1989 on a daily bases. The results were reasonable for large rainfall years.

(2) Method for making data-set with 2 X 2 minutes resolution, which describes surface runoff in a large basin was developed using the both of simplified river networks and ridges of mountaines dividing drainage area of each major tributaries.

(3) New regression equation, which derives monthly mean air-temperature with 2 X 2 minutes resolution over the Asian Continent using NOAA AVHRR GAC data, were applied to the Asian Continent. The results were fairly good.

(4) Data-set on observed monthly mean air-temperature over the Asian Continent were made for evaluating the estimated monthly mean air-temperature mentioned above.

1. Objectives

The purpose of this study is to develop the RWB model(Regional Water Balance model) with 0.5° x 0.5 ° resolution. The model could be used to assess the variation of water resources and soil moisture over the wide area in detail due to the anomaly of Asian Monsoon activity. The RWB model predicts river discharge, water contents in the soil, storage amount of water in the ground as potentially utilizable water, snow deposit, snow melt and actual evapotranspiration on each area with 0.5 ° x 0.5 ° in latitude and longitude. The model gives appropriate information for assessing hydrological regime in detail comparing general circulation models. The study had started with developing the model. Through applying to various places, the RWB model over the Asian Continent will be developed as the final goal of this study.

2. Methods

The RWB model is made on the basis of the concepts of Tank Model(Sugawara, 1984). The Tank Model have been applied to many river basins in the world, such as tropical humid area, snow covered area, semi-arid area, etc. As shown in Figure 1, the RWB model is composed of four sub-models,

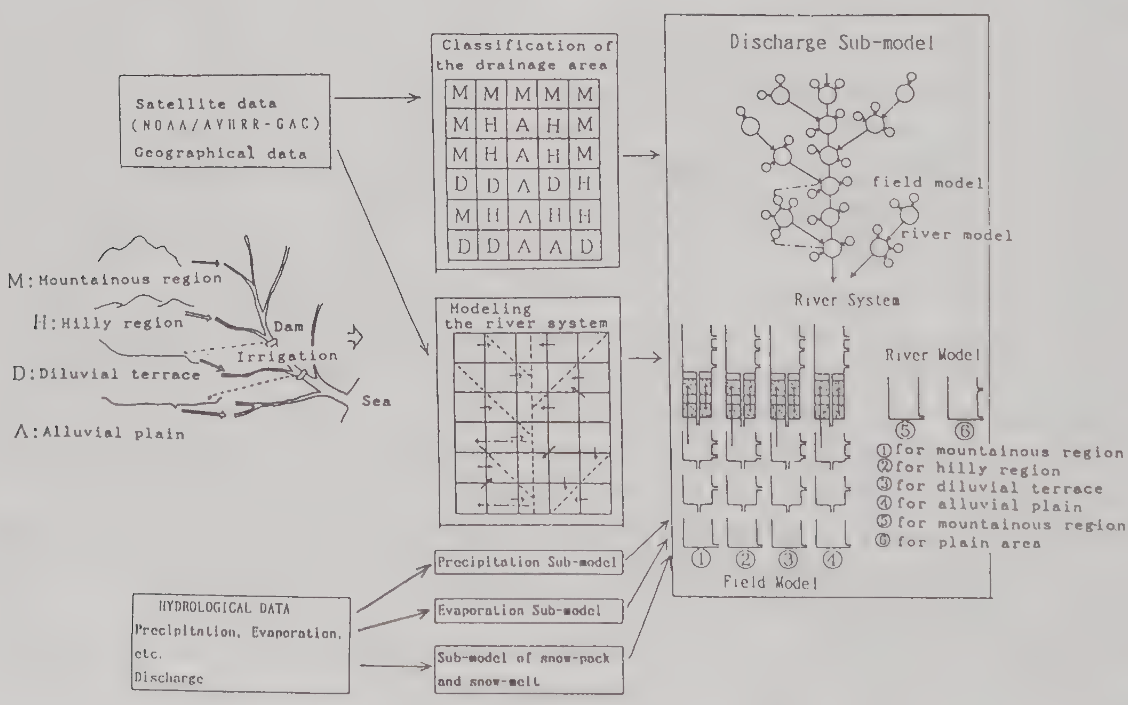


図1　広域水収支モデルの概略

Fig.1 Outline of the Regional Water Balance Model.

namely, a discharge sub-model, an evaporation sub-model, a sub-model of snow-pack and snow-melt, and a precipitation sub-model. The discharge sub-model is composed of many field models and river models. The field models, which are composed of four tanks arranged vertically in series respectively, are applied to each grid areas of simply categorized fields. Field models are four types according to the categorization of fields, namely mountainous type, hilly type, diluvial type and alluvial type. River models composed of one tank are used as the river runoff model on the simplified river system. River models are also three types according to river conditions, such as mountainous type, plain type and swampy type. These field models and river models are linked like a tree structure. The evaporation sub-model calculates evaporation in grid area by combining conventional pan-evaporation data at several points and estimated regional evaporation from satellite data. The sub-model of snow-pack and snow-melt calculates water equivalent of snow-pack and snow-melt on grid areas using daily precipitation and daily mean air-temperature, which has some local factors related to humidity and wind. The precipitation sub-model calculates the areal precipitation on grid areas by combining conventional rain gage data and seasonal patterns of the cloud cover, which are derived from satellite data. Up to this time, the prototype of the discharge sub-model had been developed. The sub-model had been applied to Chaophraya River basin with 110 thousand km^2 in Thailand. The results were fairly good, though the weather condition in the basin changes from dry to wet alternately. Now, the same model was applied to Huaihe River basin with 121 thousand km^2 in China. The study to develop the RWB model over Asian Continent was also curried out. In this study, making data-set for basin's conditions is important. These data-set are consist of simply categorized field and river system, which describe how rain-water flows into the river mouth through the river system. It is hard to make these data-set, especially river system, because of huge data and complicated river system over the Asian Continent. In this year, the method for making these data-set were investigated continuously.

The model requires huge conventional observed data for input data. However, it is difficult to acquire these data over the wide area densely, especially evaporation. Therefore, it is necessary to estimate evaporation in wide area by using satellite data. Because the satellite could observe Brightness Temperature and Albedo, which are related with evaporation, on the land from the space globally and frequently. Evaporation relates with air-temperature strongly(Thornthwaite, 1948). The air-temperature is

potentially derived from split window data of infrared channel on NOAA AVHRR GAC data. In our institute, W-RSI(Weekly Regional Satellite Image) data covering the area from 60° N to 20° S in latitude and from 30° E to 160° E in longitude are being made from NOAA AVHRR(Advanced Very High Resolution Radiometer) GAC(Global Area Coverage) data on a weekly basis(Yazaki, 1990 and Nakane, 1990). The map projection of W-RSI data is a grid coordinate system with 2 minutes equal intervals of latitude and longitude. W-RSI data unfortunately contain many cloud, which prevent to transmit information from land surface to satellite because of absorbing radiation and reflection from the land. Therefore, M-RSI(Monthly Regional Satellite Image) data are made by composing data of cloud free area on W-RSI data during a month. M-RSI data could be used for estimating M-AT(monthly mean air-temperature) successfully(Nakane, 1991). Up to now, the new regression equation described in Equation 1, which was improved former regression equation, had been obtained for estimating the M-AT from M-RSI data.

$$M\text{-}AT = K1 \times SR3 + K2 \times Tch4 + K3 \times (Tch4 - Tch5) + K0 \qquad ----(1)$$

$$SR = \cos(\theta - \delta)$$

$$\delta = 0.4093 \times \sin(0.01698 \times (JDAY - 80))$$

$$L = 1.0 + 0.033 \times \cos(360/370 \times {*}JDAY)$$

$$Dul = -0.045/\cos(\theta)/\cos(\delta) - \tan(\theta) \times {*}\tan(\delta)$$

$$SR3 = SR \times L \times \tan^{-1}(\sqrt{}(1 - Dul \times Dul)/Dul) \times 2.0/\pi$$

Where, Tch4 and Tch5 are brightness temperature(unit: degree Celsius) of Channel 4(wave band: 10.5～11.5 μm) and Channel 5(wave band: 11.5～12.5 μm) on NOAA AVHRR data respectively, SR and θ are the seasonal coefficient of outer solar radiation and latitude at a target point respectively, δ is declination, JDAY is Julian Days. K0, K1, K2 and K3 are coefficients of regression equation.

The equation has four coefficients. These coefficients relate with the latitude of target points, though coefficients are variable from place to place. Because, these coefficients relate with water vapor in the atmosphere and the distribution of water vapor depends on the latitude. Now, the new regression equation was applied to the Asian Continent, and the obseved data-set was made using 1,000 stations over the Asian Continent for evaluating estimated M-AT.

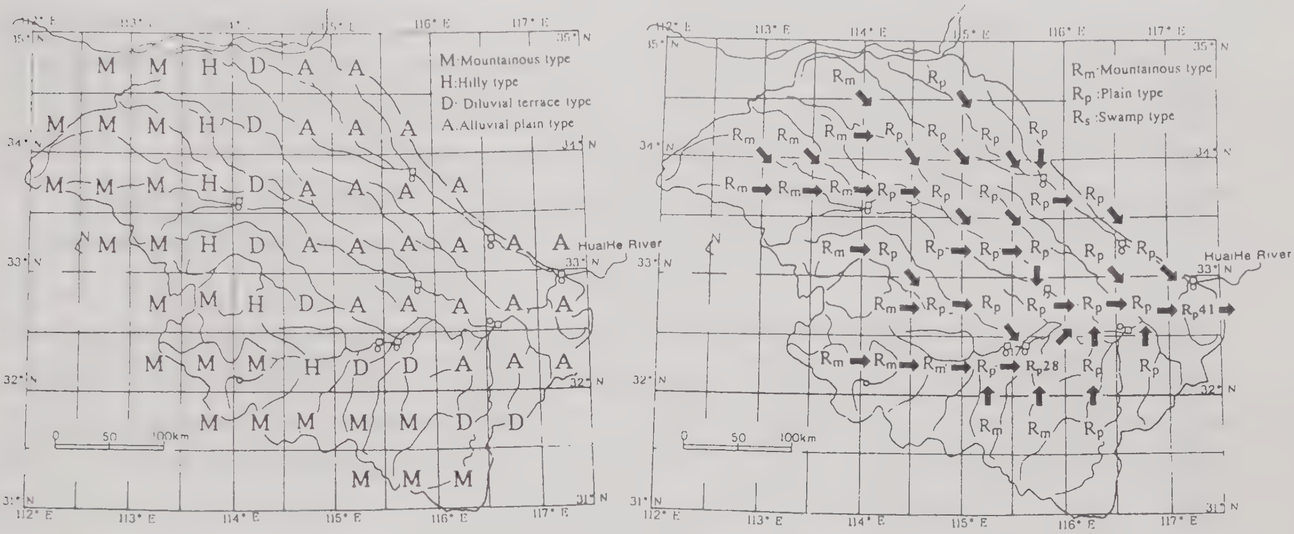
3. Results

In this fiscal year, the RWB model was applied to Huaihe River basin, and the new regression equation, which estimated M-AT from NOAA AVHRR GAC data, was applied to the Asian Continent. These results are summarized as

follows;

(1)Application of the Regional Water Balance model to Huaihe River basin

the RWB model had been developed and applied to the Huaihe River basin in China, where the analyzing catchment area is 121 thousand km². Figure 2 shows the classification of the basin and simplified river system in the Huaihe River basin respectively. For model input data, 38 precipitation data measured by rain gauges, 15 evaporation data measured by evaporation pan with 20cm diameter and discharge data just below of 6 big dams were used. Areal precipitation and evaporation on grid areas were estimated by weight mean method using above observation data in this time. In calculations, the



Classification of the basin　　Simplified river system

図２　淮河流域（対象流域面積:121,330km2）における流域分類及び単純化した河川網

Fig.2 Classification of the basin and simplified river system in Huaihe River Basin.

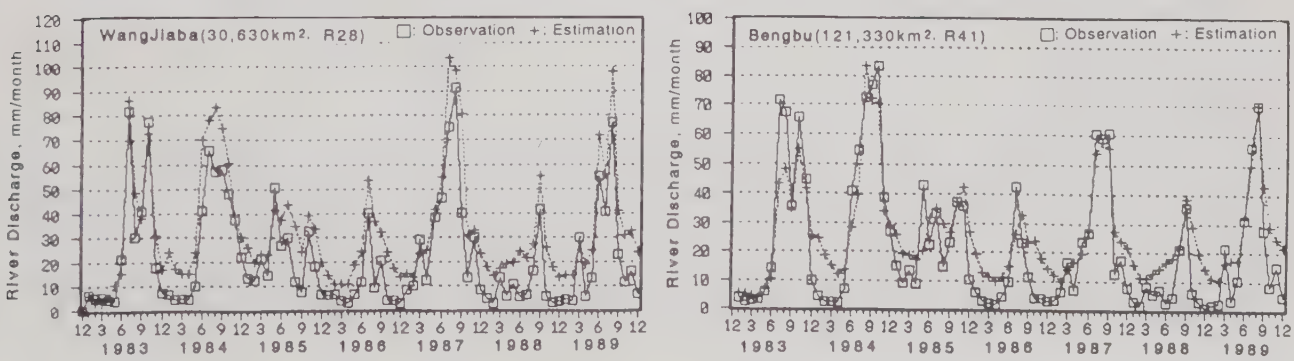


図４　淮河流域における月流量の推定結果

Fig.3 Estimation for monthly discharge in Huaihe River Basin.

extra coefficient depending on the altitude for both precipitation and evaporation were not used because of little information for the dependency on the latitude. The important thing of this experiment is same parameters of the RWB model in the Chaophraya River basin, Thailand were used. Figure 3 shows estimations for monthly discharge from 1983 to 1989 at WangJiaba station, where the catchment area is 30,630 km^2, and BengBu station, where the catchment area is 121,330 km^2. These estimations are reasonable on a whole. In detail, estimation for low flow and flood shape are not adequate.

(2)Developing the method for flow direction of surface runoff

In the development of the RWB model over Asian Continent, data-set for simplified river system is important. The half automatic method for making vector data describing flow directions of surface runoff were developed using simplified river system, ridges of mountains and digital elevation data with 2 × 2 minutes resolution over the Asian Continent.

(3)Application of the new regression equation to the Asian Continent

The regression equation, which derives M-AT by using M-RSI data, was improved. The solor term in the equation was considered not only seasonal change of the sun angle, but also both of the distance between sun and earth and the duration of sun shine. Relations between coefficients of the new regression equation, and both of the latitude and the elevation at the target point were found. From these relations, applicable coefficients in wide area were obtained. The regression equation gave reasonable estimations of M-AT with 2 × 2 minutes resolution over the Asian Continent using these coefficients(see Figure 4 and 5).

(4) Observed data-set on M-AT data over the Asian Continent

The data-set was made for evaluating the estimated M-AT mentioned above using about1,000 stations. The observed data were offered by Japan meteorological agency.

4. Discussions

The RWB model, which used same model's parameters in case of Chaophraya River basin in Thailand, had applied to Huaihe River basin from 1983 to 1989. These estimations are reasonable on a whole. In detail, estimation for low flow and flood shape are not adequate. The cause seems to arise from irrigation and flood control. These problem will be clear through the further detail estimation using data on irrigation and flood control in the basin.

Study for making data-set of RWB model over the Asian Continent was curried out. The half automatic method for making vector data describing

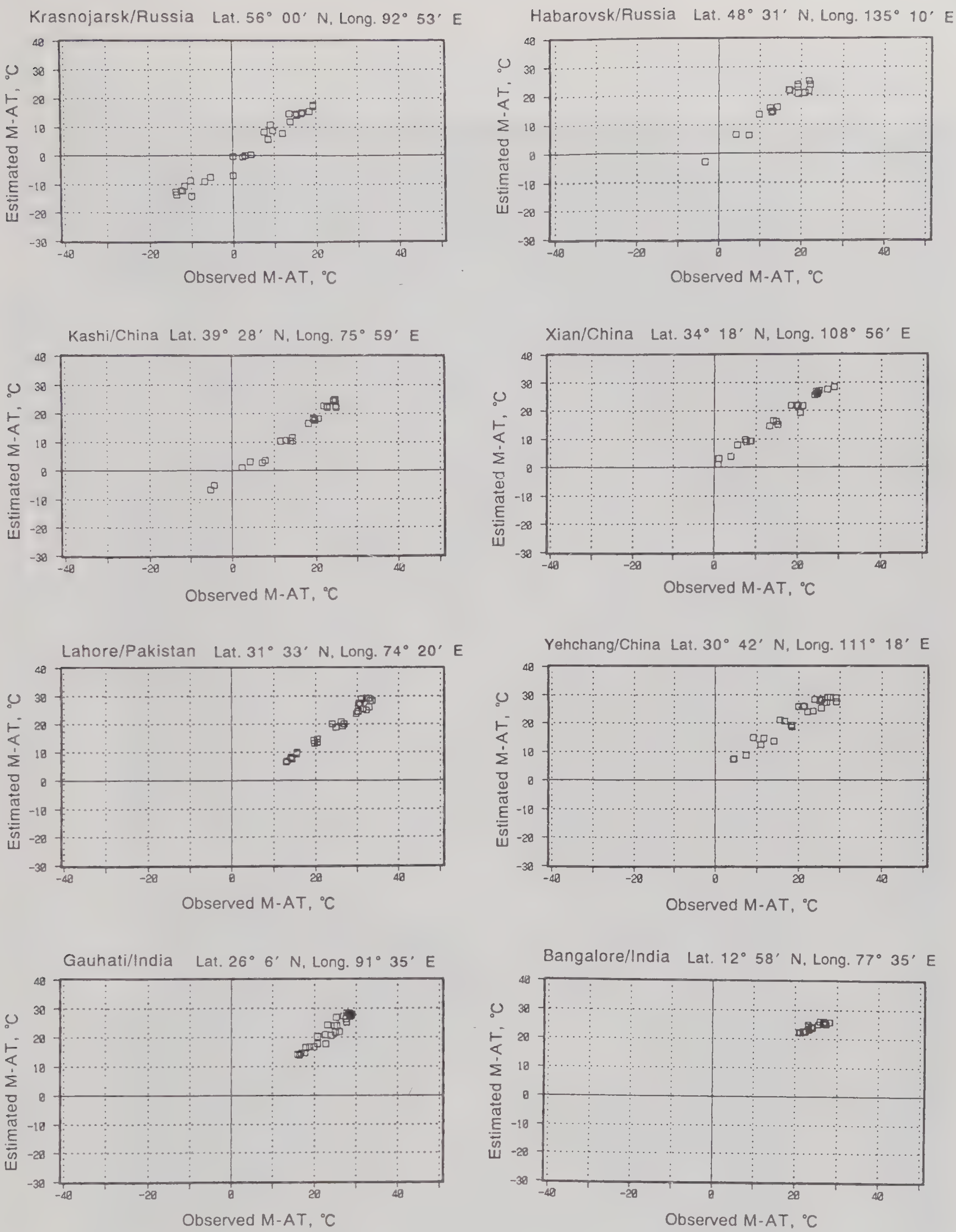


図4　緯度及び標高の関数として求めた係数を用いた月平均気温の推定

Fig.4 Estimation of M-AT by using coefficients (K0, K1, K2 and K3) derived by functions of the latitude and elevation at target point.



図５　緯度及び標高の関数として求めた係数を用いたアジア大陸の月平均気温推定結果

Fig.5 Estimation of M-AT over the Asian Continent by using coefficients (K0, K1, K2 and K3) derived by functions of the latitude and elevation at target point.

flow directions of surface runoff was developed using simplified river system, ridges of mountains and didital elevation data with 2 × 2 minutes resolution over the Asian Continent. These simplified river system and ridges of mountaines were identified by human judgement using data-set on the both of DTM with 5 x 5 minutes resolution and river network in World Data Bank II. The method is still hard to use in wide area.

The new regression equation was developed for estimating the M-AT. Appropriate coefficients of the new regression equation in wide area were obtained as functions of the latitude and the elevation at each target point. These coefficients were applied to estimate M-AT over the Asian Continent. Results were good on a whole compering data-set on observed M-AT data. In some area, however, estimated values had some bias. It seems that the bias will be explained by NDVI(normalized differential vegetation index). The problem will be investigated in future.

5. References

1)K. Nakane et al.; Regional Image Processing for NOAA AVHRR data Part II Composition of the wide Regional Image, Report on the 16th Remote Sensing Symposium,67-70(1990).

2)K.Nakane; Estimation of Monthly Mean Air Temperature over Asian Area using GAC Data of NOAA AVHRR, Journal of Japan Remote Sensing Vol.13 No.1, 14-26(1993).

3) K. Nakane; Regional water balance model based on the concept of the Tank Model: Development and application for Huaihe River Basin and Chaophraya River Basin, Proceedings of the Third International Study Conference on GEWEX in Asia and GAME, GAME International Science Panel, (1997).

4)K. Nakane, S. Yazaki and S.Kishi; Estimation of Monthly Mean Air-temperature over the Asian Continent using NOAA AVHRR GAC data, Proceedings of International Workshop on Global Change and Terrestrial Environment in Monsoon Asia, University of Tsukuba,164-167(1997)

5)M. Sugawara et al.; Tank Model with Snow Component, Research Notes of the National Research Center for Disaster Prevention No.65, 1-293(1984).

6)C.W. Thornthwaite; An Approach Toward a Rational Classification of Climate, Geographical Review Vol.38, 55-94(1948).

7)S. Yazaki et al.; Regional Image Proceeding for NOAA AVHRR data Part I Geometric Correction and Map Projection, Report on the 16th Remote Sensing Symposium, 63-66(1990).

6. Publication

1)K. Nakane; Regional Water Balance Model, Proceedings of 1995 Annual Conference, Japan Society of Hydrology and Water Resources, 130-131(1995).

2)K. Nakane; Regional water balance model based on the concept of the Tank Model: Development and application for Huaihe River Basin and Chaophraya River Basin, Proceedings of the International Workshop on the Climate System of Monsoon Asia, Meteorological Research Institute and Center for Climate System Research, University of Tokyo, 219-223(1996).

3) K. Nakane; Regional water balance model based on the concept of the Tank Model: Development and Application for Huaihe River Basin and Chaophraya River Basin, Proceedings of the Third International Study Conference on GEWEX in Asia and GAME, GAME International Science Panel,(1997).

4)K. Nakane, S. Yazaki and S.Kishi; Estimation of Monthly Mean Air-temperature over the Asian Continent using NOAA AVHRR GAC data, Proceedings of International Workshop on Global Change and Terrestrial Environment in Monsoon Asia, University of Tsukuba,164-167(1997)

7. International Cooperation

These studies are being carried out cooperatively with RSTAC/MWS(Remote Sensing Technology Application Center, Ministry of Water Resources in China) and SMRI/SMR/CMA(Satellite Meteorology Research Institute, Satellite Meteorology Center, China Meteorological Administration). In this fiscal year, we had cooperated as follows;

(1)Invitation of Chinese researcher from Dec. 1 to Dec. 27 in 1996

NIED(National Research Institute for Earth Science and Disaster Prevention) had invited two researchers from RSTAC/MWS. We cooperated to analyzing land surface conditions related to hydrological factors using MOS-1 data on Huaihe River basin and attended 5th Working Group Meeting of the Japanese-Sino Cooperative Project and the International workshop on the Climate System of Monsoon Asia.

(2)Visit to RSTAC/MWS and SMRI/SMR/CMA

Nakane visited RSTAC/MWS from Oct. 28 to Nov. 3 in 1996. he exchanged research ideas on analysis of the land surface conditions using satellite data and visited the Huaihe River basin for investigating hydrological stations and the irrigation condition. He also visited SMRI/SMR/CMA from Nov. 4 to Nov. 11, and he exchanged research ideas on analysis for smow cover area using satellite data and visited the agricultural observatory in Thaian City, Shanton probince for installing the soil moisture apparatus.

和文抄録
本研究は広域にわたるアジアモンスーン地域を対象として、降水、積雪・融雪、蒸発散、河川流出等の水文過程を的確にモデル化し、アジアモンスーンの変動が地域の水資源及び土壌水分に与える影響を0.5度×0.5度(約50km×50km)の等緯度経度の分解能で詳しく評価できる広域水収支モデルの開発を目的としている。本研究で開発する広域水収支モデルは広域の地表を０.５度×０.５度の領域にメッシュ分割し、降水量、蒸発量、気温等から任意の地域の河川流量、水の流域貯留量（土壌水分量、地下水量など）、実蒸発散量等を計算するモデルであり、この種の広域の計算に使用されている大気大循環モデルよりも詳細に適切な広域の水資源情報を提供する。この広域水収支モデルはタンクモデルの概念を基本とし用いている。初期的な広域水収支モデルは乾期と雨期のある熱帯域に位置するタイのチャオプラヤ川流域（解析対象面積１１万ｋm2）に適用し、良好な予測結果を得た。現在、このモデルは中国の淮河流域（解析対象面積１２万ｋm2）及び日本の大淀川流域（解析対象面積２千ｋm2）において検証・評価を行っている。また、本研究の最終目標であるアジア大陸の広域水収支モデルを構築するため、地表状態を簡略化した河川網のデータセット作成手法の研究に着手した。この広域水収支モデルは入力データとして膨大な観測データを使用するが、これら広域のデータを密に収集するのは困難である。特に、蒸発量データは困難である。そのため、衛星データを用いた蒸発量の推定研究も行っている。蒸発量は気温と密接に関係しており、NOAA AVHRR GACデータを用いた月平均気温の新しい推定手法を開発し、その一般化手法の検討を行っている。これら研究の今年度の主な成果は以下の通りである。
(1)中国の淮河流域において、広域水収支モデルの検証・評価をより詳細に行うため、３８地点の降水量、１５地点の蒸発量及び６地点のダム流量のデータを用いて、1983年から1989年の7年間のモデルシミュレーションを行った。その結果、全体的に妥当な計算結果を得た。
(2)アジア大陸の広域水収支モデル作成において、広域の地表状態を適切に簡略化し、河川網を作成することが重要であるが、データ量が膨大で人力作業が困難なため、計算機を用いた半自動的な手法を検討した。本年度は、昨年度作成した単純化した河川網データ、尾根線網データ及び標高データから表面流出の広域流出ベクトルを作成する手法を開発した。
(3)月平均気温の推定に用いた回帰式は４つの定数を持ち、それらは地域依存性を有している。この地域依存性は大気中の水蒸気量に関係しており、また、この水蒸気分布は緯度と関係していることが分かっている。そこで、４つの定数を緯度及び標高の関数として求め、それらを用いて、アジア大陸の月平均気温を推定した。それら推定値を約1,000カ所の観測データと比較した。その結果、全体的に妥当な推定値であることが分かった。しかし、地域によっては定数バイアスが生じることも分かった。

III. Synthetic Study on the Atmosphere-Ocean-Land Interactions
大気・海洋・陸面間の相互作用に関する総合研究

1. Experiment of the Atmosphere-Ocean-Land Interactions by the Use of General Circulation Models
大規模モデルによる大気・海洋・陸面間の相互作用に関する実験研究

Meteorological Research institute,
Japan Meteorological Agency
A. Kitoh, K. Mabuchi and
T. Ose
気象庁気象研究所
鬼頭　昭雄、馬淵　和雄
尾瀬　智昭

(Abstract)

The large scale background fields associated with the interannual variability of sea surface temperature anomalies (SSTA) over the South China Sea (SCS) is studied by the statistical analysis of the observational data and the atmospheric general circulation model (AGCM) experiments. The SCS SSTA can be recognized as a unique index for the Asian monsoon and the El Niño/Southern Oscillation (ENSO) system because of its special geographical location for that system.

Interannual variability of the Asian summer monsoon simulated by the MRI coupled atmosphere-ocean GCM (CGCM) is investigated. Simulated precipitation over India is negatively correlated with the equatorial Pacific SST. This corresponds to the model La Niña . The overall relationship between circulation patterns and the SST distribution in the model is consistent with the observed one (i.e., good monsoon is associated with La Niña). Lagged correlations are calculated for surface conditions over land in the preceding season. Correlations for snow mass in March-May show that spring snow is less extensive in western Eurasia in the year when summer monsoon is stronger than normal. At this time, ground is drier although statistical significance is not large. Cloudiness is less and upper tropospheric temperature is warmer in the 30°N-50°N belt over Eurasia. Cold SST anomalies, however, are already prevailing at this time in the tropical Pacific.

1. Objectives

The monsoon is an essential part of climates in the Asian countries by contributing to establish an annual cycle in many meteorological elements. For some contries the monsoon is the climate. And the interannual variability of the Asian monsoon affects climate variations not only in Asia but also in larger parts of the globe because the Asian monsoon region is located close to the ocean with the warmest sea surface temperature and is the most vigorous heating source of the atmospheric general circulation.

The purposes of the present study are to clarify the mechanism of atmosphere-ocean-land interactions in an Asian monsoon region including the Pacific and the Indian Oceans and the Eurasian continent by performing a series of numerical experiments.

2. Methods

We use an atmospheric general circulation model (GCM) which includes interactive land surface processes (in the first phase of the program) and also an ocean-atmosphere coupled GCM (in the second phase). By a series of numerical experiments with atmospheric and/or coupled GCMs, roles of land surface conditions and sea surface temperature (SST) in establishing the monsoon and its variability will be investigated.

Following a sensitivity study of the role of the South China Sea (SCS) SST anomalies on the northern hemisphere summer atmosphere by the MRI atmospheric GCM in the last fiscal year, we made a similar experiment for the northern winter season. We also made the statistical analysis using the observational data in order to clarify the relationship between the SCS SST and circulation changes associated with El Niño/Southern Oscillation (ENSO) phenomenon.

We continued an analysis of a long integration of the MRI coupled atmosphere-ocean GCM (CGCM). The model has a 15-level atmosphere GCM with the top at 1 hPa and a 21-level ocean GCM. The model was integrated for 70 years with flux adjustments. This is the control run of the transient CO_2 increase experiment (Tokioka et al., 1995). In this year, we analyzed interannual variability of simulated Asian summer monsoon and its relationship with the SST and land surface conditions.

3. Results

3.1 SST in the South China Sea

Interannual variability of the SST anomalies over the South China Sea is recognized as a unique index for the Asian monsoon and ENSO system because of its special geographical location for that system.

The following results are obtained by the statistical analysis of the observational data and the atmospheric general circulation model (AGCM) experiments.

(1) The northern summer SCS SSTA do not play the active role on the summer Asian monsoon in a viewpoint of the global scale. The summer SCS SSTA seem to be controlled by in-situ low-level wind anomalies. The weak South Asia monsoon jet is related to the weak low-level wind speed over the SCS, and furthermore the warm SCS SSTA. The westerly wind anomalies in East Asia and the easterly anomalies east of the Philippines are also found at 850 hPa in the case of the warm SCS SSTA.

(2) All years are classified into 'the BO-type years' and 'the LF-type years' by the combination of the polarities of the SCS SSTA and the Niño4 SSTA in the northern winter season. The defined two type years are considered as the in-phase and out-of-phase composition of the biennial mode and the low-frequency mode. The features of the biennial mode can be found in the BO-type years.

(3) In the northern winter, the LF-type years are distinguished from the BO-type years by a small westward shift of the global low-level vorticity anomalies under a given polarity of the tropical eastern Pacific SSTA. The SSTA with a dominant biennial oscillation are found in the regions where the directions of the low-level wind anomalies are quite sensitive to that longitudinal shift across the SCS of the vorticity anomalies. The SCS SSTA are the most typical case.

(4) Tropical eastern Pacific SSTA change significantly during the northern spring for the BO-type years. On the other hand, they tend not to change for the LF-type years. The low-level wind anomalies over the tropical western Pacific in winter may be important factors to determine the change of Niño3 SSTA during the following spring.

(5) In the northern summer, the detailed interannual variability of the SCS SSTA is associated with the fluctuations of the three major low-level wind branches over South Asia, East Asia, and the western Pacific. The typical BO-type years are distinguished from the LF-type years by the strength of zonal wind anomalies and associated geopotential height anomalies at 850 hPa in the western Pacific.

3.2 Monsoon variability in the MRI coupled GCM

The MRI CGCM has simulated some aspects of El Niño (Yukimoto et al. 1996). The SST averaged for the Niño3+4 region for June-August (JJA) is shown in Fig. 1c. It has a dominant peak periods of 3 to 6 years. Also shown is the South Asian monsoon index defined as (a) land precipitation over 60°-100°E, 10°-30°N and (b) difference of zonal winds between 850 hPa and 200 hPa averagred over 40°-110°E, 5°-20°N. Correlation coefficient between monsoon rainfall and monsoon wind shear index is 0.08 and is not significant. Correlation between monsoon rainfall and Niño3+4 SST is -0.51 and is statistically significant. Correlation becomes larger when we use Niño4 SST ($r = -0.55$), while it becomes less with Niño3 SST ($r = -0.33$). Correlation between monsoon wind shear index and Niño3+4 SST is -0.13 and is not significant. Therefore, the model reproduces the observed relationship (i.e., good monsoon is associated with La Niña).

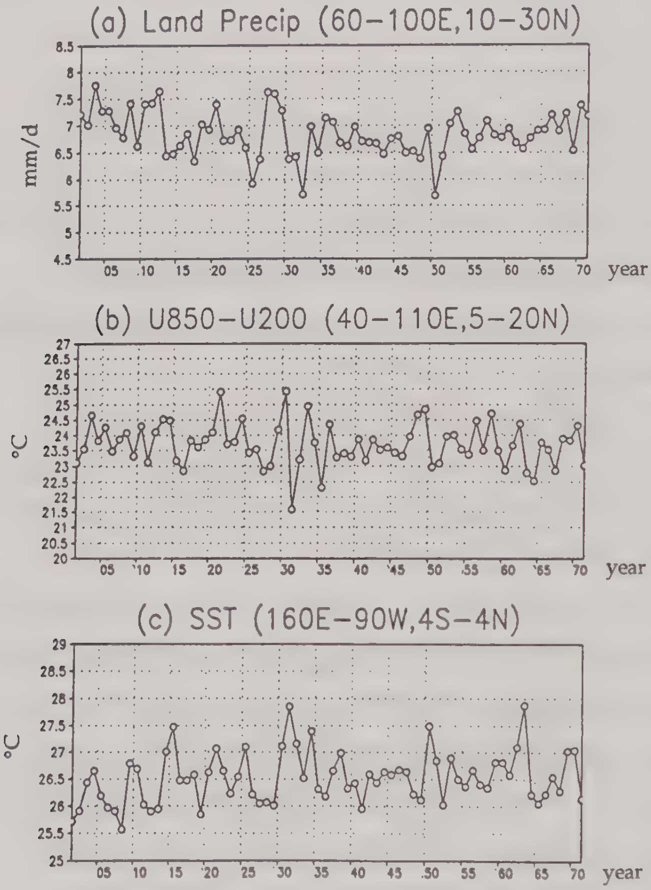


Fig. 1 Time series of the simulated (a) precipitation averaged over land for 60°-100°E, 10°-30°N, (b) zonal wind difference between 850 hPa and 200 hPa averaged for 40°-110°E, 5°-20°N, (c) SST averaged for 160°E -90°W, 4°S-4°N. All values are the JJA averages.

Figure 2 shows simultaneous correlations between the two monsoon indices (i.e., rainfall in Fig. 1a and wind shear in Fig. 1b) and SST. Precipitation in India is significantly correlated with the Pacific SST (Fig. 2a). There is a negative SST anomaly over tropical Pacific and a potitive SST anomaly in the North Pacific. The largest negative anomaly is located in the central equatorial Pacific. This simulated SST pattern in the Pacific corresponds to the model La Niña and captures the observed SST anomaly pattern. Correlations are less in the Pacific when the monsoon wind shear index was used (Fig. 2b), although a negative anomaly is larger over the Arabian Sea.

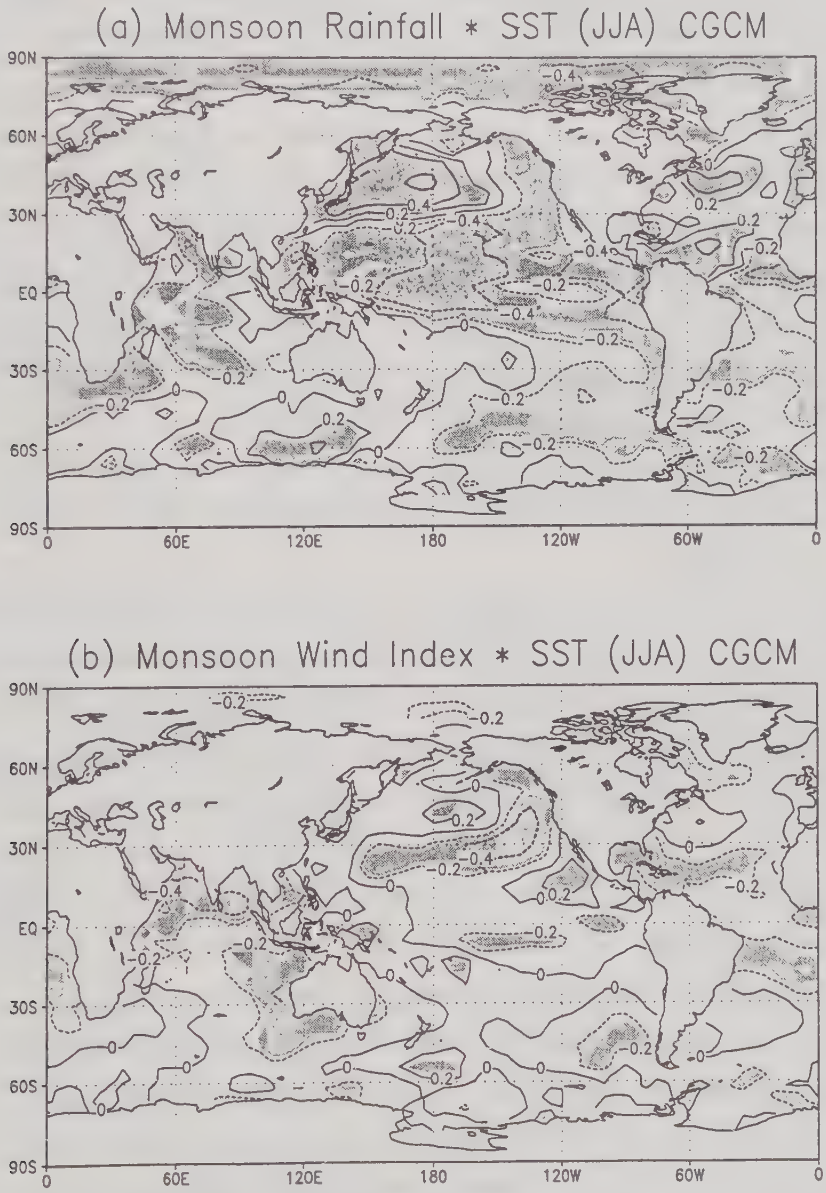


Fig. 2 (a) Simultaneous correlations between monsoon rainfall and SST in JJA. Contour interval is 0.2. Significant region is shaded. (b) As in (a) but for monsoon wind shear index.

Figure 3a shows simultaneous composite anomaly of precipitation in all grid points in JJA with respect to the Indian monsoon rainfall. Fluctuation of the JJA rainfall over India and South Arabia occurs coherently in the model. It is noted that there is negative relationship in precipitation between India and southern China. There is a trace of positive precipitation anomaly over Sahel. This feature is similar to the summer precipitation anomaly at the time of climatic optimum around 6,000 years ago. Surface air temperature (Fig. 3b) is cooler than average over a broad region from Africa through Saudi Arabia, India and over the western Pacific. Negative temperature anomaly over land is well correlated with precipitation (Fig. 3a) and soil moisture anomaly (Fig. 3c). Over the region with heavier than normal precipitation, there are more cloudiness (Fig. 3d). A belt from South China to Japan is characterized with less cloud. A broad region over the western Indian Ocean and most of Africa is covered with easterly wind anomaly at 200 hPa (Fig. 3e), corresponding to a stronger Tibetan high and a stronger monsoon easterly jet. At 850 hPa, easterly wind anomaly is found over the Arabian Sea, indicating a stronger monsoon flow. There is an easterly wind anomaly over a broad region from east of India through the equatorial western Pacific, which is consistent with La Niña type SST anomalies. These anomalous wind fields correspond to lower tropospheric moisture convergence over India, resulting in positive precipitation anomaly there. Therefore, the overall relationship between circulation patterns and the SST distribution in the model is consistent with the observed one (i.e., good monsoon is associated with La Niña).

Figure 4 shows composite of (a) snow mass, (b) ground temperature, (C) soil moisture, (d) cloudiness, (e) 200 hPa temperature, and (f) 200 hPa height averaged in January-May with respect to the Indian monsoon rainfall in JJA. Snow mass anomaly in Fig. 4a shows that spring snow is less extensive in western Eurasia in the year when summer monsoon is stronger than normal. At this time, ground temperature is above normal. Ground is drier although statistical significance is not large. Cloudiness is less and upper tropospheric temperature is warmer in the 30°-50°N belt over Eurasia. They show a consistent feature of warmer and drier conditions at the ground and in the troposphere. Cold SST anomalies, however, are already prevailing at this time in the tropical Pacific (not shown). Therefore, these circulation anomaly, and resultant ground condition, seem to be an atmospheric response to the SST anomaly in the remote tropical Pacific. Whether there is an influence of land surface conditions and monsoon variability on tropical Pacific SST changes needs further study.

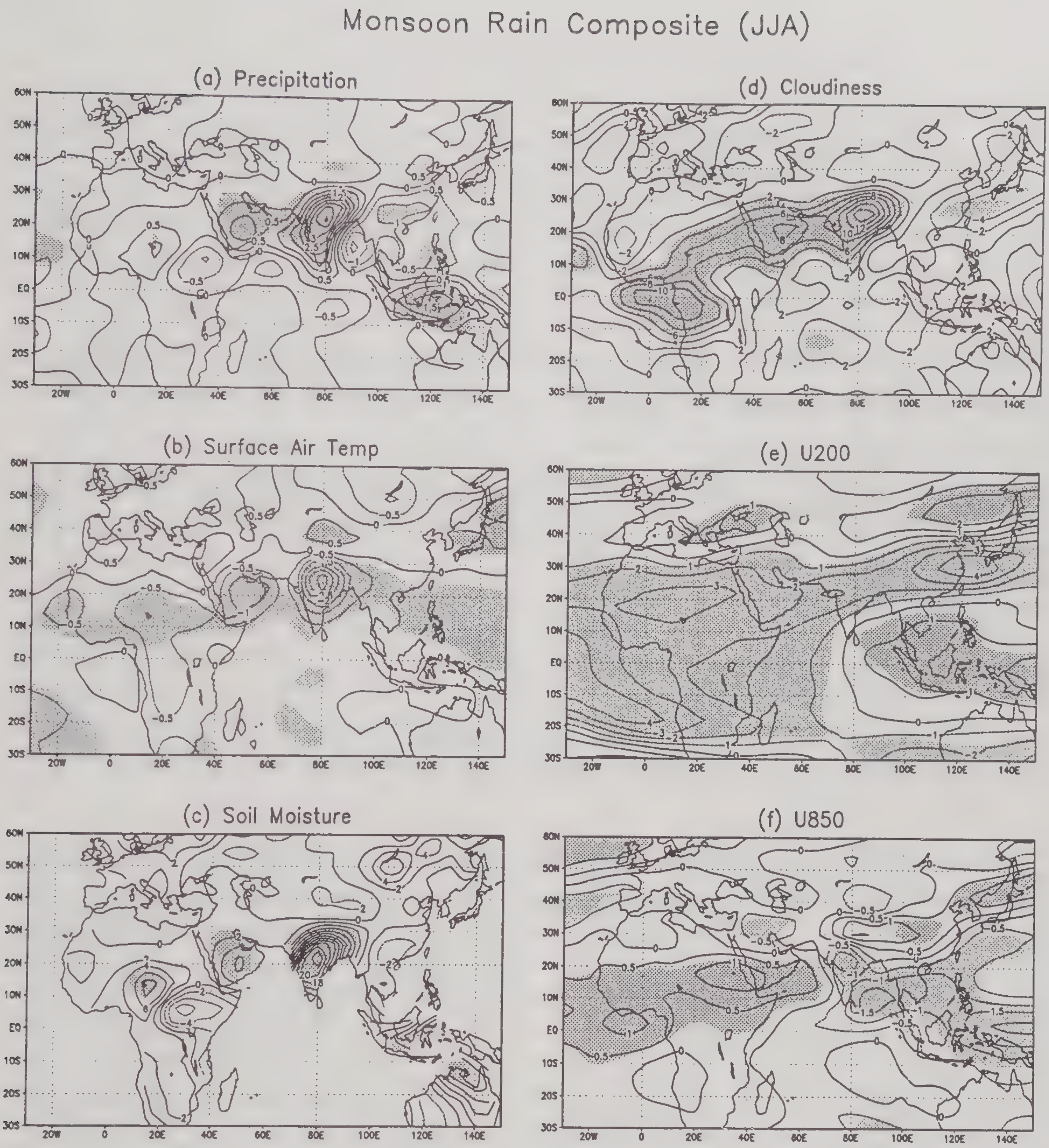


Fig. 3 Composites in JJA of (a) precipitation (contour interval is 0.5 mm/d), (b) surface air temperature (0.5° C), (c) ground wetness (2%), (d) cloudiness (2%), (e) zonal wind at 200 hPa (1 m/s), and (f) zonal wind at 850 hPa (0.5 m/s). Composite is calculated using years when JJA precipitation over India (Fig. 1a) exceeds 1 standard deviation. Shaded region is where correlation is significant at 95% level.

Monsoon Rain Composite for JFMAM

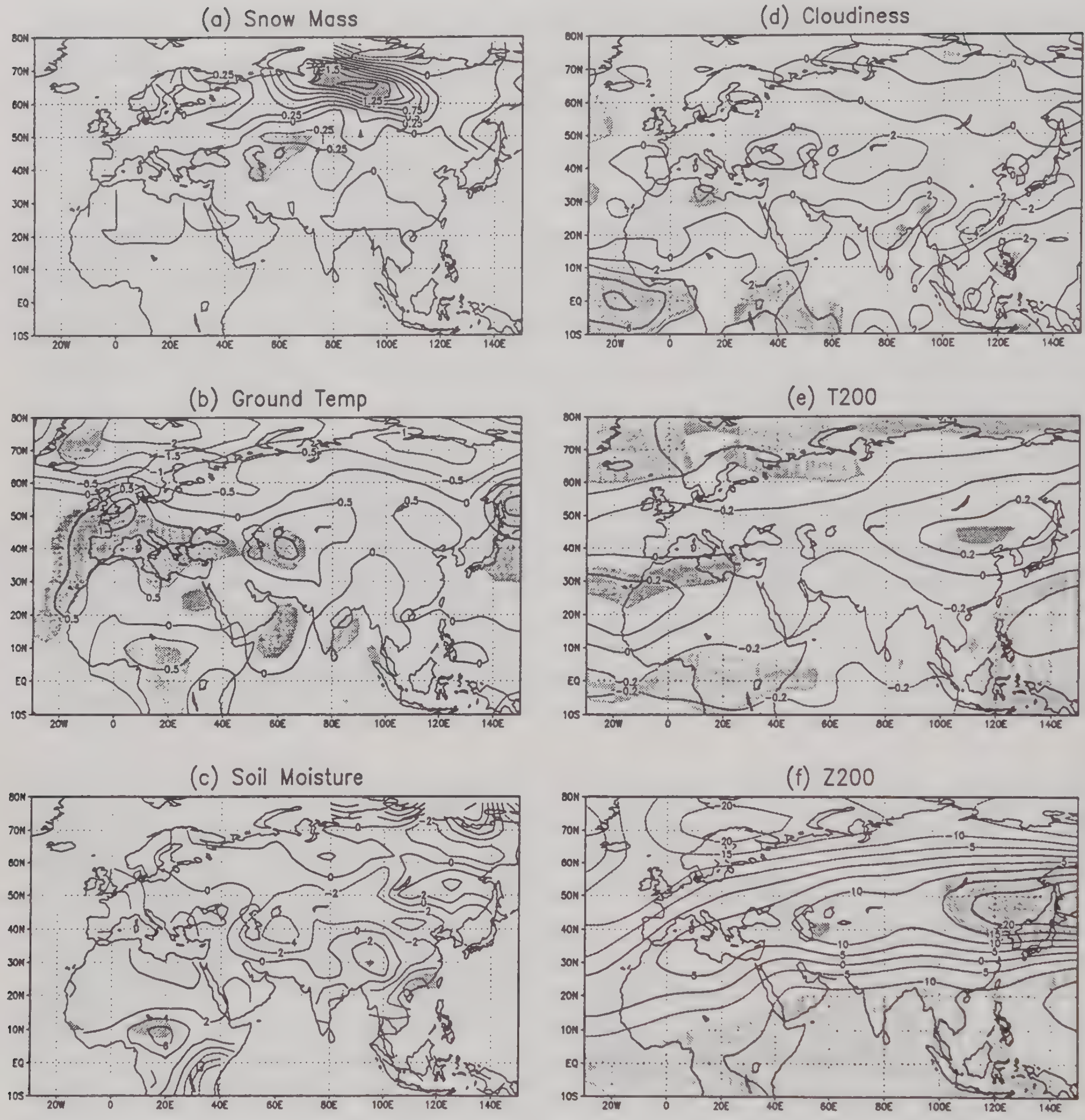


Fig. 4 Composites in January-May of (a) snow mass (contour: 0.25 kg/m^2), (b) ground temperature (0.5° C), (c) ground wetness (2%), (d) cloudiness (2%), (e) 200 hPa temperatured (0.2° C), and (f) 200 hPa height (5 m). Composite is calculated using years when JJA precipitation over India (Fig. 1a) exceeds 1 standard deviation. Shaded region is where correlation is significant at 95% level.

4. Discussions

With respect to the data analysis of the SCS SST, we confirm that the tropical atmospheric circulation anomalies are closely coupled with the SSTA. The characteristic anomalies in the tropical atmosphere are simulated by the AGCM with the observed tropical SSTA. The tropical atmospheric anomalies seem to explain the corresponding SSTA. We have neither challenged to analyze the tropical ocean data nor to use the atmosphere-ocean coupled model in order to explore the oceanic state. This work may be made in the future.

The MRI coupled model showed interannual variations, similar to the observation that a good monsoon is associated with La Niña type SST anomalies. It is also found that snow is less and the ground is generally dry in western Eurasia in spring preceding a good monsoon. However, whether land surface conditions and monsoon variability could have an impact on tropical Pacific SST changes needs further sensitivity studies.

5. References

Tokioka, T., A. Noda, A. Kitoh, Y. Nikaidou, S. Nakagawa, T. Motoi and S. Yukimoto, 1995: A transient CO_2 experiment with the MRI CGCM -Quick report-. *J. Meteor. Soc. Japan*, **73**, 817-826.

Yukimoto, S., M. Endoh, Y. Kitamura, A. Kitoh, T. Motoi, A. Noda and T. Tokioka, 1996: Interannual and interdecadal variabilities in the Pacific in an MRI coupled GCM. *Clim. Dyn.*, 12, 667-683.

6. Publications

Ose, T., Y.-K. Song and A. Kitoh, 1997: Sea surface temperature in the South China Sea - a unique index for the Asian summer monsoon and ENSO system. (Submitted to *J. Meteor. Soc. Japan*)

7. International Cooperation

Discussion on a manuscript on the South China Sea SST paper (Ose et al., 1997) was made by email between the MRI and the CAMS.

要旨

南シナ海の海面水温に関する観測値の統計的解析及び大気大循環モデルの実験から、南シナ海の海面水温の年々変動は、その地理的位置のため、アジアモンスーンとENSOシステムのユニークな指標と認識できることが分かった。夏季の南シナ海の海面水温偏差は、アジアモンスーンに対して大きな空間スケールでは積極的な役割を果たしていない。南シナ海の海面水温偏差は、むしろ下層風偏差によって決まっている。冬季の南シナ海およびNINO4海面水温偏差の正負の組み合わせによりすべての年は2つのタイプに分類される。このタイプの違いは熱帯太平洋の海面水温偏差の空間パターン、大規模な下層渦度偏差の東西方向の微強なシフトをもたらすが、南シナ海は、この東西のシフトにより渦度偏差がその東に位置するか西に位置するかの微妙な位置にあることが分かった。

気象研究所全球大気・海洋結合モデルの基準実験で得られたアジアモンスーンの年々変動の解析を行った。モデルは３～６年の周期帯のエルニーニョを再現している。観測と同様にモデルでもアジアモンスーンが強い時にはラニーニャ傾向であることが分かった。またこの時には春の西ユーラシア大陸の積雪は少なくなっており、雲量も少なく地面は乾燥し上部対流圏の気温は高い。熱帯太平洋ではこの時には既にラニーニャが進行しており大気循環場の偏差はこの海面水温偏差に応答したものとも考えられる。

III. Synthetic study of the monsoon circulations
大気・海洋・陸面間の相互作用に関する総合研究

2. Analysis of the energy balance of monsoon
モンスーンのエネルギー収支に関する解析研究

Meteorological Research Institute (MRI)
Japan Meteorological Agency
Tomoaki Ose
気象庁気象研究所
尾瀬　智昭

(Abstract)

The air column heat budget is obtained from the ECMWF re-analysis upper air level data in association with the Asian summer monsoon. The characteristics of the heat budget from spring through early summer in the Eurasian Continent are studied preliminarily.

The heat budget of Tibet is qualitatively similar to that of the arid region west of Tibet where positive sensible heat flux from the surface and radiative cooling in the upper air are found. The differences are the contribution of the downward motion to warming and the relatively active evaporation in the arid region.

The condensation heating in the upper air is common over Siberia and near Japan in early summer. The positive sensible heat flux and warm horizontal advection are extended over Siberia and near Japan, respectively.

1. Objectives

Asian monsoon is formed basically by the solar heat difference between land and ocean. In order to understand the mechanism of the Asian monsoon activities including its onset, it is one way to analyze the spatial and temporal variabilities of the energy budget associated with the Asian monsoon.

We have studied Earth Radiation Budget (ERB) at the top of the atmosphere in the Asian monsoon system. ERB at the top of the atmosphere is distributed into the other regions through the ground and ocean heat budget and through the atmospheric heat budget. It is important to know how ERB is distributed in the Asian monsoon system. The atmospheric heat budget of the Asian summer monsoon is studied with that purpose. The preliminary results are reported.

2. Methods

The ECMWF re-analysis advanced analysis upper air data set for 1985-87 is used to study the atmospheric energy budget. The data has the horizontal resolution of 2.5°x2.5°. The vertical levels for analysis are 1000, 925, 850, 775, 700, 600, 500, 400, 300, 250, 200, 150, 100, 70, 50, 30 and 10hPa. The heat budget is obtained in almost the same way as Hoskins et al. (1989) The analysis is made twice a day (0000 and 1200 UTC). The results are averaged for three periods of about 10 days in each month. The climatic surface pressure is obtained from the smoothed orography of the U.S.Navy 10-minute resolution dataset by the interpolation of the geopotential height at the standard pressure levels.

The heat budget shown here comprises the net increase of temperature, horizontal advection, vertical advection plus adiabatic compression, and Q1 (Yanai et al., 1992). The diabatic heating is separated to condensation and evaporation heating in the air, sensible heating from the ground, net radiative heating in the air. These terms are supposed from Q2 to some extent by comparing the signs and the magnitudes of Q1 and Q2. The heat budget terms are averaged vertically with mass weight in the whole air column (85hPa-surface).

The vertically integrated Q1 and Q2 are denoted as:

$Q1=R+LP+S$,

$Q2=LP-LE$,

where R, P, S and E are radiative heating rate in the air, precipitation rate, sensible heat flux from the surface and evaporation rate at the

surface, respectively.

3. Results

The preliminary results of the heat budget from spring to early summer are shown in this report. The air temperature increase is large over the Northern Continents as compared with oceanic regions in these seasons (not shown).

Figure 1 (a) and (b) shows Q1 and Q2 for March and April mean, respectively. Unit is K/day. Figure 1 (c) and (d) is the same as Fig.1 (a) and (b) except for May and June mean. March and April are the season before the summer Asian monsoon begins. May and June correspond to the early period of the monsoon.

Figure 2 is the same as Fig.1 except for the lower air column (700hPa-surface). Figure 3 are the same as Fig.1 except for vertical advection plus adiabatic compression (-VADV) in (a) and (c) and horizontal advection (-HADV) in (b) and (d).

March and April are referred to as spring, and May and June are referred to as early summer in this report.

a. Tibet region (30°-42°N,70°-100°E)

Positive Q1 and no corresponding Q2 in spring suggest that positive S+R is dominant in this season. According to the vertical distribution of Q1 and Q2 (not shown), positive S is dominant near the surface or 500hPa, and negative R is dominant at 200hPa. The cooling due to upward motion is found in spring. The qualitatively same characteristics are confirmed in early summer.

b. Arid region (30°-50°N,50°-70°E)

Negative R is found in the upper air in spring. But, the Q1 and Q2 in the lower air suggest positive sensible heat flux and evaporation from the surface. Evaporation seem to be active over lakes in this region. The difference from Tibet is that downward motion contributes to the warming. Positive sensible heat flux and evaporation from the surface are strengthen in early summer.

c. Siberia region (50°-70°N,90°-160°E)

Radiative cooling is dominant in spring when Q1 is averaged through the whole air column. Positive sensible heat flux is found near surface south of Siberia. Positive sensible heat flux and evaporation from the

surface are extended in early summer.

d. Near Japan region (30°-50°N,130°-160°E)

Positive sensible heat flux and evaporation from the surface are clearly found south of Japan in spring. The relatively cold and dry air is still advected horizontally over East Asia from the Continent. The above heat budget is drastically changed in early summer. The precipitation or condensation heating is dominant in Q1 and Q2 during early summer as compared with the sensible heat and latent heat flux at the surface. Horizontal heat advection is positive in early summer.

e. South Asia region (6°-30°N,70°-100°E)

The Q1 is well balanced by the cooling due to upward motion in most of the convective region. Evaporation is active at the surface over the ocean through the seasons. The positive sensitive heat flux is dominant in India in spring. The condensation heating is dominant in India in early spring when the Indian monsoon begins.

4. Discussions

The model results reported last year (not published at the present) seem to be rather different from the observational results. The major difference in the heat budget comes from the precipitation distribution in the model, particularly over Tibet and Siberia. The contribution of the downward motion to the continent heat budget seems to be relatively large in the model. Detailed analysis of the observational heat budget is necessary.

5. References

1) Hoskins, B.J., H.H. Hsu, I.N. James, M. Masutani, P.D. Sardeshmukh and G.H. White, 1989; Diagnostics of the global atmospheric circulation based on ECMWF analysis 1979-1989. *WMO/TD.* No.326. 217pp.

2) Yanai, M., C. Li, and Z. Song, 1992: Seasonal heating of the Tibetan Plateau and its effects on the evolution of the Asian summer monsoon. *J. Meteor. Soc. Japan*, **70**, 319-351.

6. Publications

None

7. International Cooperation

None

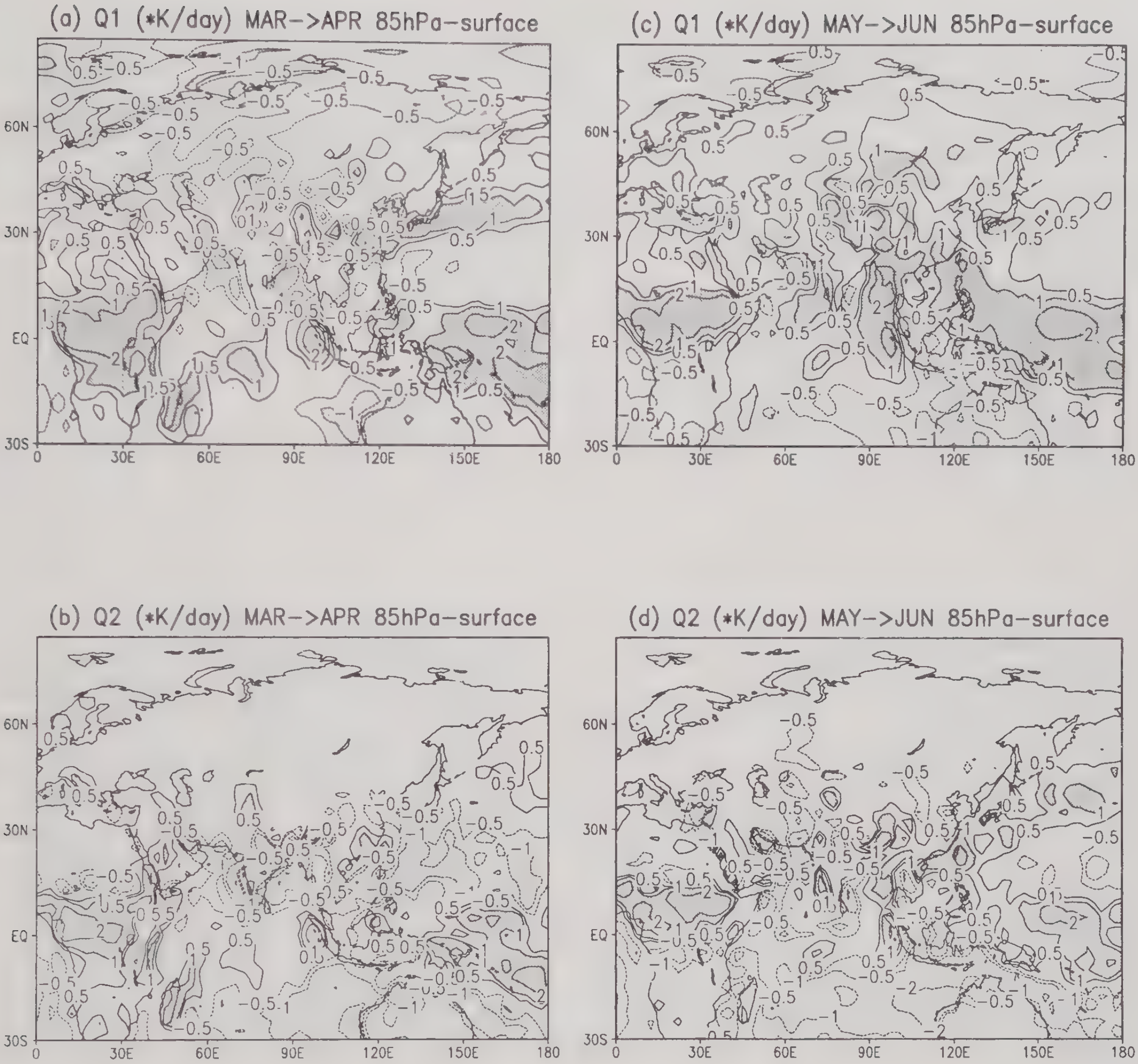


Fig.1 (a) Q1 vertically averaged between 85hPa and surface for March and April mean. (b) the same as (a) except for Q2. (c) and (d) are the same as (a) and (b) except for May and June. Contours are only -2, -1, -0.5, 0.5, 1, 2K/day.

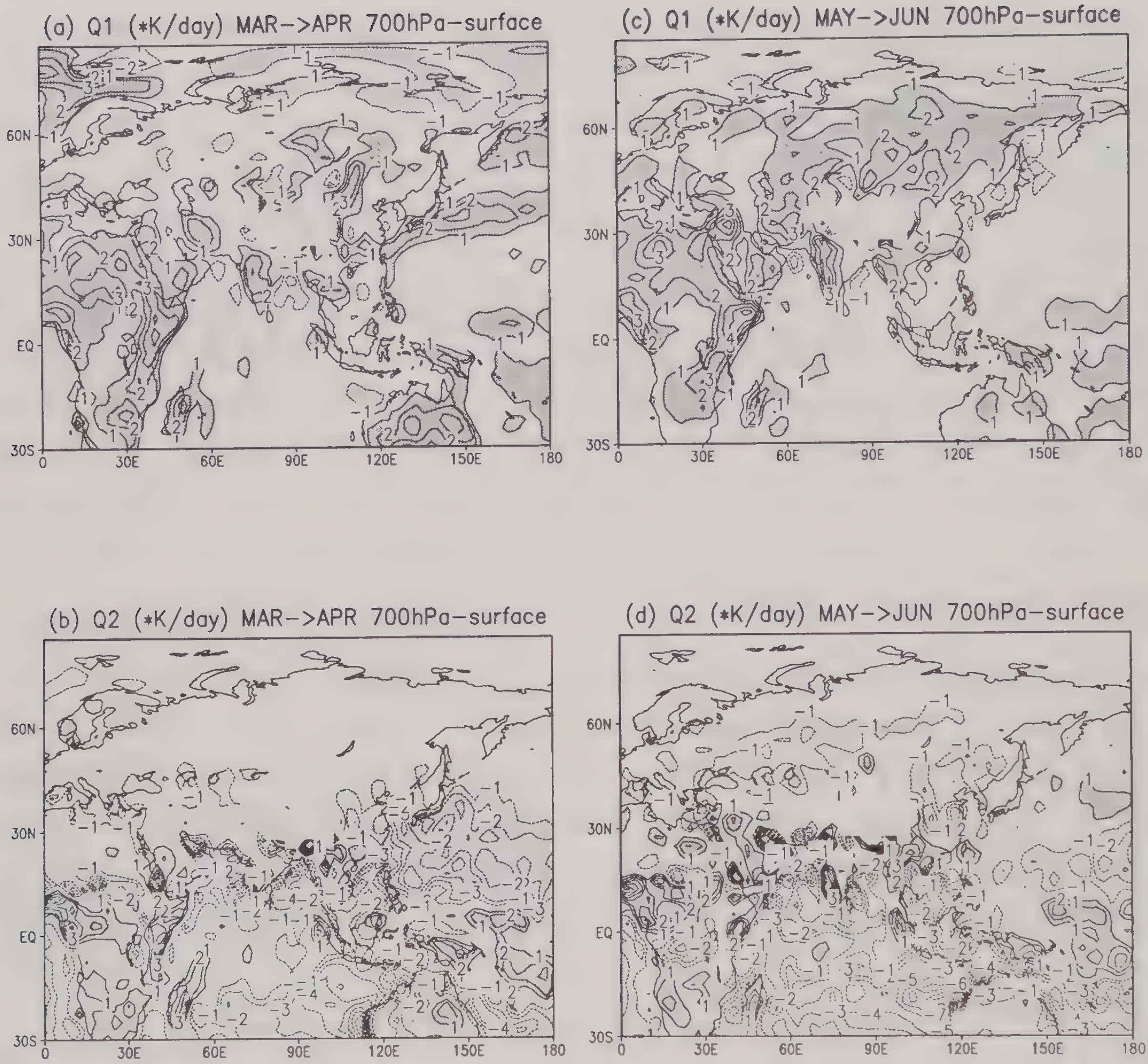


Fig.2 the same as Fig.1 except for those averaged between 700hPa and surface. Contour interval is 1K/day.

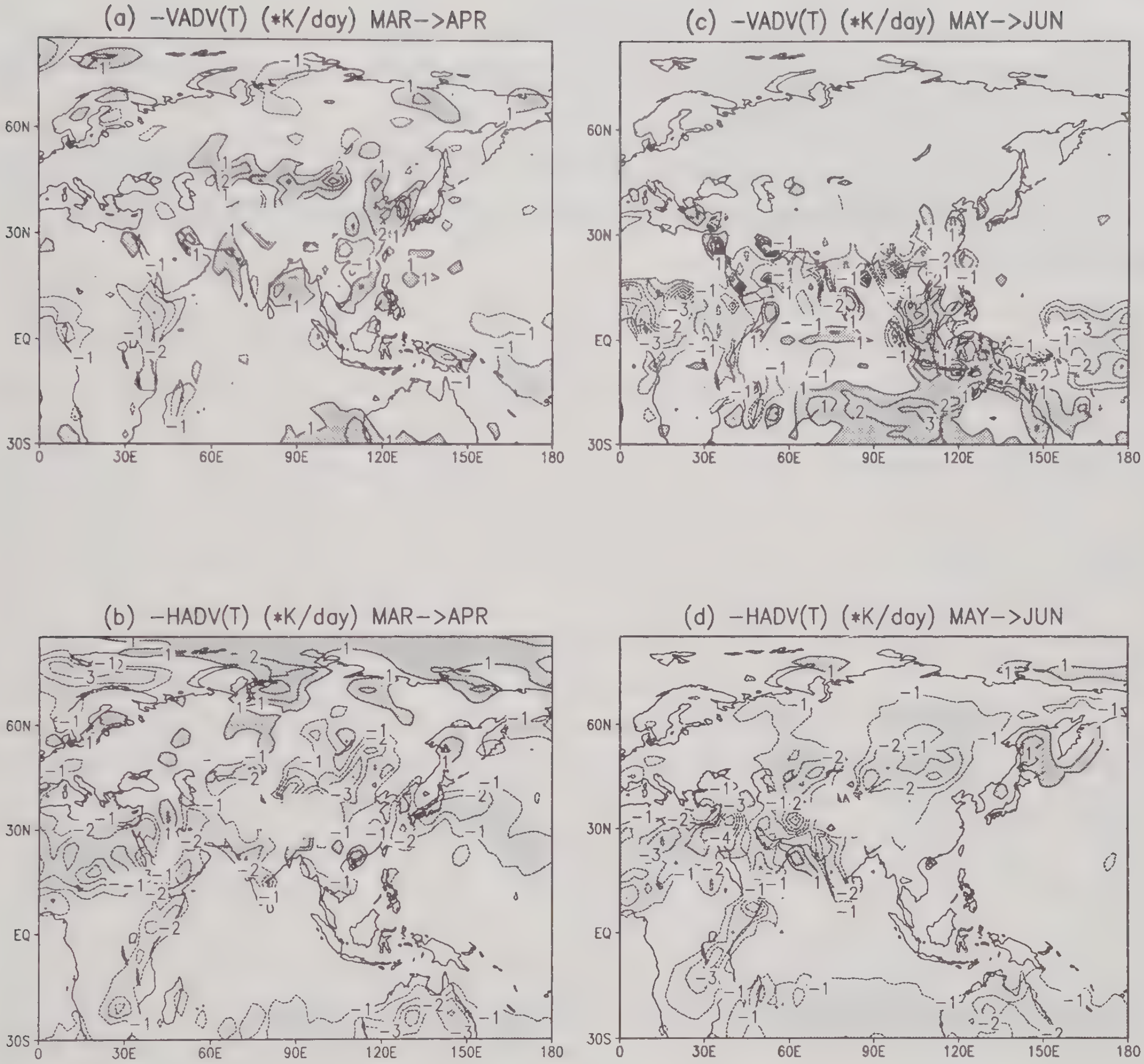


Fig.3 the same as Fig.1 except for vertical advection in (a) and (c) and horizontal advection in (b) and (d). Contour interval is 1K/day.

要旨

ECMWFの再解析上層大気データを用いて、夏のアジアモンスーンに関連した熱収支解析を行った。春から初夏にかけてのユーラシア大陸上の熱収支の特徴が、初歩的であるが解析された。

チベットの熱収支は、チベットの西の乾燥域と、地表面での正の顕熱フラックスと上層大気での放射冷却が見られるという点で定性的に似ている。乾燥域では、下降流による昇温と比較的活発な蒸発が見られるところが異なる。

シベリアと日本付近では、初夏の上層大気中に凝結熱が見られるのが共通している。シベリアでは正の顕熱フラックスが、日本付近では水平方向の暖気移流が見られる点が異なる。

Ⅲ. 大気・海洋・陸面間の相互作用に関する総合研究
Synthetic study on the atmosphere-ocean-land interactions

3.モンスーン循環系の総合解析
Synthetic study of the monsoon circulations

気象庁
気候・海洋気象部
気候情報課
藤川典久、石原幸司、多田一正
Climate Prediction Division
Climate and Marine Department
Japan Meteorological Agency
N.Fujikawa,K.Ishihara, K.Tada

(Abstract) Three indices have been proposed to represent the activity of Asian summer monsoon. The Outgoing Longwave Radiation (OLR) data observed by orbital satellites are used to estimate them under the assumption that OLR is associated with the convective activity which is one of the features in Asian summer monsoon . The proposed indices show the seasonal activity of monsoon, latitudinal and longitudinal gradients of the convective activity for summer season, respectively (hereafter, referred to as SAMOI(A), SAMOI(N) and SAMOI(W)). They also indicate the horizontal scale and the intensity of convection.

A number of simultaneous correlation coefficients between these indices and atmospheric fields, and sea surface temperature, are calculated to assess its validity. The results are consistent with our previous investigations. It is remarkable that atmospheric responses over Japan and the Philippines to SAMOI(N) are greatly different compared with those to SAMOI(W). SAMOI(N) brings the positive anomalies over Japan at 500hPa and 100hPa heights, and SAMOI(W) the negative anomalies. These differences indicate an availability for forecasts around Japan in summer seasons. They may show an annual variation of the monsoon activity state. As for forecasts, it is necessary to search for the predictors to estimate these indices before starting summer season. It will be one of the powerful tools for this research.

The snow cover is one of the possible predictors in the light of the experiment using numerical prediction models. So we investigated the relationship between these indices and the snow cover in the western Siberia in April, and it showed little correlation. It means that the snow cover in April gives little influence on the three month mean activity of Asian summer monsoon. Furthermore, we made another investigation ; the relationship between the snow cover in the western Siberia in April and Okhotsk high pressure in June. Composite maps of the 500hPa geopotential height show some influence of the snow cover on the 500hPa height field in the eastern Siberia in June. The above two results indicate that the snow-covered area to be investigated should be extended into the Eurasian continent, because the limited area of the snow cover was used in our investigation. The snow cover may give an

influence on the atmospheric circulation in June.

1. Objectives

The Asian monsoon circulation shows the variation on the time scales from several ten days to several years and has a significant influence on the climate in Japan and the world through the global atmospheric circulation. The purposes of this study are to clarify long-term variations of the monsoon circulation and to assess the influence on the climate in Japan and the world by the observational data analysis.

2. Methods

The data used for making indices are three-monthly means of outgoing longwave radiation (OLR) observed by orbital satellites. The OLR data averaged for June, July and August are calculated in the areas shown in Figure 1. The deviation from normal, which is defined as the means for 1979 to 1996, is used to calculate the following three indices and normalized statistically every index. SAMOI(A) = (−1) * OLR(W+E), SAMOI(N)= OLR(S) − OLR(N), SAMOI(W) = OLR(E) − OLR(W) , where OLR(X) indicates the deviation of OLR from the normal in the X-area. Simultaneous and lagged correlation methods are used to assess the validity of three indices.

The extension of the snow cover in the western part of Siberia is defined as the square (km^2) in the rectangular area surrounded by 50N to 60N in latitude, from 50E to 80E in longitude. Composite maps at 500hPa in the large and small snow-cover cases are made using eight years' data selected for 1971 to 1995, respectively.

3. Results

Figure 1 shows the area used for the calculation of three indices. Asian summer monsoon is a meteorological phenomenon including the circulation in the more extensive area. However, cumulus convection in the defined area on the whole are drawn attention to.

Figure 2 shows the annual variation of three indices. The values of SAMOI(A) more than a standard deviation show that the convective activities in 1984, 1985 and 1994 are stronger and correspond to the hot summer in Japan. On the other hand, those in 1979, 1983 and 1993 are weaker and correspond to the cold summer in Japan except for the year of 1979.

Figure 3 shows the simultaneous correlation between the 500hPa and 100hPa height anomalies and three indices. In the case of strong convection, the positive correlation coefficient around Japan are shown at both heights. It indicates the barotropic structure of atmospheric state, for example, as shown in the analysis of hot summer in 1994. The index of SAMOI(N) has a positive correlation with both 500hPa and 100hPa height anomalies around Japan. It means that the strong convection in the N-area causes positive anomalies over Japan at both levels. On the other hand, SAMOI(W) has a negative correlation with both height anomalies around Japan. It follows that the weak convection off the Philippine Islands leads to the negative height anomaly around Japan.

Figure 4 shows the composite maps of 500hPa height in June in the case of large and small snow cover in the western Siberia, respectively. The difference appears in

the eastern Siberia and around Japan, where the anomalies of two composite maps are out of phase. This difference results from albedo and hydrological effects of the snow cover on the atmosphere. It is also shown that the temperature anomaly at 850hPa (not shown here) had a negative simultaneous correlation with the snow-covered area in April.

4. Discussions

Asian summer monsoon is a large scale seasonal phenomenon in the area from the Arabian sea to the southeast Asia. The general characteristic features are shown in a number of papers ; the existence of monsoon trough at 850hPa, Somali jet, Tibetan high intraseasonal oscillation of convective activity and so on. The heat source by convection among them is the important factor to drive the atmosphere. Rainy fronts and atmospheric fields over Japan is more or less associated with this monsoon circulation. On the other hand, there is an annual variation of Asian monsoon activity, which seems to be essential to give an influence on the summer weather in Japan. Our previous investigations showed the relationship between the weather in Japan and the convective activity in the monsoon area principally. However, we had so far no synthetic index which represents the Asian summer monsoon activity, using homogeneous observations by satellites.

The newly developed indices represented the heat source distribution by the convection over the monsoon area. They indicate the total activity of convection in the defined area, the gradients from north to south and from east to west of convective activities, respectively. According to the simultaneous correlation maps at 500hPa and 100hPa, the atmospheric responses over Japan to the total activity show the positive coefficients in both levels. It indicates a kind of the heat source response from the monsoon area to the atmospheric circulation in mid-latitudes for summer seasons. Lau and Phillips (1986) showed the response patterns of the tropical heat source to the atmospheric winter circulation in the mid-latitudes, using OLR. The response for summer seasons is located in a few positions with the small area compared with that for winter seasons. And there are different responses of both height fields to SAMOI(N) and SAMOI(W). This difference is useful information for the weather forecasting in Japan in the summer season. We can apply these indices to the extremely hot summer in 1994 and the cool summer in 1993 over Japan. Figure 2 represents the high positive value of SAMOI(A) and SAMOI(N) in 1994. In 1993 , SAMOI(A) shows a high negative value. The positive anomalies appear in the height fields over Japan (shown in Figure 3). An analysis of hot summer in 1994 showed the positive height anomaly over Japan (Fujikawa et al., 1996). In 1993, there was the negative height anomaly at 500hPa. They correspond to the summer weather over Japan in both years.

These indices are consistent with our previous investigations. We can use them as a measure for the synthetic analysis. Our next target is to search for the predictors from the boundary conditions, which would be associated with the indices. Sea surface temperature and the extent of snow cover are one of the boundary conditions to the atmosphere. Firstly, we would draw attention to an influence of the extent of

snow cover on the atmosphere. Hahn and Shukla (1976) showed the relationship between the snow cover in Tibetan plateau and Indian monsoon rainfall. As for the numerical experiment, an influence of the extent of snow cover in Eurasia on the atmosphere is pointed out by Kodera (1989). Figure 4 represents the relationship between the extent of snow cover over the western Siberia in April and 500hPa height in June. The opposite height anomaly pattern appears in the eastern Siberia in the two cases (small and large snow cover), shown in the investigation by Ishihara (1996). However, there is little impact in the correlation between three indices and the snow covered extent in April. These results give us new investigations under the condition of the extension of snow covered area to be investigated in the Eurasian Continent, and of the production of monthly mean indices.

5. References

1) Fujikawa, N. and K.Tada, 1996 : Annual Report (Apr.1995 ~ Mar.1996) of Japanese Experiment on Asian Monsoon, 163 -167, edited by Research and Development Bureau, Science and Technology Agency, Japan.

2) Hahn, D.G., and J. Shukla, 1976 : An apparent relationship between Eurasian snow cover and Indian monsoon rainfall. J. Atmos. Sci., **33**, 2461 - 2463.

3) Kodera, K. and C. Chiba, 1989 : West Siberian spring snow cover and East Asian June 500mb height. Papers in Meteorology and Geophysics, **40**, 51 - 54.

4) Lau,K.-M and T.J.Phillips, 1986: Coherent fluctuation of extratropical geopotential time scales, J. Atmos. Sci., **43**, 1164 - 1181.

6. Publications

1) Fujikawa, N., 1997 : Reprints of the 1997 Spring Semi-annual Meeting of the Meteorological Society of Japan, 21 - 23 May, Tukuba, D104, P109.

2) Ishihara, K., et al.,1996 : Reprints of the 1996 Autumn Semi-annual Meeting of the Meteorological Society of Japan, 6 - 8 November, Nagoya, A156, P33.

7. International cooperation

none

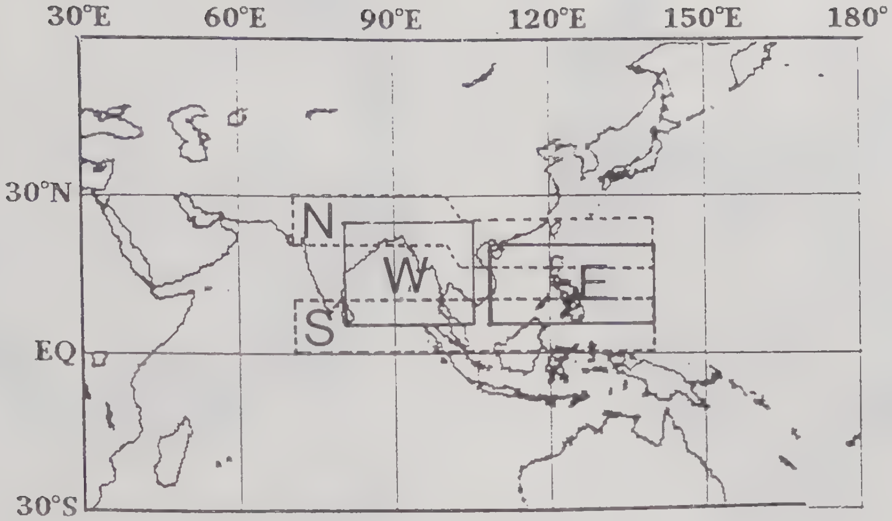


Fig.1 Regions used for development of Asian summer monsoon indices.
W area : (80E−105E, 5N−25N), E area : (107.5E−140E, 5N−25N)
N area : (70E−100E, 20N−30N) + (102.5E−140E, 15N−25N), S area : (70E−140E, EQ.−10N)

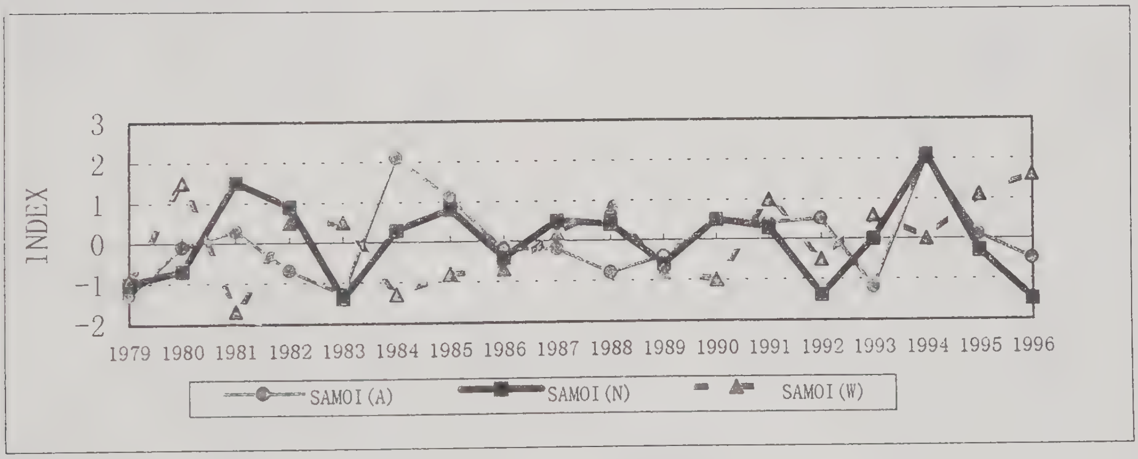


Fig.2 Annual variations of developed indices. Closed circle, square and triangular marks show SAMOI(A), SAMOI(N) and SAMOI(W), respectively.

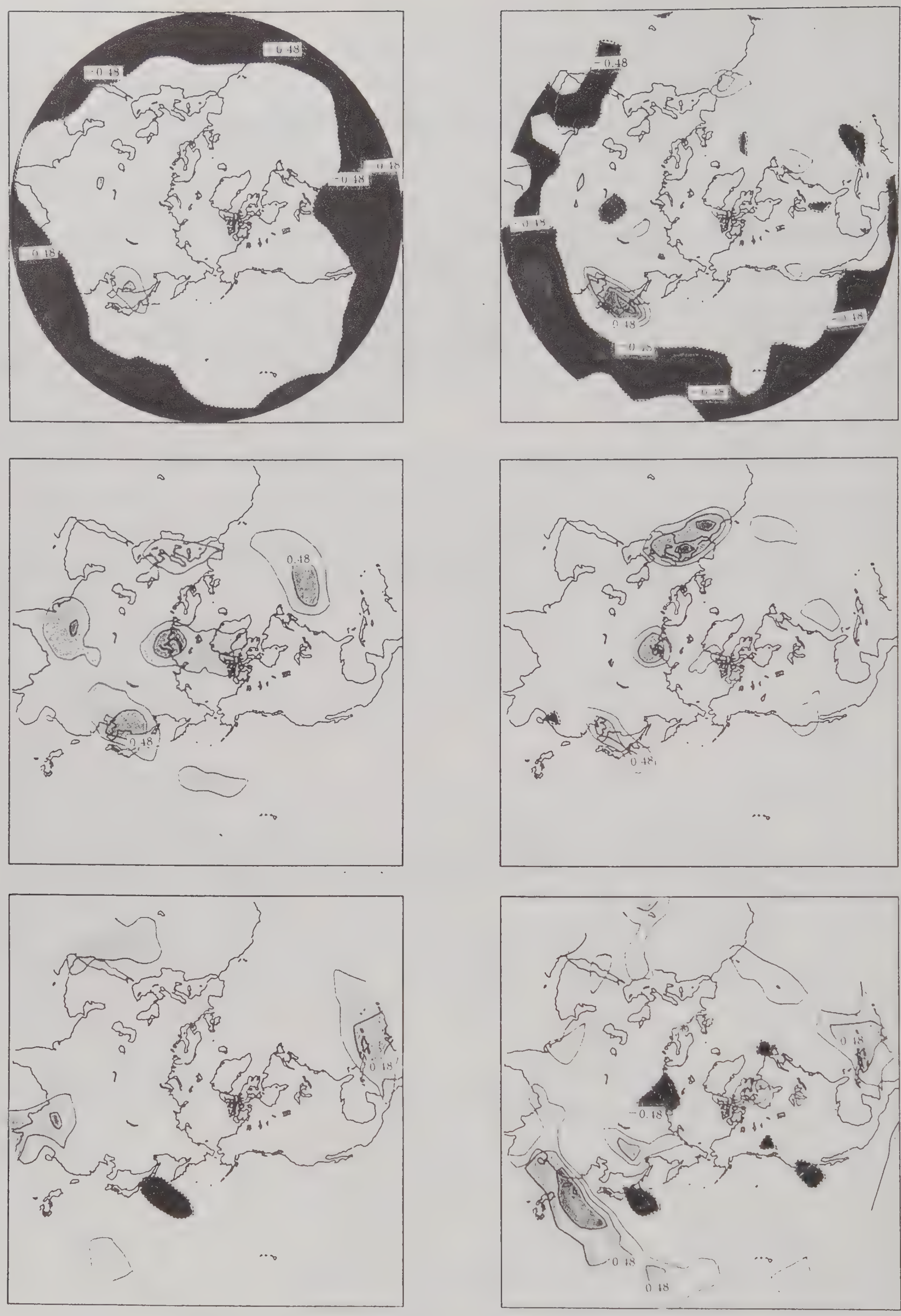
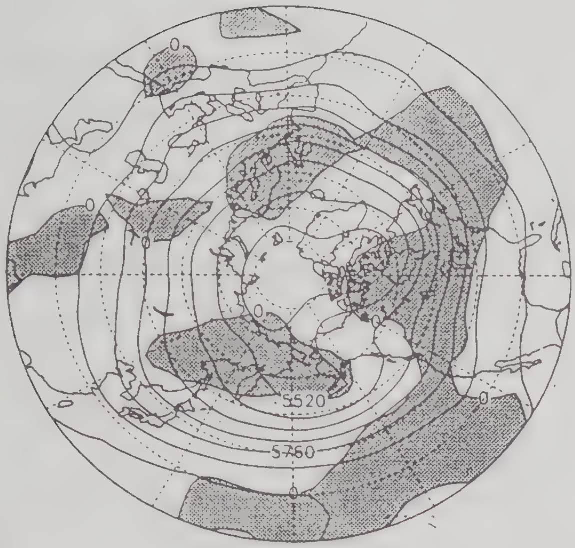


Fig.3 Correlation maps between 500hPa (right) and 100hPa (left) height anomalies and monsoon indices for June to August. Blue and orange lines mean the negative and positive values. Intervals more than 0.36 are drawn by 0.12, and shaded. Upper, middle and bottom panels show SAMOI(A), SAMOI(N), SAMOI(W), respectively.



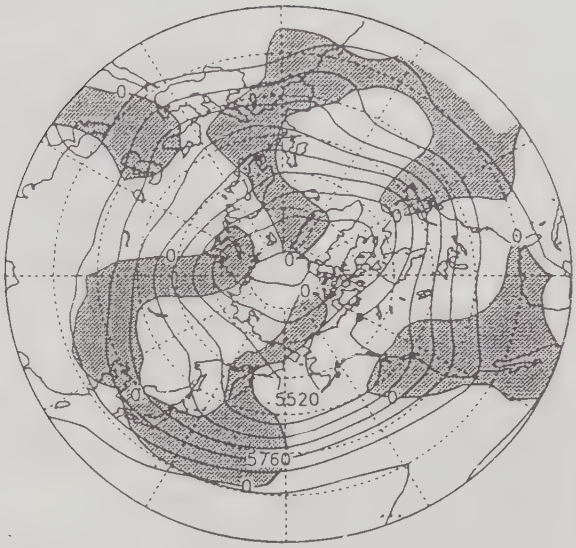


Fig.4 Composite maps of 500hPa height in the case of large (left) and small (right) snow cover.
The years in the large snow cover are 1972, 1979, 1980, 1981, 1982, 1984, 1987 and 1993.
The years in the small snow cover are 1971, 1973, 1975, 1978, 1983, 1988, 1991 and 1995.
Negative anomalies are shaded.

アブストラクト

衛星観測データである外向き長波放射量(OLR)を用い、夏期におけるアジアモンスーンの活動度を表現する指数を開発した。対流活動はモンスーンの活動を示す特徴の一つであるが、OLR は概ね対流活動に対応していることを仮定した。開発した指数は、対流活動の全体的な活動度、活動中心の南北ｼﾌﾄ、活動中心の東西ｼﾌﾄの状態を表現するものであり、熱源の強度と水平スケール及びその分布を示している。

これらの指数が循環場等と矛盾がないことを確認するために、循環場や海面水温などと同時相関係数を計算した。計算結果は、これまでの調査結果と一致するものであり、これらの指数がモンスーンの解析に有用であることを確認した。南北ｼﾌﾄと東西ｼﾌﾄの指数と高度場の同時相関係数から、両者の日本付近の大気の循環場への応答は異なっていることが分かった。両指数の大気応答の差は、夏期における日本の天候予報に有用な情報であり、今後、両指数と強く関係する境界条件及び循環場の調査を進める。

積雪分布は考えられる境界条件の一つである。調査の結果、作成指数と 4 月の西シベリア域の積雪分布には、ほとんど相関関係が見られなかった。これは、4 月の西シベリア地の積雪分布の影響は、夏期のアジアモンスーンの平均場に見ることができないことを示している。一方、 4 月の西シベリア域の積雪分布と 6 月のオホーツク海高気圧との関係調査では 500hPa の高度場に積雪分布の影響が現れている。これらの結果から、積雪分布の影響を確認するために、今後、積雪分布の対象をユーラシア大陸に拡大すること、 6 月における大気循環場との関係をさらに調査する必要がある。

観測・解析研究ディレクトリー

Directory of Observation/Analysis Data Set

1. Directory Entry Title :
GMS IR Histogram

2. Directory Entry Start and Stop Date
Start Date : 1996-01-01
Stop Date : 1996-12-31

3. Sensor Name
VISSR

4. Source Name
GMS

5. Investigator, Technical Contact, and Author
(1) Investigator
Last name : Yamazaki
First name : Nobuo
Email : nyamazak@mri-jma.go.jp
Phone : +81-298-53-8668
Address : M.R.I., 1-1 Nagamine, Tsukuba, Ibaraki 305, Japan
(2) Technical Contact
Last name : Kiyoshi
First name : Sasamoto
Email :
Phone :
Address : Meteorological Satellite Center, Tokyo, Japan
(3) Author
Last name :
First name :
Email :
Phone :
Address :

6. Data Center
(1) Data Center Name : M R I >Meteorological Research Institute
(2) Dataset ID :
(3) Data Center Contact
Last Name :
First Name :
Email :
Phone :
Address :

7. Originating Center

8. Campaign or Project
J E X A M >Japanese Experiment on Asian Monsoon

9. Storage Medium

130 CCT's 13 G Bytes

10. Parameter Measured

Earth Radiative Process > IR equivalent black body temperature

11. Discipline Keywords

Earth Science > Atmosphere

12. Coverage

Minimum Latitude: 50S
Maximum Latitude: 50N
Minimum Longitude: 80E
Minimum Longitude: 160W

13. Location Keywords

Western Pacific

14. General Keywords

15. Revision Date

16. Science Review Date

17. Future Review Date

18. References

19. Summary

Available on the basis of cooperative research

1. Directory Entry Title :
GMS Water vapor Channel Histogram

2. Directory Entry Start and Stop Date
Start Date : 1996-01-01
Stop Date : 1996-12-31

3. Sensor Name
VISSR

4. Source Name
GMS

5. Investigator, Technical Contact, and Author
(1) Investigator
Last name : Yamazaki
First name : Nobuo
Email : nyamazak@mri-jma.go.jp
Phone : +81-298-53-8668
Address : M.R.I., 1-1 Nagamine, Tsukuba, Ibaraki 305, Japan
(2) Technical Contact
Last name : Kiyoshi
First name : Sasamoto
Email :
Phone :
Address : Meteorological Satellite Center, Tokyo, Japan
(3) Author
Last name :
First name :
Email :
Phone :
Address :

6. Data Center
(1) Data Center Name : M R I >Meteorological Research Institute
(2) Dataset ID :
(3) Data Center Contact
Last Name :
First Name :
Email :
Phone :
Address :

7. Originating Center

8. Campaign or Project
J E X A M >Japanese Experiment on Asian Monsoon

9. Storage Medium 130 CCT's 13 G Bytes
10. Parameter Measured Earth Radiative Process > Water vapor Channel equivalent black body temperature
11. Discipline Keywords Earth Science > Atmosphere
12. Coverage Minimum Latitude: 50S Maximum Latitude: 50N Minimum Longitude: 80E Minimum Longitude: 160W
13. Location Keywords Western Pacific
14. General Keywords
15. Revision Date
16. Science Review Date
17. Future Review Date
18. References
19. Summary Available on the basis of cooperative research

1.Directory Entry Title XBT observation between the South China Sea and the Persian Gulf
2.Directory Entry Start and Stop Date Start Date : 07 Oct. 1990 Stop Date :
3.Sensor Name XBT > Expendable bathythermograph
4.Source Name Kashimasan Maru
5.Investigator,Technical Contact, and Author (1) Investigator (Last Name) (First Name) (Middle Name) Name : Mikawa Tetsuya Email : tmikawa@naps.kishou.go.jp Phone : +81-3-3212-8341 Ext.5135 Address : Climate Prediction Division Climate and Marine Department, Japan Meteorological Agency 1-3-4, Otemachi, Chiyoda-ku, Tokyo, 100 JAPAN (2) Technical Contact Name : Yoshida Takashi Email : yoshida@naps.kishou.go.jp Phone : +81-3-3212-8341 Ext.5129 Address : Oceanographical Division Climate and Marine Department, Japan Meteorological Agency 1-3-4, Otemachi, Chiyoda-ku, Tokyo, 100 JAPAN
6.Data Center (1) Data Center Name: Global Subsurface Data Center (2) Dataset ID : (3) Data Center Contact (Last Name) (First Name) (Middle Name) Name : Fabri Marie-Claire Email : Marie.Claire.Fabre@ifremer.fr Phone : +33-02-98-22-46-44 Address : IFREMER/ORSTOM PB 70 29280 Plouzane FRANCE
7.Originating Center
8.Campaign or Project Campaign : TOGA > Tropical Oceans and Global Atmosphere Campaign : WOCE > World Ocean Circulation Experiment

9. Storage Medium

magnetic disks

10. Parameter Measured

Ocean Dynamics > Temperature

11. Discipline Keywords

Earth Science > Ocean

12. Coverage

Minimum Latitude : 5N
Maximum Latitude : 23N
Minimum Longitude : 60E
Maximum Longitude : 121E

13. Location Keywords

Indian Ocean

14. General Keywords

15. Revision Date

16. Science Review Date

17. Future Review Date

18. References

19. Summary

Japan Meteorological Agency is operating a voluntary ship for XBT observations at South China Sea, the Strait of Malacca to Sri Lanka and the Persian Gulf. The ship, "Kashimasan Maru", is a crude oil tanker.

About 14 sections per year and 4 casts a day are observed.

1. Directory Entry Title : JEXAM drifting buoy data in teh tropical Indian Ocean
2. Directory Entry Start and Stop Date Start date : Feb. 2, 1990 Stop date :
3. Sensor Name : Surface drifter with SST sensor
4. Source Name : ARGOS
5. Investigator, Technical Contact and Author (1) Investigator Last Name : Yoritaka First Name: Hiroyuki Email : yoritaka@cue.jhd.go.jp (internet) Phone : +81-3-3541-4387 FAX : +81-3-3541-4397 Address : 5-3-1 Tsukiji, Chuo-ku, Tokyo 104 Japan (2) Technical Contact Last Name : Yoritaka First Name: Hiroyuki Email : yoritaka@cue.jhd.go.jp (internet) Phone : +81-3-3541-4387 FAX : +81-3-3541-4397 Address : 5-3-1 Tsukiji, Chuo-ku, Tokyo 104 Japan (3) Author Last Name : Yoritaka First Name: Hiroyuki Email : yoritaka@cue.jhd.go.jp (internet) Phone : +81-3-3541-4387 FAX : +81-3-3541-4397 Address : 5-3-1 Tsukiji, Chuo-ku, Tokyo 104 Japan
6. Data Center (1) Data Center Name : Japan Oceanographic Data Center (2) Data Set ID : (3) Data Center Contact Last Name : Nagai First Name: Toshio Email : jodc@osman.jhd.go.jp (internet) Phone : +81-3-3541-4295 FAX : +81-3-3545-2885 Address : 5-3-1 Tsukiji, Chuo-ku, Tokyo 104 Japan
7. Originating Center
8. Campaign or Project Project : Japanese Experiment on Asian Monsoon (JEXAM)
9. Storage Medium : Magnetic Tape, 6 Mbyte
10. Parameter Measured : Locations of drifters, SST

11. Discipline Keywords
Earth science > Tropical Indian Ocean > Oceanic currents

12. Coverage
Minimum latitude : 33 S
Maximum latitude : 24 N
Minimum longitude : 38E
Maximum longitude : 135E

13. Location Keywords
Indian Ocean > Tropical Region

14. General Keywords
Surface currents > Heat Transport

15. Revision Date
March 31, 1997

16. Science Review Date

17. Future Review Date

18. References

Hydrographic Department of Japan, Surface Currents and Upper Oecan Thermal Structure in the Indian Ocean (small atlas), 1994.

Michida, Y. and H. Yoritaka, Survivability of the surface drifters deployed by Hydrographic Department of Japan for the period from 1988 to 1993, *J. Japan Soc. Mar. Surv. Tech.* 7(2), 21-28, 1995.

Michida, Y. and H. Yoritaka, Surface currents in the area of the Indo-Pacific throughflow and in the tropical Indian Ocean observed with surface drifters, *J. Geophys. Res.* 101, 12475-12482, 1996.

1. Directory Entry Title Surface Meteorological data of AWS	
2. Dirtectry Entry Start and Stop Date Start Date: 6 July 1993 Stop Date:	
3. Sensor Name wind vane, anemometer, thermometer, hygrometer, rain gauge, barometer, soil moisture gauge, pyranometer, radiometer	
4. Source Name AWS > Automatic Weather Station	
5. Investigator, Technical Contact, and Author (1) Investigator Last Name: Shigenori First name: Haginoya E-mail: shaginoy@mri-jma.go.jp Phone: +81-298-53-8706 Adress: M.R.I., 1-1 Nagamine, Tsukuba, Ibaraki 305, Japan (2) Technical Contact Last Name: First name: E-mail: Phone: Adress: (3) Author Last Name: First name: E-mail: Phone: Adress:	
6. Data Center (1) Data Center Name: MRI > Meteorological Research Institute (2) Dataset ID: (3) Data Center Contact Last Name First name: E-mail: Phone: Adress:	
7. Originating Center	
8. Campaign or Project JEXAM > Japanese Experiment of Asian Monsoon	
9. Storage Medium FDD, 3.5" MO disk	
10. Parameter Measured wind direction, wind speed, air temperature, relative humidity,	

precipitation, air pressure, soil temperature, soil water content, global solar radiation, reflective solar radiation, net radiatioon.
11. Discipline Keywords Earth Science > Atmosphere
12. Coverage Lhasa: 29° 40'N, 91° 08'E Rikeze: 29° 15'N, 88° 53'E Nagqu: 31° 29'N, 92° 04'E Lingzi: 29° 34'N, 94° 28'E
13. Location keywords Tibetan Plateau
14. General Keywords
15. Revision Date
16. Science Review Date
17. Future Review Date
18. References
19. Summary This data set is in preparation.

1. Directory Entry Title
Sea Surface Meteorological data of AWS

2. Dirtectry Entry Start and Stop Date
Start Date: 23 Ocober 1991
Stop Date: 7 Ocober 1995

3. Sensor Name
wind vane, anemometer, thermometer, hygrometer, rain gauge, barometer, pyranometer, radiometer

4. Source Name
AWS > Automatic Weather Station

5. Investigator, Technical Contact, and Author
(1) Investigator
Last Name: Shigenori
First name: Haginoya
E-mail: shaginoy@mri-jma.go.jp
Phone: +81-298-53-8706
Adress: M.R.I., 1-1 Nagamine, Tsukuba, Ibaraki 305, Japan
(2) Technical Contact
Last Name:
First name:
E-mail:
Phone:
Adress:
(3) Author
Last Name:
First name:
E-mail:
Phone:
Adress:

6. Data Center
(1) Data Center Name: MRI > Meteorological Research Institute
(2) Dataset ID:
(3) Data Center Contact
Last Name
First name:
E-mail:
Phone:
Adress:

7. Originating Center

8. Campaign or Project
JEXAM > Japanese Experiment of Asian Monsoon

9. Storage Medium
FDD, 3.5" MO disk

10. Parameter Measured
wind direction, wind speed, air temperature, relative humidity,

precipitation, air pressure, sea surface temperature, global solar radiation, long wave radiatioon.
11. Discipline Keywords Earth Science > Atmosphere
12. Coverage Minimun Latitude:36S Maximum Latitude: 36N Minimun Longitude: 18E Maximum Longitude: 140E
13. Location keywords Indian Ocean
14. General Keywords
15. Revision Date
16. Science Review Date
17. Future Review Date
18. References
19. Summary This data set is in preparation.

1. Directory Entry Title: Lower Atmosphere Observation by Wind Profiling Radar
2. Directory Entry Start and Stop Date Start Date: Feb. 24, 1994, Stop Date: March 31, 1995
3. Sensor Name: Boundary Layer Radar & RASS
4. Source Name: Clear air turbulence and Acoustic wave
5. Investigator, Technical Contact, and Author Name : Yoshihisa Masuda, E-mail: masuda@crl.go.jp, Phone: +81-98-895-2045 Address:829-3,Daigusukubaru, Aza-kuba, Nakakgusukuson, Nakagami-gun, Okinawa 901-24, Japa
6. Data Center (1) Name: CRL(Communications Research Laboratory) (2) Contact: Name :Yoshihisa Masuda, E-mail: masuda@crl.go.jp, Phone: +81-98-895-2045 Address:829-3,Daigusukubaru, Aza-kuba, Nakakgusukuson, Nakagami-gun, Okinawa 901-24, Japa
7. Originating Center:
8. Campaign or Project:
9. Storage Medium: DOS formatted 3.5 inch flopy disk
10. Parameter Measured: Wind velocity (U,V,W)
11.Discipline Keywords: Atmospheric remote sensing with radio- and acoustic waves
12. Coverage
13. Location Keywords: Subtropical region
14. General Keywords: Asia monsoon
15. Revision Date:
16. Science Review Date:
17. Future Review Date:
18. References
19. Summary Our data-set is the Doppler spectra measured with a boundary layer radar(BLR). The target of the BLR is the clear air turbulence. The BLR can measure the tropospheric wind profiles composed with three-dimensional wind vectors, and the intensity of the turbulence up to about 3 km from 300 m over ground.

1. Data Base Name: [illegible] Atmospheric Observations by Wind Profiler [illegible]

2. Directory Entry Reference [illegible]

Start Date: Feb 28 1993 Stop Date: March 31, 1994

3. Source Name: [illegible] Space Center & NASA

4. Source Name: Center for [illegible] and [illegible]

5. Investigators, Technical Contact, and Author:

Name: [illegible]

Address: [illegible]

[illegible]

6. Data Center

10 Name: [illegible]

(2) Contact

Name: [illegible]

Address: [illegible]

[illegible]

7. Originating Agency

8. Classification of Project

9. Storage Medium: [illegible] disk

10. [illegible]

11. Descriptive Keywords: Atmospheric remote sensing with radar, and acoustic waves

12. Coverage

13. Location Keywords: [illegible]

14. Content: [illegible]

15. Revision Date

16. Science Review Date

17. Future Review Date

18. References

19. Summary

Our data set is the [illegible] measured with a [illegible] radar ([illegible]). The target of the [illegible] of the [illegible] are [illegible]. The [illegible] can measure the temperature, wind profiles [illegible] with three-dimensional wind vectors, and the intensity of the turbulence up to about 1 km from the ground.

全般の問い合せ先

〒１００　東京都千代田区霞ケ関２－２－１

科学技術庁研究開発局海洋地球課

Inquiries to:

Ocean and Earth Division,
Research and Development Bureau,
Science and Technology Agency
2-2-1, Kasumigaseki, Chiyoda-ku, Tokyo 100
Japan